The Expedition ANT-XXIII/4

of the Research Vessel Polarstern in 2006

Edited by
Karsten Gohl
with contributions of the participants

ANT-XXIII/4

To the Bellingshausen and Amundsen Sea

10 February to 11 April 2006
Punta Arenas - Punta Arenas

Fahrtleiter / Chief Scientist:
Dr. Karsten Gohl

Koordinator / Coordinator:
Prof. Dr. W. Arntz

1. Zusammenfassung und Fahrtverlauf

Karsten Gohl
Alfred-Wegener-Institut, Bremerhaven

Die FS *Polarstern*-Expedition ANT-XXIII/4 hatte einen geowissenschaftlichen Schwerpunkt mit dem Ziel, sowohl die glazial-marinen Sedimentationsprozesse als auch die tektonisch-geodynamische Entwicklung des südlichen Amundsenmeeres und der Pine-Island-Bucht im Zusammenhang mit den glazialen und interglazialen Zyklen der Westantarktis zu erkunden. Zusätzlich wurde ein Projekt zur marinen mikrobischen Ökologie, ein ozeanographisches Programm sowie der Transport von Personal und Fracht an den Forschungsstationen *Rothera* und *Jubany* durchgeführt. Nach dem Auslaufen aus Punta Arenas und dem Durchfahren der Magellanstraße, setzte FS *Polarstern* zunächst Kurs in Richtung der Station *Rothera* zwecks Personentransfers. Auf der Peter-I-Insel als dem nächsten Ziel wurden ein GPS-Instrument und ein Magnetometer installiert, um für die folgenden Wochen Messdaten aufzuzeichnen. Das GPS-Instrument zeichnete die erste Wiederholungsmessung des Messpunktes auf dieser Insel seit 1998 als Teil des westantarktischen Messnetzes auf. Das Magnetometer diente als Basisstation zur Aufnahme von zeitlichen Variationen des Erdmagnetfeldes für die helikoptergestützten magnetischen Vermessungen während der Expedition. Weiterhin wurde eine automatische Langzeit-Wetterstation auf dem Radiosletta-Plateau errichtet und Vulkanite mit der Dredge vom submarinen Hang der Insel gesammelt.

Nach einer bathymetrischen Vermessung und einigen Sedimentkern-Stationen entlang der Seamount-Kette nördlich der Insel lief das Schiff in Richtung der Hauptarbeitsgebiete im Amundsenmeer und der Pine-Island-Bucht. Ein breiter Meereisgürtel und nördliche Winde, die einen starken Druck auf das Meereis ausübten, verhinderten einen ersten Versuch, in die Pine-Island-Bucht zu gelangen. Bevor es westwärts entlang des Eisgürtels ging, wurde eine kleinere bathymetrische Vermessung auf dem äußeren Schelf durchgeführt, die deutliche großräumige glaziale Spuren erkennen ließ. Ein seismisches Profil schloss sich daran an. Bei ca. 115° W erfolgte der Durchbruch durch den Eisgürtel in die westliche Pine-Island-Bucht. In diesem Teil des Amundsenmeeres wurden reflexions- und refraktionsseismische Profile vermessen sowie ausgedehnte bathymetrische (Hydrosweep-) Kartierungen und sedimentechographische (Parasound-) Aufzeichnungen der tiefen glazialen Tröge vor dem östlichen Getz- und dem Dotson-Schelfeis durchgeführt. An ausgewählten Stationen der Tröge und Ebenen des inneren Schelfs ist eine große Anzahl von Sedimentkerne mit dem Schwerelot gezogen worden. Aufgrund der günstigen Wetterbedingungen war es möglich, das Vulkanologen-Team, das GPS-Team und die Gruppe zur Datierung von Oberflächenerosionen zu Mt. Murphy zu fliegen. Alle Gruppen absolvierten erfolgreich ihre Programme zur Beprobung bzw. Instrumenteninstallation.

In der Zwischenzeit entwickelte sich entlang der Thwaites-Gletscherzunge eine Polynja, die es dem FS *Polarstern* ermöglichte, in die östliche Pine-Island-Bucht vorzustoßen. In diesem Teil der Bucht wurden die bathymetrischen und seismischen Vermessungen sowie die Sedimentkern-Beprobungen fortgesetzt, um Erkenntnisse der Enteisungsgeschichte in dieser Region der Westantarktis zu gewinnen, wo ein

zügiger Rückzug der Pine-Island- und Thwaites-Gletschersysteme auftritt. Die Hudson Mountains von Ellsworth-Land waren Ziel von weiteren Gesteinsbeprobungen zur Untersuchung dieser vulkanischen Provinz sowie von GPS-Installationen zur Gewinnung von Parametern zur Untersuchung der tektonischen Bewegungen und des glazialen Ausgleichs der Kruste. Zusätzliche GPS-Stationen auf den Schelfeisen der Pine-Island-Bucht zeichneten Daten der Gezeiten und der Schelfeisbewegungen auf. Als Teil des ozeanographischen Programms, sind CTD-Verankerungen nahe der Schelfeise und auf dem äußeren Kontinentalschelf abgesetzt worden. Diese Instrumente sollen während einer amerikanischen Expedition im Folgejahr wieder geborgen werden.

Nachdem die Pine-Island-Bucht durch den nördlichen Meereisgürtel verlassen wurde, ist die Expedition mit reflexions- und refraktionsseismischen Profilen entlang des Kontinentalfußes nördlich der Schelfkante fortgesetzt worden, bevor das FS *Polarstern* in das Gebiet der Marie-Byrd-Seamounts gelangte. Hier erfolgte ein Dredge-Programm zur Beprobung von vulkanischen Gesteinen, die von den Flanken dieser zuvor noch nie beprobten unterseeischen Bergkuppen gebrochen wurden. Dieses Material dient der Bestimmung des Eruptionsalters und der petrologisch-geochemischen Zusammensetzung.

Als Teil des geophysikalischen Untersuchungsprogramms sind große Abschnitte des südlichen Amundsenmeeres und der Pine-Island-Bucht mit schiffsgestützter Gravimetrie und Magnetik sowie mit helikoptergestützter Magnetik vermessen worden.

Die meeresbiologische Gruppe sammelten Proben von Krill- und mikrobischen Arten aus der Wassersäule an mehreren Stationen entlang der gesamten Fahrtstrecke. An Bord wurden Experimente zur Untersuchung der mikrobischen Nahrungskette und der Einfluss auf die Biodiversität des Südozeans durchgeführt. Ein Walbeobachtungsteam registrierte Walsichtungen und -identifikationen entlang der Fahrtroute.

Auf dem Rückweg von den Marie-Byrd-Seamounts sind das GPS-Gerät und das Magnetometer von Peter-I-Island geborgen worden. Ein Besuch an der *Jubany*-Station auf der King-George-Insel erfolgte zwecks Personen- und Frachttransports und eines kurzen Programms zur Sedimentkernentnahme, bevor das FS *Polarstern* nach Punta Arenas zurückkehrte.

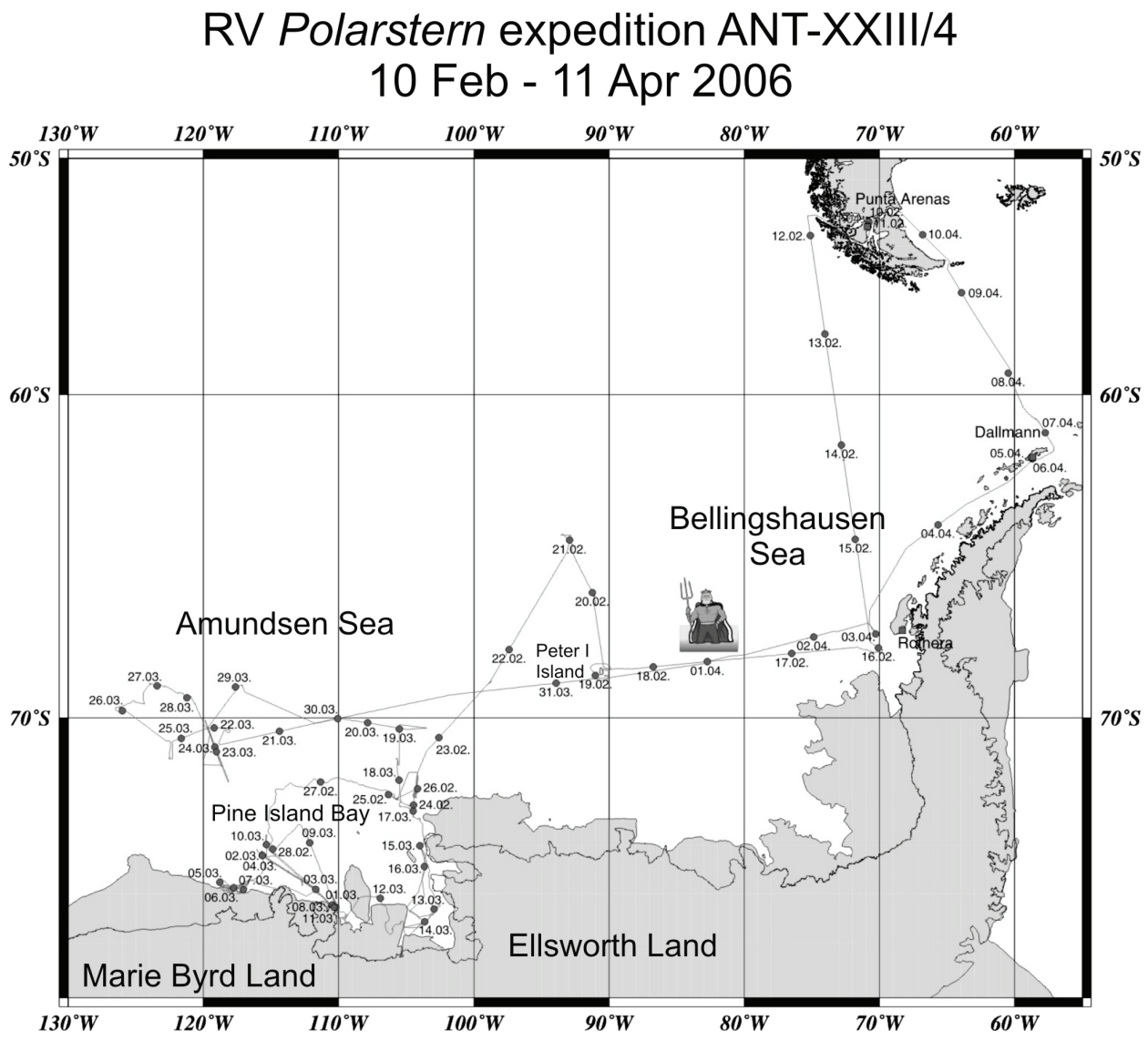

Abb. 1: Übersicht der Fahrtroute der Polarstern Expedition ANT-XXIII/4
Fig. 1: Overview track chart of Polarstern expedition ANT-XXIII/4

SUMMARY AND ITINERARY

The RV *Polarstern* expedition ANT-XXIII/4 had its main focus on geoscientific research with the goal to investigate the glacial-marine sedimentation processes and the tectonic-geodynamic evolution of the southern Amundsen Sea and Pine Island Bay for deciphering the glacial and deglacial development of West Antarctica. In addition, a programme on marine microbial ecology, an oceanographic programme and the transport of persons and freight from *Rothera* and *Jubany* Stations were conducted.

After leaving Punta Arenas and the Magellan Strait, RV *Polarstern* set course toward *Rothera* Station for personnel transfer. The ship headed to Peter I Island where a GPS station and a magnetometer were installed in order to record data for the duration of the following weeks. The GPS measurement is the first repeat measurement of a survey point on this island since it was established in 1998 as part of the West Antarctic GPS network. The magnetometer served as a base station to record temporal variations of the earth magnetic field for the helicopter-magnetic surveys of this expedition. In addition, a long-term automatic weather station was deployed on the Radiosletta plateau and volcanic rocks were dredged from the submarine slope of the island.

After a swath-bathymetric survey and sediment coring along the seamount chain north of Peter I Island, the ship headed toward the main research areas in the Amundsen Sea Embayment and Pine Island Bay. A wide sea-ice belt and strong northerly winds pressing onto the sea-ice prevented the first attempt to enter Pine Island Bay. Before moving westward along the sea-ice edge, a small bathymetric survey revealed strongly structured mega-scale glacial lineation, and a seismic profile was added to an existing line on the outer continental shelf. At about 115°W, we attempted to enter through the sea-ice belt into the western Pine Island Bay, and succeeded. In this part of the Amundsen Sea Embayment, seismic reflection and refraction profiles were recorded in addition to extensive swath-bathymetric (hydrosweep) and sub-bottom profiler (parasound) surveys of the deep glacial troughs off the Eastern Getz and Dotson Ice-Shelves (down to 1,600 m water depth). On selected sites of the troughs and plains of the inner shelf, a large number of sediment cores were taken with a gravity corer. Due to very favourable weather conditions it was possible to fly out the volcanology team, the GPS team and the surface-exposure-dating team to Mt. Murphy. All teams succeeded in their rock sampling and instrument installation programme.

In the meantime, a polynya had developed along the Thwaites Glacier ice-tongue, which allowed RV *Polarstern* to enter the inner Pine Island Bay. In this part of the bay, bathymetric and seismic surveying as well as sediment coring continued in order to obtain information on the deglaciation history of this part of West Antarctica, where

the retreat of the Pine Island and Thwaites Glacier systems occurs rapidly. The Hudson Mountains of Ellsworth Land were the destination for further rock sampling and a GPS site installation to investigate the volcanic province and to obtain parameters for tectonic and glacial rebound studies. Additional GPS sites on ice-shelves of Pine Island Bay provided data on tidal and ice-shelf motion. As part of the oceanographic programme, CTD moorings were deployed near the ice-shelves and on the outer shelf. An American expedition is planning to recover the instruments in the following year.

After leaving Pine Island Bay through the northern sea-ice belt, seismic reflection and refraction profiling continued on the continental rise off the shelf break before the ship moved into the area of the Marie Byrd Seamounts. Here, the dredging programme succeeded in collecting freshly broken volcanic rock from the slopes of several of these previously unsampled seamounts, providing material for determining their petrological-geochemical composition and their eruption age.

As part of the geophysical programme, large parts of the southern Amundsen Sea and Pine Island Bay were surveyed with shipborne gravity and magnetic profiles as well as with a dense grid of helicopter-magnetic flight lines.

The marine biology group collected krill and microbial species from the water column on several sites along the entire ship track of this leg. Experiments were conducted on board in order to investigate the microbial food web and its effect on biodiversity in the Southern Ocean. A whale observation team recorded whale sightings and identifications along the cruise track.

On the return track from the Marie Byrd Seamount area, the GPS and magnetic instruments were recovered from Peter I Island. *Jubany* Station on King George Island was the next destination for person and freight transfer and to collect sediment cores in the bay before RV *Polarstern* headed back to Punta Arenas.

2. MAGNETIC AND GRAVIMETRIC SURVEYING

Tectonic and geodynamic evolution of the Southern Pacific and the West Antarctic Continental Margin

Graeme Eagles, Volker Leinweber, Karsten Gohl, Christina Mayr, Sonja Suckro
Alfred-Wegener-Institut, Bremerhaven

Objectives

Accurate models of the geodynamic-tectonic evolution contain some of the most important parameters for understanding and reconstruction of the palaeo-environment. Magnetic and gravimetric surveys of the abyssal plain, the continental shelf and slope of the southern Amundsen Sea and Pine Island Bay allow plate-tectonic and continental crustal reconstructions. The objectives are:

- Identification of the boundaries between suspected crustal blocks and volcanic zones in Pine Island Bay. The glacier troughs and Pine Island Bay are thought to have developed along such tectonic boundaries.

- During and after separation from the Chatham Rise and Campbell Plateau (New Zealand), the continental margin of Marie Byrd Land developed as a passive margin, probably accompanied by intensive volcanism. The question is whether this volcanism occurred mainly during the rifting process or during post-rift phases, or whether it developed in relation to the West Antarctic rift system.

- Mapping of the acoustic basement and its structure to obtain the tectonic geometries and boundary conditions.

Work plan

- Installation and operation of an autonomous magnetic base station system on Peter I Island
- Collection of gravity and magnetic data using the ship's permanently installed gravity meter and a three-component magnetometer as well as the helicopter-towed caesium-vapour aeromagnetic sensor system
- Processing of the gravity data to the stage of useable free-air and Bouguer anomalies
- Processing the helicopter magnetometer data by removing the geomagnetic variation and electromagnetic noise
- Processing the ship's magnetometer data by compensating for perturbations due to magnetic fields caused by the ship's hull and superstructure, filtering and removing the geomagnetic variations

Methods and equipment

Helicopter magnetics

AWI's Scintrex caesium vapour magnetometer, towed 30 m below the helicopter to avoid magnetic disturbances, was used to collect aeromagnetic data. Inside the cockpit, this magnetometer was connected to the PICODAS data acquisition system, consisting of a PC with further connections to a GPS-antenna and radar altimeter.

Daily flight planning was done using *Matlab* algorithms, written during the cruise, which allow interactive project management. This capability is essential in an area like the Amundsen Sea where changeable ice and weather conditions meant that the ship's itinerary was often altered on short notice. Furthermore, we successfully tested software written in Bremerhaven by Matthias König that is intended to read the GPS signal over a serial port (in real time?) into a laptop computer, which might also be running the flight-planning programme during data acquisition. This capability is intended to improve the flexibility of the flight operator's response to situations in which the flight plan needs to be changed during acquisition.

PICODAS is not intended for survey plans that stretch over more than one Universal Transverse Mercator (UTM) zone. Because our target research area, the Amundsen Sea embayment, covers several UTM zones, it presented problems for PICODAS when it came to calculating and displaying project lines in the cockpit. We circumvented this problem by creating a separate project for each UTM-zone, in which the project lines passed seamlessly into those of the adjacent projects.

Data acquisition went smoothly most of the time, although we experienced problems caused by a faulty connector (now replaced) on the magnetometer cable and during VHF communication with RV *Polarstern* when the GPS signal was occasionally lost. A few tracks had to be rerouted during flight, especially during an extended period of rainy weather near the Marie Byrd Seamounts.

Shipborne magnetics

Shipborne magnetic measurements were made by two fluxgate vector magnetometers, which were permanently mounted at the crow's nest. The data were directly saved in the ship's archiving system, PODAS, at one-second intervals. To take account of the influence of the metallic bulk of the ship, the ship undertook compensation loops on 14 , 20 , and 25 February and 8 March. In the small area of a compensation loop the variations of the magnetic field due to crustal magnetisation are assumed to be negligible. The loops thus provide coefficients that relate the ship's heading, roll, and pitch movements to the variations in magnetometer measurements that they cause. Using these coefficients, it is possible to correct the shipborne magnetic measurements in the wider area around the compensation loop. This compensation process was completed using the experimental PSMAG programme written by Matthias König (AWI).

Magnetic base station

The recorded magnetic field shows not only geographical but also temporal variations due to solar radiation and other influences. In industry surveys, this variation is removed by subtracting continuous measurements taken at static base stations deployed within the survey area. Usually it is not possible to install base

stations for this purpose during ship-based surveys because of the lack of suitable locations at sea. On ANT-XXIII/4, however, we were able to install a base station magnetometer on the Michajlovodden headland of Peter I Island (Figs. 2.1 and 2.2; at 90.4266°W, 68.8634°S, somewhat outside the main survey area) during the period of 19 February to 31 March 2006. The magnetometer used for this purpose is an Overhauser Effect proton precession magnetometer, newly purchased from GEM Systems, Canada. Electrical supply to the magnetometer was achieved using 6 car batteries and 4 solar panels connected as shown in figure 2.3. The magnetometer sensor was mounted on a pole, which was fixed to a base consisting of a collapsible wooden cross suitable for transportation to the island by helicopter.

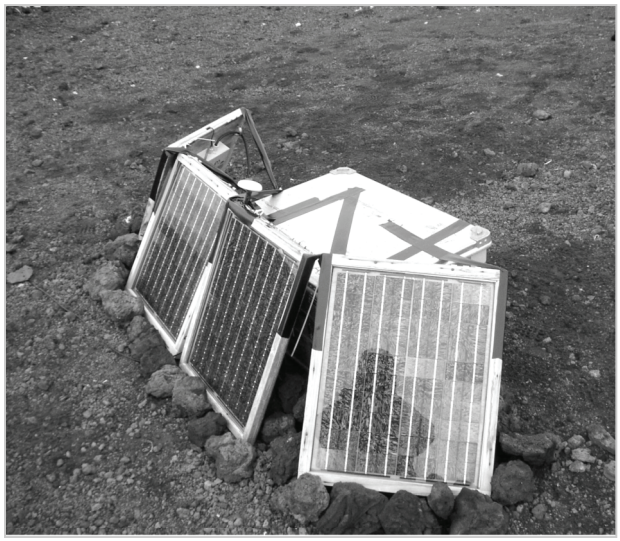

Fig. 2.1: Box containing the batteries and magnetometer console, with the solar panels and GPS antenna

Fig. 2.2: The magnetometer sensor on Peter I Island

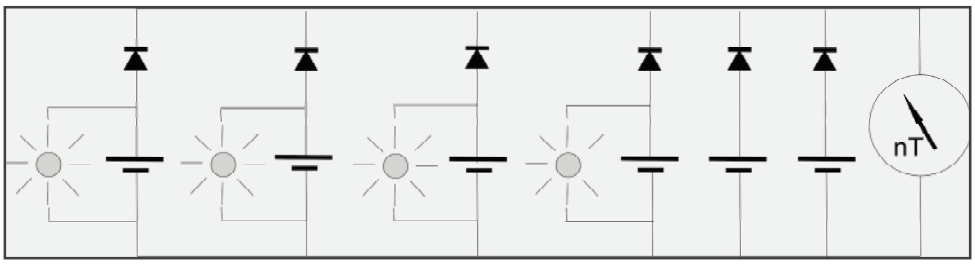

Fig. 2.3: Plan of the base station magnetometer power supply

Shipborne gravity

Gravity data were continuously acquired during the expedition using the ship's permanently-mounted KSS31 gravity meter. The data were directly archived in the PODAS system at one-second intervals. The gravity data acquisition worked without

any problems during the entire cruise leg, except for short periods when PODAS was shut down.
We conducted two measurements with a LaCoste and Romberg gravity meter at the bunker pier on Cabo Negro near Punta Arenas in order to tie the underway data to the International Gravity Station Network (IGSN). It was not possible to measure directly at the nearest located IGSN station at the Port Authority building in Punta Arenas, due to limited time between arrival in South America and the ship's departure. Instead, we used the last available gravity measurement from that station, made with the same gravity meter just before leg ANT-XXII/4 in 2005. We obtained an absolute gravity value at the bunker pier by calculating the difference between the 2005 measurement there and our measurement, and applying it to the published gravity value at the IGSN station. This value was then used to correct the KSS31-measurements.

Results

Gravity

The data from the ship's gravity meter were successfully reduced to free-air and Bouguer anomalies using standard AWI procedures. Despite having no recent measurement at the IGSN station in Punta Arenas, comparison with satellite-derived gravity anomalies revealed differences of <15 mGal over open water. Much larger variations between ship's gravity and satellite derived gravity exist in sea-ice covered areas and near ice shelves. In these areas the ship's data can be considered more accurate. Figure 2.4 shows two example data profiles.

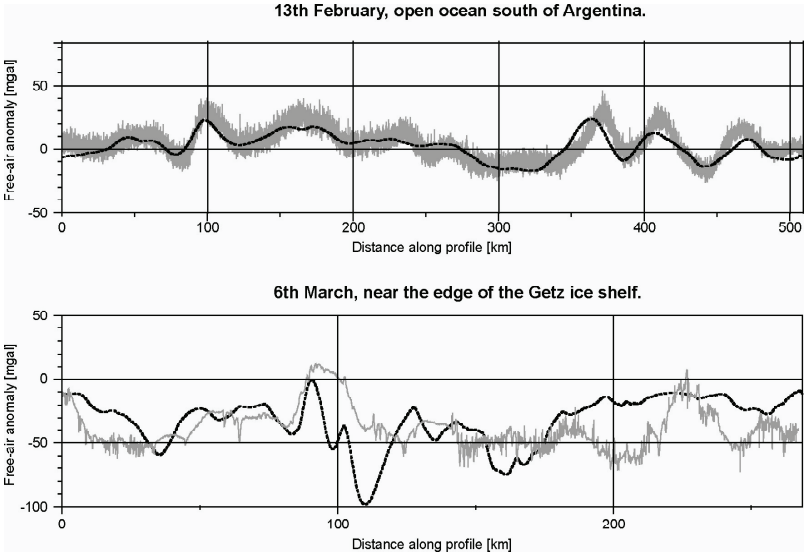

Figure 2.4: Examples of free-air gravity anomalies derived from ship's data (grey line, unfiltered) compared to satellite-derived free-air anomalies (dashed black line)

Shipborne magnetics

The ship's magnetometer data were downloaded from PODAS and processed in day-long blocks every one or two days. As well as compensation for the ship's field, processing consisted of an IGRF correction, data reduction and filtering of high frequency chatter. Regardless of which set of compensation parameters is used, some day files retain long wavelength residual anomalies after the processing. This

may be attributable to the high gradient in the geomagnetic field in the study area, meaning a set of compensation coefficients quickly becomes inadequate for full compensation as the ship progresses. Because it was impractical to complete a large number of compensation loops, these long wavelength anomalies were removed using filtering processes implemented in the Generic Mapping Tools package. At this stage, the individual days of data are useable, although in some cases alternative compensation coefficients, derived after the processing date, may yield improvements. Comparison with helicopter magnetic profiles shows that the shipborne data are reliable in that they show similar anomalies with similar amplitudes.

Helicopter magnetics
The helicopter magnetic programme took advantage of the good weather conditions to deliver a total of nearly 20,700 km of new data. Table 2.1 and figure 2.5 give an overview of magnetic flights. In mid February, the first patterns were flown off the Antarctic Peninsula margin and in the Bellingshausen Sea. A short test flight and 5 further flights in this programme revealed seafloor spreading anomalies. Upon reaching the Amundsen Sea embayment, a small regular grid built of up to 4 flight patterns was flown over the continental shelf west of Thurston Island, enabling the identification of a belt of strong magnetic variations with a possible trend parallel to the island's long axis. North of this belt, the magnetic anomalies were more subdued. Once south of the ice barrier, a regular pattern of 22 north-south and east-west flights was flown, quickly revealing a fundamental division between the magnetic styles of the inner and outer shelf. Short wavelength anomalies characterise the inner shelf and neighbouring land, but longer wavelength anomalies are visible in the north. One flight reached far enough south to cross the flights of 2005's AGASEA magnetic grid, acquired by the University of Texas, USA, in order to provide the possibility of connecting the two data sets.

After breaking through into the southeastern part of the embayment, 10 flights were flown in and around Pine Island Bay, with line spacing and orientation chosen to highlight suspected NW-trending variations as quickly as possible. In these three and a half days of surveying, we also managed a number of north-south oriented flights that connect the Pine Island Bay data set to that of the earlier flown route off Thurston Island, and flights connecting our survey to tracks of the 2005 British Antarctic Survey and AGASEA campaigns. In this region, high amplitude short wavelength magnetic anomalies appear to be related to granitic island groups that lie along NW-oriented gravity anomaly trends, but at this stage the NW trend itself is not strongly evident in the magnetic data.

After leaving Pine Island Bay we resumed flights over the deep ocean, extending AWI's 2001 helicopter magnetics data set, flown from RV *Polarstern*, to the SW and into the Marie Byrd Seamounts province. Together with the 2001 survey, these data, accumulated during a total of 24 flights, show that the late Cretaceous spreading ridge was regularly segmented by short-offset transform faults between the Udintsev and Antipodes fracture zones, something that was not evident before. The Bellingshausen–Antarctic extensional plate boundary existed in this region during its period of activity around 79–61 Ma, with the Antipodes Fracture Zone thought to represent either the Bellingshausen–Antarctic–Pacific triple junction trace or the

Bellingshausen–Antarctic plate boundary itself. After an analysis back in Bremerhaven, a set of flights concentrating on the Antipodes Fracture Zone may provide answers to this question.

Base station magnetics

Prior to deploying the base station magnetometer on Peter I Island, we conducted a brief set of tests onboard RV *Polarstern* to establish its functionality. Upon retrieval the magnetometer base unit was still working, despite having been buried under snow and ice, and tests lateron showed that each of the six car batteries was supplying a load of around 12 V. After returning the magnetometer to RV *Polarstern*, however, we were unable to switch it on again, and repairs were necessary. The problem seems to have occurred during disconnecting the magnetometer from its power supply on the island, but its exact cause remains unknown. The data from the magnetometer are of good quality, and show relatively quiet magnetic conditions during the deployment. Daily variations in a range of 40-70 nT are typical, with occasional bursts of 100 min period variation at an amplitude of around 20-30 nT, and ubiquitous short wavelength (6 s) variation at around 1-2 nT. An initial examination of the data shows that there appears to be little correlation between the 100 min variations and anomalies in the helicopter magnetic data at similar wavelengths. Therefore, it seems at this point that the base station data are not suitable for correcting the underway data, probably due to the 20–30° longitude difference between Peter I Island and the main regions of investigation.

Summary

In summary, we can see that even at this early stage the newly-acquired potential field data are undoubtedly of scientific value. In the future, after further data reduction and modelling of source body distributions, the ship's gravity and magnetic data will be useful adjuncts to the interpretation of the seismic refraction profiles, as these are co-located. Two such multidisciplinary profiles have been acquired, in the western Amundsen Sea Embayment and in the Marie Byrd Seamounts province. After further processing, possibly using the base station measurements, and levelling, the helicopter magnetic data will also contribute to these studies, as they provide information on the spatial extent of features crossed by the profiles. In the absence of extensive rock outcrops, these data will also provide key information on the near surface geology of Pine Island Bay.

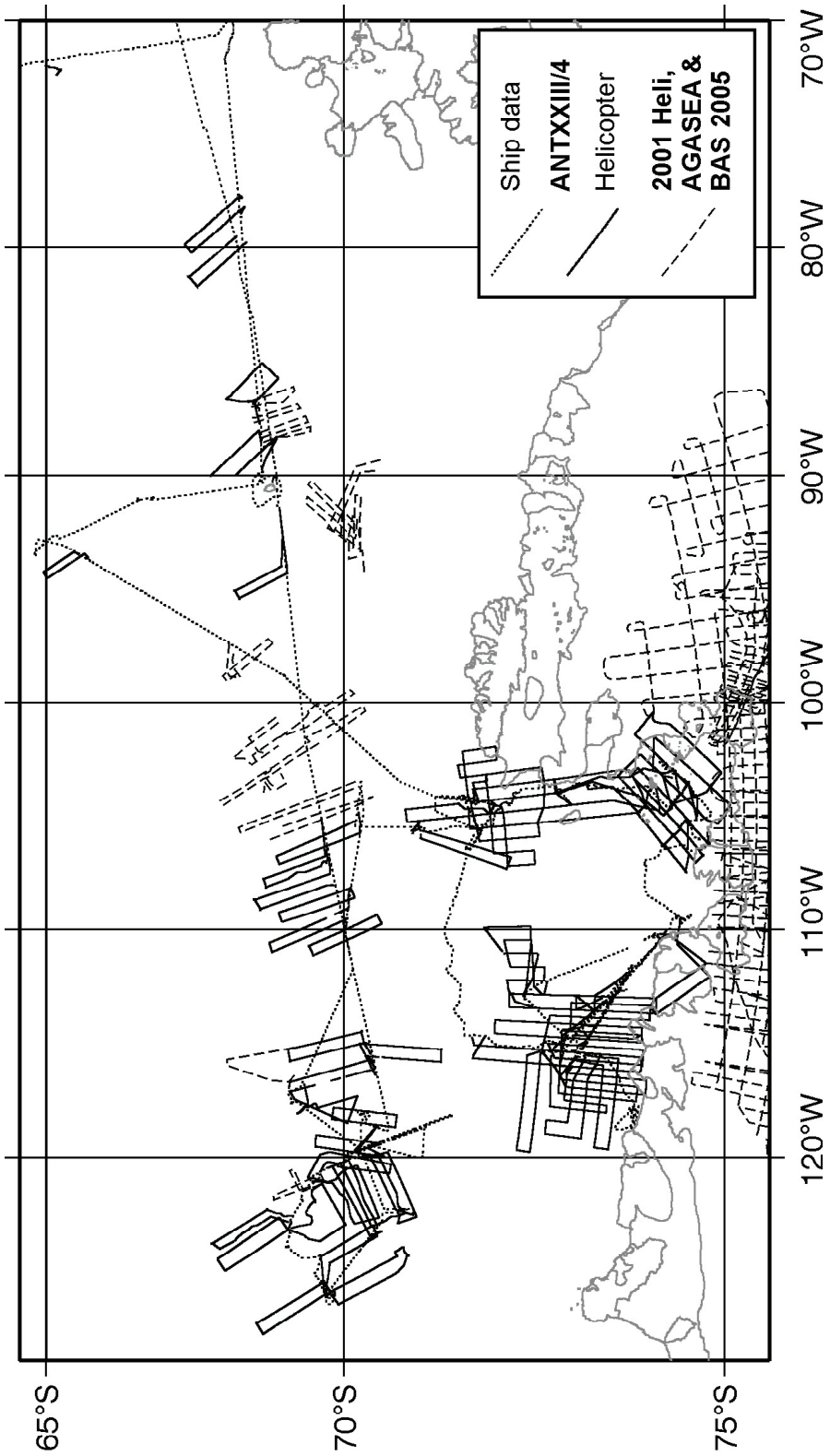

Fig.: 2.5: Selected magnetic data in the Amundsen Sea region

Tab. 2.1: Helicopter magnetic data acquisition flight details

Date	Flight no. this day	Area	No. FIDS	Filename	Duration
15.02.2006	1	Test flight	4364	0602151.raw	1:13:37
17.02.2006	1	Bellingshausen Sea	7918	0602171.RAW	2:12:03
17.02.2006	2	Bellingshausen Sea	25	6002172.RAW	0:00:24
17.02.2006	2	Bellingshausen Sea	242	0602173.RAW	0:04:37
17.02.2006	2	Bellingshausen Sea	642	0602174.RAW	0:10:41
17.02.2006	2	Bellingshausen Sea	6143	0602175.RAW	1:42:15
18.02.2006	1	near Peter I Island	7887	0602181.RAW	2:11:51
18.02.2006	2	near Peter I Island	9140	0602182.RAW	2:32:32
21.02.2006	1	near Peter I Island	5704	0602211.RAW	1:35:09
24.02.2006	1	N Pine Island Bay	7815	0602241.RAW	2:10:37
24.02.2006	2	N Pine Island Bay	7519	0602242.RAW	2:05:26
26.02.2006	1	N Pine Island Bay	8583	0602261.RAW	2:23:16
26.02.2006	2	N Pine Island Bay	7302	0602262.RAW	2:01:54
27.02.2006	1	W Pine Island Bay	8821	0602271.RAW	2:27:07
28.02.2006	1	W Pine Island Bay	8813	0602281.RAW	2:27:01
28.02.2006	2	W Pine Island Bay	9555	0602282.RAW	2:39:18
28.02.2006	3	W Pine Island Bay	8967	0602283.RAW	2:29:36
02.03.2006	1	W Pine Island Bay	7761	0603021.RAW	2:09:16
02.03.2006	2	W Pine Island Bay	8174	0603022.RAW	2:16:28
02.03.2006	3	W Pine Island Bay	7431	0603023.RAW	2:10:22
03.03.2006	1	W Pine Island Bay	6525	0603031.RAW	1:48:52
04.03.2006	1	W Pine Island Bay	6902	0603041.RAW	1:55:08
04.03.2006	2	W Pine Island Bay	8310	0603042.RAW	2:18:58
04.03.2006	3	W Pine Island Bay	8052	0603043.RAW	2:14:42
09.03.2006	1	W Pine Island Bay	8739	0603091.RAW	2:25:55
09.03.2006	2	W Pine Island Bay	7988	0603092.RAW	2:14:17
09.03.2006	3	W Pine Island Bay	9362	0603093.RAW	2:36:45
10.03.2006	1	W Pine Island Bay	7921	0603101.RAW	2:13:01
10.03.2006	2	W Pine Island Bay	8324	0603102.RAW	2:20:01
10.03.2006	3	W Pine Island Bay	8574	0603103.RAW	2:23:14
11.03.2006	1	W Pine Island Bay	9797	0603111.RAW	2:43:16
12.03.2006	1	Pine Island Bay	8271	0603121.RAW	2:17:59
12.03.2006	2	Pine Island Bay	8939	0603122.RAW	2:28:58
14.03.2006	1	Pine Island Bay	8470	0603141.RAW	2:21:09
14.03.2006	2	Pine Island Bay	8271	0603142.RAW	2:17:50
14.03.2006	3	Pine Island Bay	7792	0603143.RAW	2:09:59
15.03.2006	1	N Pine Island Bay	43	0603151.RAW	0:00:42
15.03.2006	1	N Pine Island Bay	8017	0603152.RAW	2:13:47

Date	Flight no. this day	Area	No. FIDS	Filename	Duration
15.03.2006	2	N Pine Island Bay	7948	0603153.RAW	2:12:27
17.03.2006	1	N Pine Island Bay	7456	0603171.RAW	2:05:47
18.03.2006	1	N Pine Island Bay	7643	0603181.RAW	2:07:25
18.03.2006	2	N Pine Island Bay	7515	0603182.RAW	2:05:24
19.03.2006	1	N Pine Island Bay	8549	0603191.RAW	2:22:28
20.03.2006	1	N Pine Island Bay	8651	0603201.RAW	2:24:10
20.03.2006	2	N Pine Island Bay	504	0603202A.RAW	0:08:23
20.03.2006	3	N Pine Island Bay	7038	0603202B.RAW	1:57:24
20.03.2006	3	N Pine Island Bay	7584	0603203.RAW	2:06:23
21.03.2006	1	W Pine Island Bay	8378	0603211.RAW	2:19:37
21.03.2006	2	W Pine Island Bay	984	0603212.RAW	0:16:23
21.03.2006	2	W Pine Island Bay	6776	0603213.RAW	1:52:55
21.03.2006	2	W Pine Island Bay	779	0603214.RAW	0:12:58
23.03.2006	1	W Pine Island Bay	7919	0603231.RAW	2:12:02
23.03.2006	2	W Pine Island Bay	8376	0603232.RAW	2:19:26
25.03.2006	1	Marie Byrd Seamounts	7685	0603251.RAW	2:08:04
25.03.2006	2	Marie Byrd Seamounts	8148	0603252.RAW	2:15:48
26.03.2006	1	Marie Byrd Seamounts	7601	0603261.RAW	2:06:40
26.03.2006	2	Marie Byrd Seamounts	8550	0603262.RAW	2:22:29
26.03.2006	3	Marie Byrd Seamounts	8303	0603263.RAW	2:18:05
27.03.2006	1	Marie Byrd Seamounts	8016	0603271.RAW	2:13:35
27.03.2006	2	Marie Byrd Seamounts	7826	0603272.RAW	2:10:25
27.03.2006	3	Marie Byrd Seamounts	7858	0603273.RAW	2:10:57
28.03.2006	1	Marie Byrd Seamounts	7998	0603281.RAW	2:13:17
28.03.2006	2	Marie Byrd Seamounts	7424	0603282.RAW	2:03:26
28.03.2006	3	Marie Byrd Seamounts	8669	0603283.RAW	2:24:28
29.03.2006	1	Marie Byrd Seamounts	1088	0603291A.RAW	0:18:07
29.03.2006	2	Marie Byrd Seamounts	416	0603291B.RAW	0:06:55
29.03.2006	2	Marie Byrd Seamounts	5343	0603291C.RAW	1:29:02
29.03.2006	2	Marie Byrd Seamounts	8038	0609292.RAW	2:13:57
30.03.2006	1	near Peter I Island	7816	0603301.RAW	2:10:21
30.03.2006	2	near Peter I Island	5374	0603302.RAW	1:29:33
31.03.2006	1	near Peter I Island	6528	0603311.RAW	1:48:55

3. DEEP CRUSTAL REFRACTION AND REFLECTION SEISMICS

Crustal and sedimentary structures and geodynamic evolution of the West Antarctic Continental Margin and Pine Island

Karsten Gohl[1)], Polina Lemenkova[2)], Jan Grobys[1)], Nicole Parsiegla[1)], Gesa Netzeband[3)], Philipp Schlüter[1)], Norbert Lensch[1)], Harald Bohlmann[4)], André Fahl[1)], Nick Rackebrandt[1)], Katja Zimmermann[1)], Janna Just[1)], Kristin Daniel[1)]

[1)] Alfred-Wegener-Institut, Bremerhaven
[2)] Vernadsky Institute of Geochemistry, Moscow, Russia
[3)] Institute of Geophysics, University of Hamburg
[4)] Isitec GmbH, Bremerhaven

Objectives

Accurate models of the geodynamic-tectonic evolution contain some of the most important parameters for understanding and reconstruction of the palaeo-environment. Geophysical surveys of the sedimentary sequences and the underlying basement of the shelf and slope of the southern Amundsen Sea, Pine Island Bay and its adjacent continental rise allow reconstructions of the formation of the tectonic and older sedimentary processes. The following objectives are addressed as part of a cooperative project between the Vernadsky Institute in Moscow (Dr. Gleb Udintsev) and AWI:

- Identification of the boundaries between suspected crustal blocks and volcanic zones in Pine Island Bay. The glacier troughs and Pine Island Bay are thought to have developed along such tectonic boundaries.
- During and after separation from the Chatham Rise and Campbell Plateau (New Zealand), the continental margin of Marie Byrd Land developed as a passive margin, probably accompanied by intensive volcanism. The question is whether this volcanism occurred mainly during the rifting process or during post-rift phases, or if it developed in relation to the West Antarctic rift system.
- Recording of the sedimentary sequences across the shelf, slope and the continental rise, using deep reflection seismics, sub-bottom profiler (Parasound) and swath-bathymetry (Hydrosweep) in order to derive a sedimentation model.
- Mapping of the acoustic basement and its structure with deep seismic reflection methods to obtain the tectonic geometries and boundary conditions necessary to understand sediment transport and depositional processes.

Seismic data acquisition

Two deep crustal seismic reflection/refraction and a series of multichannel seismic reflection (MCS) profiles for the imaging of sediments and basement were acquired in the Amundsen Sea Embayment and Pine Island Bay (Fig. 3.1). Due to solid ice cover in the central part of Pine Island Bay, most profiles were chosen in locations others than those originally planned. However, a good seismic coverage of the inner

continental shelf of the western embayment and the eastern Pine Island Bay as well as across the continental slope and along the continental rise was achieved. Ocean-bottom hydrophone (OBH) systems were deployed along each of the two seismic refraction and wide-angle reflection profiles; one is located across the inner continental shelf of the western embayment and the other extends from the foot of the continental slope (ice cover prevented a more southern profile start) into the Marie Byrd Seamount area.

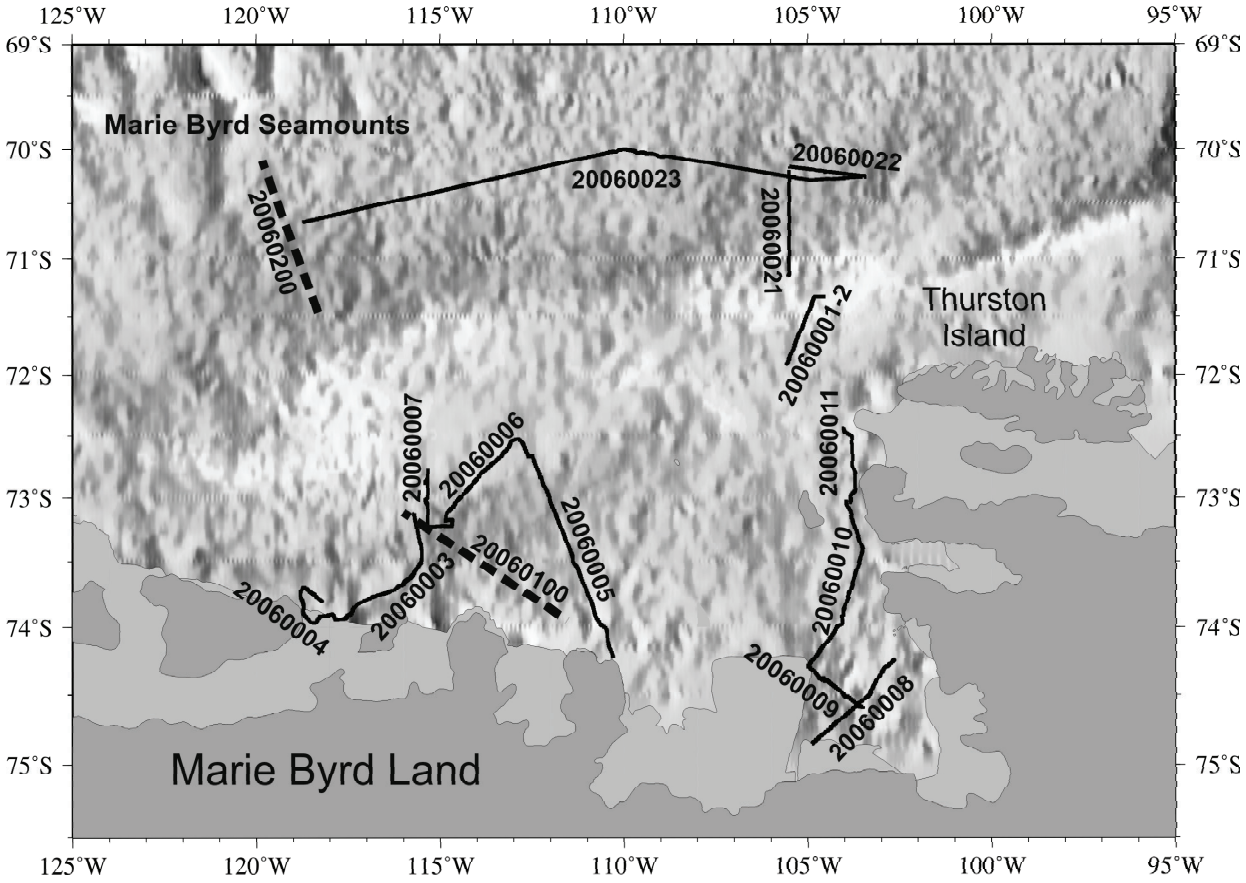

Fig. 3.1: Satellite-derived free-air gravity anomaly map (Laxon & McAdoo, 1997) of the Amundsen Sea Embayment with annotated multi-channel seismic profiles (solid lines) (see Chapter 4) and deep crustal reflection/refraction seismic profiles 20060100 and 20060200 (hashed lines) acquired during expedition ANT-XXIII/4.

Methods and equipment

OBH systems

All nine OBH systems are of similar GEOMAR-type construction. The five OBH systems of AWI (Fig. 3.2) use a different type of pressure cylinder and power supply than the four OBH systems borrowed from IFM-GEOMAR. Deployment and recovery coordinates and times are listed in tables 3.1 and 3.2.

The components of an OBH are mounted on a steel rack. Beneath a ring for deployment and retrieval purposes, the steel construction holds a floating body consisting of syntactic foam and a pressure chamber holding the power supply and seismic recording unit. The seismic hydrophone is an E-2PD sensor made by OAS Inc. The acoustic/time release unit, made by MORS/OCEANO (type RT-661 CE), is

mounted next to the recording pressure chamber. A ground weight of 60 kg as anchor is suspended 2.5 m below the release system. Communication with the release system is transmitted via a hydrophone mounted on top of the buoyancy body next to a Xenon flashlight, radio beacon, using channels C and D, of NOVATECH type, flag and a length of floating rope. The acoustic release communicates with an OCEANO Telecommand deck unit (model TT-300 B and TT-801).

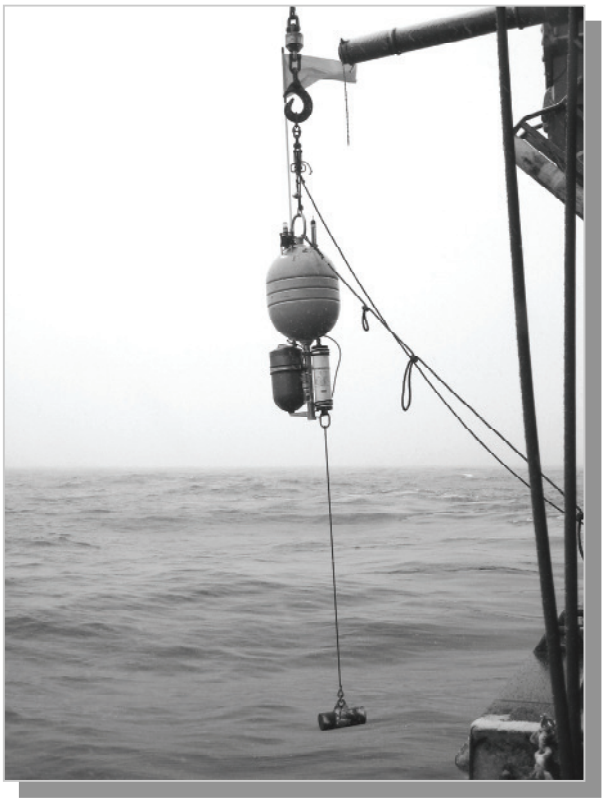

Fig. 3.2: AWI OBH-system of GEOMAR-type

The pressure chamber contains a 1-channel Marine Broadband Seismic Recorder (MBS) (AWI type OBH) or a 4-channel MBS (IFM-GEOMAR type OBH) manufactured by SEND GmbH, powered by a rechargeable lead-acid battery (12V, 33 Ah, AWI OBH) or a battery pack containing 32 monocell batteries (11,7 V, IFM-GEOMAR OBH). The pre-amplified (SN21 preamplifier) analogue input signal is digitized by the 16-bit analogue-digital converter (ADC) of the MBS. During this survey, the sampling frequency was set to 250 Hz for the hydrophone channel. From a possible scale of 1-31, the gain was set to 5. The recording parameters were set via the PC control programme SENDCOM which also controlled the time synchronisation of the internal clock with the external GPS clock. On this survey, we used a Meinberg GPS-166 clock for synchronisation, which also provided the airgun trigger pulse. Therefore, no adjustment for time-shift between clocks had to be made. The maximum skew time was -32 ms for a record of 3 days. The parameter setting and the skew time for each OBS/H are listed in tables 3.1 and 3.2.

For profile AWI-20060100, data were stored on 1 GB IBM-MicroDrives and 4 GB Hitachi MicroDrives connected to the MBS via a PCMCIA socket. Data stored on 4 GB MicroDrives were impossible to recover with onboard-means as the MBS recorders were only able to write properly on storage cards with capacities up to 2 GB because of their FAT16 file system. For profile AWI-20060200, the 4 GB MicroDrives were replaced by 128 MB and 256 MB compact flash cards. All data of the 4 GB MicroDrives were recovered after the cruise by SEND GmbH.

The recovery of the OBH systems of profile AWI 20060100 went properly. On profile AWI-20060200, the instrument at station 20060202 did not release from its anchor at first. Several tens of release signals were sent from the working deck with the OCEANO Telecommand deck unit TT-300B. This OBH was finally recovered some days later by activation of its programmed time-release. The subsequent stations were released by sending the release codes from the foreship using both telecommand units mentioned above.

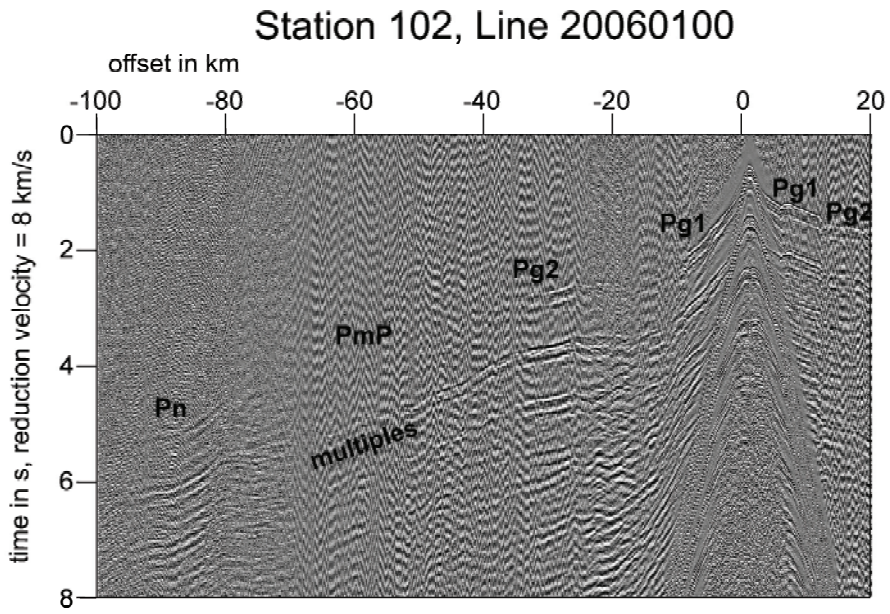

Fig. 3.3: Data example from profile AWI-20060100. P_{g1} and P_{g2} denote refracted phases from the upper and middle crust, P_mP indicates a wide-angle reflection from the crust-mantle boundray (Moho), and P_n is a refracted phase returning from the uppermost mantle.

Seismic source

As source for the deep crustal reflection and refraction seismic profiles AWI-20060100 and AWI-20060200 we used a cluster of 8 G.Guns™ (8 x 520 in^3 = 4160 in^3 = 68.17 liters in total) mounted on a metal frame and deployed sternways (Fig. 4.1). The G.Guns were towed in a depth of 10 m approximately 10 m behind the vessel. The airguns were fired once per minute at a pressure of 190 bar, leading to a nominal shot spacing of 150 m. We tried to add a single Bolt™ 800CT airgun of 2000 in^3 (32.77 liters) volume, deployed on starboard side, to the G.Gun sources for increased volume and lower frequency. The Bolt airgun was towed in a depth of 15 m approximately and 10 m behind the vessel. However, the Bolt airgun did not operate properly. Probably due to the frigid water temperature, it fired only up to 85 bar with numerous failures. Therefore, the use of this airgun had to be given up for most lengths of the profiles.

The airgun shots were simultaneously recorded by the multichannel seismic recording system and its streamer (see Chapter 4 and Table 4.1).

Processing of the OBH data
The OBH data were subject to onboard processing that consisted of the following steps:

- The MBS recorders were connected to the GPS clock and the PC running the SEND programme sendcom. Recording was ended and time skew was taken in order to obtain the time drift of the internal clock of the recorder compared to GPS time. This closed the storage card.
- The MBS data and log files were copied from the storage cards to a Windows PC and to a Linux PC. The data files were pre-processed with the Linux version of the send2x programme package (version 2.5). The routine mbsread extracts the data from the raw files. The routine seg-ywrite demultiplexes the data, adds shot and station coordinates to the trace headers and converts the data to the SEG-Y format according to a given time window provided by a shot-point coordinate file. A SEG-Y file with trace lengths of 60 s was written, beginning at the exact shot time.
- Using CWP/SU (SeismicUnix) software, the SEG-Y formatted data were converted to SU format. Shot-receiver offsets were calculated and written together with water depths at the receiver and shot point as well as source depth information into the file header. After band-pass filtering (4 - 40 Hz), travel-time reduction and optimising display parameters, the OBH records were displayed and printed for a first data analyses.
- For archive purposes the data were transferred to a UNIX SUN computer for which we had a licence to run the FOCUS processing software.
- In order to allow a first modelling of the OBH data, the data in the SU format were re-converted to SEG-Y format and further on to the ZP-format. With the programme ZP the refraction and reflection phases and the first multiples were selected and digitized.

Data quality and results
Profile AWI-20060100
Of the 9 OBH stations deployed and recovered, 4 stations could be read out on board. These stations recorded usable data from the airgun shot profile across the inner continental shelf of the western Amundsen Sea Embayment. These seismograms show good-quality refracted P-wave phases from the crust (P_{g1}, P_{g2}). This first ever recorded deep crustal seismic dataset of the Amundsen Sea Embayment reveals apparent P-wave velocities increasing from 2.5 km/s to 2.8 km/s for sediments and 4.3 – 5.0 km/s for the top of the basement to ca. 6.3 km/s for the middle to observed on two recordings. Two recordings show a low-amplitude refracted phase from the upper mantle (Pn), which is difficult to identify. P-wave arrivals can be observed at source-receiver offsets of up to 130 km.

A preliminary P-wave velocity-depth model (Fig. 3.4) was derived on board using the records of four stations. This model incorporates one sedimentary layer, two crustal layers and the uppermost mantle. Sediment velocities have been modelled with 2.0-2.6 km/s. Several basement highs separate the sedimentary layer into five subbasins

reaching a thickness of about 1.2 to 2 km. Both crustal layers show only little lateral variations in the P-wave velocity as well as in the crustal thickness, with the exception of the southern end of the profile, where the upper crustal layer thins and the lower crustal layer thickens. However, this model interface is constrained by very few intracrustal reflections and mainly introduced to allow for changes in velocity gradient. The Moho steps down from 22 km to 24 km below the seafloor (b.s.f). P-wave velocities of the uppermost mantle are about 7.8 km/s.

A resolution kernel was calculated for this profile (Fig. 3.5). The entire model has a X–value of 1.225 and a rms-misfit of 0.104 ms. The velocities of the model are well resolved for most parts of the crustal layers in the areas covered by rays, while the uppermost mantle and the sedimentary layers still have moderate resolution values. The interface nodes defining the Moho along the profile have values representing a good resolution.

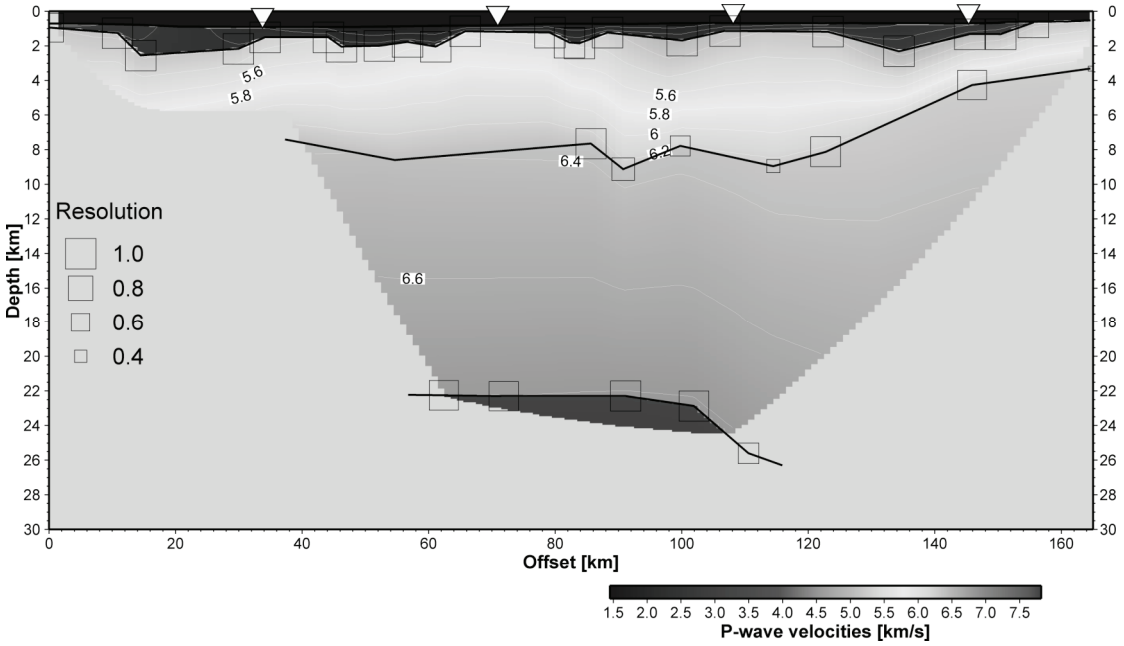

Fig. 3.4: Preliminary velocity-depth model along profile AWI-20060100 based on four OBH recordings

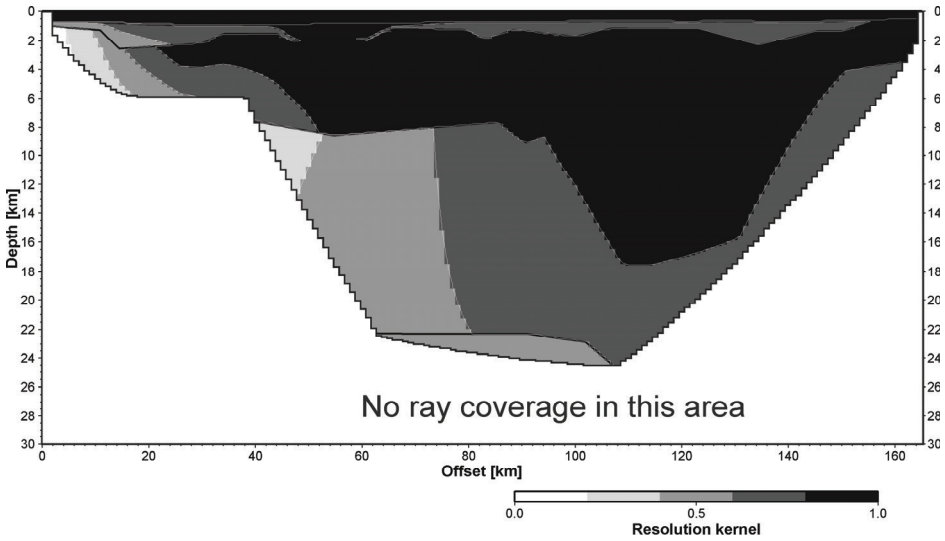

Fig. 3.5: Resolution of preliminary velocity-depth model along profile AWI-20060100. Dark areas indicate a high resolution, bright areas are less resolved.

Profile AWI-20060200

Of the seven OBH systems recovered, five recorded usable hydrophone data from the airgun shots between the continental shelf and the Marie Byrd Seamounts. The recordings of this profile exhibit a significantly poorer data quality than those of profile AWI-20060100. Apparent velocities increase from 2.0 to 2.3 km/s for sediments and ca. 5.0 km/s for the top of the basement to ca. 6.4 km/s for the middle to lower crust (P_{g1}, P_{g2}). Reflection phases from the suspected crust-mantle boundary (P_mP) could be observed on two recordings. Another set of recordings show a low-amplitude refracted phase from the upper mantle (P_n), which is difficult to identify. P-wave arrivals can be observed at source-receiver offsets of up to 80 km.

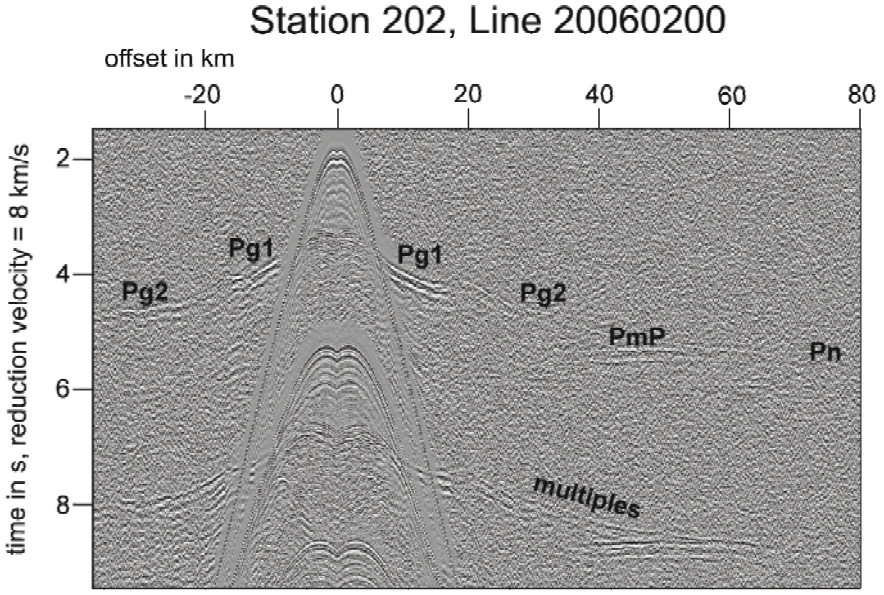

Fig. 3.6: Data example from profile AWI-20060200. P_{g1} and P_{g2} denote refracted phases from the upper and middle crust, P_mP indicates a wide-angle reflection from the Moho, and P_n is a refracted phase through the uppermost mantle.

Onboard, a preliminary P-wave velocity-depth model was calculated with all stations (Fig. 3.7). This model incorporates one sedimentary layer, two crustal layers and the uppermost mantle. Sediment velocities have been modelled with 1.8-2.6 km/s. Four major highs in the rugged basement separate the sedimentary layer into five subbasins, which reach thicknesses of up to 2.5 km. The upper crust is laterally homogeneous with velocities ranging from 5.3 to 6.3 km/s. The thickness of this layer increases from 4 km in the northwest to 5 km in the southeast. The thickness of the lower crustal layer increases from 7 km in the northwest to 10 km in the southeast. This layer is laterally homogeneous, too. The velocities at the top of this layer are between 6.3 km/s, 6.4 km/s and 6.8 km/s at the base of the crust. The Moho steps down from 12 km b.s.f in the northwest to 18 km b.s.f in the southeast of this profile. The uppermost mantle has velocities of ca. 7.9 km/s.

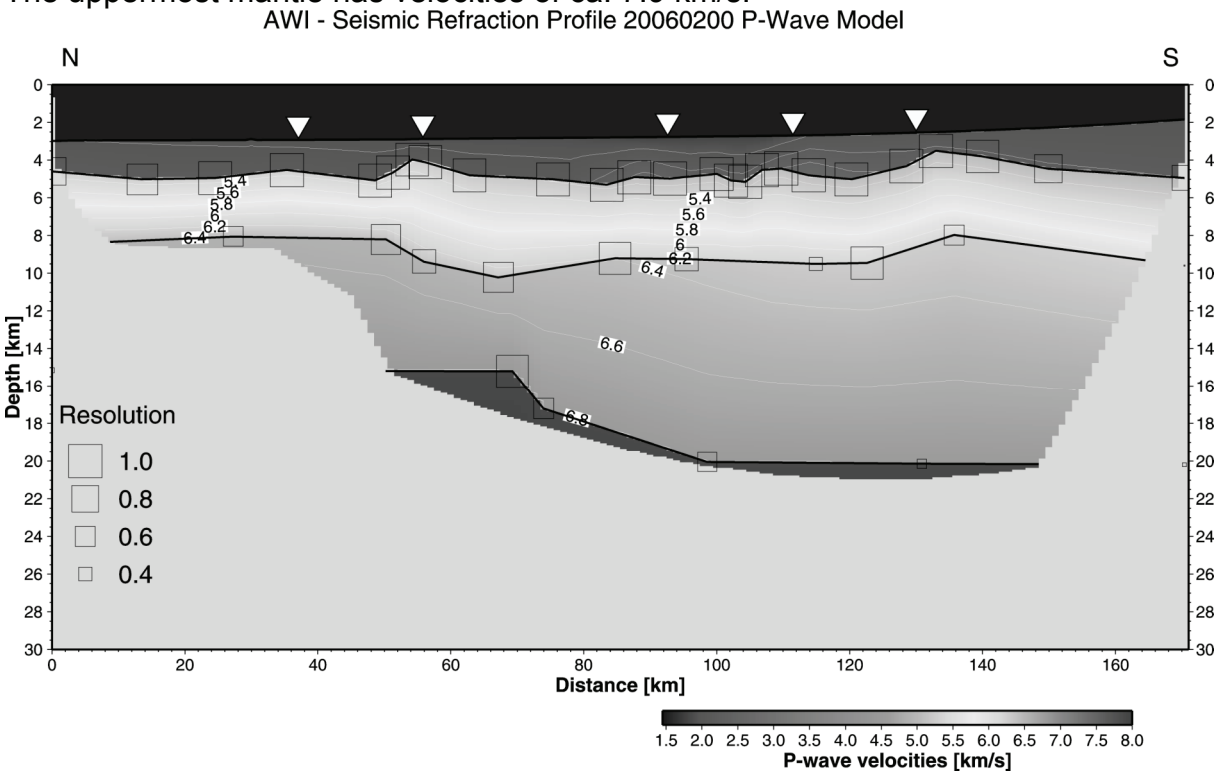

Fig. 3.7: Preliminary velocity-depth model along profile AWI-20060200

A resolution kernel was calculated for this profile (Fig. 3.8). The model has a χ–value of 1.127 and a rms-misfit of 0.112 ms. The velocities of the model are well resolved for most parts of the crustal layers in the areas covered by rays, while the uppermost mantle and the sedimentary layers still have moderate resolution values. The interface nodes defining the Moho along profile have values representing a good to moderate resolution.

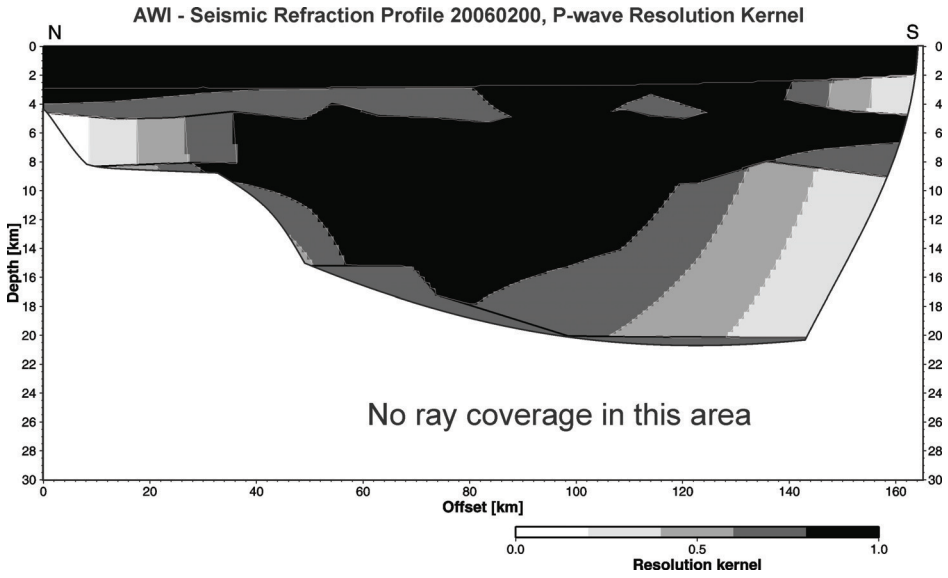

Fig. 3.8: Resolution of the preliminary velocity-depth model along profile AWI-20060200. Dark areas indicate a high resolution, bright areas are less resolved.

Tab. 3.1: Deployment coordinates and instrument description of OBH profile AWI-20060100

		Deployment					Recovery			
Station no.	**OBH ownership**	**Lat south**	**Lon west**	**Water depth (m)**	**Deployment date**	**UTC**	**Lat south**	**Lon west**	**Recovery date**	**UTC**
101	AWI	73° 55,100’	111°40,672’	557	02.03.2006	01:53	73°55,370’	111°40,240’	03.03.2006	13:48
102	GEOMAR	73°50,127’	112°10,917’	708	02.03.2006	03:11	73°50,327’	112°11,899’	03.03.2006	15:40
103	AWI	73°44,546’	112°40,827’	712	02.03.2006	04:29	73°44,599’	112°40,541’	03.03.2006	17:16
104	GEOMAR	73°39,100’	113°10,800’	684	02.03.2006	05:48	73°38,802’	113°10,685’	03.03.2006	21:30
105	AWI	73°33,823’	113°40,758’	738	02.03.2006	06:58	73°33,703’	113°41,187’	03.03.2006	23:16
106	GEOMAR	73°28,462’	114°10,328’	797	02.03.2006	08:11	73°28,347’	114°10,555’	04.03.2006	02:21
107	AWI	73°23,089’	114°40,000’	888	02.03.2006	09:26	73°23,165’	114°40,480’	04.03.2006	06:00
108	GEOMAR	73°17,767’	115°09,286’	918	02.03.2006	10:40	73°17,757’	115°09,457’	04.03.2006	08:49
109	AWI	73°12,345’	115°38,211’	804	02.03.2006	12:01	73°12,416’	115°38,045’	04.03.2006	12:10

Station no.	**Recorder type**	**Recorder S/N**	**Hydrophone type**	**Sample rate [Hz]**	**Recorded data [kB]**	**Skew time [ms]**	**Remarks**
101	MBS	010709	E-2PD	250	52736	+3	
102	MBS	000614	E-2PD	250	78048	-13	4 GB MicroDrive – FAT problem
103	MBS	020501	E-2PD	250	94752	+12	
104	MBS	001006	E-2PD	250	115104	-8	4 GB MicroDrive – FAT problem
105	MBS	010706	E-2PD	250	102560	-38	
106	MBS	020504	E-2PD	250	100608	+12	No release after first attempt, 4 GB MicroDrive – FAT problem
107	MBS	001008	E-2PD	250	89280	-16	No release after first attempt
108	MBS	010701	E-2PD	250	93184	-37	4 GB Microdrive – FAT problem
109	MBS	000609	E-2PD	250	57792	-11	

Tab. 3.2: Deployment coordinates and instrument description of OBH profile AWI-20060200

		Deployment					Recovery			
Station no.	**OBH ownership**	**Lat south**	**Lon west**	**Water depth (m)**	**Deployment date**	**UTC**	**Lat south**	**Lon west**	**Recovery date**	**UTC**
201	AWI	70°15,072’	119°41,276’	2949	22.03.2006	14:21	70°15,173’	119°41,331’	29.03.2006	00:55
202	GEOMAR	70°24,415’	119°30,778’	2923	22.03.2006	15:39	70°24,461’	119°30,675	25.03.2006	04:37
203	GEOMAR	70°33,796’	119°19,733’	2863	22.03.2006	17:01	70°33,708	119°20,280’	24.03.2006	07:37
204	AWI	70°43,007’	119°10,098’	2816	22.03.2006	18:25	70°43,020’	119°08,811’	24.03.2006	12:42
205	AWI	70°52,402’	118°58,755’	2774	22.03.2006	19:45	70°52,492’	118°58,219’	24.03.2006	14:53
206	GEOMAR	71°01,800’	118°48,274’	2697	22.03.2006	21:06	71°01,945’	118°48,992’	24.03.2006	17:01
207	GEOMAR	71°11,175’	118°37,260’	2540	22.03.2006	22:26	71°11,315’	118°37,606’	24.03.2006	19:04

Station no.	**Recorder type**	**Recorder S/N**	**Hydrophone type**	**Sample rate [Hz]**	**Recorded data [kB]**	**Skew time [ms]**	**Remarks**
201	MBS	020501	E-2PD	250	150656	+15	No release after several attempts and further attempts one day later; recovered after time release, hydrophone failure
202	MBS	000614	E-2PD	250	113952	-22	No release after several attempts; successful release one day later
203	MBS	001006	E-2PD	250	77984	-6	
204	MBS	020501	E-2PD	250	50496	+9	Hydrophone failure
205	MBS	000609	E-2PD	250	77824	-9	
206	MBS	020504	E-2PD	250	82112	+12	
207	MBS	010701	E-2PD	250	82240	-30	

4. HIGH-RESOLUTION REFLECTION SEISMICS

Quaternary West Antarctic deglaciation in the Amundsen Sea Embayment

Karsten Gohl[1)], Claus-Dieter Hillenbrand[2)], Philipp Schlüter[1)], Norbert Lensch[1)], Harald Bohlmann[3)], Jan Grobys[1)], Nicole Parsiegla[1)], André Fahl[1)], Janna Just[1)], Gesa Netzeband[4)], Nick Rackebrand[1)], Katja Zimmermann[1)], Kristin Daniel[1)], Joanne Johnson[2)]

[1)] Alfred-Wegener-Institut, Bremerhaven
[2)] British Antarctic Survey, Cambridge, UK
[3)] Isitec GmbH, Bremerhaven
[4)] Institute of Geophysics, University of Hamburg

Objectives

The Amundsen Sea Embayment lies offshore from Pine Island and Thwaites glaciers, which exhibit the most rapid elevation change/ice thinning and grounding-line retreat in Antarctica. It has been suggested that this area might be most likely the site for the initiation of a collapse of the two million km^2 West Antarctic Ice-Sheet (WAIS), which would result in a global sea-level rise of 5 to 6 m. At present it is not clear to what extent the current retreat of WAIS grounding lines is part of the ongoing recession that started more than 14,000 years ago, and to what extent it reflects more recent climatic changes. The marine record of Quaternary deglaciations in the Amundsen Sea Embayment, coupled with ice sheet models, can provide important clues to understanding the stability and climate sensitivity of the WAIS. The main objectives of this cooperative project between the British Antarctic Survey (group of Dr. Rob Larter) and AWI include:

- the glacial maximum extent of the ice sheet,
- the extent of fast ice flow in the former ice sheet, and controls on the location and onset position of fast ice flow,
- the retreat history of the ice sheet,
- whether or not the last ice sheet and its deglaciation are representative of events during earlier Quaternary glacial cycles.

This project is directly linked to Chapter 5 “Swath-bathymetric mapping” and Chapter 6 “Marine-sedimentary geology”.

Methods and equipment

Seismic source, triggering and timing

Two airgun source configurations were used (Fig. 4.1), depending on target depths/distances and required resolution of the seismic data.

The high resolution seismic reflection lines were shot using high-frequency 3 GI-Guns™ to better resolve the expected sedimentary layers. A single GI-Gun is made of two independent airguns within the same body. The first airgun (“Generator”)

produces the primary pulse, while the second airgun ("Injector") is used to control the oscillation of the bubble produced by the "Generator". We used the "Generator" with a volume of 0.74 liters (45 in^3) and fired the "Injector" with a volume of 1.72 liters (105 in^3) with a delay of 33 ms, leading to an almost bubble-free signal. The GI-Guns were towed 10 m behind the vessel in 3 m depth and were fired every 12 seconds at 190 bar, leading to an average shot interval of 25 m.

In order to accommodate the larger water depths along the seismic profiles off the continental shelf, we reduced the 8-G.Gun cluster (see Chapter 2) to a cluster of 4 G.Guns (4 x 520 in^3 = 2080 in^3 = 34.08 liters in total). The G.Guns were towed in a depth of 10 m approximately 10 m behind the vessel. The G.Guns were fired every 15 seconds at 190 bar.

Seismic data acquisition requires a very precise timing system, because seismic sources and recording systems must be synchronised. A combined electric trigger-clock system was in operation in order to provide the firing signal for the electric airgun valves, to provide the time-control of the seismic data recording and to synchronize the internal clocks of the OBH system.

Mitigation methods
Three observers constantly visually monitored the survey, depending on the weather conditions, around the vessel for possible whale appearance before and during seismic profiling. In case of whale sighting within a radius 1 km or less, seismic shooting was stopped instantly. Airguns were fired with gradually increasing working pressure at the beginning of a profile and after shot interruptions (soft start).

Multi-channel reflection recording system
As part of the multi-channel reflection data acquisition system, a 600 m long (active sections), 96 channel (hydrophones groups) analogue streamer (Type Prakla) was used. The data were recorded in SEG-D format on 3480 cartridge magnetic tapes via a Geometrics EG&G 2420 recording system.

Processing of multi-channel reflection seismic data
Seismic data were recorded at 1 ms, 2 ms or 4 ms sampling intervals. For "rebuilding" them into traces, the samples have to be demultiplexed, which was done right after finishing every profile. Afterwards, the demultiplexed data were linked to navigation data. Normally, the data would have been CDP-sorted and stacked later on. Due to a software problem, which occurred during demultiplexing, the profiles could not be processed any further. The profiles could be only read in, in pieces of approximately 20 km length. Afterwards these profile-pieces had to be refixed again. Only single channel plots of every seismic section could be processed on board. The demultiplexing was carried out on a SGI Origin 200 computer using FOCUS™ processing software. We encountered a leakage problem with most of the streamer channels which caused a coherent noise pattern across the shot gathers of all profiles. After several tests, the noise was associated with leakages in the lead-in cable of the streamer, a problem we could not fix on board. Complete processing and an attempt to remove as much of the coherent streamer noise will be performed at the AWI after the expedition.

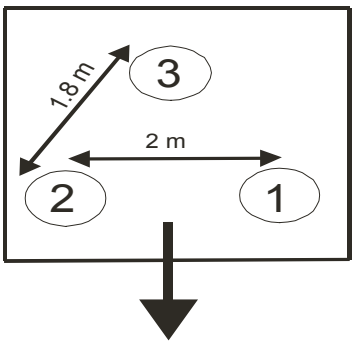

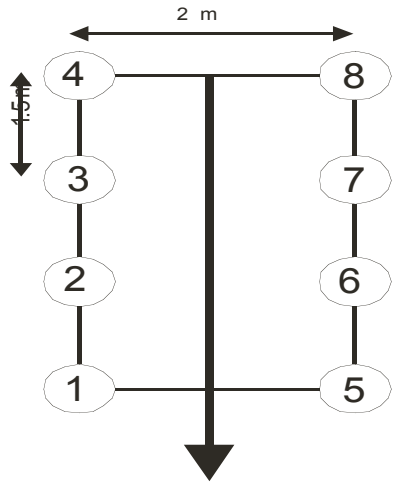

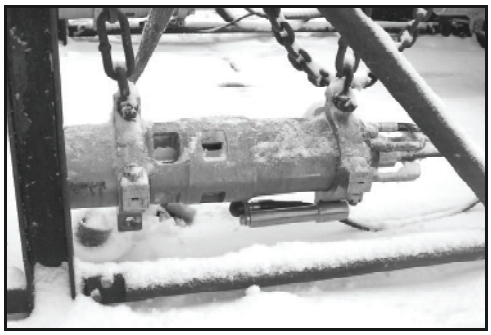

GI-Gun

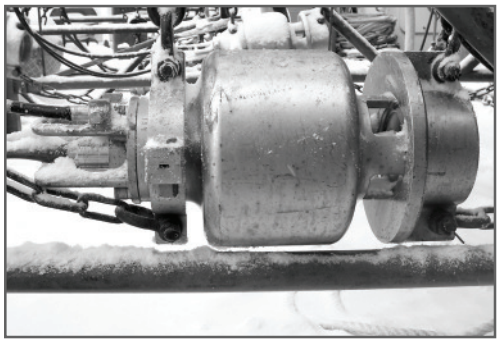

G-Gun

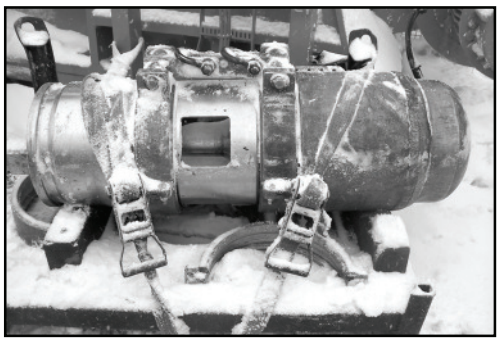

Bolt Airgun

Fig. 4.1: The upper left figure shows the GI-Gun array and the upper right figure shows the G.Guns, both are mounted on a metal frame. Arrows indicate the tow direction.

Tab. 4.1: Seismic reflection and refraction profiles

Profile	Date	Time UTC	Lat. Start	Long. Start	Lat. End	Long. End	Gun-Array	Sampling Rate (ms)	Record Length (s)	Profile length (km)
20060001	25/02/2006	14:42:36 - 19:15:00	-71.91854	-105.59457	-71.56024	-105.10662	3 x GI-Gun® = 7500 ccm	1	8	43.5
20060002	25/02/2006	19:19:24 - 23:19:24	-71.55498	-105.09920	-71.33333	-104.50683	3 x GI-Gun® = 7500 ccm	2	8	37.5
20060003	04/03/2006 - 05/03/2006	15:55:12 - 09:26:48	-73.11919	-115.70830	-73.95969	-118.50853	3 x GI-Gun® = 7500 ccm	1	8	163
20060004	05/03/2006	09:38:00 - 15:17:50	-73.95153	-118.56177	-73.81593	-118.20596	3 x GI-Gun® = 7500 ccm	1	8	55
20060005	08/03/2006 - 09/03/2006	19:09:36 - 17:57:12	-74.22959	-110.30066	-72.53731	-112.83811	3 x GI-Gun® = 7500 ccm	1	8	213
20060006	09/03/2006 - 10/03/2006	17:57:36 - 08:35:00	-72.53684	-112.84000	-73.23099	-115.28979	3 x GI-Gun® = 7500 ccm	1	8	134.5
20060007	10/03/2006	08:57:36 - 14:59:00	-73.21428	-115.33280	-72.76527	- 115.33627	3 x GI-Gun® = 7500 ccm	1	8	56
20060008	13/03/2006	03:07:00 - 13:28:48	-74.85135	-104.88598	-74.24125	-102.62963	3 x GI-Gun® = 7500 ccm	1	8	111.5
20060009	14/03/2006	11:24:12 - 17:53:48	-74.58030	-103.49286	-74.29517	-104.98350	3 x GI-Gun® = 7500 ccm	1	8	63.5
20060010	14/03/2006 - 15/03/2006	17:54:00 - 10:58:00	-74.29502	-104.98423	-73.01655	-103.95081	3 x GI-Gun® = 7500 ccm	1	8	157.5

Profile	Date	Time UTC	Lat. Start	Long. Start	Lat. End	Long. End	Gun-Array	Sampling Rate (ms)	Record Length (s)	Profile length (km)
20060011	16/03/2006 - 17/03/2006	16:43:00 - 00:43:36	-73.03743	-103.87329	-72.43232	-104.00860	3 x GI-Gun® = 7500 ccm	1	8	74.5
20060021	19/03/2006	01:15:00 - 12:56:15	-71.15269	-105.54497	-70.19563	-105.49980	3 x GI-Gun® = 7500 ccm	1	8	111
20060022	19/03/2006	13:19:00 - 20:58:00	-70.16734	-105.48742	-70.26115	-103.47911	4 x G-Gun® = 34000 ccm	1	12	81.5
20060023	19/03/2006 - 22/03/2006	21:06:15 - 03:21:00	-70.26078	-103.51841	-70.66488	-118.72814	4 x G-Gun® = 34000 ccm	1	12	589.5
20060100	02/03/2006 - 03/03/2006	14:24:00 - 12:14:00	-73.11529	-115.99294	-73.92573	-111.64914	8 x G-Gun® 1 x Bolt-Gun® = 100000 ccm	4	12	164
20060200	23/03/2006	02:59:00 - 21:29:00	-71.52305	-118.20821	-70.09611	-119.86344	8 x G-Gun® 1 x Bolt-Gun® = 100000 ccm	4	12	171.5
									Total km:	2227

Results

More than 2200 km of multichannel seismic reflection data were recorded in the Amundsen Sea Embayment and Pine Island Bay (Fig. 3.1), including the MCS recordings along the two deep crustal refraction/wide-angle reflection profiles AWI-20060100 and 20060200. Due to severe ice coverage in large parts of the embayment, we had to focus the survey in the western embayment off the Getz and Dotson Ice-Shelves, in the eastern and inner Pine Island Bay and in the deep sea off the continental shelf.

The preliminary results are summarized for the main survey areas:

Profiles AWI-20060001-02 (outer Pine Island Bay shelf): This is actually a single profile (the switch over to a different sampling rate restarted a new profile) which is in southward prolongation to the MCS profile AWI-94042 from 1994. It clearly shows the prograding sequences of the outer continental shelf.

Profiles AWI-20060003-07 (western Amundsen Sea Embayment): This set of profiles follows, crosses and parallels the glacial troughs on the inner continental shelf off the Getz and Dotson Ice-Shelves. They mark a clear boundary between northwest-dipping older strata to the north and a southern inner shelf (Fig. 4.2) that is mostly void of resolvable sediments, with the exception of some deeply incised narrow troughs which contain 100-200 m of sediments.

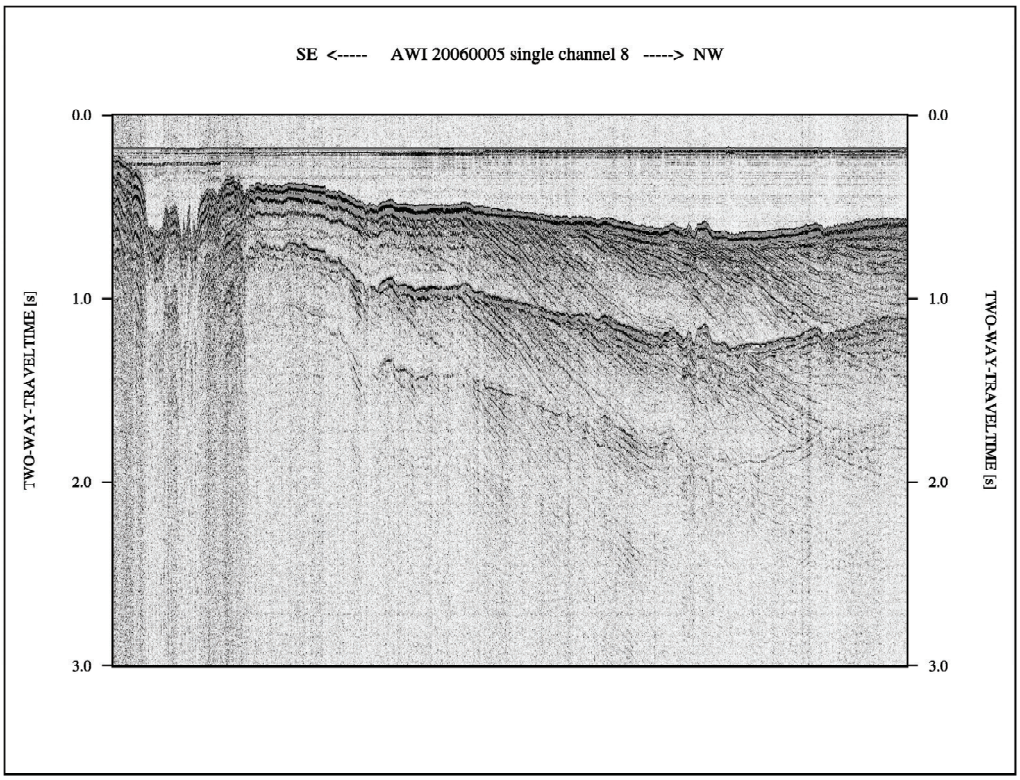

Fig. 4.2: Example of a seismic reflection profile. The single-channel display of MCS profile AWI-20060005 shows a clear boundary between northwest-dipping strata and outcropping basement to the south.

Profiles AWI-20060008-11 (eastern Pine Island Bay): Ice coverage in the central Pine Island Bay limited our survey along eastern the polynyas and off the Pine Island Ice-Shelf. The profiles also mark a clear boundary between the begin of older strata to the north and a southern inner shelf which is mostly void of resolvable sediments with the exception of some deeply incised narrow troughs off the Pine Island Ice-Shelf, containing 100-200 m of sediments.

Profiles AWI-20060021-23 (continental slope and rise): Profile 20060021 shows the shelf slope sequences from the progradation of the outermost shelf to the slope deposits and slumps of the slope and foot of the continental shelf. Profiles 20060022-23 follow the continental rise parallel to the shelf. They show numerous sediment drifts and channel-levee systems.

5. SWATH-BATHYMETRIC MAPPING

Steffen Gauger[1)], Gerhard Kuhn[2)], Karsten Gohl[2)], Thomas Feigl[2)], Polina Lemenkova[3)], Claus-Dieter Hillenbrand[4)]

[1)] Fielax GmbH, Bremerhaven
[2)] Alfred-Wegener-Institut, Bremerhaven
[3)] Vernadsky Institute of Geochemistry, Moscow, Russia
[4)] British Antarctic Survey, Cambridge, UK

Objectives
The main objective of the bathymetric working group was to perform high resolution multibeam surveys during the entire cruise for geomorphological interpretation, to locate geological sampling sites, to interpret magnetic and gravimetric measurements and to expand the world database for oceanic mapping.

Precise depth measurements are the basis for creating high resolution models of the sea surface. The morphology of the seabed, interpreted from bathymetric models, gives information about the geological processes on the earth surface.

Methods and equipment
The main characteristic of the deep water sounding system Atlas Hydrosweep DS-2 is a coverage angle of up to 120°, which results in a depth profile with a length of 3.4 times the water depth perpendicular to the ship's long axis. Most of the time, a coverage angle of 100° was applied. The acoustic signal, generated by the hull mounted transducer, has a frequency of 15.5 kHz and allows measurement up to full ocean depth. Based on the acoustic pulse 240 depth measurements with individual opening angles of about 2.3° (in deep water operation) and an accuracy of approximately 1 % of water depth were derived. In addition, the echo amplitudes were converted to multibeam sidescan (4094 pixels per swath) and angular backscatter data (59 values per swath).

For the slant range corrections of the outer sonar beams, CTD (conductivity, temperature, density) profiles, collected either on this expedition or on former expeditions of other vessels, were mostly used. Where there was no information about the water properties, the automatic crossfan calibration, which generates a swath in the direction of the ship's long axis and adjusts the vertical position of the outer beams by overlaying with the previous central beams, was used to calculate the mean sound velocity in the water column.

To assign the depth measurement to a geographic position, the GPS navigation and the ship's motion data, received from the Trimble MS750 GPS system and the MINS ringlaser gyro respectively, were applied.

To prevent the disturbance of marine mammals, the multibeam sonar system was switched off during periods, when there was no scientific necessity for surveying the

sea floor and if marine mammals were close to the ship (nearer than 100 m). After updating the multibeam system with the HDBE (High Definition Bearing Estimation) soft beam modus, the source level could be adjusted, so that the acoustic energy transmitted into the water was not higher then needed to obtain high quality measurements. The multibeam sonar was exclusively operated in the source level mode "Maximum Level", where the maximum source level was reduced manually to a minimum, depending on the water depth and hydroacoustic conditions.

Besides operating and observing the multibeam sonar system, data processing was the main part of the work on board. Erroneous depth measurements, caused by hydroacoustic disturbances i.e. because of sea ice, waves or interferences with other sounding systems, needed to be cleaned. The depth editing, as well as the cleaning of navigation spikes, was done using the Caris Hips software. Furthermore, data processing included integration of the ship's navigation into the ESRI database BatGIS, containing most multibeam survey lines of the AWI. The preparation of meta data describing each data set allows data exchange and archiving. The data preparation for terrain modelling includes the projection of geographic coordinates into metric coordinates and the recomputing of depths. In order to make depth data compatible to previous and subsequent measurements, a sound velocity of 1500 ms^{-1} has been applied.

For the interpretation of the sea bottom topography, digital elevation models (DTM's) were calculated out of the edited data and presented in preliminary bathymetric maps, using the Generic Mapping Tool (GMT) and ESRI ArcGIS software. Based on the DTM's (grid spacing up to 50 m in medium water depths), contour line maps with color-coded depth ranges (scales up to 1:100000) and additional information like coastlines and surface elevation, sea ice coverage or sampling stations were produced. Using the ArcGIS module ArcScene, virtual flights above the sea floor were prepared in regions of specific interest. These three-dimensional visualisations facilitate the interpretation of morphology and support interdisciplinary work.

Results

Peter I Island

A systematic bathymetric survey of ~32 hours was added to the existing data at Peter I. Island (69° S / 90° 30' W). The data set (with an area of approx. 4500 km^2 and a depth range of 100 m to 4200 m), representing the sea floor topography of the volcanic island, is a compilation of data sets collected on four scientific cruises by the vessels RV *Akademik B. P*etrov in 1998 and RV *Polarstern* in 1994, 2001 and 2006.

Unnamed Ridge north of Peter I Island

With three survey lines approx. 240 km north of Peter I Island (66°50' S / 91° W) a small ridge was mapped. This was discovered on a pre-existing seismic profile and its morphology is still unknown . The north-south orientated ridge is approx. 31 km long and 2 - 5 km wide. It has a height of ~950 m above the surrounding seafloor with a depth of approx. 4600 m. The ridge with slope angles of up to 40° is characterised by three tops, the southernmost being the highest.

De Gerlache Seamounts
At the western De Gerlache Seamount (65° S / 93° W) two multibeam profiles were added to the existing bathymetric data set, which was collected during the RV *Polarstern* cruise ANT-XII/4 (1995). The two new profiles crossing the top of the seamount in north-western and north-eastern directions are approx. 60 km long and show depths from 4700 m at the surrounding seafloor to 300 m on the flat top of the seamount.

Amundsen Sea Embayment
In the Amundsen Sea Embayment two major systematic bathymetric surveys were carried out, in addition to the bathymetric measurements during seismic surveys, station work or transits. Some smaller systematic surveys were carried out in the Amundsen Sea Embayment, i.e. east of Bear Peninsula (74°30' S / 110° W), where parts of the trough offshore from the Crosson Ice Shelf with depths of more than 1300 m were mapped. New bathymetric data was added to the existing data set of Pine Island Bay, mostly based on the surveys of RV *Nathaniel B. Palmer* in 1999 and 2000.

Glacial bedforms west of Abbot Ice Shelf
At the entrance to the embayment, west of the Abbot Ice Shelf (71°50' S / 104°20' W, Fig. 5.1), an 800 km^2 wide survey shows megascale glacial lineations, traces of grounded ice movements on the seabed. In depths between 550 m and 750 m four prominent individual lineations with directions varying between 2°, 10°, 25° and 35°, a maximum length of 24 km, depths of approx. 25 m and a width of approx. 600 m leaving their mark on the floor, but there are many more less dominant lineations similarly aligned. Based on the morphology of the intersection points of the lineations a relative age of the lineations can be obtained: with turning of the direction of the lineations to north-east, the age becomes younger. While in the deeper areas no scours of icebergs are visible, they are more abundant at shallower depths (<650 m).

Trough off central Getz Ice Shelf
The trough offshore from the central Getz Ice Shelf (74° S / 118° W, Fig. 5.2), a nearly 3000 km^2 wide area, was mapped during approx. 36 hours of systematic multibeam survey, in addition to one survey line of the RV *Nathaniel B. Palmer* in 2000. The investigated area is connected to the survey area of the RV *James Clark Ross* of the British Antarctic Survey in 2006. Based on the morphology the trough can be roughly divided into 2 parts, where the seabed was formed by grounded ice scratching the seafloor and melt water. The first part, directly in front of the current ice shelf, is characterised by a very rough morphology with depths varying between 700 m and 1600 m. The second part in the north-east of the trough is characterised by megascale glacial lineations, oriented in north-eastern direction, and depths of approx. 1100 m to 800 m.

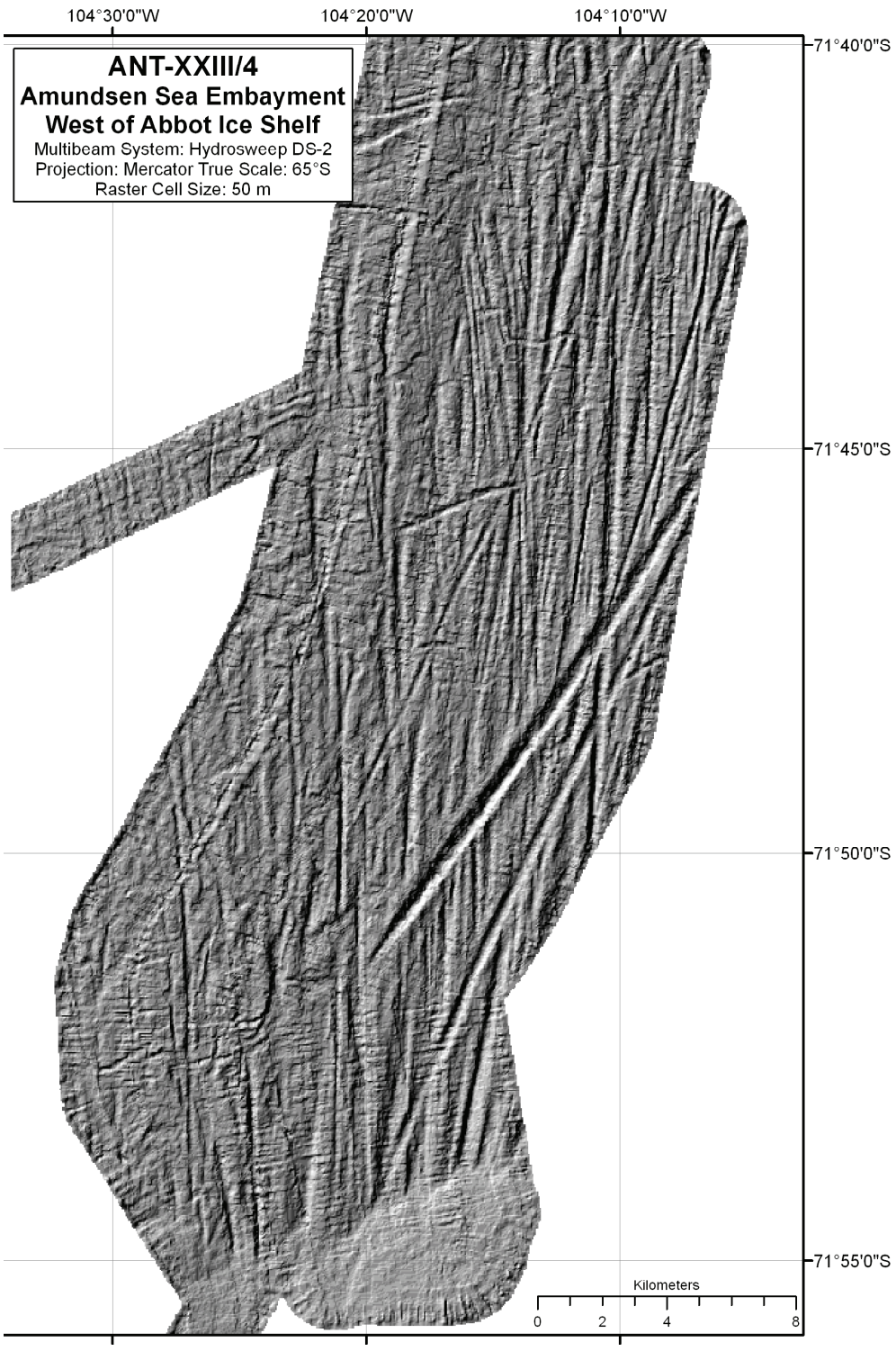

Fig. 5.1: Hillshade of the survey area west of the Abbot Ice Shelf

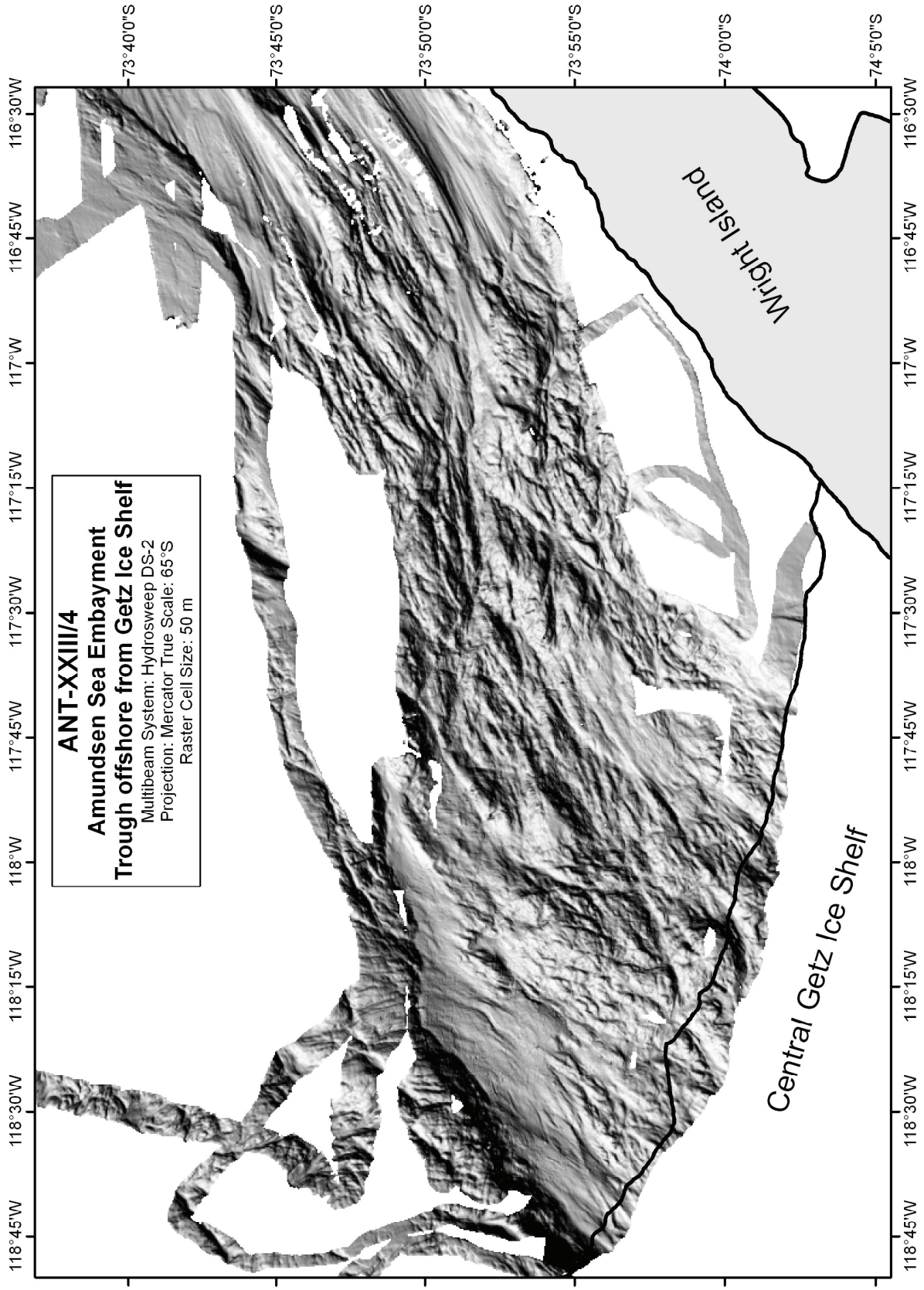

Fig. 5.2: Hillshade of the trough offshore from the Getz Ice Shelf

Marie Byrd Seamounts
In the area of the southern Marie Byrd Seamounts, where a huge seamount was shown in the Smith-Sandwell bathymetric dataset (71° S / 122°30' W), compiled from marine gravimety anomaly from satellites together with ships sonar data, the multibeam survey shows flat seafloor. The further survey mapped a north-west to south-east aligned ridge at 70°40' S / 122°30' W with two overlapping profiles.

The south-eastern part of a seamount at 69°45' S / 126°20' W (Fig. 5.3), which was never mapped before, was surveyed within approx. 16 hours. The north-west to south-east aligned seamount with a length of approx. 40 nm and a width of approx. 15 nm shows a flat top in a depth of 1200 m, steep flanks reaching the surrounding ocean floor at 3400 m water depth and lots of volcanic cones with heights of approx. 200 m.

The seamount at 69°35' S / 124°45' W, which was partly mapped before by RV *Nathaniel B. Palmer* in 1996, was crossed on a line north of the existing survey profile to create connected bathymetry data sets. The seamount at 69°05' S / 123°30' W, which was completely mapped before by RV *Nathaniel B. Palmer* in 1996, was crossed on a line at the southern slope. The Hubert Miller Seamount at 69°15' S / 121°30' W, which was partly mapped before by RV *Polarstern* in 2001, was crossed on a line at the southern slope, which added new bathymetry information to the existing data set. The seamount at 69°12' S / 117°30' W, which was previously discovered by RV *Polarstern* in 2001, was crossed with one line.

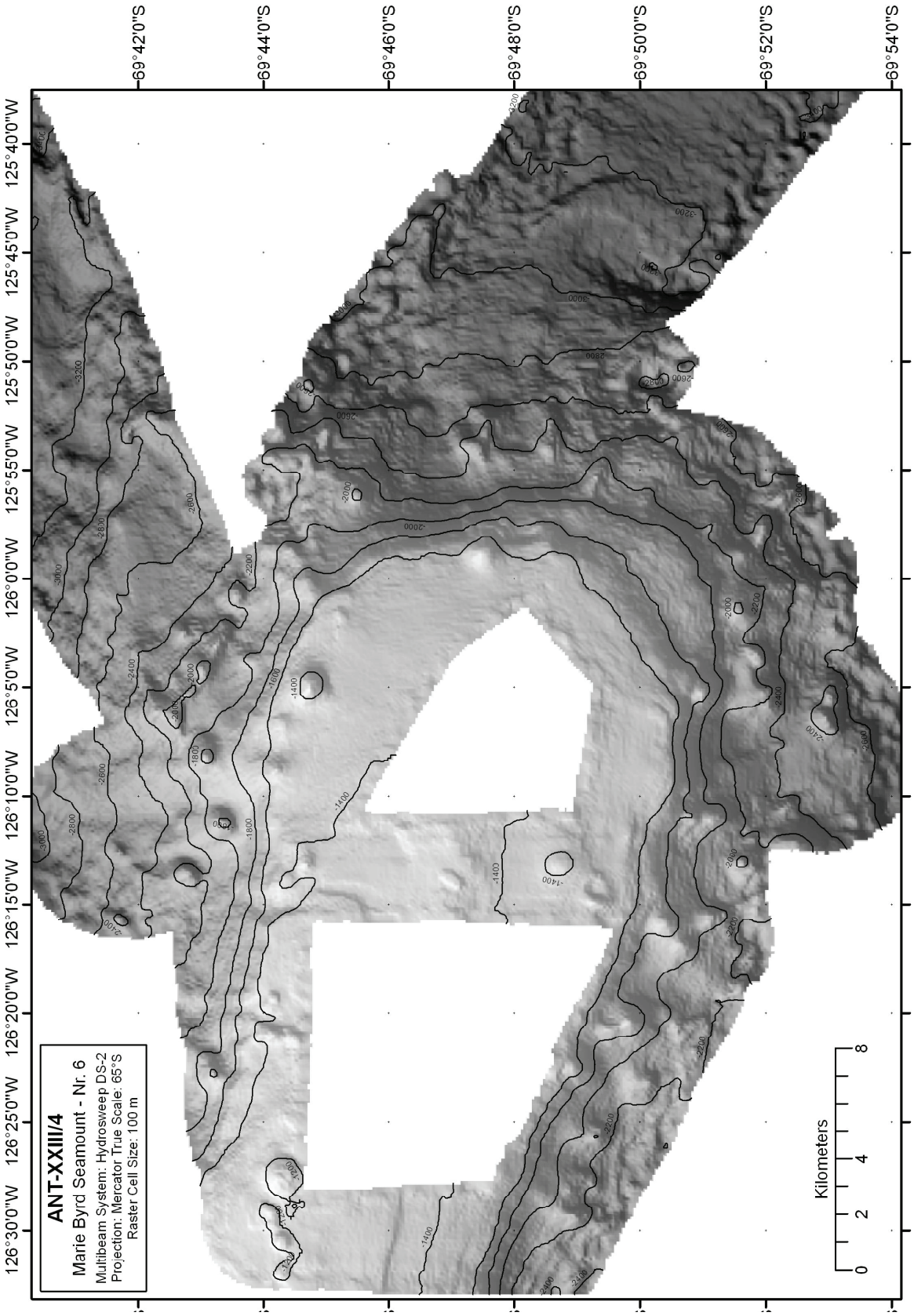

Fig. 5.3: Bathymetry of seamount no. 6 of the Marie Byrd Seamounts

Deep-sea channel in the southern Amundsen Sea
In addition to the bathymetric survey by RV *Polarstern* in 1994, a deep sea channel system was completely mapped. The channel system consists of three channels in a water depth of approx. 3000 m south of a seamount with a height of 500 m, where the biggest channel has a length of 28 km, a depth of 50 m and a width of up to 2.5 km. All channels are situated in a north-eastern direction and disembogue into a common basin.

King George Island
In addition to former surveys by RV *Polarstern*, the Maxwell Bay and the Potter Cove was mapped during approx. one day of systematic surveying and station work. The mapped area of approx. 50 km^2 shows depths between 50 m and 500 m.

6. MARINE-SEDIMENTARY GEOLOGY

Dynamic behaviour of the West Antarctic ice sheet in the Amundsen Sea Embayment during the later quaternary climatic cycles, pliocene to quaternary palaeoceanography in the Southwest Pacific, and holocene climate history of Maxwell Bay, King George Island

Gerhard Kuhn[1)], Claus-Dieter Hillenbrand[2)], Christian Hass[1)], Norbert Lensch[1)], Matthias Forwick[3)], Kristin Daniel[1)], Martin Kober[1)], Stefan Krüger[4)], Manuel Petitat[1)], Andreas Veit[5)]

[1)] Alfred-Wegener-Institut, Bremerhaven
[2)] British Antarctic Survey, Cambridge, UK
[3)] Dept. of Geology, University of Tromsø, Norway
[4)] Institute of Geophysics & Geology, University of Leipzig
[5)] Institute of Geosciences, University of Jena

Objectives

1) The Amundsen Sea Embayment lies offshore from Pine Island and Thwaites glaciers, which exhibit the most rapid elevation change/ice thinning and grounding-line retreat in Antarctica. It has been suggested that this area might be the most likely site for the initiation of a collapse of two million km^2 West Antarctic Ice-Sheet (WAIS), which would result in a global sea-level rise of 5 to 6 m. At present it is not clear to what extent the current retreat of WAIS grounding lines is part of the ongoing recession that started more than 14,000 years ago and to what extent it reflects more recent climatic changes. The marine record of Quaternary deglaciations in the Amundsen Sea Embayment, coupled with ice sheet models, can provide important clues to understanding the stability and climate sensitivity of the WAIS. The main objectives of this cooperative project between the British Antarctic Survey (R. Larter & C.-D. Hillenbrand) and AWI include:

- the glacial maximum extent of the ice sheet,
- the extent of fast ice flow in the former ice sheet, and controls on the location and onset position of fast ice flow,
- the retreat history of the ice sheet,
- whether or not the last ice sheet and its deglaciation are representative of events during earlier Quaternary glacial cycles.
-

This project component is directly linked to Chapter 4 “High-resolution reflection seismics” and Chapter 5 “Swath-bathymetric mapping”.

2) The palaeoceanographic history of the SE Pacific sector of the Southern Ocean should be reconstructed by the recovery of Pliocene to Quaternary pelagic sedimentary sequences from the deep-sea and submarine elevations such as the De Gerlache Seamounts. These sedimentary archives should also provide insights into the dynamics of the WAIS, i.e. if WAIS had collapsed during the late Quaternary.

3) The coring campaign in Potter Cove and Maxwell Bay aimed at providing new insights into sedimentary processes triggered and affected by rapid climate warming along the western Antarctic Peninsula. The major goal of the project is to answer the following questions:

a) How do specifically selected key areas along the western Antarctic Peninsula (here: Potter Cove and Maxwell Bay) respond to rapid climatic warming? What are the key processes with regard to the coupled terrestrial/marine depositional system?
b) How did the study area respond to warming phases during the late Holocene? Were the reactions similar to today? Is there any information which can be used for a near-future prognosis?
c) Are the processes locally confined or can the findings be applied on a broader scale?

In this approach multi-disciplinary methods will be combined in order

1) to provide information on sediment type and composition as a function of provenance, transport processes, and environmental energy, which is related to climatically triggered changes,
2) to map recent morphological structures on the seafloor using the Hydrosweep swath echosounder for the reconstruction of environmental energy and morphodynamics,
3) to reconstruct the late Holocene development of the depositional system and relate it to climate change and associated processes such as local glacier melting/calving and erosional processes.

Methods and equipment

Sub-bottom echosounding with the Parasound system

The most important tool on board for the identification, characterization and quantification of seafloor sediments is the Parasound sub-bottom echosounder. On cruise ANT-XXIII/4 a distance of 7400 miles was profiled. Parasound is a high-resolution sub-bottom echosounder, which operates with two primary frequencies generating a parametric frequency in the water column. This effect results in a secondary frequency varying from 2.5 to 5.5 kHz, which can be used for sub-bottom profiling, depending on the scientific objective. During the whole leg the following settings were used: PAR Frequency 4 kHz, 2 Periods/Pulse length, A/D frequency 50 kHz and a frequency filter at 2 - 6 kHz. Sensor operation mode "PAR-Pilot" was used in water depths below 2000 m and "PAR" in shallower waters.

Based on two channels, Parametric and NBS (18 kHz) signals were recorded and saved on different data storage units as *.asd and *.ps3 files. After real-time recording on a local hard disk, all files were copied to the main server and to a second PC for post-processing, followed by recording on LTO-Tapes. Approximately 660 GB of data were stored.

Sub-bottom profiling is not only a tool for gathering information about sediment accumulation and erosion but it is also used for locating coring positions. Parasound was particularly useful for the identification of core sites in the inner Pine Island Bay,

where a very patchy spatial distribution of sediments was recorded. Small pockets of sediment were mainly observed in deep troughs (Fig. 6.1). The acoustic information from PARASOUND at each coring location can be compared with physical properties measured on the sediment cores with the multi-sensor core logger (MSCL).

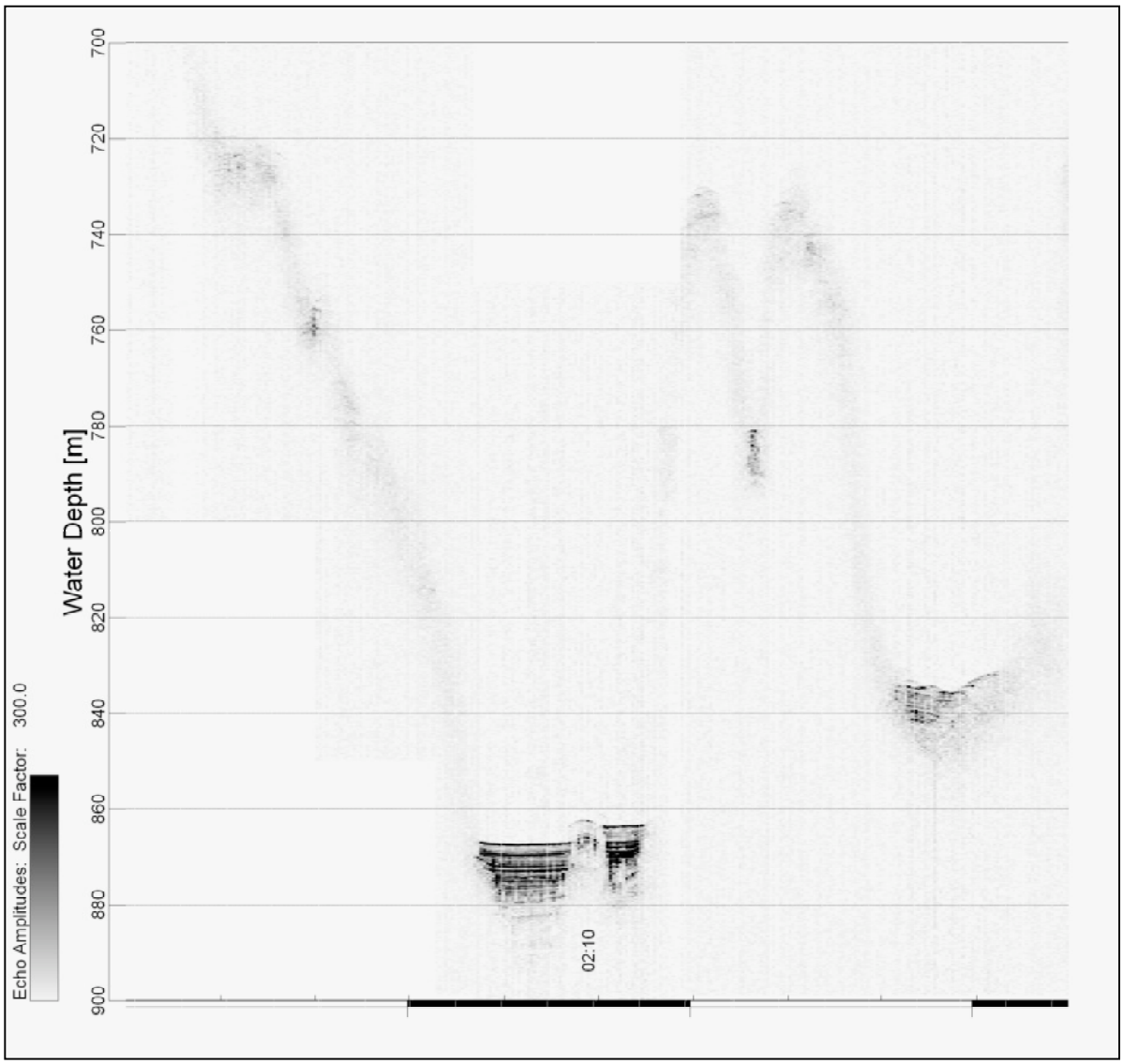

Fig. 6.1: Parasound sub-bottom profile from Pine Island Bay recorded on 13.03.2006 at 74°48'S 105°06'W to 74°49'S 105°04'W

Physical properties of sediment cores

Physical properties of the sediments such as wet bulk density, p-wave velocity, and magnetic susceptibility were detected on the collected sediment cores with a GEOTEK multi-sensor core logger (MSCL). Additionally, core diameter and temperature were measured for the calculation of these values. The parameters listed in the logger settings of the MSCL software (version 6) and given in table 6.1 were used for calibration.

All physical property data still have to be graphically corrected, and faulty values at core section boundaries have to be deleted. The data will be stored in the database PANGAEA (www.pangaea.de) after verification.

In addition, magnetic susceptibility was measured with an F-sensor at 1-cm intervals on the surfaces of the split cores. Furthermore, an image was scanned with a line scan camera (RGB values), and visual color reflectance from 400 to 700 nm (10 nm channels) was measured with a hand held Minolta spectrophotometer.

Tab. 6.1: Sensors and parameter settings for measurements with the GEOTEK multi-sensor core logger during ANT-XXIII/4

P-wave velocity and core diameter plate-transducers diameter: 4 cm transmitter pulse frequency: 500 kHz pulse repetition rate: 1 kHz recorded pulse resolution: 50 ns gate: 2800 delay: 10 µs P-wave travel time offset: 8.28 µs (KOL, 2*2.7 mm liner thickness, PS69/246 to 250) P-wave travel time offset: 7.88 µs (KOL, 2*2.7 mm liner thickness, PS69/288 upper part, PS69/309 to 332) P-wave travel time offset: 7.82 µs (processed with 11.19 µs, SL, 2*2.5 mm liner thickness, PS69/251 to 302) P-wave travel time offset: 7.78 µs (SL, 2*2.5 mm liner thickness, PS69/334 to 339) temperature = 20 °C, salinity = 35 psu, not corrected for water depth and in situ temperature; calibrated with water core of known temperature and theoretical sound velocity
Temperature bimetal sensor, calibrated with Hg-thermometer
Density gamma ray source: Cs-137; activity: 356 MBq; energy: 0.662 MeV aperture diameter: 5.0 mm (SL+KOL) gamma ray detector: Gammasearch2, Model SD302D, Ser. Nr. 3047, John Caunt Scientific Ltd.; count time 10 s Gamma ray attenuation measurement and density calculation with equation type $y=Ax^2+Bx+C$, (Coefficients A, B, and C determined with measurements on calibration cores KOL (PS69/246 to 250) A=0.0004, B=-0.0702, C=10.095 SL (PS69/251 to 302) A=0.0001, B=-0.0695, C=10.075 KOL (PS69/288 upper part, PS69/309 to 332) A=0.0004, B=-0.0729, C=10.111 SL (PS69/334 to 339) A=0.00004, B=-0.0643, C=10.023
Fractional porosity mineral grain density = 2.65, water density = 1.026
Magnetic susceptibility coil sensor: BARTINGTON MS-2C, Ser. Nr. 207 (KOL), Ser. Nr. 130 (SL) nominal inner coil diameter: 10 cm (KOL), 14 cm (SL) coil diameter: 10.8 cm (KOL), 14.8 (SL, and KOL PS69/310-1) alternating field frequency: 565 Hz, count time 10 s, precision $0.1 * 10^{-5}$ (SI) magnetic field strength: ca. 80 A/m RMS Krel: 1.44 (KOL, 8.46 cm core-ø); 1.56 (SL, 12 cm core-ø) coil sensor correction factor: 6.926 (KOL), 6.391 (SL), 14.584 (PS69/310-1); for 10^{-6} (SI)
Core thickness measurement Penny + Giles, Type HLP 190…, Ser #. 92730147, calibrated with distance pieces

Giant box corer (GKG), piston corer (KOL) and gravity corer (SL)
During ANT-XXIII/4 a giant box corer (GKG) (50 x 50 x 60 cm) was used at 19 coring sites to recover undisturbed surface sediments (Table 6.2). Seven piston corers (KOL) and 31 gravity corers (SL) with a total core barrel length of 367 m were used to recover long sedimentary sequences. The deployment of the gear types and the length of the coring devices were chosen based on lithological information derived from sediment acoustic profiles provided by the Parasound echosounding system. With the exception of three GKG sites with very low or no core recovery (sites PS69/255, PS69/280, PS68/281), all deployments were successful and resulted in a total core recovery of 254 m including 5.1 m core length recovered by the pilot corer (TC) triggering the KOL (Table 6.2). The sediment cores taken with piston and gravity corers were cut onboard RV *Polarstern* into 1 m-long sections. After the measurement of physical properties with the multi-sensor core logger, KOL and SL sections and subcores taken from the GKG were not opened onboard RV *Polarstern* but stored in a reefer container at a temperature of +4° C and transported to Bremerhaven.

Piston corers (KOL) were deployed to recover both hemipelagic-terrigenous sedimentary sequences on the Antarctic continental rise in the Bellingshausen and Amundsen seas and pelagic, biogenic sediments on the DeGerlache Seamounts (Figs. 6.2). The barrel lengths of the KOL devices were 25 m at three locations, and 20 m at four locations with the recovery ranging from 13.2 m on the continental rise in the western Amundsen Sea (PS69/310) to 20.1 m in the deep-sea of the south-western Bellingshausen Sea (PS69/250). The KOL recovery rate (ratio of core recovery to penetration depth) varied between 70 % at site PS69/309 in the western Amundsen Sea and 100 % at site PS69/250 located in the south-western Bellingshausen Sea. On the continental rise in the Amundsen Sea bending limited the penetration of the KOL at site PS69/330, while at site PS69/310 one plastic liner imploded during the penetration process (probably as a result of high penetration velocity and a faulty liner). Moreover, one segment of the sediment core collected at site PS69/310 was sheared off and slipped out of the liner, but could be saved. Core recovery of the trigger corer (TC) used for the KOL deployments varied between 0.2 m and 1.0 m. Although TC recovery spanned a broad range (Table 6.2), sediments were observed within the weight set on the top of the TC at sites PS69/247, PS69/309 and PS69/330 suggesting that the gear had fully intruded the seabed. Attempts were made to limit the penetration of the TC, but were not always successful. The gravity corer (SL) on cruise ANT-XXIII/4 was used for coring glacio-marine and subglacial deposits on the shelf of the Amundsen Sea Embayment and in Maxwell Bay of King George Island (Figs. 6.3 and 6.4). The SL deployments were carried out with 3 m to 15 m long barrels and successfully recovered sediment cores ranging from 0.9 m (site PS69/337 in Potter Cove, King George Island) to 9.9 m (site PS69/265 on the inner shelf in Pine Island Bay) in length (Table 6.2). At site PS69/288 on the inner shelf in Pine Island Bay a SL with a 5 m-long barrel recovered a 6.6 m long sediment core (1.6 m of sediment were recovered from within the weight set) and as a consequence a second SL with a 10 m-long barrel was deployed at site PS69/288, which recovered a 9.1 m-long sediment core. At site PS69/337 in Potter Cove bending of the SL in ca. 2 m depth below the seafloor resulted in low core recovery. In general, the recovery rate for the SL varied between 40 % and 90 %.

Tab. 6.2: Coring sites on cruise ANT-XXIII/4. GKG: giant box corer, KOL: piston corer, TC: trigger corer, SL: gravity corer

Station	Gear	Location	Latitude (deg/min)	Longitude (deg/min)	Water depth (m)	Penetration depth/ Deployed core length (m)	Core recovery (m)	Remarks
PS69/246-1	TC	DeGerlache Seamounts	65°12.10´S	92°40.85´W	3442	1/1	0.19	
PS69/246-1	KOL	DeGerlache Seamounts	65°12.10´S	92°40.85´W	3442	20/20	16.90	
PS69/247-1	TC	DeGerlache Seamounts	64°48.58´S	93°34.80´W	4238	1/1	0.94	core top lost
PS69/247-1	KOL	DeGerlache Seamounts	64°48.58´S	93°34.80´W	4238	19.5/20	16.24	
PS69/250-1	TC	continental rise in SW' Bellingshausen Sea	69°05.87´S	98°51.50´W	4456	1/1	0.66	
PS69/250-1	KOL	continental rise in SW' Bellingshausen Sea	69°05.87´S	98°51.50´W	4456	20/25	20.10	0-5 cmbsf disturbed
PS69/251-1	GKG	outer shelf in E' Amundsen Sea	72°06.85´S	104°48.31´W	552	0.4/0.6	0.38	
PS69/251-2	SL	outer shelf in E' Amundsen Sea	72°06.85´S	104°48.31´W	553	3/3	2.55	
PS69/255-1	SL	outer shelf in E' Amundsen Sea	71°48.08´S	104°21.09´W	640	3/3	1.65	
PS69/255-2	GKG	outer shelf in E' Amundsen Sea	71°48.00´S	104°21.17´W	640	0/0.6	0	triggered, but not closed
PS69/255-3	GKG	outer shelf in E' Amundsen Sea	71°47.83´S	104°21.67´W	640	0.4/0.6	0.33	
PS69/256-1	SL	outer shelf in E' Amundsen Sea	71°55.35´S	104°20.27´W	647	3.5/3	1.96	
PS69/259-1	SL	inner shelf NE of Bear Peninsula	74°18.10´S	110°15.92´W	250	4/3	3.06	core top lost
PS69/265-3	SL	inner shelf SW' Amundsen Sea	73°40.13´S	113°02.31´W	672	2.5/5	1.29	fallen over?
PS69/266-1	SL	inner shelf SW' Amundsen Sea	73°32.52´S	113°44.48´W	719	5/5	3.46	
PS69/267-1	SL	inner shelf SW' Amundsen Sea	73°23.71´S	114°33.55´W	832	5/5	2.97	0-5 cmbsf disturbed
PS69/267-2	GKG	inner shelf SW' Amundsen Sea	73°23.71´S	114°33.91´W	836	0.5/0.6	ca. 0.3	triggered, but not closed
PS69/269-1	GKG	inner shelf SW' Amundsen Sea	73°13.15´S	115°34.61´W	822	0.5/0.6	ca. 0.3	
PS69/269-2	SL	inner shelf SW' Amundsen Sea	73°13.11´S	115°34.28´W	824	5/5	2.09	
PS69/272-2	SL	inner shelf SW' Amundsen Sea	73°53.56´S	118°29.19´W	1538	?/5	1.565	fallen over?
PS69/272-3	GKG	inner shelf SW' Amundsen Sea	73°53.52´S	118°28.69´W	1529	0.4/0.6	0.32	
PS69/273-2	SL	inner shelf SW' Amundsen Sea	73°57.70´S	117°50.59´W	1318	?/5	3.29	
PS69/274-1	SL	inner shelf SW' Amundsen Sea	73°51.36´S	117°46.54´W	1411	6/5	4.53	
PS69/275-1	SL	inner shelf SW' Amundsen Sea	73°53.33´S	117°32.90´W	1478	6/5	4.79	
PS69/275-2	GKG	inner shelf SW' Amundsen Sea	73°53.32´S	117°32.90´W	1472	0.3/0.6	0.265	

Station	Gear	Location	Latitude (deg/min)	Longitude (deg/min)	Water depth (m)	Penetration depth/ Deployed core length (m)	Core recovery (m)	Remarks
PS69/280-1	SL	inner shelf SW' Amundsen Sea	73°56.15´S	111°37.41´W	604	?/5	1.42	fallen over?
PS69/280-2	GKG	inner shelf SW' Amundsen Sea	73°56.17´S	111°37.32´W	600	?/0.6	0	box bent
PS69/281-2	GKG	inner shelf SW' Amundsen Sea	74°19.76´S	110°12.44´W	203	?/0.6	0	first attempt not triggered second attempt not closed
PS69/283-5	GKG	inner shelf SW' Amundsen Sea	72°45.86´S	115°22.62´W	588	0.4/0.6	0.34	
PS69/283-6	SL	inner shelf SW' Amundsen Sea	72°45.86´S	115°22.66´W	592	2.5/5	1.74	
PS69/284-1	SL	inner shelf SW' Amundsen Sea	73°01.40´S	115°24.20´W	734	5/5	4.47	
PS69/284-2	GKG	inner shelf SW' Amundsen Sea	73°01.20´S	115°24.11´W	736	0.5/0.6	0.50	
PS69/288-1	SL	inner Pine Island Bay	74°24.91´S	102°59.60´W	744	7/5	6.62	sections 0-48 cmbsf and 48-148 cmbsf in KOL liner
PS69/288-2	GKG	inner Pine Island Bay	74°24.91´S	102°59.52´W	742	0.45/0.6	0.44	
PS69/288-3	SL	inner Pine Island Bay	74°24.94´S	102°59.48´W	744	12/10	9.12	
PS69/289-3	SL	inner Pine Island Bay	74°30.42´S	103°21.55´W	910	10/10	6.11	
PS69/291-1	SL	inner Pine Island Bay	74°41.16´S	104°09.51´W	988	12/10	9.86	
PS69/292-2	SL	inner Pine Island Bay	74°40.92´S	105°11.61´W	1361	11/10	6.83	
PS69/292-3	GKG	inner Pine Island Bay	74°40.95´S	105°11.60´W	1359	0.4/0.6	0.36	
PS69/295-1	SL	Pine Island Bay transect	74°28.73´S	104°06.09´W	1113	5.5/5	4.86	
PS69/296-1	SL	Pine Island Bay transect	74°21.41´S	104°45.08´W	1393	14/15	9.09	
PS69/297-1	GKG	Pine Island Bay transect	74°04.79´S	103°40.06´W	460	0.4/0.6	0.36	
PS69/298-1	SL	Pine Island Bay transect	73°42.13´S	103°49.95´W	886	?/5	1.90	fallen over?
PS69/299-1	GKG	Pine Island Bay transect	73°26.62´S	103°38.89´W	685	0.45/0.6	0.39	
PS69/300-1	SL	Pine Island Bay transect	73°16.23´S	103°40.76´W	738	3/5	1.41	
PS69/302-3	GKG	outer shelf Pine Island Bay	71°07.81´S	105°39.04´W	544	0.3/0.6	0.27	
PS69/302-4	SL	outer shelf Pine Island Bay	71°07.80´S	105°38.99´W	540	4/5	1.56	
PS69/309-1	TC	continental rise in W' Amundsen Sea	70°33.67´S	119°20.23´W	2778	1.2/1	0.87	core top lost
PS69/309-1	KOL	continental rise in W' Amundsen Sea	70°33.67´S	119°20.23´W	2778	22.5/25	15.70	0-10 cmbsf disturbed

Station	Gear	Location	Latitude (deg/min)	Longitude (deg/min)	Water depth (m)	Penetration depth/ Deployed core length (m)	Core recovery (m)	Remarks
PS69/310-1	TC	continental rise in W' Amundsen Sea	71°08.94´S	119°57.55´W	2048	1.1/1	0.75	
PS69/310-1	KOL	continental rise in W' Amundsen Sea	71°08.94´S	119°57.55´W	2048	15/20	13.19	217-303 cmbsf sediment slipped out of liner; 1260-1301 cmbsf liner shattered
PS69/330-1	TC	continental rise in Amundsen Sea	70°08.12´S	111°45.04´W	3327	1.1/1	0.96	ca. 0-30 cmbsf lost
PS69/330-1	KOL	continental rise in Amundsen Sea	70°08.12´S	111°45.04´W	3327	15/25	13.32	bent at ca. 15m
PS69/332-1	TC	continental rise in Bellingshausen Sea	68°31.40´S	82°44.16´W	3412	1/1	0.77	
PS69/332-1	KOL	continental rise in Bellingshausen Sea	68°31.40´S	82°44.16´W	3412	20/20	16.66	
PS69/334-2	GKG	Potter Cove, King George Island	62°14.77´S	58°42.42´W	138	0.5/0.6	0.49	
PS69/335-1	GKG	Maxwell Bay, King George Island	62°15.51´S	58°46.39´W	447	0.6/0.6	0.60	
PS69/335-2	SL	Maxwell Bay, King George Island	62°15.50´S	58°46.34´W	446	15/15	9.43	
PS69/336-1	SL	Maxwell Bay, King George Island	62°17.32´S	58°41.68´W	430	14/15	8.53	
PS69/336-2	GKG	Maxwell Bay, King George Island	62°17.34´S	58°41.50´W	428	0.5/0.6	0.48	
PS69/337-1	SL	Potter Cove, King George Island	62°14.77´S	58°42.12´W	110	2/10	1.26	gravity corer bent at 2m; ca. 0-4 cmbsf lost
PS69/337-2	SL	Potter Cove, King George Island	62°14.79´S	58°42.11´W	110	2/5	0.86	gravity corer bent at 2m; stratigraphy disturbed
PS69/338-1	SL	Maxwell Bay, King George Island	62°14.30´S	58°48.80´W	434	6/10	5.40	
PS69/339-1	SL	Maxwell Bay, King George Island	62°12.07´S	58°51.49´W	258	11/10	7.28	

Sampling and documentation
During ANT-XXIII/4 two surface sediment samples (100 cm^3 and 400 cm^3, respectively) were taken from the giant box cores for various sedimentological analyses and archiving. Two subcores (diameter: 6.2 cm) were recovered from the box cores and immediately cut into 1 cm thick slices at fixed intervals (0-1, 1-2, 2-3, 3-4, 4-5, 7-8, 10-11, 15-16, 20-21, 25-26 cmbsf, etc.). Another subcore (diameter: 6.2 cm) was frozen as archive core. If possible, two additional subcores (diameter: 12.5 cm) were taken from the box core.

Twelve subcores taken from giant box cores and eight gravity cores corresponding to 30.7 core meters were opened and sampled (Table 6.2). After opening and splitting, the sections were photographed. High resolution color scans and measurements of magnetic susceptibility (at 1-cm intervals using a point-sensor) as well as a sediment description (Appendix 6.1) were carried out on the archive half. Microscopical analyses of smear slides and investigations of x-radiographs (developed onboard RV *Polarstern* during the cruise) were used to identify the lithologies and sedimentary structures in the cores. Sediment colours were determined using a “Munsell Soil Color Chart“. Lithological classification followed the scheme depicted in Appendix 6.1. Sampling procedures of the cores followed standard methods at AWI and were exclusively carried out on the work half. Sampling types and intervals (usually 5, 10, or 15 cm) varied in response to the identified lithologies of the recovered sediments. The general sampling plan included sampling of a 25 x 10 x 1 cm sediment slab for x-raying (no x-radiographs were taken from core PS69/266 SL). Samples (10 cm^3 in volume each) for the determination of bulk parameters (water content, density, $CaCO_3$, TOC and opal content) and grain-size distribution including clay mineral analysis were taken with syringes and stored in whirlpak bags, which were pre-weighed in the case of bulk samples. Sediment slices (ca. 40 cm^3 volume) for investigations on the coarse grained fraction (>63 _m) were sampled with a spatula and stored in whirlpak bags. Laboratory analyses will be carried out on the individual samples at AWI and BAS. Information regarding the sample types and volumes will be available in the PANGAEA data bank at AWI (http://www.pangaea.de).

Results
In the Amundsen Sea box and gravity cores were recovered from the shelf west of Thurston Island (sites PS69/251 to PS69/256 and site PS69/302), north of the central and eastern Getz and the Dotson ice shelves (sites PS69/259 to PS69/284), the inner shelf in Pine Island Bay and west of the Abbot and Cosgrove ice shelves (sites PS69/288 to PS69/300) (Figs. 6.2, 6.3). Mapping with the Parasound subbottom profiler revealed that the seafloor on the inner shelf is mainly formed by bedrock. Sediments are only present at the deepest locations in the troughs directly offshore from the front of the present ice shelves. However, sedimentary coverage is not observed at all of the deepest parts of these troughs. Furthermore, sedimentary sequences detected by Parasound north of the Pine Island and Thwaites Glaciers are often thicker than sequences observed directly offshore from the Getz and Dotson ice shelves. At site PS69/275 offshore from the central Getz Ice Shelf a gravity core recovered a 2 m thick bioturbated terrigenous mud unit, which may consist of particles derived from meltwater plumes. These plumes are likely to have been produced by basal melting under the Getz Ice Shelf, possibly in response to upwelling of Circumpolar Deep-Water (CDW). Below the terrigenous mud unit at site

PS69/275 a 0.4 m thick diatom-bearing sedimentary unit is observed, which is underlain by 2.5 m of horizontally and cross bedded sandy and gravelly sediments, which often exhibit normal gradation. The sedimentary structures observed in this lowermost unit indicate reworking of sediments by gravitational down-slope processes such as turbidity currents and debris flows.

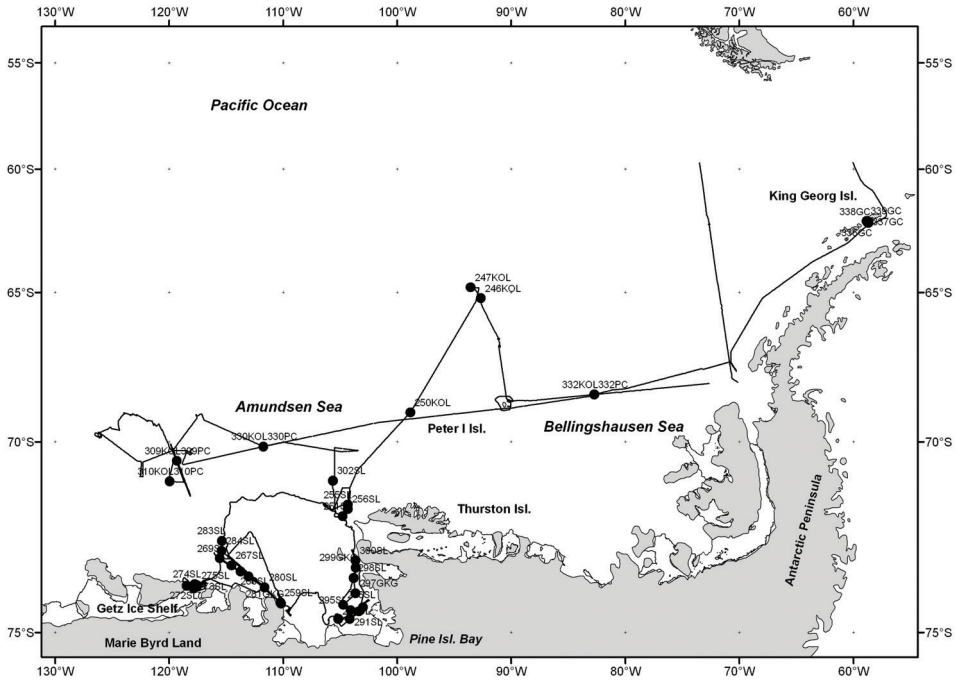

Fig. 6.2: All core sites (black dots) of cruise ANT-XXIII/4. Black line depicts the cruise track.

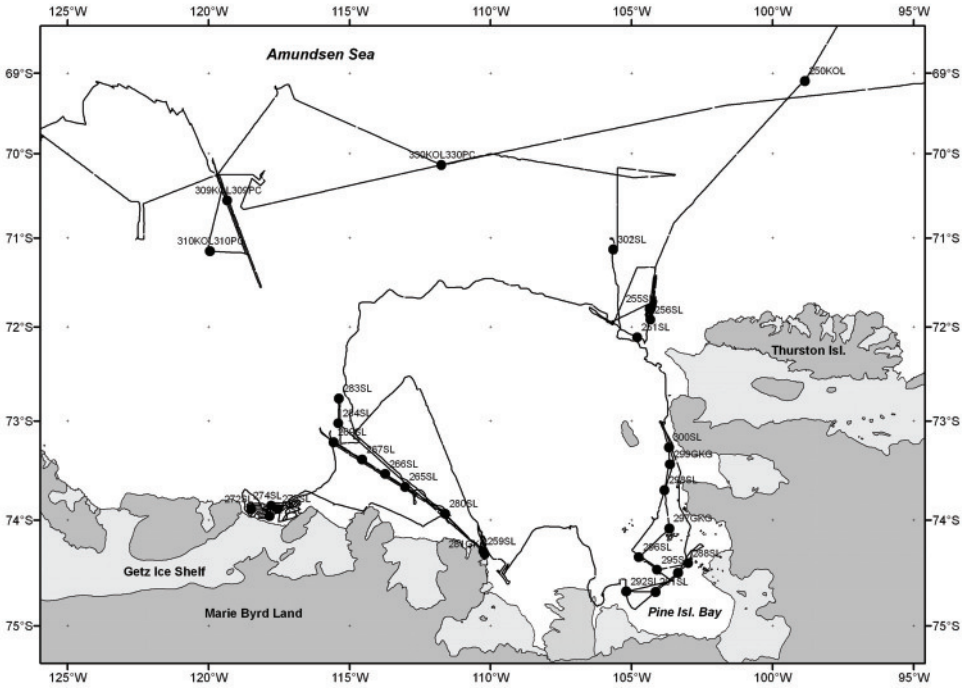

Fig. 6.3: Core sites (black dots) in the Amundsen Sea Embayment and Pine Island Bay of cruise. Black line depicts the cruise track.

Most surface sediments on the shelf (assumed to be Holocene in age) consist of purely terrigenous sandy muds, muds and silty clays. Brown diatom-bearing muds are found on the inner shelf north of the eastern Getz Ice Shelf (PS69/269). On the outer shelf of Pine Island Bay (sites PS69/255 and PS69/302) surface sediments consist of olive-brown foraminiferal muds and foraminifera-bearing sandy muds. The foraminiferal assemblage is dominated by the planktonic species *Neogloboquadrina pachyderma* sin. The foraminiferal carbonate will be used for AMS ^{14}C dating. Gravel grains and cobbles lie on top of surface sediments recovered from the outer shelf of the study area. The gravels and cobbles, which are interpreted as dropstones, are often covered with thin manganese coatings pointing to sedimentation rates less than 1 cm/kyr. The occurrence of silt- and clay-sized particles within the surface sediments supports the idea that these deposits represent condensed units rather than residual sediments.

In all cores recovered from the shelf of the Amundsen Sea the abundance of microfossils decreases downcore within the uppermost 0.5 m. The underlying purely terrigenous sediments, which often contain significant amounts of sand and gravel, were probably deposited at the transition from the last glacial to the present interglacial period. The basal sediments in cores collected from the shelf often consist of terrigenous diamictons. The diamictons were probably deposited during the last glacial period and represent tills deposited subglacially by ice streams (particularly in areas, where megascale glacial lineations are observed, e.g. at site PS69/251), debris flow deposits, which were deposited in close vicinity to the grounding line of a grounded ice mass, and/or sub-ice shelf deposits. On the outer shelf, the deposition of a diamicton may alternatively result from the grounding of an iceberg, which is suggested by numerous iceberg furrows observed in that area. These diamictons can be interpreted as iceberg turbates.

One piston core (site PS69/250) from the deep-sea in the western Bellingshausen Sea and two piston cores (sites PS69/246 and PS69/247) from the DeGerlache Seamounts were recovered for studying the Pliocene and Quaternary oceanography in the SE Pacific sector of the Southern Ocean. Four piston cores (sites PS69/309, PS69/310, PS69/330 and PS69/332) were recovered from the continental rise in the Amundsen Sea and the Bellingshausen Sea for investigating a relatively proximal record of the behaviour of WAIS during the late Quaternary and its relation to climatic changes and oceanographic processes.

Aerial photographs had previously revealed mud plumes in the area around King George Island. These plumes were produced by tidewater glaciers in bights such as Potter Cove. The mud plumes appear to exit the bights along the bights' left coastlines (in flow direction) possibly as a result of the Coriolis force. Inner Maxwell Bay was mapped using Hydrosweep and Parasound in order to reconstruct the sources of the sediment that is draped upon the deeper part of Maxwell Bay. During the survey three subbasins were detected that carry acoustically well stratified sediments. A total of 6 gravity cores and 3 boxcores (sites PS69/334 to PS69/339, total length: 34 m) were taken from the target areas described. The aim was to collect sediment cores within Potter Cove for detailed understanding of the processes involved in a single bight. Sediment cores were also taken from the inner and the outer Maxwell Bay where acoustically well-structured sediments were detected.

These cores are thought to represent different stages of sediment input into inner Maxwell Bay and to reflect multiple environmental signals in outer Maxwell Bay.

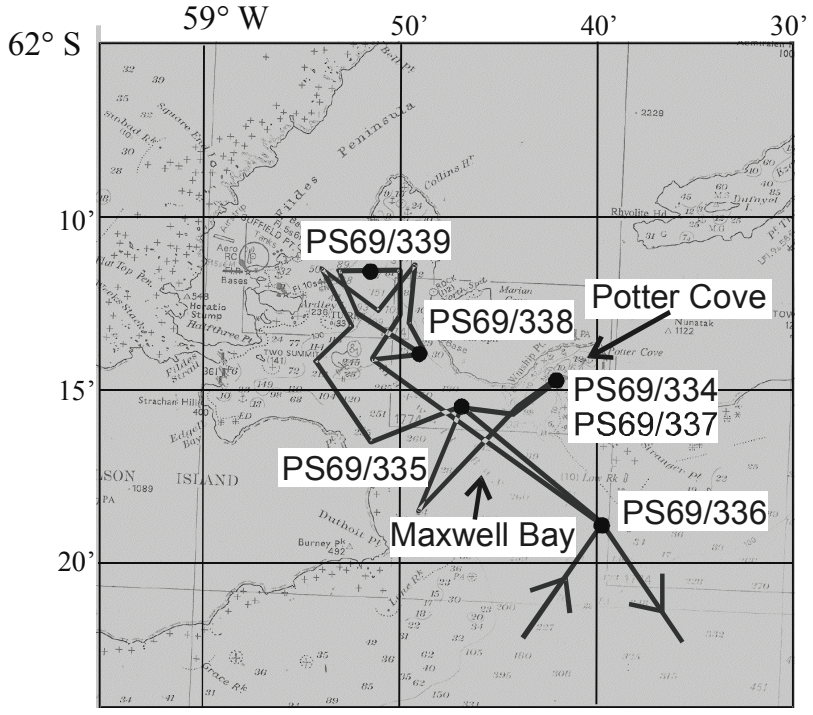

Fig. 6.4: South King George Island showing Maxwell Bay and Potter Cove. Lines mark PARASOUND and Hydrosweep transects, black dots mark core locations.

7. DREDGING

Origin and effects of magmatism at the Marie Byrd Seamounts and other seamounts of the Amundsen and Bellingshausen Seas

Reinhard Werner[1)], Folkmar Hauff[2)], Kristin Daniel[3)], Silke Hauff[2)], Jan Just[3)], Joanne Johnson[4)], Andreas Veit[5)], Katja Zimmermann[3)]

[1)] Tethys GmbH, Kiel
[2)] IFM-GEOMAR, Kiel
[3)] Alfred-Wegener-Institut, Bremerhaven
[4)] British Antarctic Survey, Cambridge, UK
[5)] Institute of Geosciences, University of Jena

Objectives

The hard rock sampling programme on RV *Polarstern* cruise ANT-XXIII/4 focussed on the Marie Byrd Seamounts, a large submarine volcanic province located in the southern Amundsen Sea between ~68° and ~71°S and ~114° and ~131°W off the shelf of Marie Byrd Land (Fig. 7.1). The individual volcanoes rise up to 3,000 m above the seafloor from abyssal plain depths of ~3,500 – 4,000 m. However, rock samples have not been recovered from the Marie Byrd Seamounts thus far and their origin and geological history remained enigmatic. On cruise ANT-XXIII/4, we therefore carried out mapping and an extensive dredging campaign of the Marie Byrd Seamounts to constrain their age and magma sources as well as their volcanological and magmatic evolution. Minor mapping and hard rock sampling were additionally carried out at Peter I Island, an isolated ocean island volcano in the western Bellingshausen Sea. Our investigations address two overall scientific topics:

(1) Since the introduction of plate tectonics, intraplate volcanism has generally been attributed to continental rifting (e.g., East African volcanoes) or mantle plumes (e.g., Hawaii, Reunion, Canary Islands), which are believed to carry hot mantle material from the Earth's interior - possibly from as deep as the boundary between the Earth's core and lower mantle at 2,900 km depth – to the base of the lithospheric plates, causing extensive volcanic activity. Recently, however, a global debate has developed on the origin of intraplate volcanism (the so-called "Great Plume Debate") in response to increasing problems in explaining intraplate volcanism in many areas (in particular in the southern Pacific region). The Marie Byrd Seamounts appear to be a typical example for such enigmatic intraplate volcanism since their wide and irregular distribution and their location on oceanic crust are difficult to explain alone with the „classic" models for the origin of intraplate volcanism. The investigation of the Marie Byrd Seamount volcanism should therefore provide new insights in the magmatic and geodynamic processes which cause intraplate volcanism.

(2) The volcanism in the area of the Marie Byrd Seamounts may also originate from tectonic or magmatic processes related to the break-up of the Cretaceous supercontinent Gondwana (consisting of Africa, South America, Antarctica, Australia, India, and the New Zealand micro-continent). The break-up of Gondwana began with the separation of Africa and South America at ~130 Ma, whereas the separation of New Zealand and Australia from Antarctica occurred at ~105 Ma, thus representing the final phase of the so called Gondwana break-up which lead to the present configuration of the continents. Within this complex plate tectonic puzzle, today's Antarctic Marie Byrd Land was still attached to the New Zealandic micro-continent 110 million years ago and according to magnetic seafloor anomalies did not fully separate from New Zealand prior to 84 Ma (Weaver et al. 1994, Bradshaw et al. 1997). Therefore the Marie Byrd Seamounts, located on oceanic crust off the shelf of Marie Byrd Land, may represent a relict of the final phase of the Gondwana break-up. Investigations of this seamount province may therefore contribute to a better understanding of geodynamic processes which cause continental break-up, and to the reconstruction of the plate tectonic evolution of the southwest Pacific.

Methods and equipment

Rock sampling on ANT-XXIII/4 was carried out using rectangular chain bag dredges. Chain bag dredges are similar to large buckets with a chain bag attached to their bottom and steel teeth at their openings, which are dragged along the ocean floor by the ship´s winch.

Selection of Dredge Sites

General station areas were chosen based on satellite gravity maps, bathymetric maps derived from gravity data (Smith and Sandwell 1997), and bathymetric data gained on former cruises (RV *Nathaniel B. Palmer* in 1996, RV *Polarstern* ANT-XI/3 in 1994 and ANT-XVIII/5a in 2001). The final selection of dredge sites in un-mapped areas was critically dependent on detailed Hydrosweep DS2 surveys carried out at each station before dredging. Final positioning of the vessel over the dredge sites was done using GPS and the bathymetric data gained on the surveys, and allowing for weather and drift conditions. Dredge tracks were usually located - depending on the morphology of the structures - on steep slopes, at plateau edges, at scarps or at small cones on the flanks of the seamounts. This was done (1) to avoid areas of thick sediment cover and (2) to receive rocks as young and accordingly as fresh as possible.

Taking into account the widespread ice-rafted debris in the Bellingshausen and Amundsen Seas, detailed analysis of the rocks yielded by dredging was carried out to identify *in-situ* rock fragments. The criteria used for distinction include, but are not restricted to, (1) shape of the fragments (angular vs. well-rounded), (2) existence of fresh surfaces formed by tearing away from the bedrock outcrops, and (3) homogeneity of the dredged material.

Shipboard procedure

Once on board, a selection of the rocks was cleaned and then examined with a hand lens and grouped according to their lithologies and degree of marine weathering. The immediate aim was to determine whether *in-situ* material being suitable for

geochemistry and age dating had been recovered. Suitable volcanic rock samples have an unweathered and unaltered groundmass, empty vesicles, glassy rims (ideally), and - if present - any fresh phenocrysts. If suitable *in-situ* samples were present, the ship moved to the next station. If they were not, then the importance of obtaining samples from the station was weighed against the available ship-time. Additional dredges nearby the same station were sometimes possible.

Fresh blocks of representative volcanic rock samples were cut for thin section and microprobe preparation as well as geochemistry and were further processed to remove possible manganese crusts, weathering rinds etc. Each of these sub-samples, together with any remaining bulk sample, was described, labelled, and finally sealed in plastic bags for transportation to IFM-GEOMAR or cooperating institutions. Carbonate crusts and biological material were also sampled for cooperating working groups.

Land based analyses
Magmatic rocks sampled by the RV *Polarstern* from the ocean floor will be analyzed using a variety of different geochemical methods. The age of whole rocks and minerals will be determined by $^{40}Ar/^{39}Ar$ laser dating. Major element geochemistry by XRF and EMP will constrain magma chamber processes within the crust, and also yield information on the average depth of melting, temperature and source composition to a first approximation. Phenocryst assemblages and compositions will be used to quantify magma evolution, e.g. differentiation, accumulation and wall rock assimilation. Petrologic studies of the volcanic rocks will also help to constrain the conditions under which the melts formed (e.g., melting depths and temperatures). Further analytical effort will concentrate on methods that constrain deep seated mantle processes. For example, trace element data by ICPMS will help to define the degree of mantle melting and help to characterize the chemical composition of the source. Long-lived radiogenic isotopic ratios by TIMS and MC-ICPMS such as $^{87}Sr/^{86}Sr$, $^{143}Nd/^{144}Nd$, $^{206}Pb/^{204}Pb$, $^{207}Pb/^{204}Pb$, $^{208}Pb/^{204}Pb$, and $^{187}Hf/^{188}Hf$ are independent of the melting process and reflect the long term evolution of a source region and thus serve as tracers to identify mantle and recycled crust sources. Additionally, morphological studies and volcanological analyses of the dredged rocks will be used to constrain eruption processes, eruption environment and evolution of the volcanoes. Through integration of the various geochemical parameters, the morphological and volcanological data, and the age data the origin and evolution of the sampled structures can be reconstructed.

Results
The base of Peter I Island and several volcanoes in selected areas of the Marie Byrd Seamount Province were successfully dredged on RV *Polarstern* cruise ANT-XXIII/4. Out of the 19 dredges on the cruise, 10 contained igneous rocks (excluding dropstones), 5 Mn-Fe oxides, 2 semiconsolidated sediments or carbonate crusts, and 4 biological samples. One dredge was lost. Additional samples from Peter I Island could be taken from a peninsula at its eastern coast using a helicopter. Furthermore a potentially volcanic structure north of Peter I Island has been surveyed with the Hydrosweep DS2 multi-beam echo-sounding system without identifying possible dredge targets. This section gives background information and short summaries of the structures sampled through dredging and/or mapping and summarizes the results

of sampling and mapping. Refer to tables 7.1 and 7.2 for latitude, longitude and depth of dredge sites. Distances between seamounts are given between the seamount tops and are approximate only; dimensions and heights are preliminary and are included only to give a rough idea of seamount dimensions.

Peter I Island
The N-S elongated, ~20 x 10 km Peter I Island is located in the western Bellingshausen Sea some 500 km north of the Antarctic mainland. The island represents the top of a large volcano which measures ~65 km in diameter at its base and rises from abyssal plain depths of ~3,500 – 4,000 m to an elevation of 1,640 m above sea level. The volcano is situated on a linear, N-S-striking gravity ridge (abandoned rift?) which also runs through the DeGerlache Seamounts located some 400 km north of Peter I Island. The subaerial part of the volcano is composed of alkali basalts, hawaiites, and trachytes with geochemical signatures similar to ocean island basalts (OIB, Hart et al. 1995). The volcano may be considered active as indicated by young ages of the Peter I lavas (< 0,33 m.y., Prestvik et al. 1990, Prestvik and Duncan 1991) and jagged and precipitous scoria deposits on its flanks (see below). Prestvik and Duncan (1991) postulate that construction of the island may have started 10 – 20 m.y. ago, based on estimated volumes and eruption rates. Despite the lack of a clear hotspot track, a plume-related origin has been proposed for Peter I Island (e.g., Prestvik et al. 1990, Hart et al. 1995).

The submarine base of Peter I Island was partially surveyed before cruise ANT-XXIII/4 but has not successfully been sampled yet (apart from dredge hauls off the coast of the island some 80 years ago, Broch 1927). The bathymetric maps reveal several small cone- and ridge-like structures on the flanks of the base and a steep canyon at its western side which appeared to be the most promising site for dredging. However, dredging at the canyon proved difficult because of the wind conditions. Therefore a dredge haul was carried out at a small, ~150 m high ridge located in ~1,800 m water depth on the NE slope of the island. Dredge PS69-244-1 yielded ~400 kg angular volcanic fragments and minor amounts of dropstones. Predominant lithologies are (1) up to ~50 cm large vesicular pillow fragments and (2) fragments of the surface of a sheet lava flow. Both lava types are plagioclase-phyric and have up to 1 cm thick glassy rims on their surfaces. The rocks appear to be surprisingly fresh. Vesicles are generally unfilled and only some glassy surfaces show early stages of palagonitization. Considering the 1,800 m water depth at which these lavas erupted, their high vesicularity is somewhat unusual and may indicate that the initial volatile concentrations of these melts were relatively high. A second dredge (PS69-245-1) was made on a small cone-like structure in 1,500 m water depth on the eastern slope of the base of the island. Unfortunately the dredge got stucked and was lost after both safety cables sheared off for unknown reasons.

The small peninsula Michajlovodden, being located at the eastern coast of Peter I Island, was selected for a GPS and a magnetometer station (see Chapters 2 and 10). At the end of cruise ANT-XXIII/4, the opportunity was given to study and sample the upper rock units of Michajlovodden during undeployment of the GPS and magnetometer stations. Michajlovodden measures ~300 x 180 m and represents the steep-sided, oval-shaped remains of a small volcanic edifice. It rises to a flat plateau at 65 m above sea level and is connected with the main island by a small ice-covered

ridge. A succession of different volcanic deposits forms the top area of Michajlovodden. The lowermost studied deposit is a >1.5 m thick layer of partly red oxidized, aphyric agglutinates outcropped in the northern part of the peninsula (sample PS69/PI-3). The agglutinates are overlain by a massive, at least 1 m thick lava flow. The lava is fresh, aphyric and has ~5 % vesicles (sample PS69/PI-2). Similar but more vesicular lava (~15 % vesicles, sample PS69/PI-1) forms the eastern edge of the flattish top of Michajlovodden. Due to the snow cover it is difficult to say if this lava represents an individual thin lava flow or whether it is the top of the lava flow overlying the agglutinates. The lava flow(s) which form the plateau of Michajlovodden prevent or at least slow down further erosion of the volcano by the sea. The uppermost unit of Michajlovodden is a fall out deposit consisting of reddish ash, lapilli and bombs. The reddish bombs are up to > 50 cm in size and have 10 – 20 % vesicles (sample PS69/PI-4). It is notable that these volcaniclastic deposits on top of Michajlovodden are not completely eroded by ice yet. This observation may suggest a relatively young age for this volcano (max. some thousand years?).

A seismic line (BAS923-30), recorded during a RV *James Clark Ross* cruise in 1992/93, reveals a submarine volcanic structure ~200 km north of Peter I Island. A Hydrosweep survey at this site revealed a N-S-striking, slightly undulating ridge-like volcanic structure. The ridge is 25 km long, up to 5 km wide and rises from its base at 4,600 m below sea level to ~800 m above the sea floor. However, no appropriate dredge sites were found to sample this possible volcanic ridge.

Marie Byrd Seamount Province

The Marie Byrd Seamount Province comprises 8 large volcanoes (up to 75 x 50 km at their base) and numerous minor volcanic and tectonic (?) structures. Many of these volcanoes are aligned in E-W-direction and form a chain which extends ~800 km sub-parallel to the shelf of Marie Byrd Land (Fig. 7.1). Most of the large volcanoes appear to be elongated in an E-W or NW-SE-direction. According to the bathymetric maps derived from satellite gravity data (predicted bathymetry; Smith and Sandwell 1997) smaller volcanoes and ridge-like structures appear to be scattered irregularily between this chain and the shelf. Multi-beam mapping of four of the Marie Byrd Seamounts on former cruises (RV *Nathaniel B. Palmer* [1996], RV *Polarstern* ANT-XI/3 [1994], and ANT-XVIII/5a [2001]) revealed oval-shaped or round, flat-topped, guyot-type seamounts with several small volcanic cones on their tops and flanks (e.g., Miller and Grobe 1996, Feldberg 1997).

On cruise ANT-XXIII/4 five Marie Byrd Seamounts and associated features have been surveyed and dredged (Fig. 7.1). Additionally a multi-beam survey has been carried out between the Marie Byrd Seamounts and the shelf of Marie Byrd Land, in an area where the satellite-derived bathymetry maps show a large, roughly circular seamount (~28 km in diamater and 1,300 m high) and many smaller features being possibly of volcanic origin (Fig. 7.1). However, the multi-beam data revealed that the satellite-derived bathymetry failed, i.e. the large seamount and other individual volcanic edifices appearing in the predicted bathymetry do not exist. The area is dominated by flat, sediment-covered ocean floor and two ridge-like structures which strike in N-S and NW-SE-direction, respectively. Small cone-like structures, being most likely of volcanic origin, are situated on both ridges and may point to a volcanic rather than to a pure tectonic origin for the ridges. Appropriate dredge sites, however,

could not be identified in this area. Therefore the decision was made to stop any survey south of the Marie Byrd Seamounts and to continue further north at the major volcanoes.

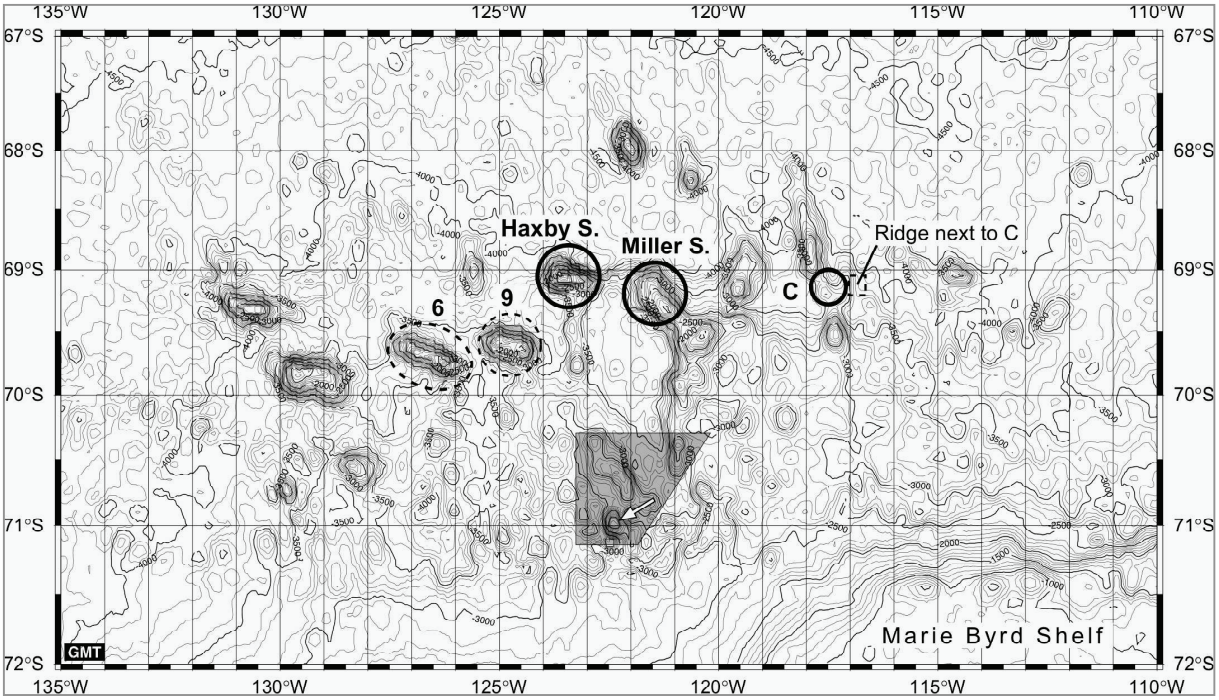

Fig. 7.1: Bathymetric map derived from gravity data (Smith and Sandwell 1997) showing the Marie Byrd Seamount Province. Dredging on cruise ANT-XXIII-4 yielded in-situ volcanic rocks at the Haxby and Hubert Miller Seamounts and Seamount "C" (marked by thick black circles). Sampling of in-situ volcanic rocks failed at Seamounts "6" and "9" and a ridge-like structure east of Seamount "C" (marked by dashed lines). A multi-beam survey between the Marie Byrd Seamounts and the shelf (shaded area) did not reveal any sites appropriate sites for dredging. Note that the large cone-like structure (marked by white arrow) at the southern edge of the survey area does not exist.

Mapping and sampling of the Marie Byrd Seamounts was originally planned along a W-E profile comprising most of the largest seamounts. However, due to time constraints the profile had to be reduced to the "central part" of the Marie Byrd Seamounts (Fig. 7.1). The westernmost studied seamount (hereafter called "Seamount 6") appears to be one of the largest Marie Byrd Seamounts and has not been surveyed previously. Multi-beam mapping of its eastern part revealed the seamount to be a huge guyot with a oval-shaped, steep-sided base and flat top except for several smaller volcanic cones. The base of the seamount lies at ~2,800 – 3,000 m below sea level (b.s.l.), measures ~80 x 20 km (length according to satellite-derived bathymetry), and strikes in WNW-ESE-direction. The flat top (~1,600 m b.s.l. at the edges and ~1,350 m b.s.l. in the centre) is interpreted to be an erosional platform being formed by wave activity at sea level. The younger volcanic cones appear to be well preserved, rise to depths of 1,140 m b.s.l. and must have formed after the seamount subsided below wave base. Three dredge hauls were made at Seamount 6: PS69-311-1 on a small cone on the southwest slope, PS69-312-1 on a steep slope just beneath the eastern plateau edge and PS69-314-1 on a small cone

on its northern flank. All dredges yielded large amounts of dropstones but failed to produce any *in-situ* material (except of a few biological samples).

Another large seamount (hereafter called “Seamount 9”) appears on the satellite-derived bathymetry maps approximately 25 nm east of Seamount 6. A WNW-ESE-running multi-beam track across Seamount 9 recorded on RV *Nathaniel B. Palmer* cruise in 1996 (J.M. Stock pers. comm. 2006) reveals a guyot with an oval-shaped, ~25 km long base that rises to a flat, wave-eroded plateau. The outer part of the plateau occurs at a depth of 1,600 m b.s.l. and the interior at a depth of ~1,500 m. Small cones and ridges are situated on the flanks and on top of the plateau. Several cones form a WNW-ESE-trending chain which emanates from the base of the volcano in WNW direction. These aligned cones are interpreted as volcanic rift zone. A single dredge (PS69-315-1) of a cone-like structure belonging to the volcanic rift on the western flank produced – apart from huge amounts of dropstones – Mn-crusts, fossil corals and two lava fragments of unclear origin (porhyric evolved lava and heavily altered basalt). In view of the shallower slope angles compared to the Haxby Seamount (see below), no further dredging was attempted.

The Haxby Seamount (provisionally named) lies approximately 40 nm northeast of Seamount 9 and has completely been mapped on the RV *Nathaniel B. Palmer* cruise in 1996 and morphologically studied in detail by Feldberg (1997). Haxby is an roughly circular guyot volcano, ~30 km in diameter. It rises from the abyssal plain at ~4,000 m b.s.l. to a flat top between 1,600 - ~1,200 m and has numerous <2 km diameter cones constructed on its flanks and top. The most remarkable feature of Haxby is the presence of a slightly curvilinear volcanic rift system with abundant cones on its top emanating from the eastern edge of the guyot and extending > 30 km to the east. A less pronounced, ~12 km long chain of volcanic cones and ridges emanates to the west and may be the western continuation of the volcanic rift system. Four dredge hauls were made on Haxby: PS69-316-1 on the lower S-slope of the western volcanic rift yielded only dropstones. PS69-317-1 was made on the upper southern slope beneath the plateau edge and contained, besides dropstones, several up to 70 x 40 cm sized, freshly broken fragments of carbonate cemented volcanic breccia. The breccia contains numerous aphyric basaltic clasts up to 8 cm in size, representing the first *in-situ* volcanics which have ever been sampled at the Marie Byrd Seamounts. Dredge haul PS69-318-1 on the south-eastern plateau edge yielded two pieces of completely altered volcanic breccias, Mn- and dolomitic ((?)) crusts, fossil corals and numerous dropstones. A similar result produced dredge PS69-319-1 on the southern flank of the eastern volcanic rift.

The Hubert Miller Seamount is located ~40 nm ESE of Haxby and has been partially surveyed on RV *Polarstern* cruise ANT-XVIII/5a in 2001 (K. Gohl pers. com. 2005). Miller appears to be the largest of the Marie Byrd Seamounts, being some 75 x 50 km at the base and elongated in a NW-SE direction. It rises from ~3,600 – 4,000 m b.s.l. to a plateau between 1,600 - 1,200 m b.s.l.. Small cones and ridges occur frequently on the flanks but only rarely on the top plateau of the volcano. Several small, up to 8 km long ridges, interpreted to be volcanic rift zones, emanate from the base mostly towards western, north-western, and northern directions. Out of six dredges carried out at Miller Seamount four contained *in-situ* lava fragments (besides volcanics of unclear origin, various crusts and varying amounts of

dropstones): PS69-320-1 was made on a small volcanic rift on the lower NW-slope and yielded vesicular, aphyric lava. PS69-321-1 produced several ol-cpx-phyric lava fragments from a steep slope just beneath the SE plateau edge. PS69-324-1 was carried out on the lower SE slope beneath a cone-like structure and yielded dense, (ol)-fsp-cpx-phyric basalt lava fragments and numerous pieces of a carbonate((?))-cemented, Mn-encrusted volcanic breccia. PS69-325-1 yielded vesicular fsp-phyric lava fragments from a cone-like structure on the upper southern flank of Miller Seamount. PS69-322-1 carried out on the southern slope was empty and PS69-323-1 on the slope beneath the southern plateau edge contained only a few dropstones.

On RV *Polarstern* cruise ANT-XI/3 in 1994, a seamount some 75 nm east of Miller Seamount has been mapped (Miller and Grobe 1996). This seamount (hereafter called „Seamount C“) does not appear in the bathymetric maps derived from satellite gravity data. The mapping showed Seamount C to be a smaller volcano than the other studied volcanoes, ~17 km in diameter at the base (depth 3,500 m b.s.l.). It is a guyot with a crudely circular base that rises to a flat plateau (~7 km in diameter). The outer part of the plateau occurs at a depth of 2,400 m and the interior at a depth of 2,200 m. Small cones and ridges were identifiable on the flanks and on the top plateau. Volcanic rifts emanate from the base in northern and southern directions. A single dredge (PS69-327-1) of a cone at the lower western flank of Seamount C yielded numerous vesicular, ol-fsp-phyric pillow fragments and dense, fsp-phyric pillow fragments. Approximately 15 nm east of Seamount C appears a N-S-striking, ridge-like structure in the multi-beam maps. The ridge has steep flanks and a flat top, is 7 – 8 km wide, ~300 m high and shows some small volcanic cones on its flanks and top area. Two attempts were made to dredge the western flank of this ridge: PS69-328-1 produced large amounts of semiconsolidated sediment which contained some small lava fragments of unclear origin, PS69-329-1 was empty.

Marie Byrd Seamount Summary (Morphology)

The most striking feature of all studied Marie Byrd Seamounts is their guyot-like form, characterized by steep sides and a relatively flat top. The morphology of these seamounts is consistent with an erosional origin for these platforms. They have once formed island volcanoes which were eroded at sea level and subsequently subsided to their present position. The inward shoaling of the platforms is consistent with subsidence occurring contemporaneously with erosion at sea level to form the platform. The total net subsidence of seamounts 6, 9, Haxby, and Miller, represented by the depth of the basal erosional platform, is ~1,600 m and indicates that these seamount/ocean island complexes may have formed at approximately the same time. The plateau of Seamount C, however, is situated significantly deeper (2,400 m b.s.l.). This observation suggests either higher subsidence rates for the eastern Marie Byrd Seamounts or formation of Seamount C prior to the other seamounts. Small cones located on the top platforms of most guyots must have formed after the erosional platforms subsided below wave base and therefore represent a late stage or post-erosional phase of volcanism. The multi-beam data gained on former cruises and the new data of cruise ANT-XXIII/4 furthermore confirm the predominance of E-W or NW-SE-trends of structural features as it is indicated by the satellite-derived bathymetry at least for the central Marie Byrd Seamounts. Farther east at Seamount C, however, N-S-directions appear to dominate.

References

Bradshaw JD, Pankhurst RJ, Weaver SD, Storey BC, Muir RJ, Ireland TR (1997) New Zealand superterranes recognized in Marie Byrd Land and Thurston Island. The Antarctic Region: Geological Evolution and Processes: 429-436.

Broch OA (1927) Gesteine von der Peter I.-Insel, West Antarktis. Avh Nor Vid Akad Mat Naturv Kl 9: 1 – 41.

Feldberg JM (1997) A Geophysical Study of Seamount E, Bellinghausen Sea, Antarctica. Unpubl. Bachelor thesis, Wesleyan Univ, Middletown, Connecticut: 84p.

Hart SR, Blusztajn J, Craddock C (1995) Cenozoic volcanism in Antarctica: Jones Mountains and Peter I. Island. Geochim Cosmochim Acta 59, no 16: 3379 – 3388.

Prestvik T, Duncan RA (1991) The geology and age of Peter I. Øy, Antarctica. Polar Research 9: 89 – 98.

Prestvik T, Barnes CG, Sundvoll B, Duncan RA (1990) Petrology of Peter I. Øy (Peter I. Island), West Antarctica. J Volcanol Geotherm Res 44: 315 – 338.

Miller H, Grobe H (1996) Die Expedition ANTARKTIS-XI/3 mit FS *Polarstern* 1994, Berichte zur Polarforschung 188: 1 – 115.

Smith WHF, Sandwell DT (1997) Global seafloor topography from satellite altimetry and ship deep soundings. Science 277: 1956-1962.

Weaver SD, Storey BC, Pankhurst RJ, Mukasa SB, DiVenere VJ, Bradshaw JD (1994) Antarctica-New Zealand rifting and Marie Byrd Land lithospheric magmatism linked to ridge subduction and mantle plume activity; Geology 22: 811-814.

8. GEOLOGY ON LAND

Composition and evolution of cenozoic volcanic complexes and the crystalline basement of Marie Byrd and Ellsworth Land

Reinhard Werner[1)], Kristin Daniel[2,4)], Folkmar Hauff[3)], Andreas Veit[4)]

[1)] Tethys GmbH, Kiel
[2)] Alfred-Wegener-Institut, Bremerhaven
[3)] IFM-GEOMAR, Kiel
[4)] Institute of Geosciences, University of Jena

Objectives

The land geology programme proposed by the University of Jena for RV *Polarstern* cruise ANT-XXIII/4 originally focussed on the Cenozoic Hudson Mountains volcanic field, located in western Ellsworth Land east of the inner Pine Island Bay (Fig. 8.1). The planned studies included facies analyses and sampling of several nunataks and detailed studies of tephra layers which are believed to have formed during an eruption in 1985 and should be preserved within snow and ice profiles. These investigations aimed at reconstructing the original, magmatic, and volcanic evolution of the Hudson Mountains and the interaction of volcanism with the West Antarctic Ice Sheet. However, the field work in the Hudson Mountains was restricted to a reconnaissance field programme at two nunataks since RV *Polarstern* could stay in the inner Pine Island Bay only for a few days due to ice conditions on the shelf of Marie Byrd Land. Instead, a second field expedition could be carried out to Mt. Murphy, a large volcano located further to the west in eastern Marie Byrd Land and south of the western Pine Island Bay (Fig. 8.1). The field studies, reconnaissance sampling and subsequent land based analyses of the volcanic rock samples from Mt. Murphy and the Hudson Mountains aim to reconstruct the composition and origin of the studied volcanoes in order to contribute to a better understanding of causes and effects of the Cenozoic intraplate volcanism in West Antarctica. Considering that Mt. Murphy and the Hudson Mountains are situated on different crustal blocks, the comparison of the data obtained from both volcanic complexes may also help to characterize the influence of the crustal structure and composition on the composition and eruption processes of these volcanoes. Furthermore, volcanological studies could provide information on the paleo-ice presence and thickness at times of activity of the volcanoes in both areas.

The discovery of accessible basement outcrops at the coast of Marie Byrd Land led to the integration of an additional land geology programme into the cruise schedule. This programme comprised several expeditions and helicopter surveys, mainly carried out in combination with the GPS deployment or helicopter magnetics flights, in order to collect samples of the crystalline basement in eastern Marie Byrd Land and to survey and sample island chains in the inner Pine Island Bay (Fig. 8.1). The primary goal of these investigations is to contribute to the characterization of the

composition and age of the basement and to constrain the nature of the islands (e.g., volcanic or crystalline basement??). The data yielded by the observations during helicopter flights and analyses of the basement rock samples should provide important background information for the geophysical studies on RV *Polarstern* cruise ANT-XXIII/4 and may contribute to a model of the geodynamic evolution of the West Antarctic continental margin and Pine Island Bay. In the frame of this new land geology programme we also tried to identify and sample mafic dykes, which have penetrated the crystalline basement. Storey et al. (1999) have described such dykes from Marie Byrd Land and relate them to the final phase of the Gondwana break-up, i.e. the Late Cretaceous separation of the New Zealand micro-continent from Marie Byrd Land (see also Chapter 7). Geochemical analyses of the rock samples yielded from those dykes may therefore provide valuable information on the geodynamic processes which caused the continental break-up (cf. Storey et al. 1999), and therefore will complement the studies of the Marie Byrd Seamounts (see Chapter 7).

Methods and equipment

Most land expeditions have been carried out by the helicopters of RV *Polarstern*. The high level of experience of the pilots from HeliTransair and their willingness to support our studies made it possible to access outcrops in remote areas even in difficult flight conditions. One basement outcrop has been sampled using a zodiac of RV *Polarstern*. In volcanic areas, all units being accessible from the landing site have been described, documented using digital cameras, and sampled. Suitable samples of sheet and pillow lavas have an unweathered and unaltered groundmass, empty vesicles, glassy rims (ideally), and - if present - fresh phenocrysts. Additionally representative samples of volcaniclastic rocks (i.e., hyaloclastites) have been taken from most units. Sampling of basement outcrops and dykes was aimed at receiving a rather large volume of fresh material to enable us to carry out material-consuming land-based analyses, such as separation of zircons and monazite from granitic rocks for age dating. Once back on board, all samples were described in detail and photographed. Representative samples were cut for thin section and microprobe preparation, geochemistry, and further processed to remove alteration products on their surfaces. Each of these sub-samples, together with any remaining bulk sample, was labelled and finally sealed in plastic bags for transportation to IFM-GEOMAR or the University of Jena.

Results

Altogether 26 volcanic rocks samples, 16 samples of crystalline basement rocks (incl. 2 xenolithes enclosed in granites), and a sample of a mafic dyke have been taken during the land expeditions of ANT-XXIII/4. This section gives background information on the sampled structures and short summaries of the sampled rocks. Refer to table 8.1 (volcanic rocks) and table 8.2 (basement rocks and dykes) for latitude and longitude of sampling sites and sample descriptions.

Hudson Mountain volcanic field

The Hudson Mountains are located in western Ellsworth Land in West Antarctica at 73°45’ to 74°55’S and 98°20’ to 100°30’W east of Pine Island Bay (Fig. 8.1). The volcanic field extends ~150 km in N-S direction, is ~60 km wide and consists of numerous small volcanic nunataks (< ~500 m high) and a couple of larger volcanic structures, among them Mt. Moses (749 m) and Mt. Manthe (567 m) and Shepherd

Dome, believed to be the centre of an eruption in 1985. Until today, not much is known of this large volcanic field, because prior to ANT-XXIII/4, the Hudson Mountains were studied only once during a reconnaissance field campaign in 1968 (e.g., Wade and La Prade 1969, Wade and Wilbanks 1972). Based on observations during the 1968 campaign it was proposed that the Hudson Mountains volcanic field is formed by 3 major units: (1) lower (subaqueous??) lava flows, (2) a middle hyaloclastite sequence, and (3) upper subaerial lava flows. Sparse geochemical data suggest that alkaline olivine-phyric basalt dominates in the Hudson Mountains. K/Ar-dating of clasts found in the hyaloclastite sequence and of the upper lavas yielded ages of ~5-6 Ma (LeMasurier and Rex 1982).

Shepherd Dome was originally a major target of the ANT-XXIII/4 land expeditions to the Hudson Mountains, in particular for detailed tephra studies. However, pictures taken by the British Antarctic Survey (BAS) in 2004 and our own helicopter survey proved that Shepherd Dome is almost completely covered by snow and ice, apart from a few small and isolated hyaloclastite outcrops. Considering the available time for field work and the necessity to get an appropriate sample set for land-based analyses, we decided to focus instead on Mt. Moses whose upper part appeared almost completely exposed on the BAS pictures (Fig. 8.2a).

Mt. Moses is located at ~74°33,5´S and 99°11,0´W in the central part of Hudson Mountains volcanic field and consists of a wide basal complex overlain by a NNE-SSW-trending ridge-like structure which forms the top area. Only relatively small areas of Mt. Moses are covered by ice or snow, and outcrops are common. Most slopes of the volcano are strewn with lava fragments, predominately cm- to dm-sized pillow lava fragments which cover *in-situ* pillow lavas or, more rarely, hyaloclastites. Field work and a helicopter survey proved that Mt. Moses has significantly been eroded. Wall-like outcrops of dykes in the top area indicate that the volcano was considerably higher prior to erosion.

Field work and sampling was carried out over 2,5 hours on the western slope of Mt. Moses between ~480 and 580 m elevation. One team concentrated work upslope SE of the landing site on a small plateau at 74°32.79´S and 99°10.31´W in 500 m elevation (Fig. 8.2a), where a complex series of hyaloclastite deposits were exposed and covered upslope by pillow lava. A second team sampled a large pillow lava field and adjacent hyaloclastite deposits west of the landing site. Six units of Mt. Moses were documented and sampled:

(1) A lower, massive hyaloclastite body. The hylaloclastites are very homogeneous, coarse-grained, contain only a few larger lava clasts and appear to form large parts of the western base of the volcano (Sample P26).

(2) A large lower pillow lava complex formed on (the flank) of the massive hyaloclatites. This pillow lava field extends from the helicopter landing site all the way down slope to the base of the mountain. The pillow tubes are mostly between 0.3 and 0.8 m in diameter. The lava is quite aphyric, fresh, and contains 20 - 25 % unfilled vesicles. In places E-W striking glacial lineations indicate that the rocks were covered by ice after emplacement and experienced glacial movements (Samples P12 – P14).

(3) A layered middle hyaloclastite sequence being deposited on the massive lower hyaloclastites (1) and obviously banked against the lower pillow complex (2). The hyaloclastites are bedded with normally graded beds ranging in thickness from a few cm to 1 – 2 m. Fine-grained, thinly bedded (cm-range) layers show cross-bedding, ripples, dunes etc. which suggest a transport direction from N or NNW towards S or SSE (Samples P24 and P25).

(4) A (partly irregular) layered upper hyaloclastite sequence which appears to cover hyaloclastite (3). These hyaloclastites show a broad variety of sedimentary structures which have not been studied in detail due to lack of time. This hyaloclastite sequence is at least 50 m thick and probably (mainly) epiclastic. Vesicular, aphyric pillow-like lavas have penetrated the upper part of this sequence in some places (Sample P21).

(5) An upper pillow complex, being most likely quite large as suggested by extensive areas covered by pillow lava fragments east of the upper hyaloclastite (4). Except of a few tubes, the *in-situ* pillows are almost completely covered by debris. The pillows are fresh, vesicular and quite aphyric (Sample P20).

(6) A small (~20 x 50 x 5 m) pillow complex in unclear stratigraphic position. These pillows cannot easily be linked to the pillow complexes (1) or (5). Field relationships suggest that these pillows may have been intruded in the lower part of the upper hyaloclatites (4) or, alternatively, have been covered by these hyaloclatites. The lava is fresh, highly vesicular, and has a fine-grained matrix with small olivine and feldspar phenocrysts (Sample P22).

Apart from the units described above, a SE-NW-striking dyke has been sampled which has penetrated the lower pillows (2). The dyke rocks are ol-fsp-phyric with a fine grained matrix and clearly show columnar jointing perpendicular to the surfaces of the dyke (Sample P23).

Additionally a GPS deployment at Mt. Manthe has been used to sample a lava plateau at the west side of this volcano at 74°46,8´S and 99°22,2´W in 528 m elevation. The plateau is formed by a succession of (subaerial?) lava flows which cover huge hyaloclastite cliffs. Massive and layered hyaloclastites (Sample P16), partly penetrated (??) by pillow-like lavas, have also been deposited on the plateau forming lava flows. The lavas exposed on the surface of the plateau are vesicular ol-cpx-fsp-phyric basalts with a fine-grained matrix (Samples P17 - 19).

A first evaluation of our field observations in the Hudson Mountains suggests that at least Mt. Moses consists of a complex succession of pillow lavas and various hyaloclastite complexes. Helicopter surveys and field work proved that thick successions of subaerial lava flows do not exist at Mt. Moses (however, we cannot exclude the occurrence of minor subaerial deposits). Taken together, the volcanic deposits forming Mt. Moses appear to be not consistent with the succession lower lavas - middle hyaloclastite - upper subaerial lavas being previously proposed for the Hudson Mountain volcanic field.

Mt. Murphy volcano

Mt. Murphy is about 25 km in diameter and rises 2,445 m above sea level. Its complex edifice is marked by an E-W elongated central part, three prominent ridge-like structures which extend to the northeast and north, respectively, and a less prominent ridge-like extension at its western side (Fig. 8.2b). By contrast to the Hudson Mountains (see above), Mt. Murphy belongs to the more intensely studied volcanoes of Antarctica (e.g., LeMasurier and Rex 1982, Smellie 2000, Smellie 2001, LeMasurier 2002, Wilch and McIntosh 2002). The lower half of the volcano is dominated by basaltic pillow lavas and hyaloclastite breccias with intercalated tillite. This basal section is overlain by subaerial basalt and trachyte lavas (Smellie 2000). Smellie points out that the main edifice of the volcano has been constructed relatively quickly between 8 and 9 Ma. Younger satellite centres on the west side, being active between 7 and 4.5 Ma, are considered as remains of several small dissected, predominantly basaltic Surtseyan volcanoes. Mt. Murphy underwent postvolcanic overriding by ice sheets as indicated by striated surfaces and basement-derived erratic found up to 1,800 m above sea level on the flanks of the volcano. According to LeMasurier (1990) Mt. Murphy is considered a dormant volcano.

The upper 2,000 m of Mt. Murphy elevate above the surrounding ice sheet and are partly outcropped. The majority of the relatively easily accessible outcrops are located at the west side of the volcano (Smellie, pers. com. 2006). Therefore the decision was made to start field work at Turtle Rock (Fig. 8.2b), a superbly exposed, steep-sided complex with a relatively flat top. The field work and sampling had been carried out over ~2 hours in its top area around the landing site at 75°22.16´S and 111°17.65´W in 700 m elevation. A couple of days later additional sampling was possible during pick up of the GPS station. The top area of Turtle Rock mainly consists of massive hyaloclastites with various amounts of lava clasts and intercalated (pillow) lavas. Two pillow-hyaloclastite sequences, a hyaloclastite complex (incl. lava clasts), and a lava flow have been documented and sampled. A common feature of the lavas is their high vesicularity. They are fresh and contain ol+fsp(±cpx)-phenocrysts in a fine grained matrix (Samples P1, 2, 7, and 10). The hyaloclastites (Samples P3, 5, and 9) are relatively coarse-grained, mostly massive, and contain various amounts of lava clasts (Samples P4, 5, and 9). Helicopter observations suggest that the entire exposed volcanic edifice of Turtle Rock mainly consists of thick hyaloclastite sequences with minor intercalated lavas.

A subsequent helicopter survey proved that the southern part of Mt. Murphy was completely covered by snow and ice. By contrast huge cliff sections, apparently consisting mainly of hyaloclastite, are exposed in the central and north-eastern part of the volcano. However, it proved difficult to find appropriate landing sites in this area because of the jagged morphology and the wind conditions. However, it was possible to land further to the north on a small plateau formed by a succession of (most likely subaerial) lava flows. The plateau is located at 75°17.05´S and 110°15.25´W in 600 m elevation at the western edge of the eastern ridge-like extension of Mt. Murphy (Fig. 8.2b). According to helicopter observations the ridge-like structure consists of huge hyaloclastite successions overlain by a ~50 to 100 m thick sequence of (most likely subaerial) lava flows. Accordingly the plateau is formed by a lava flow with a heavily eroded surface and covered with lava fragments obviously mainly derived from the same flow. An *in-situ* sample from this relatively

dense, ol-cpx-fsp phyric lava could be taken at a small step within in plateau (Sample P8).

Marie Byrd Land basement

The crystalline basement of Marie Byrd Land was sampled at two sites at the coast of the western Pine Island Bay (Fig. 8.1). At the north-western coast of Wright Island, steep cliffs, exposed beneath shelf ice, have been surveyed by helicopter. The cliffs proved inaccessible, but a small island appeared accessible. The island obviously consists of the same lithology as the cliffs and could be successfully sampled by zodiac. The obtained rocks are fresh and represent relatively fine-grained quartz-granodiorite. Dark, biotite-rich inclusions and very small dykes (mainly cm-range) are common (Samples PS69/277-1-1 to –7).

A second basement outcrop was sampled by helicopter at the western coast of Bear Peninsula (Fig. 8.1). The exposed rocks in the area of the landing site are very fresh, coarse-grained biotite granites. A weakly developed foliation of the granites, the common occurrence of dark xenolithes (most likely meta-sediments), and intercalated “chert-like” layers may indicate that this outcrop represents the edge (or roof) of a batholith (Samples BI-1 to -7).

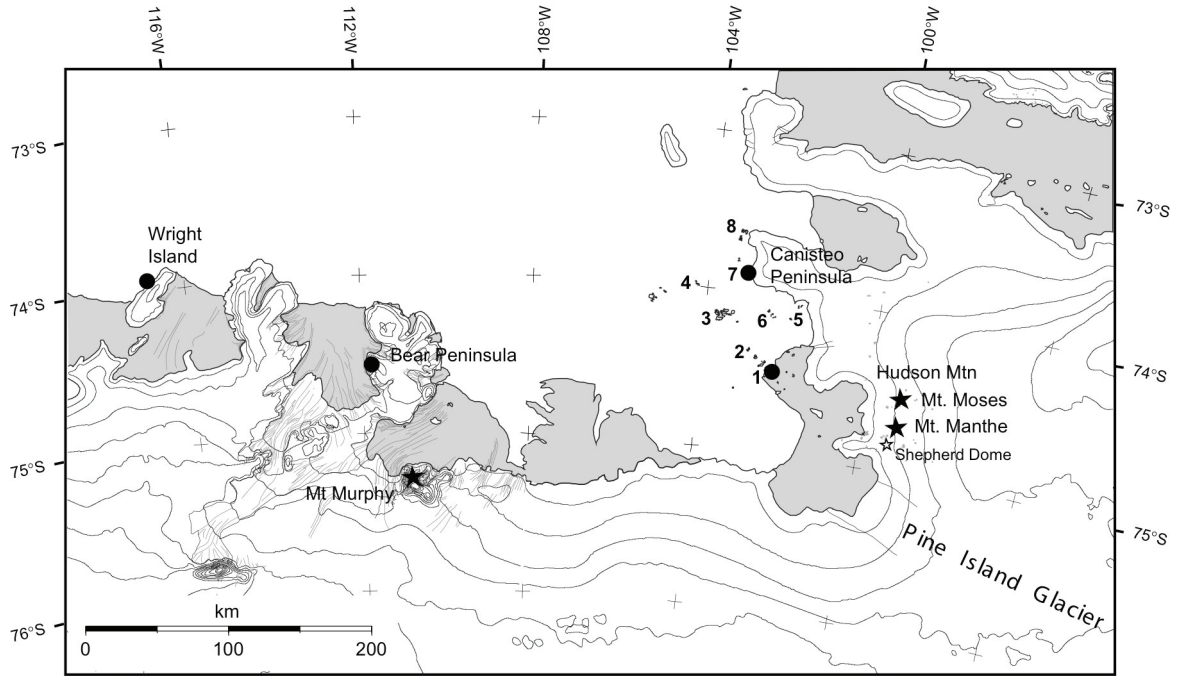

Fig. 8.1: Overview map of the Pine Island Bay area showing the surveyed islands (marked by numbers) and sampling sites on land. Stars indicate studied volcanoes, black dots sampled outcrops of crystalline basement (1 – Backer Islands SE, 2 – Backer Islands NW, 3 – Brownson Islands, 4 – Jaynes Islands, 5 – McKinzie Islands, 6 – Suchland Islands, 7 – Edwards Islands, 8 – Lindsey Islands).

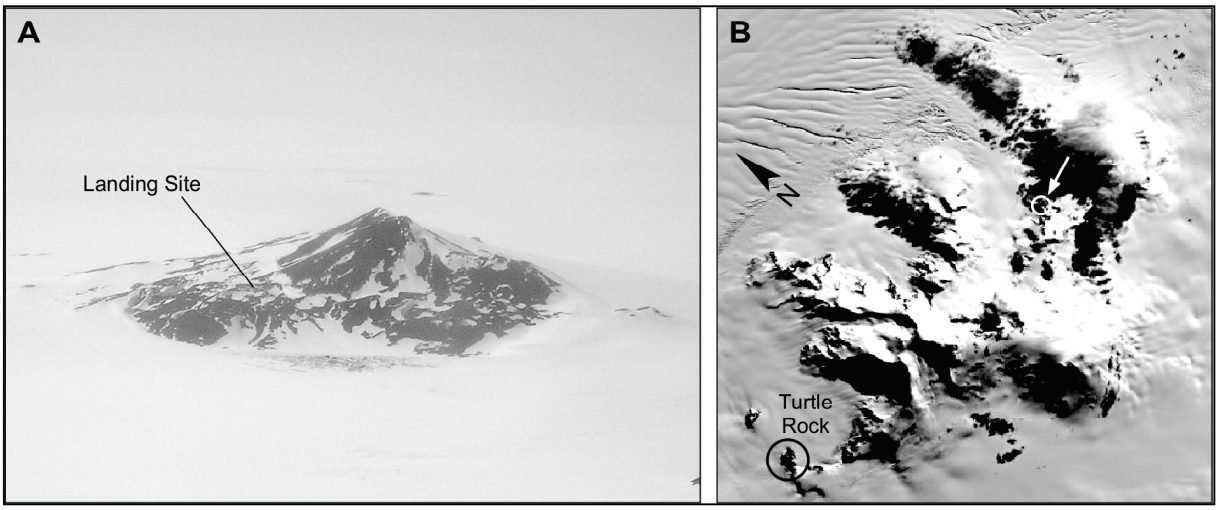

Fig. 8.2: (A) Air photograph showing Mt. Moses. (B) Satellite picture of Mt. Murphy. Samples were taken from Turtle Rock (black circle) and from a lava plateau at the western edge of the eastern ridge-like extension of Mt. Murphy (white circle and arrow; sampling site covered by clouds).

Islands of the eastern Pine Island Bay

Altogether 8 islands and island groups, respectively, were surveyed in the eastern Pine Island Bay (Fig. 8.1, Table 8.2). Four of them (e.g., Backer Islands SE and NW, Brownson Islands, Jaymes Islands) belong to a prominent SE-NW-striking island chain which extents from southern Ellsworth Land ("Evans Knoll") over the ice shelf of the Pine Island Glacier into the bay. All of these islands appear to consist mainly of granitic rocks. A GPS station has been deployed on an unnamed island in the southern area of the Backer Island group. During pick up of this GPS station we had the possibility to visit and sample this island which is mainly formed of biotite granite. Meter-sized blocks of quartz-feldspar granite, possibly formed by metasomatic processes, occur as inclusions in the biotite granite. Fine-grained leuco-granite occurs as minor lithology on this island (Samples PS69/PIB-1 to –3).

Additionally 4 island groups off the coast of Canisteo Peninsula were surveyed. The McKinzie and Suchland Islands, being located south of Canisteo Peninsula, appear to consist also entirely of granite. On the Edwards and Lindsey Islands west off Canisteo Peninsula, however, approximately E-W-striking mafic dykes cut through the granitic bedrock. One of the Edwards Islands, being inhabited by elephant seals, has been sampled by helicopter. The dykes are up to some meters thick and consist of dense, fine-grained volcanic rocks with ~20 % feldspar phenocrysts (up to 1 cm in size). The granitic bedrock contains up to 50 % metasomatized quartz (Samples PS69/LI-1 to -3).

Taken together, crystalline basement rocks dominate on the island groups of the Pine Island Bay, indications for Cenocoic volcanic activity or rocks have not been found. It is remarkable, however, that the discovery of mafic dykes occurs commonly on the island groups west of Canisteo Peninsula.

Tab. 8.1: Sampling site locations at land volcanoes and rock sample descriptions (Mt. Murphy, Mt. Manthe, Mt. Moses).

MOUNT MURPHY

complex shield volcano

location Turtle Rock, W of Mount Murphy, lat 75°22.158'S , long 111°17.652'W

SAMPLE #	altitude [m]	DESCRIPTION
P1	713	vesicular pillow lava that intruded into wet hyaloclastite. Dark matrix with few phenocrysts of fresh olivine and minor feldspar. Flow structures are preserved
P2	713	outer part of pillow lava P1 with radial cooling structures, matrix is similar to P1 and contains olivine.
P3	713	hyaloclastite into which pillow lava P1 and P2 intruded, free of sediment structures, unsorted material (1mm- several cm), contains different components such as lava clasts often with glass crusts, or small palagonitic glass fragments
P4	695	inner part of a lava fragment located within a hyaloclastite complex, denser than samples P1 and P2, matrix is light grey containing olivine and pyroxene phenocrysts, yellowish surface alteration
P5	695	hyaloclastite (hostrock of lava fragment P4), consisting for the most part of small lava clasts 0.5-15mm (always with glass crusts), but also bigger fragments occur which are sometimes covered with glass crusts. Lots of free olivine crystalsare present between the clasts
P6	695	bigger lava fragment recovered from hyaloclastite P5, similar to sample P4 but contains more olivine
P7	695	lava sample of a larger flow, vesicular lava for the most part but denser vesicle free parts also exist, fine grained greyish matrix with olivine, fsp, px phenocrysts.
P9	695	hyaloclasite, no sedimentary structures visible, contains mostly clasts ranging from <0,5mm to 2cm size, smaller fragments often consists of glass (palagonitic) crusts, bigger clasts are not always associated with glass. Overall samples is quite fresh with partial surface alteration.
P10	695	pillow rim from a smaller lava flow or intrusion into wet hyaloclastite (P9), typical radial cooling structures, vesiculs (<8mm), fine grained matrix with altered olivine, fsp (1-5mm), px (~1mm)
P11	695	lava fragment recovered from hyaloclastite P9, rim area is quite vesicular with subparallel aligned vesicles, inner part is dense with essentially no vesicles. Here the matrix is dark grey and contains 0,5 - 3mm sized ol, fsp and px phenocrysts

location in eastern part of Mt. Murphy, lat 75°17.048'S, long 110°15.254'W

SAMPLE #	altitude [m]	DESCRIPTION
P8	600	sample of a lava flow, mostly very dense with only small vesicles (<0,5mm), very fine grained matrix, contains olivine (0,5 - 1mm), px, fsp (1 - 3mm), but fsp- megacrysts > 2 cm also occur

MOUNT MANTHE

glacial volcano with a huge plateau

on top of the plateau, lat 74°46.752'S, long 99°22.086'W

SAMPLE #	altitude [m]	DESCRIPTION
P16	528	hyaloclastite desposited on the plateau forming lava flow, subparallel sediment structures which are internally unsorted and contain variable fragments: lava clasts with glass crusts, angular xenoliths (palagonitic?), olivine, fsp, px phenocrysts are also present
P17	528	basalt, from plateau formimg lava flow. Fine grained greyish matrix with olivine (1- 2mm), px (~0,5mm), fsp (~1mm) phenocrysts, vesicular.
P18	528	similar to P17 except for different structure of vesicles
P19	528	similar to P17

MOUNT MOSES
complex sub/englacial volcano
lat 74°32.790'S, long 99°10.310'W

SAMPLE #	altitude [m]	DESCRIPTION
P12	471	pillow lava 200m SW of helicopter landing spot. Vesicular, fine grained matrix with phenocrysts (fsp, some olivines), matrix itself contains small fsp- crystals (0,2- 0,5mm) and px (<0,5mm) Pillow lava tube, 0.3m in diameter. Slight secondary alteration along cooling cracks.
P13	471	glass sand, out of weathered glass crusts of the pillow lava, 90% are glass fragments ~10% are small vesicular lava fragments, average size of all: 1- 2mm
P14	471	rims of pillows (10- 15cm thick) with 0,5- 1cm thick glass crusts, different forms of vesicles show cooling structures, dark grey matrix, fine grained with phenocrysts (fsp, ol, px, all ~0,5mm in size)
P15	471	sub rounded 10x8x5cm pebble of ol rich lava fragment from the landing spot. 15-20% 1-2mm fresh olivine phenocrysts that are evenly distributed in the vesicular (15%) matrix, idicating a non-cumulus origin. Vesicles are unfilled and < 0.4mm. Although this sample is not in-situ, it stems very likely from this volcano.
P20	557	vesicular pillow lava, vesicles mimic flow structures, 0,5-1cm thick glass crust, not always preserved, only in the inner part grey, fine grained matrix with fsp and minor olivine phenocrysts
P21	477	hyaloclastite, below P20, contains internal sediment structures that are defined through different percentages of lava and glass clasts (palagonitic), with only little matrix, the smaller fragments are mostly glass clasts, some olivines are also present (<1mm)
P22	480	basalt from a smaller pillow unit, with glass crusts (2- 3cm thick), basalt shows typical cooling structures, dark grey fine grained matrix with fsp, ol phenocrysts
P23	470	basalt lava from a dyke, fine grained greyish matrix with phenocrysts fsp 0,5- 1mm, olivine ~0,5mm
P24	470	very fine grained hyaloclastite, mostly consists of small glass fragments and some minerals, no matrix, (palagonitic), sedimentary structures with ripples and some antidunes, the finer layers are more resistant to weathering
P25	470	hyaloclastite, 1m below P24, more coarsly grained in the upper part of the sample but finer in the lower, similar to P24
P26	464	hyaloclastite, about 5m below P24 and P25, unsorted but very homogenous, yellow color comes from palagonite, average size of fragments 1- 7mm, fragments are mostly glass clasts

Tab. 8.2: Names, positions and major lithologies of islands in the eastern Pine Island Bay which was surveyed and partly sampled by helicopter.

Islands	Lat.	Long.	Lithologies
SE-NW-trending island chain:			
Backer Islands SE (GPS-Station)	74°30,7´S	102°26,4´W	Granite (Samples PIB 1 – 3)
Backer Islands NW	74°20,9´S	102°50,7´W	Granitic Rocks
Brownson Islands	~74°10´S	~103°40´W	Granitic Rocks
Jaynes Islands	~73°58´S	~104°15´W	Granitic Rocks
Islands off Canisteo peninsula:			
McKinzie Islands	74°02,7´S	101°44,4´W	Granitic Rocks (?)
Suchland Islands	~74°05´S	~102°32´W	Granitic Rocks
Edwards Islands	73°51,2´S	102°59,3´W	Granite, mafic dykes (Samples ELE 1 – 3)
Lindsey Islands	73°37,5´S	103°02,5´W	Granite (?), mafic (?) dykes

References

LeMasurier WE (1990) Mary Byrd Land. In LeMasurier WE and Thomas JW (eds) Volcanoes on the Antarctic Plate and Southern Oceans. Antarctic Res Ser 48: 182-194

LeMasurier WE, Rex DC (1982) Volcanic record of Cenozoic glacial history in Marie Byrd Land and western Ellsworth Land – Revised chronology and evaluation of tectonic factors. In: Craddock C (ed) Antarctic Geoscience. University of Wisconsin Press, Madison: 725-734

Storey BC, Leat PT, Weaver SD, Pankhurst RJ, Bradshaw JD, Kelley S (1999) Mantle plumes and Antarctica-New Zealand rifting: Evidence from mid-Cretaceous mafic dykes, J Geol Soc London 156: 659-671

LeMasurier WE (1990) Mary Byrd Land. In LeMasurier WE and Thomas JW (eds) Volcanoes on the Antarctic Plate and Southern Oceans. Antarctic Res Ser 48: 182-194

LeMasurier WE (2002) Architecture and evolution of hydrovolcanic deltas in Marie Byrd Land, Antarctica. In: Smellie JL; Chapman MG (eds) Volcano-Ice Interaction on Earth and Mars. Geol Soc Lond Spec Pub 202: 115-148

LeMasurier WE, Rex DC (1982) Volcanic record of Cenozoic glacial history in Marie Byrd Land and western Ellsworth Land – Revised chronology and evaluation of tectonic factors. In: Craddock C (ed) Antarctic Geoscience. University of Wisconsin Press, Madison: 725-734

Smellie JL (2000) Subglacial Eruptions. In: Sigurdsson H, Houghton BF, McNutt SR, Rymer H, Stix J (eds) Encyclopaedia of Volcanoes, Academic Press, San Diego: 403-418

Smellie JL (2001) Lithofacies architecture and construction of volcanoes erupted in englacial lakes: Icefall Nunatak, Mount Murphy, eastern Marie Byrd Land, Antarctica. In White JDL and Riggs N (eds) Volcaniclastic Sedimentation in Lacustrine Settings, Blackwell, Oxford: 9-34

Storey BC, Leat PT, Weaver SD, Pankhurst RJ, Bradshaw JD, Kelley S (1999) Mantle plumes and Antarctica-New Zealand rifting: Evidence from mid-Cretaceous mafic dykes, J Geol Soc London 156: 659-671

Wade FA, La Prade KE (1969) Geology of the King Peninsula, Canisteo Peninsula, and Hudson Mountains areas, Ellswort Land, Antarctica. Antarct J US 4 (4): 92-93

Wade FA, Wilbanks JR (1972) Geology of Marie Byrd and Ellsworth lands. In: Adie RJ (ed) Antarctic Geology and Geophsics. Universitetsforlaget, Oslo: 207-214

Wilch TI, McIntosh WC (2002) Lithofacies analysis and 40Ar/39Ar geochronology of ice-volcano interactions at Mt. Murphy and the Crary Mountains, Marie Byrd Land, Antarctica.. In: Smellie JL (ed) Volcano-Ice volume. Geol Soc Lond Spec Pub 202: 237-253

Wade FA, La Prade KE (1969) Geology of the King Peninsula, Canisteo Peninsula, and Hudson Mountains areas, Ellswort Land, Antarctica. Antarct J US 4 (4): 92-93

Wade FA, Wilbanks JR (1972) Geology of Marie Byrd and Ellsworth lands. In: Adie RJ (ed) Antarctic Geology and Geophsics. Universitetsforlaget, Oslo: 207-214

9. SURFACE EXPOSURE DATING

Assessing timing of Quaternary deglaciation in the Pine Island/Thwaites Glacier area, using cosmogenic surface exposure dating

Joanne Johnson, Terence O'Donovan
British Antarctic Survey, Cambridge, UK

Objectives

The Pine Island and Thwaites glaciers exhibit the most rapid elevation change/ice thinning and grounding-line retreat in Antarctica. It has been suggested that this area may be the most likely site for the initiation of collapse of the two million km^2 West Antarctic Ice Sheet (WAIS), which would result in a global sea-level rise of 5 to 6 m. The strongest evidence that the present-day WAIS may be prone to collapse would come from a record of well-dated observations of changes in the extent and thickness of the ice sheet earlier in the Quaternary.

The aim of this project was to collect rock samples from glacially-derived erratic boulders lying on bedrock surfaces, for cosmogenic surface exposure dating. Surface exposure dating is a direct way of measuring the length of time these rocks have been exposed on the surface to cosmic rays rather than being covered by ice. We can therefore use this method to assess changes in the extent and thickness of an ice sheet over geological time. We planned to collect samples from nunataks in the Pine Island Glacier area at different elevations, in order to construct an age versus elevation record that could be used to constrain the vertical thinning of the ice sheet.

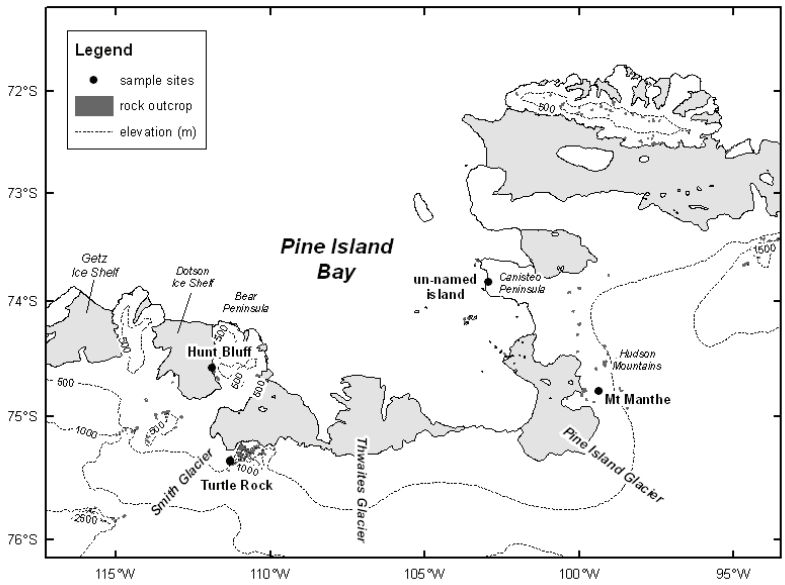

Fig. 9.1: Sample sites for cosmogenic surface exposure dating in the Pine Island Bay region

Methods and equipment

Figure 9.1 shows the sample sites visited in the Pine Island Bay region. The focus of our fieldwork was originally on the Southern Hudson Mountains, which lie adjacent to Pine Island Glacier. However, we were also able to visit two sites in Marie Byrd Land: Turtle Rock (near Mount Murphy) and Hunt Bluff, Bear Peninsula, as well as an unnamed island west of Canisteo Peninsula. In total, 2 full days and 2 half days of fieldwork were undertaken.

Glacial geomorphology was used to identify previously ice-covered areas on the nunataks visited. We looked for the presence of glacially-derived erratic boulders, drift limits and striated rock surfaces, which, if found, would all be evidence that an area had previously been covered by ice. Erratic boulders are usually of non-local lithologies (Fig. 9.2), or local lithologies that are perched on bedrock, and therefore must have been transported by ice. The surfaces of these boulders are often facetted or polished, reflecting abrasion occurring during glacial transport. Striations are also evidence for glacial erosion, and where these were found, their orientation was measured to give an indication of the potential ice-flow direction. The distribution of erratics on each nunatak was noted, in particular whether an upper altitudinal limit could be seen. Such a limit would indicate that ice had not covered the upper part of a nunatak. These observations can show over which areas of rock the ice passed, and which were left untouched by it.

Fig. 9.2: Rounded granitoid erratic boulder, lying on hyaloclastite breccia bedrock. The difference in lithology shows that the boulder has not come from a local source

Several criteria should be used when choosing an erratic boulder for sampling. Firstly, the rock must be of a suitable lithology for cosmogenic surface exposure dating. For analysis of ^{10}Be and ^{26}Al (the most commonly used nuclides), quartz-bearing rocks are most suitable; the surfaces of olivine- and pyroxene- bearing rocks, such as basalts, can be dated using cosmogenic ^{3}He or ^{21}Ne. The geomorphological context of a sample is also critically important. The boulder should be as large as possible, particularly in height off the ground, to avoid the possibility that it could have rolled, or been covered by snow. These scenarios might result in cosmic rays not penetrating the rock, even though it is not covered by ice. There should be no evidence of spalling of the rock surface (which would result in the loss of cosmogenic nuclides produced in the upper surface), and a smooth horizontal sample surface is

preferable (to reduce the adjustments required in shielding calculations for inclined surfaces).

Once we had chosen a sample based on the above criteria, other measurements were made (which will later be entered into the equations used to calculate the surface exposure ages). The elevation of the sample was measured using a hand-held Garmin E-Trex Summit GPS, whose elevation was set in the morning on the working deck of the ship, and then checked again upon return. Very accurate elevations and latitude/longitude positions will also be available for locations on Turtle Rock, Bear Peninsula and Mount Manthe, from the GPS programme of Reinhard Dietrich and Andreas Richter. These will provide a check on the accuracy of our elevation measurements. We also estimated the elevation of surrounding ice/glaciers, using the helicopter altimeter (barometric). The topographic shielding affecting a sample must also be measured. We used an Abney level for this, measuring the inclination of the surrounding hills to the horizon, at the following points of the compass: magnetic N, NE, E, SE, S, SW, W and NW. These were then corrected for the declination (difference between magnetic and true north), which is significantly large in this area:

Location	**Declination**
Turtle Rock	55º13'E
Hunt Bluff	54º22'E
Mount Manthe	44º04'E
Un-named island near Canisteo Peninsula	47º35'E

It is desirable to collect the top 5 cm of the chosen erratic boulder, but this can be difficult with a hammer and chisel if the rock surface is very smooth and rounded, as is often the case with glacially-transported boulders. We therefore used a Stihl TS400 petrol-powered cut-off saw to make a grid on the rock surface (Fig. 9.3) and then chiselled out each block. Approximately 3 kg of sample was collected from each boulder (Fig. 9.4).

Fig. 9.3: Petrol-powered cut-off saw in use on granite boulder on the un-named island west of Canisteo Peninsula

Fig. 9.4: Granite blocks removed using the Stihl saw and then a hammer and chisel. 'T' marks the upper surface of each block.

Results

Time at the sample sites was very limited, hence only a small number of samples were collected. Nevertheless, additional information was gleaned which will greatly assist in planning for a British Antarctic Survey-supported field season in the Hudson Mountains in 2007/08. In total we collected 3 erratic samples from Turtle Rock, 1 erratic and 1 bedrock sample from Hunt Bluff, 2 erratics and 1 bedrock sample from Mount Manthe, and 1 erratic sample from the un-named island (Table 9.1). Four extra samples (lava, hyaloclastite breccia and a dyke) were also collected as a record of the general context of each site.

With the exception of Hunt Bluff, the erratic boulders were all granites or granitoids. At Hunt Bluff, a few metasediment (?) boulders were perched on top of the granite bedrock (Fig. 9.5). Another small erratic was found, which may be basaltic, although it is difficult to tell at this stage because the outer surface of the sample is very weathered. We unfortunately had insufficient time at the site (due to sudden deterioration in the weather) to determine whether other basaltic erratics were present. At Hunt Bluff and Mount Manthe, the abundance of erratic boulders was very low indeed (only 3 were observed at Hunt Bluff and ~5 at Mt Manthe; Fig. 9.6). In contrast, there were several, mostly small, erratic boulders at Turtle Rock. These were predominantly coarse-grained, pink orthoclase-rich granites, with some finer-grained greyish granitoids (Fig. 9.7). The largest boulder was 80 cm long. At the un-named island, there were many erratics strewn across the landscape, varying in size from 10 cm to 1 m in diameter (Fig. 9.8). These appeared to be mostly pink orthoclase-rich granites, as well as some more brownish granites and grey granitoids. At all sites, there was very little geomorphological evidence to indicate past ice levels, so we concentrated our efforts on collecting erratics from different elevations. Striated bedrock was only found at one site, Hunt Bluff (Fig. 9.9). The orientation of the striations is N-S (corrected for declination), suggesting that ice flowed over this area either northwards or southwards.

Fig. 9.5: General view of Hunt Bluff site, with small erratic boulder (metasediment?) perched on granite bedrock next to the hammer.

Fig. 9.6: Sparse erratic boulders on Mount Manthe, Hudson Mountains: a lone granite erratic can be seen in the foreground.

The main result of this fieldwork is a new collection of samples, which can now be processed and analysed to obtain surface exposure dates for the nunataks and island visited. Although small, this dataset will give us a first impression of the retreat history of the ice sheet in the Pine Island Bay and Marie Byrd Land regions. In particular, surface exposure dates from Mount Manthe in the Hudson Mountains will give information about the thinning of Pine Island Glacier, to which it lies adjacent. The island sample will give us a date for the lateral retreat of the ice sheet from the continental shelf. This site is one that will certainly not be visited in 2007/08 because it can only be accessed by helicopter or small-boat from a ship. Turtle Rock and Hunt Bluff will provide dates for thinning of the ice sheet in the western part of Pine Island Bay and, in particular, information about the retreat of Smith Glacier (Fig. 9.1). Our terrestrial cosmogenic dates will complement radiocarbon dates from marine sediments (collected on this cruise and the British Antarctic Survey cruise JR141) that will be used to assess the lateral retreat of the WAIS across the continental shelf. Finally, a question that has arisen from this fieldwork is: From where have these granite erratics come? The answer most likely lies elsewhere in Marie Byrd Land, but we will have to examine ice flow directions in the region to determine the most likely source.

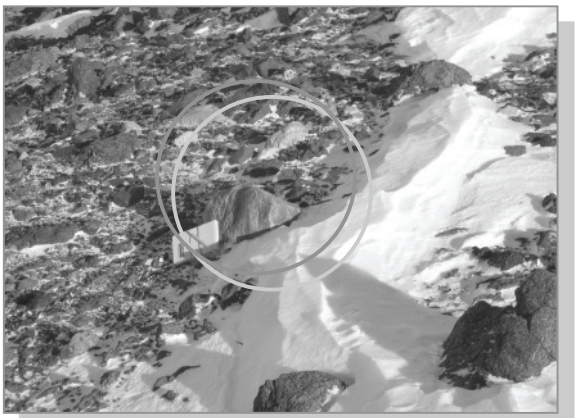

Fig. 9.7: Granite/granitoid erratic boulders (circled) strewn on top of hyaloclastite breccia at Turtle Rock. Notebook is for scale.

Fig. 9.8: Erratic boulders of varying size on the un-named island near Canisteo Peninsula.

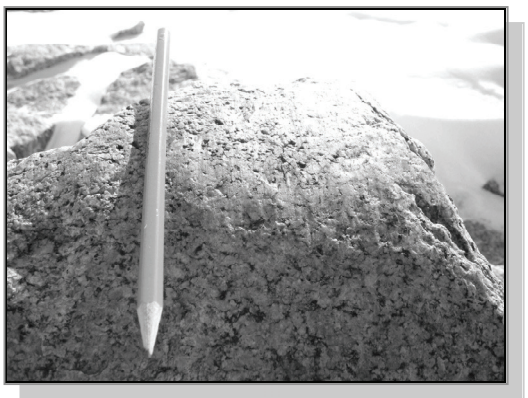

Fig. 9.9: Striations on granite bedrock at Hunt Bluff, W Bear Peninsula. The pencil shows the striation orientation.

Tab. 9.1: Details of all samples collected for surface exposure dating

Sample no.	Collection Date	Place Name	Region	Latitude (°)	Longitude (°)	Elevation (m)	Rock Type	Comment
R5.401.1	01/03/2006	Turtle Rock	Marie Byrd Land	75.36888	111.29758	690	hyaloclastite breccia	bedrock
R5.401.2	01/03/2006	Turtle Rock	Marie Byrd Land	75.36888	111.30023	712	basalt	subaerial lava on top of subaqueous hyaloclastites
R5.403.1	01/03/2006	Turtle Rock	Marie Byrd Land	75.36902	111.29908	700	granite	erratic boulder lying on hyaloclastite brecccia
R5.403.2	01/03/2006	Turtle Rock	Marie Byrd Land	75.36922	111.29727	676	granite	erratic boulder lying on hyaloclastite brecccia
R5.404.1	01/03/2006	Turtle Rock	Marie Byrd Land	75.37073	111.29123	631	granite	erratic boulder lying on hyaloclastite brecccia
R5.404.2	01/03/2006	Turtle Rock	Marie Byrd Land	75.37107	111.28965	629	granite	erratic boulder lying on hyaloclastite brecccia
R5.405.1A	11/03/2006	Hunt Bluff	W Bear Peninsula	74.57910	111.88675	508	?metasediment	erratic boulder lying on granite bedrock
R5.405.1B	11/03/2006	Hunt Bluff	W Bear Peninsula	74.57910	111.88675	508	?metasediment	erratic boulder lying on granite bedrock
R5.405.1C	11/03/2006	Hunt Bluff	W Bear Peninsula	74.57910	111.88675	508	?metasediment	erratic boulder lying on granite bedrock
R5.405.1D	11/03/2006	Hunt Bluff	W Bear Peninsula	74.57910	111.88675	508	?basalt	erratic boulder lying on granite bedrock
R5.405.2	11/03/2006	Hunt Bluff	W Bear Peninsula	74.57910	111.88675	508	granite	bedrock
R5.406.1	13/03/2006	Mount Manthe	Hudson Mountains	74.78067	99.36952	529	basalt	capping lava

Sample no.	Collection Date	Place Name	Region	Latitude (°)	Longitude (°)	Elevation (m)	Rock Type	Comment
R5.406.2	13/03/2006	Mount Manthe	Hudson Mountains	74.77745	99.36722	521	granite	erratic boulder lying on vesicular lavas
R5.406.3	13/03/2006	Mount Manthe	Hudson Mountains	74.77745	99.36722	521	basalt	vesicular lava
R5.406.4	13/03/2006	Mount Manthe	Hudson Mountains	74.77575	99.34950	498	tuffaceous sandstone	within hyaloclastite breccia
R5.406.5	13/03/2006	Mount Manthe	Hudson Mountains	74.77575	99.34950	498	hyalotuff	contains fragments of vesicular lava
R5.406.6	13/03/2006	Mount Manthe	Hudson Mountains	74.77597	99.35950	479	granite	erratic boulder lying on hyalotuff
R5.407.1	15/03/2006	un-named island	near Canisteo Peninsula	73.82300	102.94118	8	granite	erratic boulder lying in guano
R5.407.2	15/03/2006	un-named island	near Canisteo Peninsula	73.82300	102.93900	10	igneous	one of several dykes making up the island

10. GPS MEASUREMENT PROGRAMME

Determination of vertical and horizontal deformations of the Earth's crust and of ice shelves in West Antarctica by GPS observations

Reinhard Dietrich, Andreas Richter
Institute for Planetary Geodesy, Technical University Dresden

Objectives

The determination of the recent deformation of the Earth's crust in Antarctica plays an important role for the understanding of the tectonic situation and for the investigation of the glacial history. While the coherent motion of East Antarctica and the Antarctic Peninsula with respect to a common Euler pole has already been proven by the SCAR GPS campaigns (Dietrich et al. 2004), the recent deformation status of West Antarctica is still unknown to a great extent. Here the GPS observations on bedrock as performed during this expedition will contribute to answer this open question for the area of investigation. Glacial isostasy is the reason that the earth's crust in Antarctica experiences remarkable vertical motions as well (Ivins and James 2005). In West Antarctica, past and present ice mass changes are of much greater magnitude than in East Antarctica. Especially in the Pine Island Bay a much larger extent of the grounded ice during the Last Glacial Maximum was recorded, and the Pine Island and Thwaites glaciers shows the largest present-day ice mass imbalance in the entire Antarctic. If repeated GPS measurements are carried out, vertical and horizontal motion rates can be inferred with accuracy in the sub-centimetre level.

In the area of investigation (Fig. 10.1) all GPS sites were occupied for the first time with one exception: The station at Peter I Island, observed for the first time in 1998, has been re-observed during the present expedition. While all new sites on bedrock need a future re-occupation in order to infer horizontal and vertical crustal movements, the sites on the ice shelves will reveal precise surface heights, horizontal flow velocities and vertical tidal motions.

Methods and equipment

For the field observations, geodetic GPS receivers (Trimble 4000SSi) were used. Solar panels provided the power. On bedrock, fixed monuments (steel screws) have been set up, which allow a precise re-occupation during a second survey (Fig. 10.2). On ice, the antennas were mounted on the top of a steel tube, resp. a tripod, which were removed after occupation (Fig. 10.3).

For all GPS sites occupation protocols and geodetic site descriptions were formulated. In addition, for the sites on bedrock the geology group provided a geological site description as well.

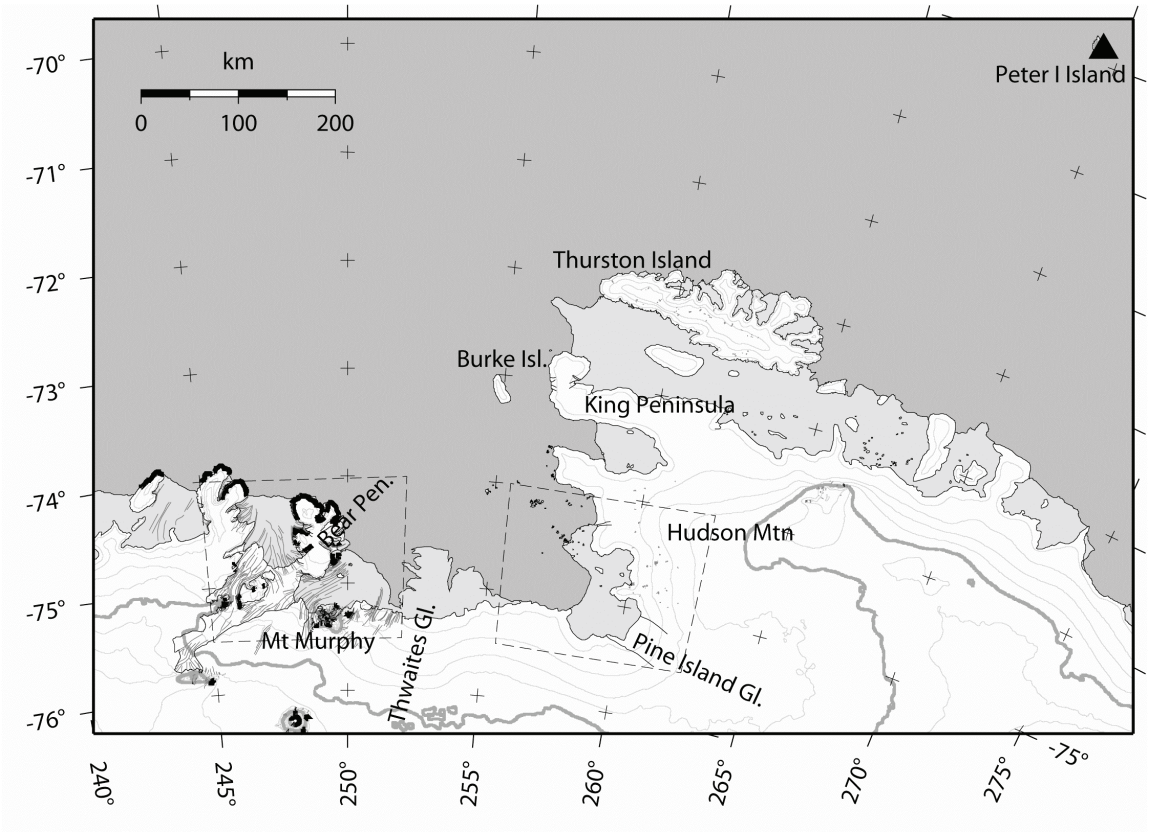

Fig. 10.1: Overview map of Amundsen Sea and Pine Island Bay. The outlines of detailed maps of the operation areas (Figs. 10.4 and 10.5) are indicated by dashed lines. Map source: Antarctic Digital Database 4.0.

Fig. 10.2: Setup of GPS antenna and receiver hardware (stored in the Zarges box) at the site ROCK2 on Turtle Peak, west of Mount Murphy, as an example for the stations on bedrock

Fig. 10.3: Setup of the GPS station on Crosson Ice Shelf as an example for the stations on ice

Results

The locations and the occupation times for all GPS sites are summarized in table 10.1. Altogether, five sites on bedrock were occupied: The existing site at Peter I Island and four new sites south of the Amundsen Sea (Figs. 10.4 and 10.5).

On ice, 4 sites (plus some additional excenters with short-term observations) could be set up on the Dotson Ice Shelf, the Crosson Ice Shelf and the northern Pine Island Ice Shelf (Figs. 10.4 and 10.5). Here, the receivers could be set up at locations of former tracks of the Icesat satellite.

The analysis of the data with the Bernese GPS software will provide precise positions for all sites in the global terrestrial reference frame with sub-cm accuracy. For the site on Peter I Island the neotectonic movements will be determined by comparison with the observations from 1998. For the positions on ice, position changes with time related to ice flow and to ocean tides shall be obtained in addition. Ice surface heights, velocities and tides will be compared to existing knowledge from satellite data and models and may help to improve them.

References

Dietrich, R.; Rülke, A.; Ihde, J.; Lindner, K.; Miller, H.; Niemeier, W.; Schenke, H.-W.; Seeber, G.: Plate Kinematics and Deformation Status of the Antarctic Peninsula based on GPS. Global and Planetary Change, Ice Sheets and Neotectonics, Volume 42, Issues 1-4, July 2004, Pages 313-321.

Ivins, E.R. and T.S. James: Antarctic glacial isostatic adjustment: A new assessment. Antarctic Science, 17(4), 537-549, 2005.

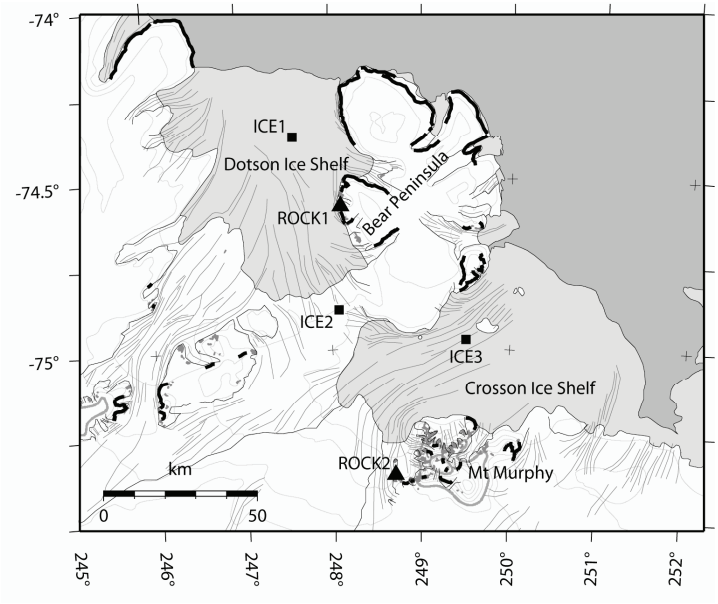

Fig. 10.4: Map of the western working area: Bear Peninsula, Dotson and Crosson Ice Shelves and Mount Murphy. Locations of the GPS markers on bedrock are shown by triangles, stations deployed on floating ice are marked by squares.

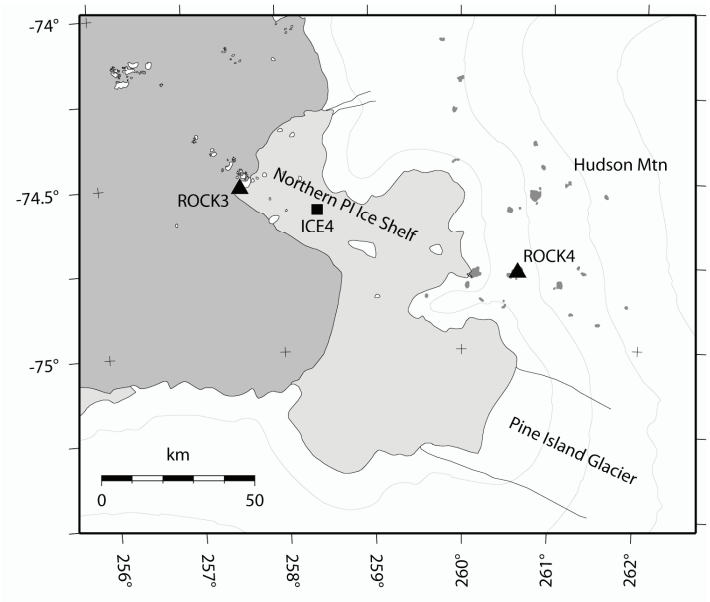

Fig. 10.5: Map of the eastern working area: Hudson Mountains and Pine Island Glacier, symbols according to Fig. 10.4

Table 10.1: Summary of the GPS observations during ANTXXIII-4 cruise

Site	Approx. coordinates		Station occupation		Location
	S (deg min)	W (deg min)	Start	End	
PET1	68 51.8	90 25.6	18.02.06	31.03.06	Peter I Island
ROCK1	74 34.7	111 53.2	03.03.06	11.03.06	Bear Peninsula
ROCK2	75 22.2	111 17.6	01.03.06	11.03.06	Mount Murphy
ROCK3	74 30.7	102 26.4	13.03.06	15.03.06	Backer Islands
ROCK4	74 46.7	99 22.1	13.03.06	15.03.06	Mount Manthe
ICE1	74 22.5	112 24.1	03.03.06	11.03.06	Dotson Ice Shelf
ICE2	74 53.0	111 55.4	03.03.06	11.03.06	Ice Shelve Junction
ICE3	74 56.8	110 24.1	01.03.06	11.03.06	Crosson Ice Shelf
ICE4	74 34.9	101 35.7	13.03.06	15.03.06	North. Pine Island Ice Shelf

11. OCEANOGRAPHY OF THE AMUNDSEN SEA CONTINENTAL SHELF

Frank Nitsche[1)], Raul Guerrero[2)]

[1)] Lamont-Doherty Earth Observatory, Palisades, USA
[2)] INIDEP, Mar del Plata, Argentina

Objectives

In the Amundsen Sea, the floor of the continental shelf is largely blanketed by 'warm' Circumpolar Deep Water (CDW) which gains access across and around shoals on the outer shelf. This inflow appears to be strongest in the eastern sector, fills deep troughs and extends under the local ice shelves. As this water can be more than 3 degrees above the *in-situ* melting point of ice, it rapidly erodes the ice shelves, which are reported to be thinning in this area, along with their incoming ice streams. From RV *Nathaniel B. Palmer* cruises in 1994 and 2000, we obtained snapshots of the late summer ocean properties on the shelf, and of the shelf bathymetry that controls the deep circulation. But as yet we can only estimate dimensions and conditions within the ice shelf cavities, and guess how the ocean density field varies over an annual cycle.

Time series measurements are needed in order to assess potential seasonal changes in the CDW inflow, and its evolution on the shelf. This RV *Polarstern* cruise presented an opportunity to access the region and deploy several simple recording instruments at appropriate sites along its cruise track, for recovery during an RV *Nathaniel B. Palmer* cruise scheduled in early 2007. As prior measurements have indicated that local thermohaline properties are well correlated and important inflows are associated with the troughs, it is feasible to focus primarily on temperature variability near the sea floor.

In addition to these long-term measurements, we performed CTD casts to obtain detailed salinity and temperature profiles at the mooring locations and several other spots on the shelf. In addition to serving as calibration points for the moorings, the CTD observations will provide information on the temperature-salinity properties of the CDW in the austral summer 2006.

We also provided temperature, salinity, and fluorescence profiles as well as water samples for the biology group.

Methods and equipment

Moorings

To determine long-term variations of bottom temperature and salinity on the shelf we deployed five moorings. Three long moorings consisted of an ORE CART release unit, a SBE37 temperature and salinity sensor near the bottom, and a second SBE39 temperature sensor ~95 m above the bottom. One short mooring consisted of an

ORE CART release unit and a SBE39 temperature sensor. And one short mooring with an additional current meter attached below the temperature sensor.

CTD measurements
At the location of the each mooring, at several positions near the shelf ice and at the biological stations we conducted CTD casts. Temperature, salinity and fluorescence profiles were obtained with the shipboard SeaBird Electronics SBE 911+ CTD system fitted with one sets of ducted conductivity-temperature sensors and a Dr Haardt fluorometer (Table 11.1). Data were acquired using Seasave software version 5.3. Raw data were copied over the network and pre-process with Seabird routines as suggested by the supplier. Pre-process data were generated in 1 m bin interval soon after leaving each station. A 24-position SBE 32 Carousel sampler with 10 litre 'Bullister' bottles completed the CTD system.

Tab. 11.1: Details of the CTD 911+ sensor set

Sensor	Serial number	Calibration date	Comments
Pressure (on SBE9 fish)	SBE9-68997	07-Jul.-1997	
Temperature	SBE3plus-2423	23-Feb--2005	
Conductivity	SBE4C-2078	15-Feb.-2005	
Fluorescence	Dr. Haardt	Not available	0-10V lineal output to 0-50 mg/l

In total, we did 32 CTD casts at various depths. Casts over or near 1,000 m water depth were conducted without the fluorometer since this is the maximum depth allowed for this sensor. Each measurement started with recording the surface value, lowering the rosette/CTD system to a depth of 20 m to allow priming of the plumbing system and starting of the pump. From there we brought the CTD back to the surface and lowered it down to the desired depth with speeds changing from 0.5 m/s (usually the upper 100 m) to 1.0 m/s (usually below 200 m). On the way up the rosette/CTD was stopped at chosen depths to take water samples for salinity calibration and/or to obtain water for the biology group. We took samples at intervals of 500 m, 300 m, 180 m, 160 m, 140 m, 120 m, 100 m, 80 m, 60 m, 40 m and 20 m, and sampled the surface for biological purposes, while sample depths for salinity were chosen in regions with homogeneous layers, water column extrema (e.g. T_{max} and T_{min}) and near the sea floor and the sea surface.

Salinity calibration
182 water samples were drawn from the rosette for onboard analyses of salinity. Salinity analyses are done primarily for standardizing the CTD conductivity sensor. Autosal 8400B, located in a highly stable air-conditioned lab, was used for salinity measurements. Calibration was performed at the beginning of each run with batch P144 (OSI) from September 2003. No re-standardizing was required between runs, which indicated an excellent stability of the lab temperature and good performance of the salinometer. Error in salinity remained constant throughout the cruise (Fig. 11.1). Salinity error, denoted as DeltaS, is reported as rosette salinity minus CTD salinity. Mean Delta S was +0.0009 with a standard deviation of 0.00233. For the estimation

of this error, 156 points out of 182 (85 %) were used. Points excluded were greater than 2 times the standard deviation of the mean error.

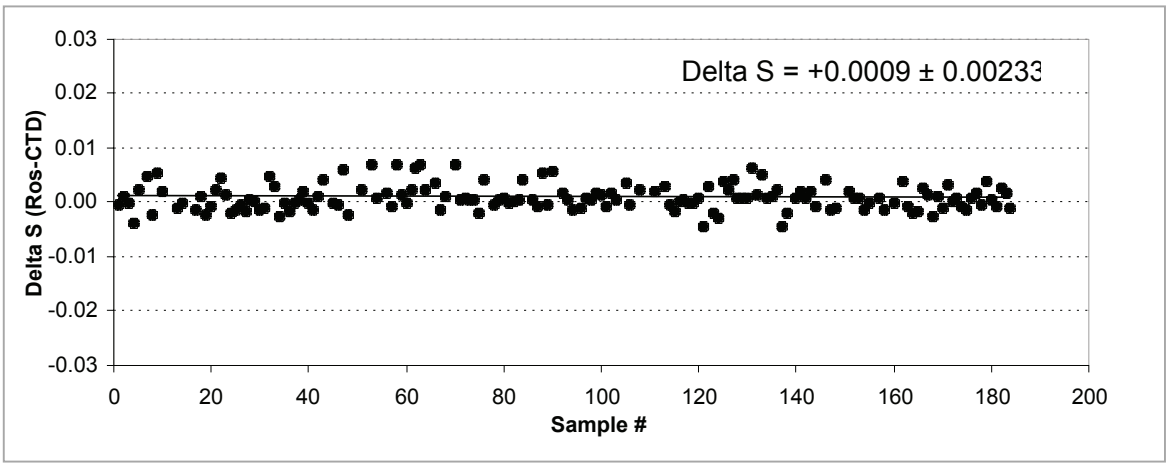

Fig. 11.1: Salinity difference, DeltaS (rosette-CTD), vs. sample number for conductivity sensor. A constant offset fit the DeltaS through the cruise.

Results

Moorings

During this cruise we deployed 4 moorings on the inner shelf and 1 on the outer shelf in the Amundsen See (see table and map for location and individual mooring configurations). It was planned to deploy the sixth mooring on the outer Amundsen Shelf as well, but time and ice conditions did not allow this. Thus the sixth mooring was deployed on the outer shelf of the Bellingshausen Sea. Locations of each mooring were established by taken the ship GPS position when the anchor weight was slipped at the end. We conducted a CTD within a mile of each mooring site except the mooring in the Bellingshausen See. The moorings are supposed to be retrieved during the RV *Nathaniel B. Palmer* cruise NBP07-02 in 2007.

CTDs

In total we performed 32 CTD casts. The primary target area was the Amundsen Sea shelf. Previous reports described relative warm and saline bottom water in the deeper troughs on the inner shelf (Jacobs et al. 1996; Hellmer et al. 1998). Our CTD casts confirmed the existence of relative warm and saline bottom water in the trough systems, but also indicated that the troughs in front of the Getz-Dotsen Ice shelf and the system in front of the Thwaites and Pine Island shelf ice belong to different systems.

References

Jacobs, S.S., Hellmer, H.H. and Jenkins, A., 1996. Antarctic ice sheet melting in the Southeast Pacific. Geophysical Research Letters, 23: 957-960.

Hellmer, H.H., Jacobs, S.S. and Jenkins, A., 1998. Oceanic Erosion of a Floating Antarctic Glacier in the Amundsen Sea. In: S.S. Jacobs and R. Weiss (Editors), Ocean, Ice, and Atmosphere: Interactions at the Antarctic Continental Margin

Antarctic Research Series. American Geophysical Union, Washington, D.C., pp. 83-99.

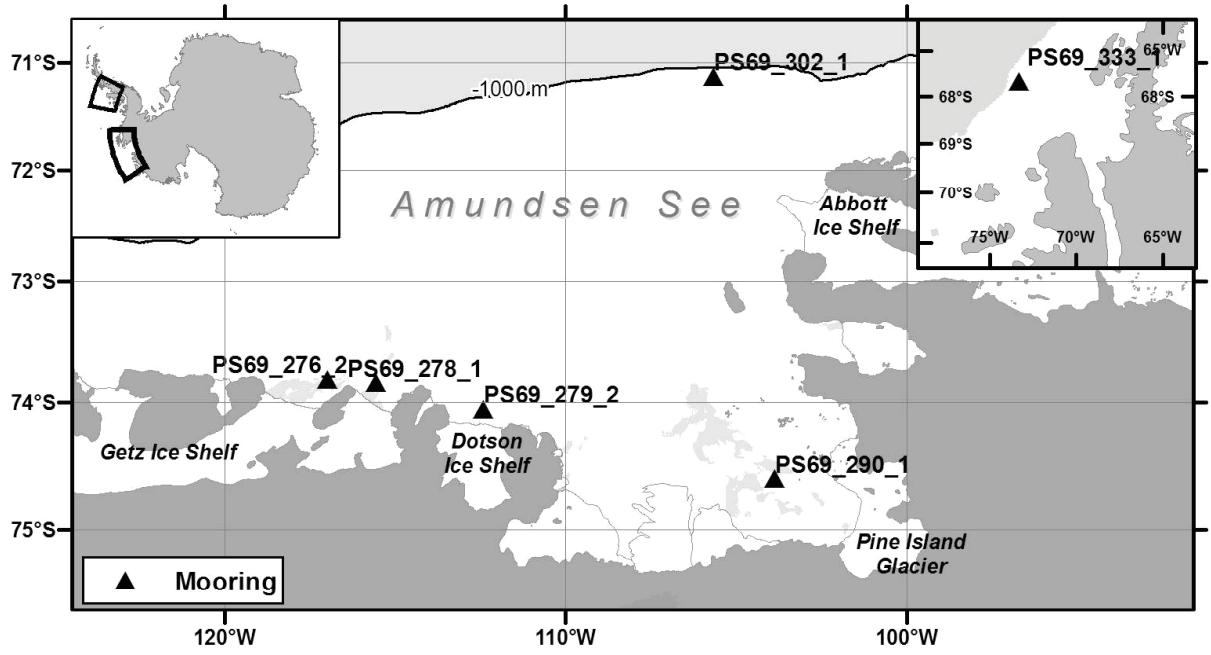

Fig. 11.2: Locations of the five moorings on the Amundsen Sea shelf in the main map and the mooring on the Bellingshausen See shelf in the right inset

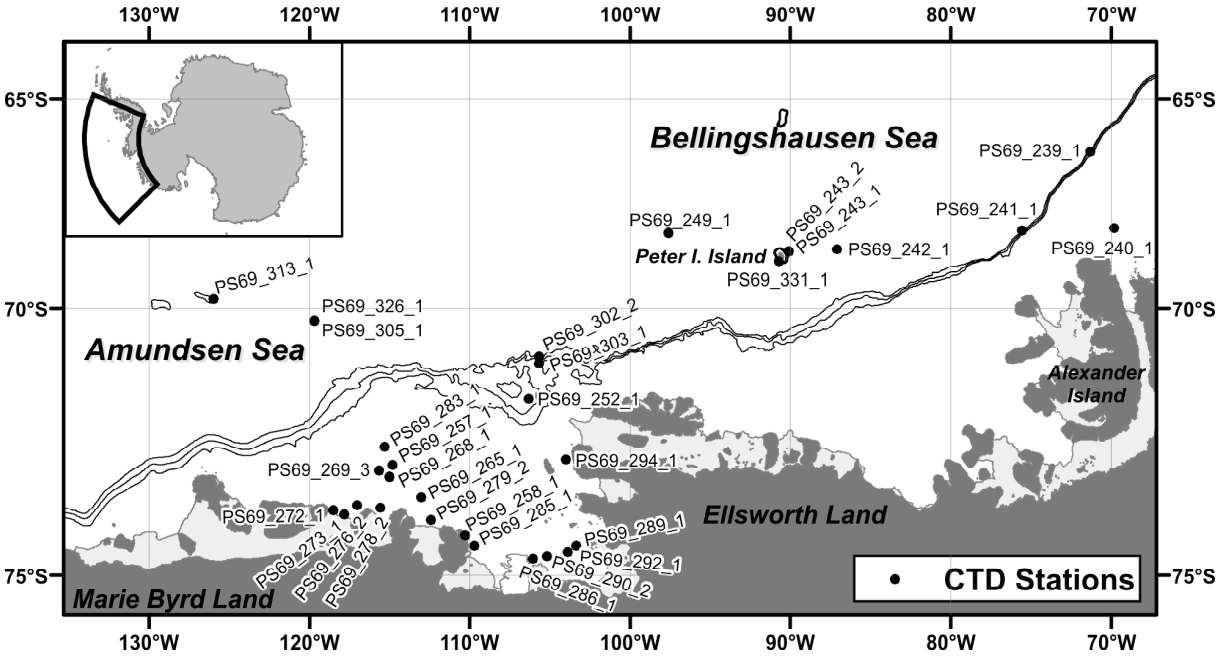

Fig. 11.3: Locations of the CTD stations

Tab. 11.2: Mooring locations and details

Station	Location	Latitude	Longitude	Date	Depth	Type
PS69_276_2	Central Getz	-73.81683	-116.99850	07.03.2006	806 m	SBE37, SBE39 90 m
PS69_278_1	East Getz	-73.84650	-115.57133	07.03.2006	939 m	SBE39
PS69_279_2	Dotson	-74.05816	-112.41783	08.03.2006	881 m	SBE39 and current meter
PS69_290_1	Pine Island Bay	-74.60850	-103.87267	14.03.2006	850 m	SBE37, SBE39 90 m
PS69_302_1	Outer shelf	-71.13683	-105.66617	18.03.2006	540 m	SBE37, SBE39 90 m
PS69_333_1	Bellingshausen Shelf	-67.677667	-73.33600	02.04.2006	496 m	SBE37, SBE39 90 m

Tab. 11.3: CTD stations (F-meter indicates the presence of a fluorometer)

Station	Location	Latitude	Longitude	Date	Depth m	CTD depth	F-meter
PS69_239_1	Shelf edge, Rothera	-66.35633	-71.28433	15.02.2006	1017	500	yes
PS69_240_1	Rothera	-68.20167	-69.80567	16.02.2006	496	478	yes
PS69_241_1	Shelf edge, Rothera	-68.26800	-75.55533	17.02.2006	1080	499	yes
PS69_242_1	Bellingshausen Sea	-68.68000	-87.10200	18.02.2006	344	505	yes
PS69_243_1	Peter I Island	-68.72650	-90.08350	18.02.2006	2948	980	yes
PS69_243_2	Peter I Island	-68.73233	-90.08400	18.02.2006	2964	2758	no
PS69_249_1	Amundsen Sea	-68.31773	-97.57800	22.02.2006	4574	500	yes
PS69_252_1	Outer Shelf	-71.85792	-106.3200	25.02.2006	563	549	yes
PS69_257_1	Mid shelf	-73.09817	-114.80483	28.02.2006	727	700	yes
PS69_258_1	Near Crosson	-74.32883	-110.26917	01.03.2006	276	160	yes
PS69_265_1	Mid shelf	-73.66767	-113.03173	03.03.2006	695	663	yes

Station	Location	Latitude	Longitude	Date	Depth m	CTD depth	F-meter
PS69_268_1	Mid shelf	-73.31683	-115.00250	04.03.2006	880	880	yes
PS69_269_3	Mid shelf	-73.20683	-115.63417	04.03.2006	782	780	yes
PS69_272_1	Central Getz	-73.89777	-118.49950	06.03.2006	1545	500	yes
PS69_272_2	Central Getz	-73.89377	-118.50640	06.03.2006	1527	1528	no
PS69_273_1	Central Getz	-73.96417	-117.83483	06.03.2006	1327	1317	no
PS69_276_2	Central Getz	-73.80940	-117.00520	07.03.2006	918	896	no
PS69_278_2	East Getz	-73.84733	-115.57350	07.03.2006	923	923	yes
PS69_279_2	Dotson Ice Shelf,	-74.05950	-112.41417	08.03.2006	859	835	yes
PS69_283_1	Mid shelf	-72.77267	-115.32083	10.03.2006	600	590	yes
PS69_285_1	Crosson Shelf	-74.50250	-109.69950	11.03.2006	825	790	no
PS69_286_1	Thwaites Glac.	-74.71517	-106.06200	12.03.2006	678	667	no
PS69_289_1	Pine Island Bay	-74.50800	-103.35733	13.03.2006	900	876	yes
PS69_290_2	Pine Island Bay	-74.60717	-103.87450	14.03.2006	813	810	yes
PS69_292_1	Pine Island Bay	-74.68150	-105.19250	14.03.2006	1368	1336	no
PS69_294_1	Pine Island shelf	-72.99933	-103.99283	15.03.2006	530	521	yes
PS69_302_2	Pine Island shelf	-71.13378	-105.66475	18.03.2006	550	540	yes
PS69_303_1	Pine Island slope	-71.00083	-105.66117	18.03.2006	1520	600	yes
PS69_305_1	Amundsen Sea	-70.25067	-119.68700	22.03.2006	2887	600	yes
PS69_313_1	Marie Byrd Seamounts	-69.78955	-125.97520	26.03.2006	1590	600	yes
PS69_326_1	Marie Byrd Seamounts	-70.25167	-119.68700	29.03.2006	2936	666	no
PS69_331_1	Peter I Island	-68.96917	-90.699176	31.03.2006	1271	600	yes

12. MARINE MICROBIAL ECOLOGY

The effects of krill larvae and copepods on the diversity and function of the Antarctic microbial food web

Stephen Wickham[1)], Nina Kamennaya[2)], Elke Neubacher[1)], Ulrike Steinmair[1)], Torben Walter[1)]

[1)] Dept. of Organismic Biology, University of Salzburg, Austria
[2)] Dept. of Botany & Environmental Ecology, Hebrew University Jerusalem, Israel

Objectives

Since Pomeroy's (1974) seminal paper, it has become increasingly clear that microbes and the microbial food web play a pivotal role in most marine food webs. The microbial food web is composed of heterotrophic and autotrophic prokaryotes (bacteria and cyanobacteria), and very small (picoplanktonic) eukaryotic algae, which are preyed upon primarily by flagellated protists. Small flagellates (and to a lesser extent, bacteria and picoplanktonic autotrophs) are in turn preyed upon by ciliated protists and dinoflagellates, which then can be consumed by the metazoans of the "classic" marine food web. Organic compounds released by heterotrophs are remineralized by heterotrophic bacteria, providing both new production and inorganic nutrients to sustain autotrophic production. The microbial food web plays a central role in most aquatic systems; this is particularly true in the Antarctic during the austral fall and winter, when primary production is minimal and the food web is net heterotrophic. The central question of the project is: to what degree is the microbial food web in the Antarctic connected to the classic food web, and what is the role of biodiversity in modulating this connection? It is well established that predation can alter the diversity of prey communities, and this can reduce the impact of predators on total prey biomass: less predation-vulnerable species increase as the competitively dominant prey species are grazed down. Recent work has proposed that this interaction between predation and biodiversity of prey is dependant on the productivity of the system, with predation having less impact on prey biodiversity as productivity declines (Worm et al. 2002). It is often difficult to show strong connections between the microbial and classic food webs since changing biomass in upper trophic levels has little or no effect on the heterotrophic and autotrophic flagellates or bacteria of the microbial food web. Previous work by the project leader showed that in late fall, removing almost all ciliate biomass through predation by the furcilia larvae of krill had no measurable effect on the trophic levels beneath ciliates. A possible explanation for this is that there were changes in abundance of individual species, but not in the community as a whole. The project addressed these questions during the cruise, as primary productivity was declining.

A second part of the project focused on the distribution and diversity of cyanobacteria. Cyanobacterial presence and their seasonal blooms in the Southern Ocean have been previously described, but in our project we aspired to determine

the diversity of cyanobacterial communities in less explored area of the antarctic waters. The main goals of this part of the project were:

(1) Molecular-based determination of cyanobacterial diversity in less explored regions of Antarctic Zone waters.
(2) Determination of nutrient (N) conditions of the water column.
(3) Determination of the abundance and distribution of picoautotrophs in the water column.

The determination was based on two techniques:

- Comparison of the *ntcA* gene, allowing the identification of cyanobacterial strains at a very fine level
- Flow cytometry, to analyze the abundance of different cell types according to their size and autofluorescence.

Methods and equipment
The project consisted of two main parts. First, *in-situ* diversity was examined at 23 stations (Table 12.1), using CTD/Niskin bottle casts. Both the continental shelf and the open ocean waters between 69°48' and 125°59'W were sampled. In conjunction with the physical oceanography group (Chapter 11), water was routinely sampled at the surface, at 20-meter intervals to 180 m and at 300 and 500 m. Simultaneously, profiles were taken for chlorophyll *a* (measured as *in-situ* algal autofluorescence), temperature and salinity. The parameters measured from the casts are given in table 12.2. Briefly, samples were taken for bacterial and flagellate as well as ciliate abundance and morphological diversity, for flagellate and ciliate molecular diversity, for cyanobacterial abundance and morphological diversity, for cyanobacterial molecular diversity, for total DNA concentration, and for inorganic nitrogen. The parameters measured and the methods of fixation and analysis are given in table 12.2.

For the molecular analyzes, 4.45 l water were prefiltered with 20 µm mesh in order to remove the fractions larger than nanophytoplankton, and then filtered onto 0.45-mm Supor-450 membranes. The membranes were immersed in storage buffer and stored at -80°C until nucleic acid extraction. For the flow cytometry analyses, 1.5 ml of unfiltered sea water were fixed in 0.1 % gluteraldehyde and frozen in liquid nitrogen.

The general abundance of microbiobial organisms was quantified with a Quant-iT™ PicoGreen® dsDNA kit, which measures the amount of double-stranded DNA in solution. For this purpose 1 ml of 100 µm mesh prefiltered sea water was incubated overnight with 0.1 % of gluteraldehyde and the dsDNA concentration was measured with TBS-380 fluorometer using the PicoGreen® assay.

In order to quantify phytoplankton biomass, Chlorophyll *a* concentrations were measured in 100 µm mesh prefiltered sea water. Chlorophyll *a* was extracted from 250-ml samples, collected on GF/F filters, extracted in 90 % acetone for 24 h at 4°C and measured on a TBS-380 fluorometer.

The concentrations of inorganic nitrogen in the water column were also analyzed. Ammonium concentrations were determined with OPA-reagent assay and measured with TBS-380 fluorometer. For nitrite and nitrate determination 15 ml sea water samples were collected for later spectrophotometric analysis.

The second part of the project was the experimental manipulation of predator densities to determine the impact of predation on abundance and diversity of components of the microbial food web. The interaction between productivity and predation on diversity was examined by repeating the same experimental design over the course of the cruise, as productivity declined with shorter day lengths and the onset of the austral fall. Three different predators were used in the experiments: The small (0.7 – 1.0 mm) cyclopoid copepod *Oithona similis*, a medium-sized (ca. 2.5 mm) calanoid copepod preliminarily identified as *Calanoides* sp, and the furcilia larval stage of the antarctic krill, *Euphausia superba*. The experiments had a so-called "Lehman-type" design, where varying numbers of either copepod or furcilia were added to seawater pre-filtered through a 250 µm mesh to remove larger zooplankton (Lehman and Sandgren 1985). Water was collected in Nisken bottle casts from 20 m water depth. The experiments were run in 4.45 l polycarbonate bottles, with three replicas per predator density. The bottles were incubated in on-deck 500 l basins with seawater flowing through them to maintain near *in-situ* temperatures. The basins were covered with near-transparent plastic covers to reduce light levels, approximating the condition of the 20 m depth in which the water for the experiments was collected. The predator densities used in the experiments as well as the stations where water and grazers were obtained are listed in table 3. The experiments had a duration of 48 h. Growth rates from beginning to end of the experiment of the various prey types will be calculated and regressed against the predator concentration or biomass. The slope of the regression is the clearance rate of the predator. This approach allows the measurement of predator-specific clearance rates on a complete prey community. The experimental design also allows the evaluation of the hypothesis that diversity should be highest at intermediate predation rates. Moreover, by repeating the same design as productivity declines, we can test the hypothesis that there is an interaction between predation and productivity on the net impact on biodiversity. The same parameters as in the profiles (listed in Table 12.2) were measured in the experiments. The exceptions were cyanobacterial diversity, dissolved N and in vivo DNA, which were not measured in the experiments.

A second set of experiments was designed to measure grazing on bacteria, and the role of predator diversity in modulating predation pressure. So-called FLB (fluorescently labelled bacteria) were used as a tracer, and were added to whole water, prefiltered through a 250 µm mesh to remover larger zooplankton. Samples taken at the beginning and end of the experiments allow the loss rate of the FLB to be calculated, and by extension, of the natural bacterial community. Samples were taken for bacterial and flagellate abundance, for flagellate and ciliate molecular diversity, and for ciliate abundance and morphological diversity. In order to determine whether nanoflagellates (those < 20 µm in size) or ciliates and dinoflagellates were the primary grazers on bacteria, three size fractions were used. Water filtered through a 250 µm mesh contained ciliate, dinoflagellate and nanoflagellates grazers, while 20 µm filtered water excluded most ciliates and dinoflagellates. A < 0.2 µm fraction should have contained no bacteria or gazers on bacteria, and had FLB

added to it to measure the non-grazing loss of FLB. Three replicates were used per size fraction, and the experiments were run in the on-deck incubators for 24 h. Three FLB experiments were conducted, with water from stations given in table 12.3.

In addition, at four stations (two shelf stations, PS 69-260 and PS 69-283 one shelf break station PS 69-303; one deep water station, PS 69-331) zooplankton samples were taken using a Hydrobios Midi Multinet with a 55 µm mesh size. The stations and depths sampled are given in table 12.4. These samples were taken on behalf of Dr. S. Schiel (AWI).

As well as the work mentioned above, at three Stations (PS 69-257, PS 69-265 and PS 69-269) *Phaeocystis antarctica* (a bloom-forming, colonial cyanobacteria) colonies were isolated and brought into culture. Samples were also taken for molecular analysis. This work was done at the request of Ms. Steffi Gaebler (AWI).

Results

As all samples can only be counted or analyzed in the home laboratories, no results can be presented at this time.

Tab. 12.1: The stations sampled by the marine microbial ecology group using the CTD-rosette, Bongo net or Multinet, and the parameters measured at the stations. At all CTD-rosette stations, samples were taken for dissolved N (NH4+, NO2-, NO3-), cyanobacterial molecular diversity, and picoautotroph abundance. Listed in the table are the additional parameters sampled. “Bact.”, flag.”, and “cil.” are bacteria, flagellate and ciliate, respectively. In the column “Equipment run”, “C” refers to the CTD-rosette, “B” to the Bongo net and “M” to the Multinet.

Station	Latitude S	Longitude W	Depth (m)	Equipment run	Addition parameters sampled
PS 69-239	66°21.388'	71°16.988'	500	C, B	
PS 69-240	68°12.103'	69°48.321'	469	C	Bact., flag. & cil. abundance, cil. morphological diversity, cil. & flag. molecular diversity
PS 69-241	68°16.137'	75°33.418'	499	C	Bact., flag. & cil. abundance, cil. morphological diversity, cil. & flag. molecular diversity
PS 69-242	68°40.794'	87°6.084'	505	C	Bact., flag. & cil. abundance, cil. morphological diversity, cil. & flag. molecular diversity
PS 69-243	68°43.94'	90°5.04'	2962	C	Bact., flag. & cil. abundance, cil. morphological diversity, cil. & flag. molecular diversity
PS69-248	65°2.234'	92°57.895	905	B	
PS 69-249	68°19.099'	97°34.748'	4589	C	*in vivo* DNA
PS 69-251	71°51.377'	106°19.053'	544	C	*in vivo* DNA
PS 69-257	73°6.078'	114°48.441'	700	C, B	*in vivo* DNA
PS 69-258	74°19.729'	110°16.191'	262	C	Bact., flag. & cil. abundance, cil. morphological diversity, cil. & flag. molecular diversity, *in vivo* DNA
PS 69-260	74°19.76'	110° 16.21'	269	M	
PS 69-265	73°40.090'	113°2.101'	662	C, B	*in vivo* DNA
PS 69-268	73°18.974'	115°0.099'	800	C	*in vivo* DNA

Station	Latitude S	Longitude W	Depth (m)	Equipment run	Addition parameters sampled
PS 69-269	73°12.409'	115°38.050'	784	C, B	
PS 69-270	73°12.402'	115°38.054'	781	C	*in vivo* DNA
PS 69-272	73°53.353'	118°30.679'	1520	C	*in vivo* DNA
PS 69-273	73°57.846'	117°50.316'	1316	C	*in vivo* DNA
PS 69-276	73°48.612'	117°0.589'	897	C	*in vivo* DNA
PS 69-278	73°50.844	115°34.425'	950	C, B	
PS 69-283	72°46.337'	115°19.241'	591	C, B, M	Bact., flag. & cil. abundance, cil. morphological diversity, cil. & flag. molecular diversity, *in vivo* DNA
PS 69-289	74°30.468'	103°21.334'	876	C B	*in vivo* DNA
PS 69-294	72°59.980'	103°59.658'	519	C, B	
PS 69-303	72°0.056'	105°39.418'	1515	C, B, M	Bact., flag. & cil. abundance, cil. morphological diversity, cil. & flag. molecular diversity, *in vivo* DNA
PS 69-305	70°15.030'	119°41.209'	2890	C, B	Bact., flag. & cil. abundance, cil. morphological diversity, cil. & flag. molecular diversity, *in vivo* DNA
PS 69-313	69°47.359'	125°58.523'	600	C, B	Bact., flag. & cil. abundance, cil. morphological diversity, cil. & flag. molecular diversity, *in vivo* DNA
PS 69-326	70°15.08'	119°41.31'	2944	C	
PS 69-331	68°51.146'	90°41.839'	1263	C, B, M	

Tab. 12.2: The parameters measured, and the methods used to analyze them, in the CTD/rosette profiles listed in Table 12.1. “Glut” is Glutardialdehyde.

Parameter	Sampling/fixation method
Bacterial abundance	Glut.-fixed; frozen in liquid N; stored at –80°C, counted with flow cytometry
Flagellate abundance	Glut.-fixed; DAPI stained stored at 4°C; counted with epifluorescence microscopy
Ciliate/Dinoflagellate/Microalgal abundance & morphological diversity	Bouins-fixed; counted on inverted microscope (post cruise); Protarol-stained
Flagellate & ciliate molecular diversity	Filtered onto GF/F filters; analyzed with DGGE
Chlorophyll *a* concentration	Filtered onto GF/F filtered; extracted with acetone; analyzed spectrophotometrically
Zooplankton abundance	Collected on 44 µm (copepods) or 500 µm mesh (furcilia); formalin-fixed
Cyanobacterial abundance & diversity	Flow cytometry and analysis of the variation in the ntcA gene
Dissolved N (NH_4^+, NO_2^-, NO_3^-) concentration	Analyzed spectrophotometrically
In vivo DNA content, <20 µm fraction	PicoGreen dsDNA kit; spectrophotometrically

Tab. 12.3: Experiments conducted during the cruise. “FLB” are fluorescently labelled bacteria, used as a tracer to measure grazing on bacteria. “Furcilia” are the furcilia larval stage of the antarctic krill *Euphausia superba*, and *O. similis* is the cyclopoid copepod *Oithona similis*.

Experiment	**Date**	**Station**	**Manipulation**
Grazing Expt. 1	17-19Feb06	PS 69-239 (animals) PS 69-241 (water)	0, 0.45, 0.90, 1.35, or 1.8 Furcilia L^{-1}
Grazing Expt. 2	22-24Feb06	PS 69-248 (animals) PS 69-249 (water)	0, 4, 8, 16, or 32 *O. similis* L^{-1}
Grazing Expt. 3	26-28Feb06	PS 69-252	0, 0.45, 0.90, 1.35, or 1.8 *Calanoides* L^{-1}
Grazing Expt. 4	1-3Mar06	PS 69-257	0, 0.67, 1.3 2.0 or 2.7 Furcilia L^{-1}
Grazing Expt. 5	5-7Mar06	PS 69-269	0, 0.67, 1.3 2.0 or 2.7 *Calanoides* L^{-1}
Grazing Expt. 6	11-13Mar06	PS 69-283	0, 0.67, 1.3 2.0 or 2.7 Furcilia L^{-1}
Grazing Expt. 7	19-21Mar06	PS 69-303	0, 4, 8, 16, or 32 *O. similis* L^{-1}
Grazing Expt. 8	23-25Mar06	PS 69-305	0, 0.67, 1.3 2.0 or 2.7 *Calanoides* L^{-1}
Grazing Expt. 9	27-29Mar06	PS 69313	0, 4, 8, 16, or 32 *O. similis* L^{-1}
FLB Expt. 1	8-9Mar06	PS 69-278	<250, <20, & <0.2 µm size fractions
FLB Expt. 2	16-17Mar06	PS 69-294	<250, <20, & <0.2 µm size fractions
FLB Expt. 3	23-24Mar06	PS 69-305	<250, <20, & <0.2 µm size fractions

Tab. 12.4: Stations and depths sampled with the multinet sampling gear. The latitude, longitude and depth of the stations are given in Table 12.1.

Station	Date	Depths sampled (m)	Fixation method
PS 69-260	01Mar06	200-160; 160-120; 120-80; 80-40; 40-0	Formol
PS 69-283	10Mar06	501-300; 300-200; 200-100; 100-50; 50-0	Formol; Ethanol
PS 69-303	18Mar06	1000-500; 500-200; 200-100; 100-50; 50-0	Formol; Ethanol
PS 69-331	31Mar06	1000-500; 500-200; 200-100; 100-50; 50-0	Formol

13. MONITORING OF WHALES

Marlen Blume, Mara Schmiing, Julia Strahl
Alfred-Wegener-Institut, Bremerhaven

Objectives

Studying whales in the wild is challenging. They are rarely seen at the surface and often stay under water for a long time. Ship based visual monitoring is the most common method to study distribution, behaviour and migration of whales (e.g. Line Transect Method). It is possible to estimate population sizes of whales according to their occurrence in a defined area.

Data from antarctic waters are sparse, especially from the Amundsen Sea. Existing data have been received from the Japanese Sightings Survey Programme, the International Whaling Commission/International Decade of Cetacean Research Programme, the Southern Ocean Whale and Ecosystem Research Programme and the Southern Hemisphere Minke Whale Assessment Programme (Branch & Butterworth 2001). It is believed that most of the whales migrate out of the Southern Ocean from February onwards (Kasamatsu et al. 1996). In general, distribution and abundance of whales depend on their food resources and on sea ice conditions. Thus, it is a major target of the whale monitoring programme during this cruise to obtain more information about occurring species, distribution and number of whales. Various whale species of the suborders Odontoceti and Mysticeti can be found in waters surrounding Antarctica. Most species have high latitudinal summer feeding grounds in the southern hemisphere and migrate annually to warm tropical waters in the winter to breed and calve. Regarding the investigated area during that cruise, known whale species included in the suborder Odontoceti are the Hourglass Dolphin (*Lagenorhynchus cruciger*), the Sperm Whale (*Physeter macrocephalus*), the Orca (*Orcinus orca*) and different Beaked Whales like the Southern Bottlenose Whale (*Hyperoodon planifrons*) and the Arnoux´s Beaked Whale (*Berardius arnuxii*). All known species of the suborder Mysticeti belong to Rorqual Whales: Antarctic Minke Whale (*Balaenoptera bonaerensis*), Humpback Whale (*Megaptera novaeangliae*), Sei Whale (*Balaenoptera borealis*), Fin Whale (*Balaenoptera physalus*) and Blue Whale (*Balaenoptera musculus*) (Branch & Butterworth 2001, Gill & Evans 2002). Species can be identified by their dorsal fin, fluke, blow, size, shape, colour/pattern, diving/breathing sequence and special behaviours like breaching, spy-hopping etc. (Carwardine 2002, Reeves et al. 2002).

The observations took place along the track of RV *Polarstern* during the cruise ANT–XXIII/4. Each day during daylight hours, marine mammal observers (MMO) looked out for whales and recorded each sighting, as well as sighting conditions. Additionally, the behaviour of the whales was recorded. To expand the observations, sightings spotted incidentally by other scientists as well as helicopter sightings were recorded and included in the evaluation.

In addition to this daily standard survey, observations were intensified during seismic profiling and geological stations to mitigate contingent negative effects on nearby whales through shut-down of hydroacoustic equipment.

Methods and equipment

Visual whale surveys took place from 15 February to 4 April 2006 on the bridge of the RV *Polarstern* during all hours of daylight. Most observations covered a forward azimuth of 180°. Schirmer binoculars (7 x 50) were used to identify observed whales. However, the use of bearing diopter was not practical due to their fixed position and complicated handling during heavy seas. Each sighting was recorded in a whale survey protocol. This is the standard observation protocol for all RV *Polarstern* expeditions and includes: date and time of the observation, observer information, ship's position, water depth, whale species and certainty of identification, numbers of adults and juveniles, description and behaviour of the whales, direction of travel of the animals in relation to the ship, geographical swimming direction, distance between the whales and the ship, activity of ship, wind direction and velocity, state of sea and visibility. In addition, acoustic activities of the ship such as Doppler Log (DoLog), Deep Water Sounder (DWS-Lot), Parasound, Hydrosweep and Airguns were noted (see Appendix 1). For the sake of completeness a daily weather protocol was taken which included state of sea, clouds, reflection of the sun, wave height, visibility, ice conditions and precipitation. To supplement the observation from the ship, helicopter-magnetic flights were used for visual whale survey. Similar to the visual survey from the ship, Schirmer binoculars (7 x 50) were used. The whale survey protocol for the flights included: date and time of the observation, observer information, GPS positions of waypoints and sighting, weather conditions, observed whale species and number of individuals. The standard whale survey was carried out by three MMO's. To optimize best results during the visual whale survey, especially during bad weather conditions, varying watch procedures were performed for three cases:

1. Standard observation

Depending on daytime length, two watch systems proved successful. During days with more than twelve hours of daylight each watch took three hours, during which the observer was at least two hours on duty. The duty switched every two hours if daytime length was less than twelve hours.

2. Mitigation monitoring

a) Watch during seismic operations

Before the begin of seismic profiling, the area was observed continuously by two MMO's 90 minutes before airgun operations started and during their soft start of about 20 minutes. During seismic profiling, each watch of one observer took two hours. The airguns were switched off in cases when a whale was observed within the distance of 1000 m to the ship. After 20 minutes with no sightings of whales, the airguns were switched on again using a soft start procedure.

b) Watch during geological stations

During geological stations, two MMO's observed the area continuously. The MMO's rotated every two hours. The Parasound and Hydrosweep sources were switched off in cases when a whale was within a 100 m radius of RV *Polarstern*. Only standard

whale observations were performed during biological stations as the use of hydroacoustic equipment was not necessary for these stations.

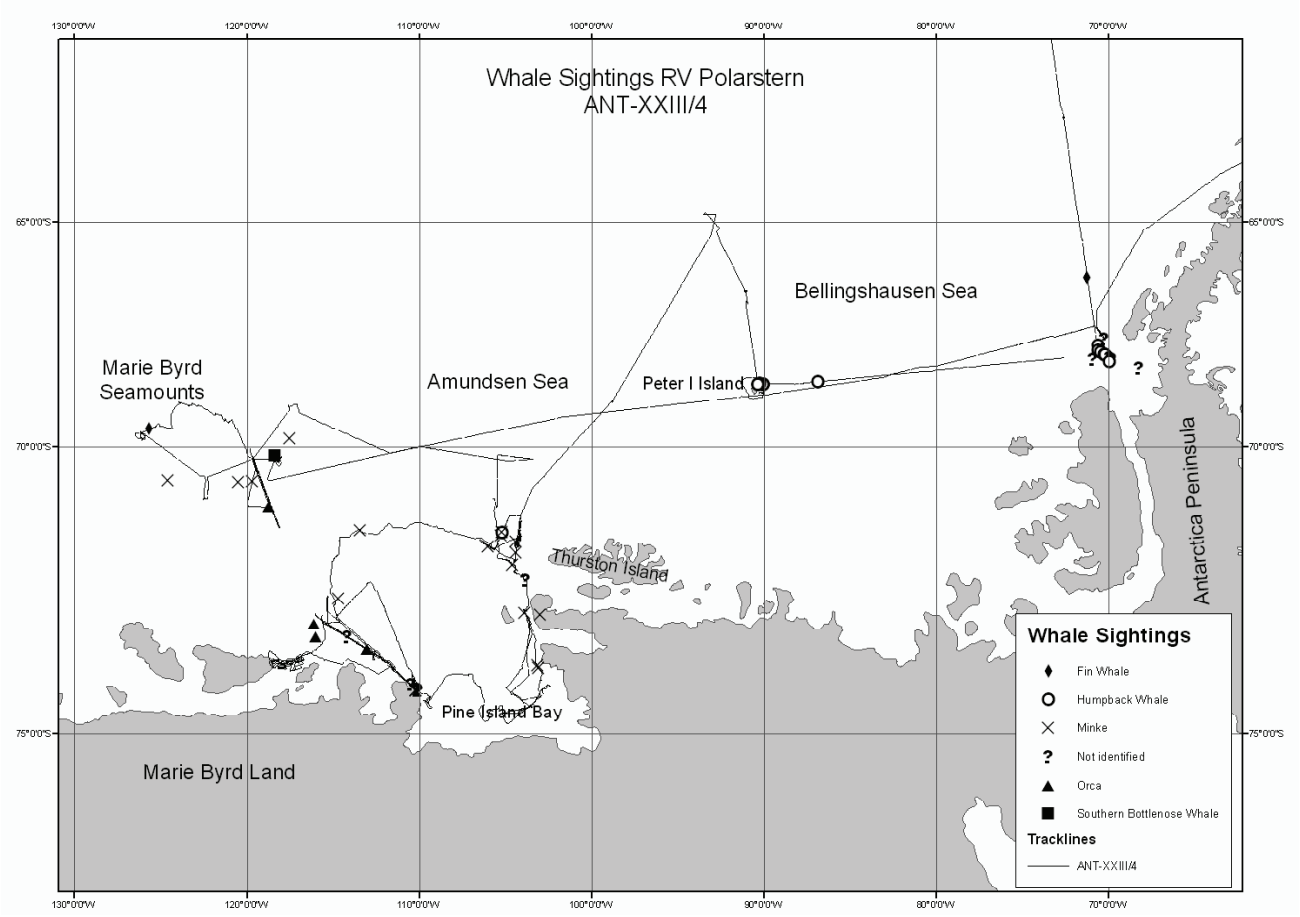

Fig. 13.1: Map overview of whale sightings made from RV Polarstern and helicopter during cruise ANT-XXIII/4. Cruise track is given for the time during between 15 February and 4 April 2006. Each species is marked with a different symbol.

Results

Of the ten known whale species known for the area of the expedition, only three species could be seen several times during this cruise. These were identified as Humpback Whale, Minke Whale and Orca. Two sightings of Fin Whales were made and two Southern Bottlenose Whales were seen during a flight of the helicopter magnetic investigations. Sightings of Humpback Whales were made only in the Bellingshausen Sea near the coast of the Antarctic Peninsula and Peter I Island. Antarctic Minke Whales could be seen frequently in the Amundsen Sea around Thurston Island, up to Pine Island Bay and on the way to, and in the area of, the Marie Byrd Seamounts. In the inner Pine Island Bay no whales were sighted. In total, most whale sightings were made near the coast and only sporadic sightings of Orcas, Fin Whales and Minke Whales were made more than 100 miles off the coast. Based on the daily weather protocols different observation conditions can be

excluded as explanation for this pattern. Possible reasons such as differences in food resources or migration remain speculative. In sea ice, six whale sightings were made contrary to all expectations: five Minke Whales and one unidentified whale. One Minke Whale was swimming under the ice and twice Minke Whales slid their jaw up through a hole in the ice or even broke through the ice. Orcas were not seen in areas with dense sea ice cover but in regions with ice floes, perhaps because they were hunting seals, which were also observed in the area. In February, numerous sightings were made around the Antarctic Peninsula near the BAS station *Rothera* (16.02.2006: 29-34 Humpback Whales, 5-7 not identified whales) and around Peter I Island (18.02.2006: 10 Humpback Whales). By contrast, at the end of March and the beginning of April, only two sightings of whales were made near *Rothera* (03.04.2006: two not identified whales). This supports the assumption that most whales migrate out of the Southern Ocean from February onwards (Kasamatsu et al. 1996). On the other hand, it has to be considered that the observation conditions at the end of March and the beginning of April were limited due to bad weather.

Disregarding the days steaming through areas with dense sea ice cover, the sighting conditions (wave action, visibility etc.) were favourable most of the time. With forty observations of approximately 100 whales, important could be collected for the previously unsurveyed Amundsen Sea.

Discovery of Southern Elephant Seals in Pine Island Bay

During the helicopter-magnetic survey in the eastern Pine Island Bay, a large group of Southern Elephant Seals was discovered on 15 March on a small rocky island (73°49.4'S, 102°56.5'W) off Canisteo Peninsula. The group consisted of about 90 young bulls retreating to the island for moulting. A discovery of this species at this high latitude is rather unusual and has never been reported for Pine Island Bay. They probably migrated quite a large distance to Pine Island Bay from the breeding colonies at King George Island or Macquarie Island. During a visit to the island for geological sampling on 16 March, the colony was documented via photos and films.

Fig. 13.2: Discovery of Southern Elephant Seals on a rocky island off Canisteo Peninsula of Pine Island Bay

Tab. 13.1: Sightings of whales made during ANT-XXIII/4. Information about date, species, position and number of individuals are given. *Sighting made during helicopter flights, Seismic = Seismic gear was running during sighting; +Airguns were switched off when whales were within an distance of 1000 m to RV Polarstern, n.i. = not identified species, indiv. = individuals.

Sighting No.	Date	Species	Latitude (S)	Longitude (W)	Indiv.	Remarks
1	15/2/2006	Fin Whale	66°21.82'	71°17.47'	1	
2	16/2/2006	Humpback Whale	67°53.56'	70°40.06'	15-20	
3	16/2/2006	Humpback Whale	68°00.79'	70°37.29'	2	
4	16/2/2006	Humpback Whale	68°02.92'	70°28.25'	3	
5	16/2/2006	Humpback Whale	68°05.62'	70°16.82'	3	
6	16/2/2006	Humpback Whale	68°06.11'	70°14.67'	4	
7	16/2/2006	n.i.	68°09.93'	69°58.35'	1	
8	16/2/2006	n.i.	68°11.21'	69°52.90'	1	
9	16/2/2006	n.i.	68°12.16'	69°51.45'	1	
10	16/2/2006	Humpback Whale	68°15.30'	69°58.86'	2	
11	16/2/2006	n.i.	68°12.19'	70°55.83'	2-3	
12	18/2/2006	Humpback Whale	68°40.19'	86°54.10'	2	
13	18/2/2006	Humpback Whale	68°44.15'	90°05.07'	2	
14	18/2/2006	Humpback Whale	68°44.00'	90°05.16'	2	
15	18/2/2006	Humpback Whale	68°43.32'	90°15.18'	1	
16	18/2/2006	Humpback Whale	68°43.74'	90°21.84'	2	
17	18/2/2006	Humpback Whale	68°44.09'	90°21.29'	1	
18	23/2/2006	Minke	71°48.90'	104°23.25'	3	
19	23/2/2006	Minke	72°00.79'	104°25.25'	1	Sea ice
20*	24/2/2006	Minke	72°65.00'	103°01.00'	2	Sea ice
21	25/2/2006	Minke	71°54.14'	106°02.58'	2	
22	25/2/2006	Minke	71°41.81'	105°17.27'	1	Seismic
23	25/2/2006	Humpback Whale	71°38.81'	105°13.43'	2	Seismic
24	25/2/2006	Minke	71°38.03'	105°12.23'	5	Seismic+
25	27/2/2006	Minke	71°36.76'	113°26.17'	3	
26	28/2/2006	n.i.	74°13.95'	110°31.23'	1	
27	28/2/2006	n.i.	74°19.56'	110°12.70'	1	
28	1/3/2006	n.i.	74°17.50'	110°10.46'	1	
29*	2/3/2006	Minke	72°48.29'	114°42.70'	4	
30	3/3/2006	Orca	73°40.10'	113°01.53'	8-9	
31	3/3/2006	n.i.	73°28.34'	114°10.76'	1	
32*	4/3/2006	Orca	73°15.30'	116°08.00'	4-5	Seismic

Sighting No.	Date	Species	Latitude (S)	Longitude (W)	Indiv.	Remarks
33*	4/3/2006	Orca	73°27.90'	116°01.10'	5-6	Seismic
34	11/3/2006	Minke	74°19.54'	110°12.24'	4	
35	11/3/2006	Minke	74°19.63'	110°12.07'	1	
36	11/3/2006	n.i.	74°18.92'	110°04.90'	1	
37*	14/3/2006	Minke	73°55'	103°10'	1	Sea ice; Seismic
38	15/3/2006	Minke	73°57.75'	103°06.85'	2	
39	16/3/2006	Minke	73°03.90'	103°52.72'	2	Sea ice
40	16/3/2006	n.i. (Big Baleen)	72°29.59'	103°51.78	1	Sea ice; Seismic^{+}
41	17/3/2006	Minke	72°13.59'	104°36.74'	1	Sea ice
42	24/3/2006	Orca	71°09.30'	118°42.92'	7-8	
43	24/3/2006	Minke	70°40.16'	119°42.41'	2	
44*	26/3/2006	Minke	70°39.7'	124°34.5'	2	
45	26/3/2006	Fin Whale	69°39.32'	125°42.95'	1	
46*	28/3/2006	Minke	70°41.05'	120°29.00'	1	
47*	29/3/2006	Southern Bottlenose Whale	70°11.4'	118°24.1'	2	
48*	29/3/2006	Minke	69°49.9'	117°32.6'	2-3	
49*	3/4/2006	n.i. (Big Baleen)	68°23'	68°15'	1	
50	3/4/2006	n.i.	67°44.43'	70°17.26'	1	
				Total	121-132	

References

Branch, TA & Butterworth, DS (2001) Estimates of abundance south of 60°S for cetacean species sighted frequently on the 1978/79 to 1997/98 IWC/IDCR-SOWER sighting surveys. Journal of Cetacean Research and Management 3(3): 251-270.

Carwardine, M (2002) Whales, Dolphins and Porpoises. 2 Edition, Smithsonian Handbooks, Dorling Kindersley Limited, London, pp. 256.

Gill, A & Evans, PGH (2002) Marine mammals of the Antarctic in relation to hydro acoustic activities. Study on behalf of the German Federal Agency for Nature Conservation (BfN), Oxford.

Kasamatsu, F, Joyce, GG, Ensor, P & Mermoz, J (1996) Current occurence of baleen whales in Antarctic waters. Reports of the International Whaling Commission 46: 293-304.

Reeves, RR, Stuart, SBS, Clapham, PJ, Powell, JA (2002) Guide to Marine Mammals of the world. National Audubon Society, Alfred A. Knopf, Inc., New York, pp. 527.

14. MARINE MAMMAL AUTOMATED PERIMETER SURVEILLANCE (MAPS)

Marc Ritter
Alfred-Wegener-Institut, Bremerhaven

Objectives

Ship-based detection of marine mammals has a broad range of applications. Ecologists with focus on marine mammal abundances and migratory patterns are interested in effective methods for conducting a census of marine mammals. On the other hand, users of hydroacoustic instruments (e.g. scientific sonars) are interested in how to most effectively implement reliable mitigation methods if adverse reactions of marine mammals to the ship's presence are observed. MAPS combines a passive hydroacoustic system (towed linear hydrophone array) and an optical system (visual and infrared camera) to achieve highest possible detection rates. While the acoustic system is built to detect submerged marine mammals by their underwater vocalizations, the infrared system detects whales resting on the surface by their warm blow standing out against the cold antarctic environment.

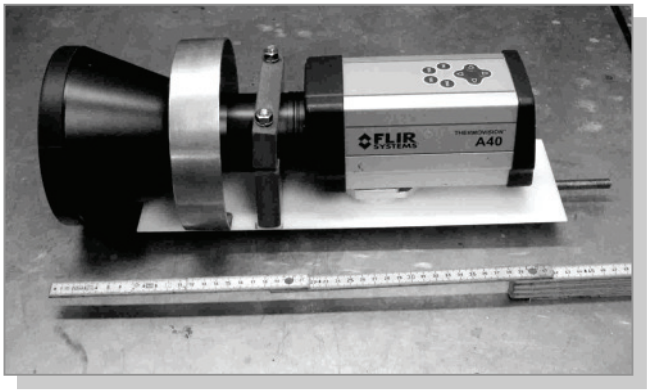

Fig. 14.1: The infrathermal camera from FLIR Systems with a telephoto lens of 7 degree with a handmade socket and latch

Fig. 14.2: Drawing some cables with Martin Fröb (left) in front of the cameras in the crow's nest

Work at sea

Scientific work at the ANT-XXIII/4 expedition focused on testing different lenses (24°, 12° and 7°) for the infrared camera and improving the camera software for recording and automated detection. At the beginning of the cruise the existing software was modified to handle up to 2 cameras (visual and/or infrared) in parallel. Also a new graphical user interface (GUI) was developed. This GUI guarantees also inexperienced users an easy and fast access to all necessary camera parameters like timer-triggered recordings, preview availability, different parameters for the auto-detection functions and several functions for the cameras itself. Also a new detection

algorithm was implemented in the software. In the course of the cruise one additional infrared camera was assembled. Now, 3 cameras (2 infrared and one visual camera) have been mounted in waterproof housings at the crow's nest – about 30 meters above sea level. The two infrared cameras are working with a 12° and a 7° lens.

Preliminary results

A total amount of 330 GB of camera data (visual and infrared) were acquired for further analysis and improvement of the detection algorithm. The software is now running stable and collects a 30 sec video clip of all cameras every 90 sec. The detection algorithm was improved and allows real-time detection on 2 cameras in parallel. In the future, the algorithm should detect whale spouts under varying environmental conditions, especially different light conditions (day/night). Unfortunately the infrared camera with the 7° lens was not running stable due to technical problems. These problems are going to be solved and the camera will be integrated in the system on expedition ANT-XXIII/6 (June - August 2006). In the future, the video signal of the infrared cameras could be spliced into the board video net as a steering help for nautical officers during night time.

Fig. 14.3: Three cameras - visual, infrared 12 degree and infrared 7 degree (up to down).

Fig. 14.4: Visual camera with a FOV of 24 degree during a bright day

Fig. 14.5: The same scence as in Pic 4 from the IR camera using a 12 degree telephoto lens with a better resolution of the landscape

15. WEATHER AND SEA-ICE OBSERVATION

Manfred Gebauer, Klaus Buldt
Deutscher Wetterdienst, Hamburg

Objectives
The ship's meteorological office has to supply ship and science as well as flight missions with meteorological data and predictions.

Methods and equipment
In order to do the whole range of meteorological measurements, the standard equipment, which is used by the DWD (Deutscher Wetterdienst), the official German meteorological office, has to be installed on the ship. The meteorological data are stored on the ship's own computer system and can be later found in the storage system of the Alfred-Wegener-Institut, Bremerhaven.

Results
Weather and sea-ice observations were performed by the staff of the ship's meteorological office. Additional sea-ice data were obtained by email and passed on to the chief scientist. Meteorological forecasts were done and also passed on to the ship's and the science's leadership, to the scientific staff as well as to the helicopter pilots.

Short weather description during ANT-XXIII/4
When the research vessel RV *Polarstern* had left Punta Arenas on 11 February, a strong westerly wind blew in the Magellan Strait, which the ship followed westwards. Next day we arrived at the western exit of the Magellan Strait and the ship continued forward on a southerly course. The wind came mainly from west to northwest and the wind force reached 6-8 Bft. When the ship arrived near *Rothera* Station a favourable easterly wind blew at 3-6 Bft.

Accompanied by southeasterly winds at 5-6 Bft the ship moved to Peter I Island, which is situated at the southern edge of Amundsen Sea and Bellingshausen Sea. Here the weather was marked by good flight conditions.

Until the end of February the ship's working area was west and southwest of Peter I Island. For a short time the weather changed, when a depression passed us at 70° S, with strong to stormy northerly winds.

The next research area in the southern Amundsen Sea south of 70° S was near the edge of the antarctic ice-shelf. Here the ship went to hardly accessible polynyas, where extensive research work was done by means of helicopter during changeable weather and visibility conditions. Due to mostly high pressure above the Antarctic continent and the influence of low pressure near 70° stormy easterly winds with –10 °C were expected near the edge of the shelf ice. Occasionally there was snowfall and

low ceiling, thus inducing the danger of icing, with a strong relevance for the flight weather. Very cold air flew out from the Antarctic continent.

During the second half of March the ship left this area and steamed to the Marie Byrd Seamounts again. Some depressions passed eastwards near 70° S. They caused a quick change of weather conditions with snow showers and storm for a short time. Occasionally there was only a gentle breeze. The weather prediction was difficult especially for the long range helicopter flights doing magnetic research.

Once more Peter I Island was visited using the helicopter for research purposes on GPS, Magnetometer and the automatic weather station. A ridge of high pressure caused acceptable flight weather with good clouds and ceiling conditions.

At the end of March a depression approached from northwest accompanied by stormy winds. Finally the ship headed home to Punta Arenas. *Rothera* was passed in order to do logistic works by means of helicopter during fair weather. The ship proceeded to *Jubany*. Despite occasional snowfall extensive logistic chores were done by helicopters. On the second day offshore *Jubany* the weather became a little better.

Crossing through Bransfield Strait and Drake Passage in the direction of Magellan Strait and Punta Arenas was strongly influenced by a heavy storm that passed through Drake Passage.

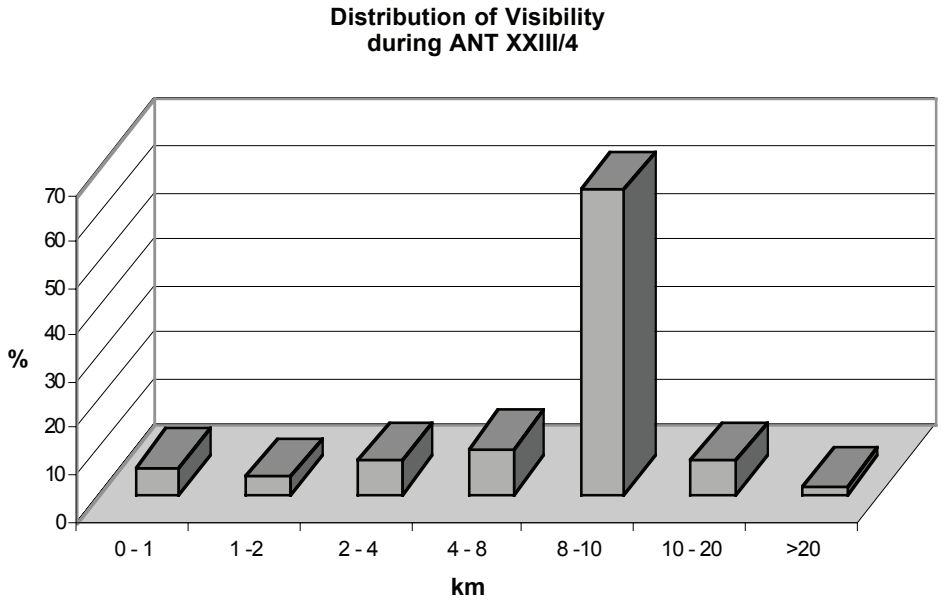

Fig. 15.1: Relative distribution of visibility

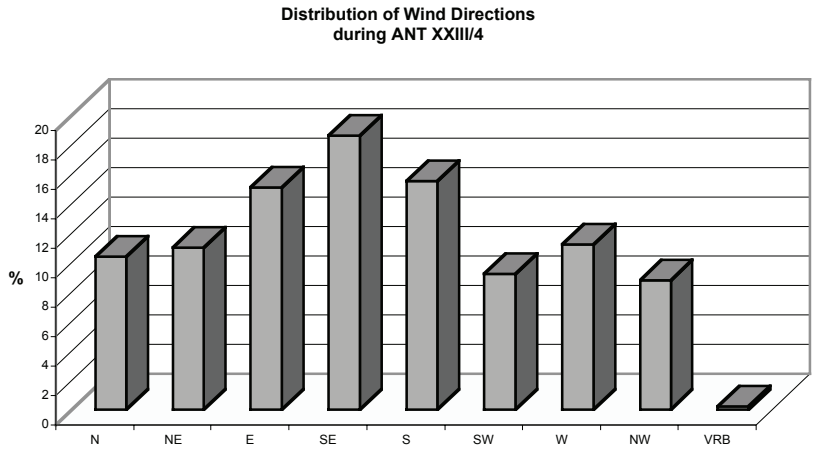

Fig. 15.2: Relative distribution of wind direction

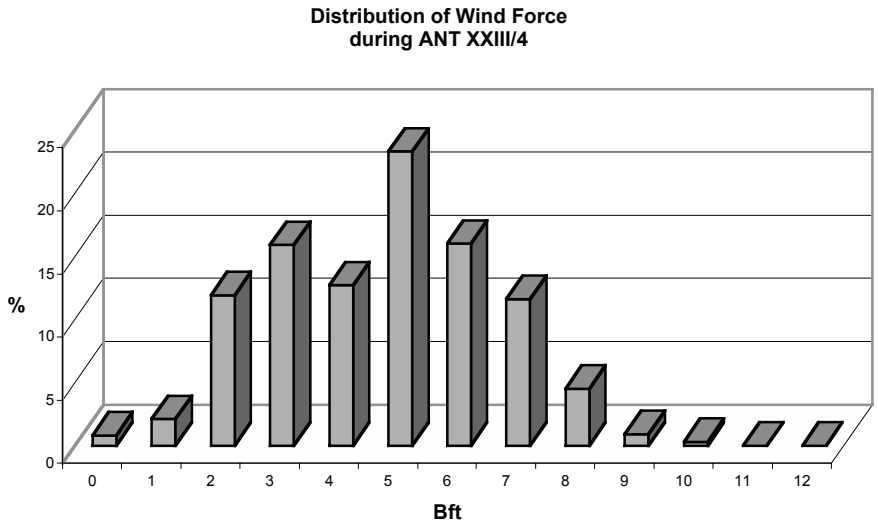

Fig. 15.3: Relative distribution of wind force

16. AUTOMATIC WEATHER STATION ON PETER I ISLAND

Frank Nitsche[1)], Raul Guerrero[2)], Terence O'Donovan[3)], Klaus Buldt[4)], Felix Riess[5)]

[1)] Lamont-Doherty Earth Observatory, Palisades, USA
[2)] INIDEP, Mar del Plata, Argentina
[3)] British Antarctic Survey, Cambridge, UK
[4)] Deutscher Wetterdienst, Hamburg
[5)] Fielax GmbH, Bremerhaven

Background

The Automatic Weather Station (AWS) programme in Antarctica began in 1980 when the first AWS units were installed. The programme is headed by the Antarctic Meteorological Research Center of the University of Wisconsin (USA) and funded by the U.S. National Science Foundation (NSF). The AWS units collect data critical to the understanding of Antarctic and global meteorology and climate. The AWS data are combined with relevant Global Telecommunications Systems data, satellite imagery, and the National Meteorological Center global analyses for comprehensive meteorological data which are available to the scientific community.

As part of this programme, there are currently 40 AWS tower units in the field. The remote regions of the Bellingshausen Sea and Amundsen Sea are rarely visited and present a large and critical gap in this network of weather stations. Based on the initiative of Stan Jacobs (Lamont-Doherty Earth Observatory), AWI was approached to help install an additional station in this area during the expedition ANT-XXIII/4.

Description of the station

The AWS consists of a 5 m tower with a wind, temperature, and humidity sensor located on top as well as a pressure sensor in the main electronic box. A solar panel recharges sealed gel-cell batteries. The wind monitor is a RM Young aerovane with a nominal 5-degree dead zone and is oriented towards north.

The AWS station with the ID 8933 transmits its data every 400 s through the ARGOS system. During fly-over of ARGOS satellites, these signals are collected and redistributed.

Deployment

After reconnaissance of Peter I Island, we decided to install the station on the northern Radiosletta plateau as this plateau allows easy access and minimal wind disturbance for prevailing wind directions from the north and west. The tower was anchored by three guy wires and dead man into the hard snow, bedrock or ice (Fig. 16.1).

The AWS was installed on 19 February 2006, after about three hours of work. It started its transmission after installation was finished at about 16:00 UTC. The location was measured using a handheld GPS at 68°46.163'S and 90°30.317'W (Fig. 16.2). Barometric and GPS determination of the height for the base of the tower yield 128 m and 135 m, respectively.

After receiving the necessary information for decoding the transmitted signal, the meteorologists on RV *Polarstern* were able to receive and decode the data. We received 3 to 4 data packages per overflight from a satellite.

Fig. 16.1: Installed tower on Peter I Island with the peak of the island in the background (looking south)

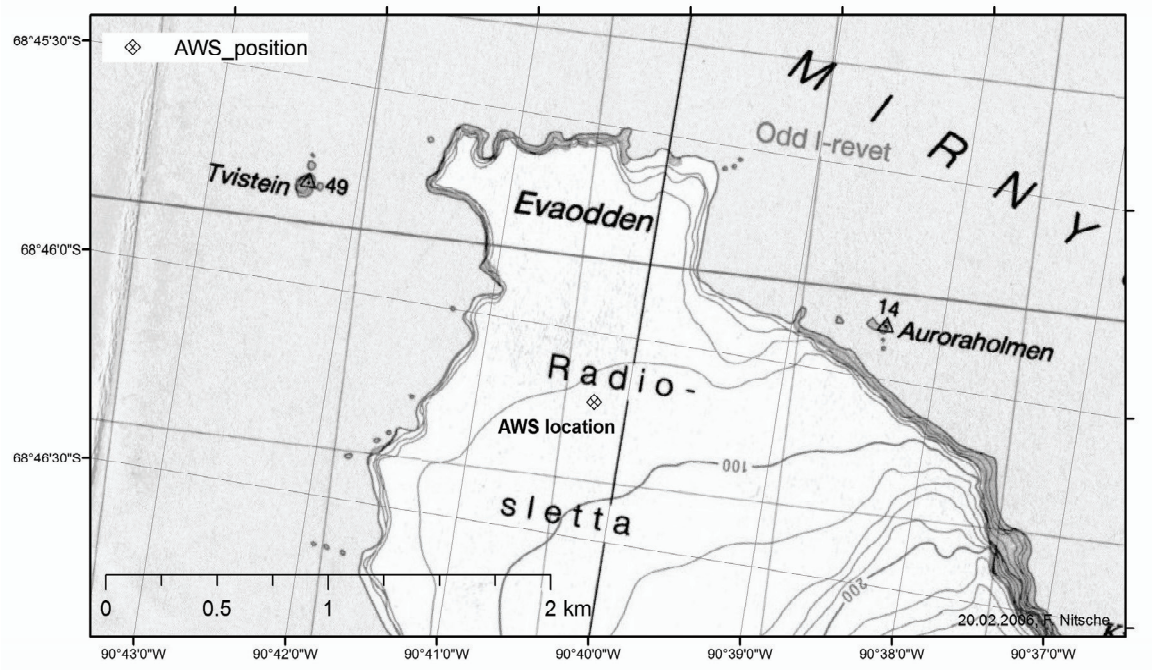

Fig. 16.2: Map showing the location of the AWS 8933 on Peter I Island on the northern plateau marked by the diamond shaped symbol

Inspection and calibration measurements

On the way back we had the opportunity to revisit the weather station on 31 March 2006. We found the station in perfect condition with only minimal snowdrift accumulation of a few centimetres. The solar panel was ice-free. We measured temperature, wind speed and direction as well as pressure, and determined relative humidity using calibrated instruments from RV *Polarstern*. The results were compared with data from the station that where received via satellite at 16:56 UTC. The results show that the AWS data are in good agreement with the measurements except that the pressure seems to be 3-4 hPa too low and the humidity much less then measured (Table 16.1). However, the measurement of the humidity might have been influenced by the higher amount of snowdrift near the base of the station compared to the top of the tower.

Tab. 16.1: Comparison of AWS data and calibration measurements

	AWS data	**Measurements**
Time	16:56 UTC	17:00 UTC
Temperature	-2.9°C	-2.8°C
Wind speed	10.3 m/s	10-11 m/s
Wind direction	244°	220° + 30° magn. declination
Pressure	960.9 hPa	964 hPa
Rel. humidity	50%	66%

Contact person for questions and long-term data storage of the station:
Matthew Lazzara
Antarctic Meteorological Research Center
947 Atmospheric, Oceanic and Space Sciences
Space Science and Engineering Center
University of Wisconsin-Madison
1225 West Dayton Street, Madison, WI 53706, USA
http://amrc.ssec.wisc.edu;
E-mail: mattl@ssec.wisc.edu

17. LOGISTICS

Karsten Gohl[1)], Uwe Pahl[2)] [1)] Alfred-Wegener-Institut, Bremerhaven
[2)] Reederei Laeisz GmbH, Rostock

***Rothera* Station (Adelaide Island)**
RV *Polarstern* called at *Rothera* Station on 16 February and on 3 April for person and freight transfer. All transports were made by helicopter transfer.

Fuel depot in Hudson Mts. (Ellsworth Land)
Upon request of the British Antarctic Survey, a small fuel depot was set up in the Hudson Mountains between Mt. Manthe and Shepard Dome on 13 March. The depot consists of 6 drums filled with aircraft kerosine and will be used for a scientific programme of BAS in the area during the following seasons.

***Jubany* Station / *Dallmann Lab* and *Bellingshausen* Station (King George Island)**
RV *Polarstern* arrived in Maxwell Bay of King George Island on 5 - 6 April to pay a visit to *Jubany* Station and *Dallmann* Laboratory as well as *Bellingshausen* Station for person and freight transfer. During this stay, an Argentine delegation from *Jubany* Station as well as a delegation and film team from the Uruguayan *Artigas* Station led by the Health Minister of Uruguay and the German Ambassador visited RV *Polarstern*. AWI Director Prof. Thiede visited the Antarctic research stations of several countries on King George Island and signed a new German-Argentine scientific cooperation contract at *Jubany* Station.

18. BETEILIGTE INSTITUTE / PARTICIPATING INSTITUTES ANT-XXIII/4

	Adresse /Address
AWI	Stiftung Alfred-Wegener-Institut für Polar- und Meeresforschung in der Helmholtz-Gemeinschaft Postfach 12 01 61 27515 Bremerhaven / Germany
BAS	British Antarctic Survey High Cross, Madingley Road Cambridge, CB3 0ET/ UK
DWD	Deutscher Wetterdienst Hamburg Abteilung Seeschifffahrt Bernhard-Nocht Str. 76 20359 Hamburg / Germany
FIELAX	FIELAX Gesellschaft für wissenschaftliche Datenverarbeitung mbH Schifferstraße 10-14 27568 Bremerhaven / Germany
University Jena	Friedrich-Schiller-Universität Jena Institut für Geowissenschaften Burgweg 11 07749 Jena / Germany
HeliTransair	HeliTransair GmbH Am Flugplatz 63329 Egelsbach / Germany
IFM-GEOMAR	Leibniz-Institut für Meereswissenschaften IFM-GEOMAR Düsternbrooker Weg 20 24105 Kiel / Germany
INIDEP Argentina	Instituto Nacional de Investigacion y Desarrollo Pesquero (INIDEP) Pasco Victoria Ocampo 1 7600 Mar del Plata / Argentina

	Adresse /Address
ISITEC	ISITEC GmbH Stresemannsr. 46 D-27570 Bremerhaven / Germany
LDEO	Lamont-Doherty Earth Observatory Columbia University LDEO / P.O. Box 1000 61 Route 9W Palisades, NY 10964-1000 / USA
Tethys	Thethys Geoconsulting GmbH Wischhofstr. 1-3 24148 Kiel / Germany
TU Dresden	Technische Universität Dresden Institut für Planetare Geodäsie 01062 Dresden / Germany
University Hamburg	Universität Hamburg Institut für Geophysik Bundesstr. 55 20146 Hamburg / Germany
University Jerusalem	Hebrew University Jerusalem Department of Botany and Environmental Ecology Giv'at Ram Campus Jerusalem 95701 / Israel
University Leipzig	Universität Leipzig Institut für Geophysik und Geologie Talstr. 35 04109 Leipzig / Germany
University Salzburg	Universität Salzburg FB Organismische Biologie Hellbrunner Str. 34 A-5020 Salzburg / Austria
UniversityTromsø	Universitetet i Tromsø Department of Geology, 9037 Tromsø / Norway
VIG	Vernadsky Institute of Geochemistry 19, Kosygin Street Moscow 117975 /Russian Federation

19. FAHRTTEILNEHMER / PARTICIPANTS

Name Vorname/ Name, First Name	Institut Institute	Beruf / Profession
Blume, Marlen	AWI	Biologist
Bohlmann, Harald	Isitec	Technician
Buldt, Klaus	DWD	Technician
Daniel, Kristin	FSU Jena	Student, geology
Dietrich, Reinhard	TU Dresden	Geodesist
Eagles, Graeme	AWI	Geophysicist
Fahl, André	AWI	Student, geophysics
Feigl, Thomas	Univ. Graz/AWI	Student, geodesy
Feldt, Oliver	HeliTransair	Technician
Forwick, Matthias	Univ. Tromsø	Geologist
Gebauer, Manfred	DWD	Meteorologist
Gohl, Karsten	AWI	Chief-Scientist, Geophysicist
Grobys, Jan	AWI	Geophysicist
Guerrero, Raul	INIDEP Argentina	Oceanographer
Hass, Christian	AWI Sylt	Geologist
Hauff, Silke	IFM-GEOMAR	Technician
Hauff, Sven Folkmar	IFM-GEOMAR	Geologist
Heckmann, Hans-Hilmar	HeliTransair	Pilot
Heise, Katja	AWI	Biologist
Hillenbrand, Claus-Dieter	BAS	Geologist
Johnson, Joanne	BAS	Geologist
Just, Janna	AWI	Student, geophysics
Kamennaya, Nina	Univ. Jerusalem	Student, biology
Kober, Martin	Univ. Jena	Student, geology
Krüger, Stefan	Univ. Leipzig/AWI	Geologist
Kuhn, Gerhard	AWI	Geologist
Leinweber, Volker	AWI	Student, geophysics
Lemenkova, Polina	VIG/Univ. Moscow	Cartographer

Name Vorname/ Name, First Name	Institut Institute	Beruf / Profession
Lensch, Norbert	AWI	Technician
Mayr, Christina	AWI	Student, geophysics
Netzeband, Gesa	Univ. Hamburg	Physicist/Geophysicist
Neubacher, Elke	Univ. Salzburg	Student, biology
Nitsche, Frank	Lamont-Doherty	Geophysicist
O'Donova, Terence	BAS	Technician
Parsiegla, Nicole	AWI	Geophysicist
Petitat, Manuel	AWI	Student, geology
Rackebrandt, Nick	AWI	Student
Richter, Andreas	TU Dresden	Engineer
Ritter, Marc	AWI	Engineer
Schlüter, Philip	AWI	Geophysicist
Schmiing, Mara	AWI	Student, biology
Steinmair, Ulrike	Univ. Salzburg	Student, biology
Strahl, Julia	AWI	Student, biology
Suckro, Sonja	AWI	Student, geophysics
Thiede, Jörn	AWI	Geologist
Veit, Andreas	Univ. Jena	Geologist
Walter, Torben	Univ. Salzburg	Student, biology
Werner, Reinhard	Tethys/Geomar	Geologist
Wickham, Stephen	Univ. Salzburg	Biologist
Wiencke, Christian	AWI	Biologist
Winter, Stefan	HeliTransair	Pilot
Zeidler, Martin	HeliTransair	Mechanic
Zimmermann, Katja	AWI	Student, geophysics
Gauger, Steffen	Fielax	Engineer

20. SCHIFFSBESATZUNG / SHIP'S CREW

Reederei F.Laeisz G.m.b.H — Reise/journey ANT-XXIII/4
Nationality : GERMAN — Punta Arenas - Punta Arenas

No.	Name	Rank
1	Pahl, Uwe	Master
2	Grundmann, Uwe	1. Offc.
3	Ziemann, Olaf	Ch.Eng.
4	Hering, Igor	2. Offc.
5	Wunderlich, Thomas	2. Offc.
6	Bratz, Herbert	3. Offc.
7	Türke, Helmut	Doctor
8	Koch, Georg	R. Offc.
9	Simon, Wolfgang	1. Eng.
10	Schnürch, Helmut	3. Eng.
11	Wanke, Steffen	3. Eng.
12	Haefke, Bernd	ElecEng.
13	Feiertag, Thomas	ELO
14	Fröb, Martin	ELO
15	Muhle, Helmut	ELO
16	Riess, Felix	ELO
17	Clasen, Burkhard	Boatsw.
18	Neisner, Winfried	Carpenter
19	Burzan, Gerd-Ekkeh.	A.B.
20	Hartwig-Lab.,Andreas	A.B.
21	Kreis, Reinhard	A.B.
22	Lamm, Gerd	A.B.
23	Moser, Siegfried	A.B.
24	Pousada Martinez, S.	A.B.
25	Schröder, Norbert	A.B.
26	Schultz, Ottomar	A.B.
27	Beth, Detlef	Storek.
28	Dinse, Horst	Mot-man
29	Fritz, Günter	Mot-man
30	Hoppe, Kurt	Mot-man
31	Krösche, Eckard	Mot-man
32	Watzel, Bernhard	MotMan
33	Fischer, Matthias	Cook
34	Martens, Michael	Cooksmate
35	Tupy, Mario	Cooksmate
36	Dinse, Petra	1.Stwdess
37	Tillmann, Barbara	Stwdss/Kr
38	Deuß, Stefanie	2.Stwdess
39	Hu, Guo Yong	2.Steward
40	Möller, Wolfgang	2.Steward
41	Schmidt, Maria	2.Stwdess
42	Sun, Yong Sheng	2.Steward
43	Yu, Chung Leung	Laundrym.
44	Felsenstein, Thomas	Apprentice

APPENDICES

A.1 Expedition itinerary

A.2 Summary of hard rock sampling

A.3 Station list

A.1 EXPEDITION ITINERARY

day	date	approx. ship time	hours from UTC	program & events	weather
Fr	10.02.	14:30 22:00	-3	Punta Arenas: arrival of participants on board; measurement of gravity reference at Cabo Negro	fine
Sa	11.02.	09:00	-3	departure of Polarstern from Cabo Negro; transit through western Magellan Strait	cloudy; rain; heavy winds
Su	12.02.	02:00	-3	leaving Magellan Strait; course southward; working deck closed	heavy winds, cloudy
Mo	13.02.	 23:00	 -4	transit; working deck closed; crossing of unmapped seamount rising to 500 m from 4300 m at 60°00'S, 73°24'W	heavy winds calming down; cloudy
Tu	14.02.	13:00	-4	magnetometer compensation track; erroneous coordinate shift of Hydrosweep (MINS problem)	calm; cloudy
We	15.02.	 10:00 16:00	-4	erroneous coordinate shift of Hydrosweep (MINS problem), change to other MINS; test flights helicopter & test flight heli-mag; CTD/Rosi 500 m, Bongo 200 m;	calm, cloudy, snow showers
Th	16.02.	 5:00 10:00	-4	arrival Marguerite Bay; whale observation begins; sightings of numerous whales; 2 heli-flights to Rothera; pick-up C.D. Hillenbrand; CTD/Rosi 500 m;	fine, cloudy, calm winds
Fr	17.02.	05:00 10:30	-4	CTD/Rosi 20 m, 500 m; heli-mag; short course on environmental behaviour; heli-mag;	fine, cloudy, calm winds
Sa	18.02.	09:00 16:30 21:00	-4	CTD/Rosi 500m; heli-mag; Peter I Island: CTD/Rosi 2500 m (Hydrosweep calibration & biology); 2 flights to island for recovery of seismometer, visit of ham radio camp and deployment of GPS unit; dredging with good recovery of volcanics	cloudy, fine, sunny
Su	19.02.	 09:00 10:00 14:00	-4	dredging flight to island for deployment of automatic weather station (AWS) and magnetometer; flights for crew and scientists; departure from Peter I Island;	cloudy, calm
Mo	20.02.	02:00 05:00 19:00	-4	DGGA seamount: bathymetric survey, decision not to dredge due to lack of steep flanks; magnetometer compensation track; west. De Gerlache Seamount: piston core 17 m;	foggy; winds getting stronger
Tu	21.02.	01:00 08:30	-4	west. De Gerlache Seamount: piston core 16 m; Bongo 200 m; transit toward Pine Island Bay margin; heli-mag;	hazy, strong winds, calming down
We	22.02.	09:00 15:00 15:30	-4	CTD/Rosi 500 m; crossing DSDP 324; piston core 20 m;	hazy, foggy, medium sea-state

day	date	approx. ship time	hours from UTC	program & events	weather
Th	23.02.	09:00 14:00 20:00 24:00	-4	releaser test cancelled due to heavy seas; arrival at Pine Island Bay margin; course through increasing sea-ice; severe press-ice conditions; stop course through ice; just drifting SW-ward;	strong winds; heavy seas
Fr	24.02.	08:30 23:00 23:30	-4	heli reconnaisance flight showed no wide pathway southward, polynia seen only in far south distance; ship made little distance in breaking through press ice in westward direction toward open water; heli-mag; reaching open water; grab sampler and gravity corer 500 m;	winds calming down; good view
Sa	25.02.	07:00 08:30 09:00 19:00 19:30	-4	bongo 200 m and CTD 500 m; hydroacoustic streamer, no whale vocalisation; begin reflection seismic profile 20060001; processing of first tape revealed unusual coherent noise in data; changing sampling rate (20060002) did not improve records; premature end of seismic profile 20060002: bathymetric survey of outer shelf, megascale lineations and iceberg scours observed;	almost no winds; hazy
Su	26.02.	 09:00 09:00 11:00	-4	continued bathymetric survey of trough; gravity cores and grab-sampler; heli reconnaisance flight showed no wide pathway and polynia along eastern PIB shore; decision to abandon attempt to move into PIB; bathymetric survey continues; heli-mag; transit along sea-ice edge westward;	no winds; cloudy, first hazy to clear, then foggy
Mo	27.02.		-4	continuing westward transit along ice-edge; breaking through ice cover southward at about 114°W; heli-mag;	calm then stronger winds; partly cloudy
Tu	28.02.	 08:30 18:00	-4	entering ice-free western PIB; transit toward Crosson Ice-Shelf; CTD 500 m, Bongo 300 m; heli-mag; arrival north of Crosson ice-shelf, cannot continue southward due to unbroken sea-ice; hydrosweep survey;	strong winds; cloudy; clear; sunny; strong winds
We	01.03.	09:00 10:00 15:00 22:00	-4	heli flights to Mt. Murphy (60 nm south) for geology, GPS and surface exposure program; good work conditions; OBH releaser test; gravity core; CTD 270 m; GPS tidal station on ice-shelf; multi-net; begin OBH deployment profile 20060100;	clear; sunny; strong winds; -13°C
Th	02.03.	08:00 10:00	-4	end OBH deployment; begin seismic shot profile 20060100; heli-mag;	partly cloudy, calm winds

day	date	approx. ship time	hours from UTC	program & events	weather
Fr	03.03.	03:00 08:30 09:00 09:30 14:00 19:00 21:30	-4	circumvening ice-fields; end seismic shot profile at OBH-1; begin OBH recovery; GPS stations on Dotson Ice-Shelf and western Bear Peninsula; gravity core; bongo; CTD; heli-mag; gravity core; gravity core; box core;	cloudy, calm winds
Sa	04.03.	01:00 02:00 03:00 08:00 08:30 12:00 17:00	-4	gravity core; CTD; gravity core; end OBH recovery; CTD/bongo net; life-boat manoevre; heli-mag; begin seismic profile 20060003; celebrating 3000th heli flight hour of Stefan Winter;	partly cloudy, calm winds sunny; no wind
Su	05.03.	11:30 12:00	-4	end seismic profile 20060005; begin bathymetric survey central Getz Ice-Shelf trough;	cloudy; intermediate winds
Mo	06.03.	all day and night	-4	end bathymetric survey central Getz Ice-Shelf trough; trough is about 1550 m deep; lots of sea-ice in bay; several CTD and gravity core stations in trough; CTD & oceanogr. mooring;	cloudy; no wind
Tu	07.03.	09:00 11:30 16:00 23:00	-4	geol. sampling at exposed rocks at west coast of Wright Island with zodiac, good samples of granites & granodiorites; departing from central Getz ice-shelf; bongo, CTD & oceanogr. mooring in trough off eastern Getz ice-shelf; CTD & oceanogr. mooring in trough off Dotson ice-shelf;	very hazy; low clouds, calm winds
We	08.03.	02:00 09:00 15:00	-4	gravity core & box core north of bay; arrival north of Crosson ice-shelf; bongo net, box core; waiting for better weather for heli reconnaissance; snow storm continued; begin seismic profile 20060005;	very hazy; strong southerly winds with snow; very cold (-13°C)
Th	09.03.	all day and night	-4	continuing seismics 20060005, 20060006 and 20060007; heli-mag;	strong southerly winds; cloudy
Fr	10.03.	11:00 12:00 18:00 19:00	-4	end seismics 20060007; heli-mag; CTD, bongo, multi-net, gravity core, box core; gravity core, box core; transit to position north of Crosson ice-shelf; heli-mag;	partly cloudy, clear; strong winds

day	date	approx. ship time	hours from UTC	program & events	weather
Sa	11.03.	08:00 09:00 12:00 13:30 18:00	-4	arrival at position north of Crosson ice-shelf; heli reconnaissance for transit to PIB, plenty of new sea-ice, but break-trough along polynya around B22 seems feasible; transit through new sea-ice cover into ice-free area off Crosson ice-shelf; heli-flights to Mt. Murphy and Bear Pensinsula for GPS recovery and redeployment and geological sampling; heli-mag; CTD (+1.2°C at bottom); hydrosweep survey off Crosson ice-shelf; Bergfest; transit along polynya north of B22A ice-tongue toward PIB;	clear and sunny, strong southeasterly winds
Su	12.03.	08:00 18:00 23:00	-4	entry into PIB through thick but breakable new sea-ice; hydrosweep track around ice-edge of ice-free bay off Thwaites ice-shelf; partly breaking through thick new sea-ice ridges; heli-mag; numerous ice-bergs at ice-shelf edge; CTD (+0.98°C at bottom); transit into area off Pine Island ice-shelf; begin seismic profile 20060008 parallel to ice-shelf;	clear and sunny, strong southeasterly winds
Mo	13.03.	09:30 10:00 10:30 17:00	-4	begin reconnaissance flights to Hudson Mts.; transport of surface exposure group to Mt. Manthe; end seismic profile 20060008 at NE end of ice-shelf; begin heli-transport of 6 fuel drums (for BAS) in 3 heli-flights to Hudson Mts.; heli transport of GPS team to Mt. ??? and ice-shelf; heli-transport of geologists to Mt. Moses; heli-transport of GPS team and geologist to small island off ice-shelf with granite outcrops; CTD, bongo net, gravity core, box core; gravity/box core program during night;	clear and sunny, southeasterly winds, cold
Tu	14.03.	07:00 12:00	-4	begin seismic profile 20060009 northward; begin seismic profile 20060010;	cloudy, calm winds
We	15.03.	07:00 17:00 21:00	-4	end seismic profile 20060010; CTD, bongo net; return hydrosweep transit to PI ice-shelf; heli-mag; sightings of elephant seals on a rocky island; arrival PI ice-shelf; flights to collect GPS from coast and Mt. Manthe; spectacular flight along PIG icestream; gravity core & bos core stations;	partly cloudy, calm winds
Th	16.03.	 12:00 21:00	-4	continuing gravity core & box core stations; begin seismic profile 20060011 northward; landing on Lindsey Island group to investigate rock outcrop and elephant seals; end seismic profile 20060011; begin northward transit through ice belt to leave PIB;	hazy, calm winds

day	date	approx. ship time	hours from UTC	program & events	weather
Fr	17.03.	all day & night	-4	continuing transit through ice belt; heavy ice conditions; heli-mag;	hazy, clearing; calm winds
Sa	18.03.	09:00 11:00 15:00 21:00	-4	leaving ice belt; arriving outer shelf; heli-mag; oceanogr. mooring, CTD, gravity core, box core; CTD, multi-net, bongo, multi-net; begin seismic profile 20060021, into deep sea;	partly cloudy, calm winds
Su	19.03.	all day & night	-4	continuing seismic profile 20060021, 20060022, 20060023;	cloudy, wind increasing
Mo	20.03.	all day & night	-4	continuing seismic profile 20060023;	cloudy, moderate winds
Tu	21.03.	all day 23:00	-4	continuing seismic profile 20060023; end seismic profile 20060023;	cloudy, calm winds
We	22.03.	00:00 08:00 09:30 22:00	-5	small hydrosweep survey along channel south of Marie Byrd Seamounts; CTD, bongo net; begin OBH deployment for 20060200; begin shot profile 20060200; Bolt-gun umbilicals caught on ice-floe;	hazy, winds becoming stronger
Th	23.03.	19:00 20:30	-5	end shot profile 20060200; begin OBH recovery; OBH-1&2 did not return;	cloudy, intermediate winds
Fr	24.03.	03:00 14:00 17:00 23:00	-5	piston core; recovery of OBH-7; return to OBH-1&2; piston core; recovery OBH-2; OBH-1 did not return;	hazy, calm winds
Sa	25.03.	02:00 all day	-5	transit to begin of dredge program at southern MB seamounts; hydrosweep surveying of southern seamount region; no dredge site found; seamount according to satellite map does not exist; heli-mag; transit to western seamounts;	cloudy with snow showers, calm winds; clearing
Su	26.03.	03:00 08:00 11:30	-5	hydrosweep survey of western seamount; several dredge sites; heli-mag; CTD, bongo net; dredging;	partly cloudy, calm winds
Mo	27.03.	all day & night	-5	dredging; heli-mag;	partly cloudy, sunny, no winds
Tu	28.03.	 19:00 20:00	-5	dredging; transit to OBH-1 (time-release); heli-mag; CTD at OBH-1 station; recovery of OBH-1 (with time-release); transit to eastern seamount;	cloudy, snow showers; low winds, increasing
We	29.03.	04:00 14:00	-5	dredging at eastern MB seamount; heli-mag; transit to Peter I Island;	cloudy, calm winds
Th	30.03.	00:30	-5	piston core; transit to Peter I Island; heli-mag;	cloudy, snow showers, winds getting stronger

day	date	approx. ship time	hours from UTC	program & events	weather
Fr	31.03.	 11:30 13:00	-5	last heli-mag flight; arrival Peter I Island; heli-flights to island for recovery of GPS and magnetometer equipment and checking on weather station; CTD, multi-net; begin transit to Rothera;	partly cloudy, intermediate winds
Sa	01.04.	06:00 13:00 18:00	-5	piston core; continuing transit to Rothera; Polartaufe; Fest;	cloudy, strong winds
Su	02.04.	 14:30	-5	continuing transit to Rothera; slowing down due to storm; deploying oceanogr. mooring;	storm in the morning; winds calming down;
Mo	03.04.		-4	heli-flight to Rothera; transport of blood samples and data tapes from Neumayer; CTD, mooring;	
Tu	04.04.		-4	transit;	
We	05.04.	08:00	-4	arrival Jubany; heli-flights to stations for cargo and person transport; visit to King Sejong Station; visit of Uruguayan delegation to Polarstern;	hazy; intermediate winds
Th	06.04.	 13:30 14:30 15:00 18:00	-4	continuing heli-flights to stations; hydrosweep survey and coring in Maxwell Bay and Cotter Cove; visit of Argentinian delegation to Polarstern; visit of Uruguayan delegation to Polarstern; Prof. Thiede et al. coming on board; departure Jubany and transit to Punta Arenas;	cloudy; calm winds
Fr	07.04.		-4	transit to P.A.;	cloudy, strong winds
Sa	08.04.		-4	transit to P.A.;	cloudy, strong winds
Su	09.04.		-4	transit to P.A.;	cloudy, winds calming down
Mo	10.04.		-4	transit to P.A.;	clear, sunny, intermediate winds
Tu	11.04.	08:00	-4	arrival in Punta Arenas	

A.2 Summary of hard rock sampling carried out on RV Polarstern cruise ANT-XXIII/4

Type	Station	Name	Wt dredge	Rock summary	Latitude	Longitude	Max	Min	Rock	Mn	Sed	Bio
	PS69-		kg		deg_min	deg_min	depth m	depth m				
DR	244-1	Peter I Island: NE	400	glassy pillow and sheet flow lava	68°44.47'S	90°20.87'W	1853	1610	1	0	0	0
DR	245-1	Peter I Island: E	0	dredge was lost	68°54.30'S	90°18.52'W	1509	1429	0	0	0	0
Zodiac	277-1	Wright Island	50	fresh qz granodiorite with cm sized biotite rich inclusions	73°57.72'S	116°52.38'W	3m absl	3m absl	1	0	0	0
Heli	BI	Bear Island	30	very fresh, slightly foliated, coarse grained biotite granite	74°34.74'S	111°53.38'W	490m absl	470m absl	1	0	0	0
Heli	PIB	Backker Islands	20	very fresh, coarse grained biotite granite and qz-kfsp granite	74°30.66'S	102°26.36'W	6m absl	6m absl	1	0	0	0
Heli	LI	Edwards Island	40	Fsp rich dike cutting biotite granite in which qz appears highly altered	73°51.17'S	102°59.33'W	5m absl	5m absl	1	0	0	0
DR	311-1	Seamount 6: SE	500	dropstones	69°51.29'S	126°05.85'W	2107	1763	0	0	0	0
DR	312-1	Seamount 6: E	500	dropstones	69°47.47'S	125°56.87'W	1993	1593	0	0	0	1
DR	314-1	Seamount 6: N	500	dropstones	69°43.51'S	126°11.54'W	2003	1873	0	0	0	0
DR	315-1	Seamount 9: W	500	dropstones; fossil corals, evolved volcanics of unclear origin, Mn crusts	69°35.50'S	125°19.76'W	2409	2369	1	0	0	1
DR	316-1	Haxby Seamount: E	20	dropstones	69°06.92'S	123°58.20'W	3361	2963	0	0	0	0
DR	317-1	Haxby Seamount: S	500	dropstones, carbonate crusts with basalt pebbles	69°10.32'S	123°25.46'W	1983	1584	1	1	1	0
DR	318-1	Haxby Seamount: S	500	dropstones, carbonates, Mn crusts, volcanic breccias, corals	69°08.64'S	123°13.35'W	1788	1480	1	0	0	1
DR	319-1	Haxby Seamount: E	500	dropstones, fossil corals, biology, Mn crusts	69°10.43'S	122°52.60'W	2009	1475	0	0	0	1
DR	320-1	Miller Seamount: NW	200	dropstones, one in-situ volcanic, others to be checked	69°21.09'S	121°52.12'W	2500	2432	1	1	0	0
DR	321-1	Miller Seamount: S	500	ol-cpx phyric basalt of in-situ origin, aphyric basalt pieces to be cross-checked for similarities, Mn crusts, minor dropstones	69°21.53'S	121°31.94'W	1670	1431	1	1	0	0
DR	322-1	Miller Seamount: S	0	empty dredge	69°28.51'S	121°22.30'W	2249	1956	0	0	0	0
DR	323-1	Miller Seamount: S	20	granitic dropstones	69°26.81'S	121°23.16'W	1676	1369	0	0	0	0
DR	324-1	Miller Seamount: S	400	dropstones, Mn-crusts, lava fragments of possible in-situ origin, volcaniclastic breccias	69°30.07'S	121°04.00'W	2622	2205	1	1	0	0
DR	325-1	Miller Seamount: S	500	dropstones, fsp phyric vesicular lava (in-situ); single basalt with possible in-situ origin, several very fine grained greyish rocks that could be either basalts or sediments	69°27.23'S	120°55.38'W	1560	1527	1	0	0	0
DR	327-1	Seamount C: W	500	vesicular, ol phyric pillow lava; dense lava of possible in-situ origin; Mn-crusts; dropstones	69°11.05'S	117°38.65'W	2957	2515	1	1	0	0
DR	328-1	Ridge E of Seamount C	500	white semiconsolidated sediment, small lava fragments of unknown origin, small dropstones	69°09.95'S	117°08.80'W	3136	3015	1	0	1	0
DR	329-1	Ridge E of Seamount C	0	empty, repeat of 328-1 due to incorrect map	69°09.76'S	117°07.80'W	3276	2984	0	0	0	0
Heli	PI	Peter I Island: E	40	lava, scoria and volcanic bombs from small eruption center	68°51.81´S	90°25.56´W	50m absl	30m absl	1	0	0	0
Total			6720						15	5	2	4

Rock sampling locations and descriptions for Marie Byrd Seamounts, Peter I Island and crystalline basement samples from Marie Byrd Land and Ellsworth Land

STATION 244-1: PETER I ISLAND

small ridge on NE slope

Dredge on bottom UTC 19/02/06 0122hrs, lat 68º44.15'S, long 90º21.25'W, depth 1853m

Dredge off bottom UTC 19/02/06 0242hrs, lat 68º44.47'S, long 90º20.87'W, depth 1610m

400kg, mostly fresh angular volcanic rocks, minor dropstones

SAMPLE #	SIZE & SHAPE & ROCK TYPE	DESCRIPTION	TS	CHEM	Ar GLS / MIN	ARCH	PICT	A.VEIT	Paulina Katja Mn	NOTES
P69/244-1-1	20x10x15cm angular pillow lava	vesicular pillow lava with 0.8cm fresh glass rind; some palagonatite. Yellowish surface alteration along cooling cracks.	Y	Y	Y Y		Y	Y		15-20% unfilled vesicles 0.5-1mm
P69/244-1-2	30x15x10cm angular pillow lava	vesicular pillow lava with fresh glass rind similar to PS69/244-1-1. Groundmass contains 10% small (<0.5mm) plagioclase.	Y	Y	Y Y		Y	Y		40% unfilled vesicles increase from <0.5mm on margin to 3mm in the interior of the pillow.
P69/244-1-3	20x10x10cm angular sheet lava	highly vesicular (>50%) outer rim of a lava flow. Glass on outer and inner part. Some flow structures are also preserved.	Y	Y	Y Y		Y	Y		Glass should be prepared from the lower side of the sample
P69/244-1-4	20x20x15cm angular to subangular pillow lava. May not belong to P69/244-1-1 through -3 lava type	pillow with no glass, 30% open vesicles. Groudmass contains abundand small plag. <<0.5 mm up to 10% in vol. Brownish-yellowisk surface alteration along cooling cracks.	Y	Y	Y		Y	Y		Plagioclase appears to have crystallized relatively fast, possibly when the lava finally cooled
P69/244-1-5	20x10x8cm angular lava fragment.	lava with 5% unflilled vesicles (0.5-1mm). 30% plag. phenocrysts (0.2-0.4mm).	Y	Y	Y		Y	Y		similar to other samples of this dredge, except no glass.
P69/244-1-6	10x10x5cm angular sheet lava	upper part of a lava with 1cm glassy margins. Surface palagonitization of glass.	Y	Y	Y		Y	Y		similar to P69/244-1-3
P69/244-1-7	30x20x15cm angular pillow	similar to P69/244-1-1,-2; with glass.				Y	Y			nice columnar joints
P69/244-1-8	15x8cmx8cm angular pillow	similar to sample P69/244-1-1,-2. Contains greenish-yellow xenoliths of unknown composition. Ol?, Peridotite?	N				Y			Needs special cutting to prepare xenolith
P69/244-1-9	20x10x10cm angular pillow	similar to P69/244-1-1,-2; with glass				Y	Y			
P69/244-1-10	30x20x20cm angular pillow	similar to P69/244-1-1,-2; with glass				Y	Y			
P69/244-1-11	15x10x8cm angular sheet lava	similar to P69/244-1-3; with glass				Y	Y			
P69/244-1-12	30x20x15cm angular sheet lava	similar to P69/244-1-5, but with minor fresh glass				Y	Y			multiple cm wide banding of vesicular and dense lava layers

STATION 244-1 (continued)

SAMPLE #	SIZE & SHAPE & ROCK TYPE	DESCRIPTION	TS	CHEM	Ar	GLS / MIN	ARCH	PICT	A.VEIT	Paulina	Katja	Mn	NOTES
P69/244-1-13	30x20x15cm highly vesicular, angular lava fragment	lava with up to 40% unfilled vesicles up to 1cm					Y	Y					Not clear whether this sample is insitu or comes from upslope
P69/244-1-14	50x40x40cm angular pillow. Largest pillow recovered	similar to P69/244-1-1,-2. Thick 1cm highly vesicular glass rim. Some surface palagonite. 5% small plagioclase phenocrysts <<0.5mm.		Y		Y	Y	Y					One piece saved into WORKING HALF ARCHIEVE SAMPLE still contains a lot of fresh glass
P69/244-1-15	20x20x10cm sheet lava.	similar to sample P69/244-1-3,-6. Abundant fresh glass.				Y							serves as backup for WORKING HALF
P69/244-1-16	20x10x6cm redish, angular scoria of possible subaerial origin	20-30% unfilled vesicles. Quite heavy for scoria, may contain basaltic core.											In situ origin questionable
P69/244-1-17	30x20x15cm highly vesicular lava fragment.	Vesicles are up to 1cm in diameter. Vesicles are lined with sandy-silty material (hyaloclastite?).											In situ origin questionable
P69/244-1-18	40x30x20cm subrounded pillow lava	15% unfilled vesicles.					Y						Piece appears more rounded than other samples of this dredge
P69/244-1-19	20x15x10cm angular sheet lava	similar to sample P69/244-1-3,-6. Abundant fresh glass.					Y						

STATION 245-1: PETER I ISLAND

E slope, small cone or ridge from N to S

Dredge on bottom UTC 19/02/06 0620hrs, lat 68º54.14'S, long 90º18.64'W, depth 1509m

Dredge off bottom UTC 19/02/06 0750hrs, lat 68º54.30'S, long 90º18.52'W, depth 1429m

dredge lost, both safety cables broke at 11tons and were probably sheared off

STATION 277-1: Wright Island, Western Pine Island Bay
Sampling by Zodiac of small island immediately in front of ice shelf. Shelf ice cliff consists of the same lithology

sampling UTC 07/03/06 1030hrs, lat 73º57.721'S, long 116º52.382'W, altitude 3m
50kg fresh angular pieces of qz-granodiorite

SAMPLE #	SIZE & SHAPE & ROCK TYPE	DESCRIPTION	TS	CHEM	Ar	GLS / MIN	ARCH	PICT	A.VEIT	Paulina	Katja	Mn	NOTES
P69/277-1-1	26x12x10cm angular	fresh quartz-granodiorite. Equigranular 2-3mm quartz (50%) and plagioclase (40%), 1-2mm biotite (8%), trace amounts of 3-4mm K-fdsp (2%). Minor iron staining along cracks, weathering rind 2mm max.	Y	Y	Y			Y					this piece has the least amount of biotite rich inclusions.
P69/277-1-2	15x15x10cm angular	similar to P69/277-1-1. Contains dark biotite rich inclusions up to 2-3cm. Iron staining along fractures.						Y					
P69/277-1-3	20x18x15 cm angular	similar to P69/277-1-1. 1/4 of the sample consists of cm sized biotite rich inclusions.						Y					
P69/277-1-4	16x17x4 cm angular	similar to P69/277-1-1. Contains 5x5cmbiotite rich inclusion.						Y					this piece appears more foliated than other samples
P69/277-1-5	23x20x6 cm angular	similar to P69/277-1-4.						Y					
P69/277-1-6	18x7x6 cm angular	similar to P69/277-1-1. Cut by 4cm thick biotite rich dike, which is simular to the rounded and schlieren like inclusion in the other samples	Y					Y					
P69/277-1-7	13x12x6 cm angular	dark biotite rich sample, probably represents a larger piece of the dark inclusons found in the other samples. Contains abundant 3-4mm biotite (50%), 2-3mm fdsp (45%) and 2mm quartz (5%).	Y		Y		Y	Y					

STATION Bear Island, Central Pine Island Bay
Sampling by helicopter of granite outcrops on Bear Island
sampling UTC 11/03/06 17:00hrs, lat 74º34.740'S, long 111º53.382'W, altitude 1556ft
30kg fresh angular pieces of coarse grained biotite granite

SAMPLE #	SIZE & SHAPE & ROCK TYPE	DESCRIPTION	TS	CHEM	Ar	GLS / MIN	ARCH	PICT	A.VEIT	Paulina	Katja	Mn	NOTES
PS69/BI-1	22x12x12 cm angular granite	very fresh, coarse grained biotite granite. 45% fdsp 3-4mm, single crystals up to 1cm. 40% qz 3-4mm, 15% biotite 2-3mm, elongated along weakly developed foliation. 2-3mm light brownish to orange weathering rind.		Y	Y			Y					biotite not always clearly identified. Check thin section for possible amph.
PS69/BI-2	16x12x10 cm angular granite	similar to PS69/BI-1		Y	Y			Y					few weathering rinds
PS69/BI-3	13x9x9 cm angular granite	similar to PS69/BI-1		Y	Y			Y					few weathering rinds
PS69/BI-4	16x12x7 cm angular granite	similar to PS69/BI-1. This is the most foliated sample with bi, fdps and qz being aligned into 2cm spaced foliation.		Y	Y			Y					on one side black, 7x4x1cm fine grained inclusion attached. Has sharp contact to granite.
PS69/BI-5	10x9x3 and 16x8x4cm angular granites	similar to PS69/BI-1	Y	Y	Y			Y					good for thin sections
PS69/BI-6	6x4x3cm angular xenolith in granite.	On one side of the sample is granite attached. Xenolith is dark, fine grained. Mostlikely a meta-sediment.											
PS69/BI-7	7x5x1 cm angular xenolith in granite	similar to PS69-BI-6, however more platy. One one side granite attached											

STATION GPS station on Backer islands, Eastern Pine Island Bay
Sampling by helicopter of granite outcrops on small island where a GPS station was set up
sampling UTC 13/03/06 17:30hrs, lat 74°30.66'S, long 102°26,36'W
10kg different granitic rocks

SAMPLE #	SIZE & SHAPE & ROCK TYPE	DESCRIPTION	TS	CHEM	Ar	GLS / MIN	ARCH	PICT	A.VEIT	Paulina	Katja	Mn	NOTES
PS69/PIB-1	13x10x10 & 16x12x8 angular pieces of coarse grained granite	biotite granite with 45% plag 4-10mm, 40% qz 3-6mm, 10% bi 2-3mm, 5% Kfdsp up to 1.5cm. Some of the black minerals could be amph. Cm sized rounded inclusions consist of <<1mm fdsp, bi (amph) mix.	Y	Y	Y	Y		Y					This could be a S-Type granite. Zircons are likely to have a complex history. This lithology makes up the most part of the outcrop. Sample stored in two separate packages.
PS69/PIB-2	16x12x6 & 16x16x10 cm angular pieces of coarse grained Kfdsp-Qz granite	qz-fdsp granite occuring as meter sized blocks within granite PIB-1. 45% Qz 5-10mm, 55% pinkish Kfdsp in several cm sized clusters. According to field observation of A.Veit Kfdsp becomes larger towards contact with PIB-1 type granite.	Y										Rock may have formed by a metasomatic process. Sample stored in two separate packages.
PS69/PIB-3	16x10x8 cm angular granite	fine grained 1-2mm leucogranite with 60% fdsp, 45% qz and << 5% bi. At one end type PIB-1 granite is attached with an irregular curved contact suggesting ductile rock properties at time of formation.					Y						

STATION Edwards Island, Eastern Pine Island Bay
Sampling by helicopter of island inhibited by sea elephants. Dikes cutting granite were found
sampling UTC 15/03/06 14:00hrs, lat 73º51.17'S, long 102º59.33'W, altitude 5m
30kg of dike and granite material

SAMPLE #	SIZE & SHAPE & ROCK TYPE	DESCRIPTION	TS	CHEM	Ar	GLS / MIN	ARCH	PICT	A.VEIT	Paulina	Katja	Mn	NOTES
PS69/ELE-1	10kg of angular fresh volcanic rocks	Dense, fine grained, black-grey matrix. 20% fdsp phenocrysts up to 1cm. Field observation suggests that this lithology represents a dike cutting through the granitic bedrock.	Y	Y	Y	Y		Y					age relation to granite? Is this dike related to 86Ma dike swarms found in Mary Byrd Land?
PS69/ELE-2	6kg of granite	holocrystalline rock under the binocular. With the naked eye the rocks resembles a subvolcanic rock. 50% Qz 3-5mm, altered (metasomatized) to orange -brown. 35% fdsp, 3-4mm, white with pale crystal surfaces (alteration?), 15% Bi <2mm.	Y					Y					
PS69/ELE-3	6kg of granite	similar to PS69/ELE-2, except for fdsp being slightly larger (up to 1cm). 50% Qz and 40% fdsp, both being less altered than in sample PS69/ELE-2, 10% bi.	Y	Y	Y	Y		Y					

STATION 311-1: Seamount 6
Small cone like structure at SW corner
Dredge on bottom UTC 26/03/06 1005hrs, lat 69°51.294'S, long 126°05.85'W, depth 217m
Dredge off bottom UTC 26/03/06 1120hrs, lat 69º50.029'S, long 126º04.831'W, depth 1763m
500kg dropstones; no samples taken

STATION 312-1: Seamount 6
steep slope on E side of Seamount 6
Dredge on bottom UTC 26/03/06 1258hrs, lat 69°47.470'S, long 125°56.874'W, depth 1993m
Dredge off bottom UTC 26/03/06 1458hrs, lat 69º47.396'S, long 125º58.165'W, depth 1593m
500kg dropstones; no samples taken, few biological samples

STATION 314-1: Seamount 6
small cone on northern flank
Dredge on bottom UTC 26/03/06 1833hrs, lat 69°43.040'S, long 126°11.541'W, depth 2003m
Dredge off bottom UTC 26/03/06 1939hrs, lat 69º43.519'S, long 126º10.700'W, depth 1873m
500kg dropstones; no samples taken

STATION 315-1: Seamount 9
cone in the middle part of a volcanic rift at westen slope of the seamount
Dredge on bottom UTC 26/03/06 2248hrs, lat 69°35.50'S, long 125°19.76'W, depth 2409m
Dredge off bottom UTC 26/03/06 2350hrs, lat 69º35.14'S, long 125º18.55'W, depth 2369m
500kg. dropstones; fossil corals, evolved volcanics of unclear origin, Mn crusts

SAMPLE #	SIZE & SHAPE & ROCK TYPE	DESCRIPTION	TS	CHEM	Ar	GLS / MIN	ARCH	PICT	A.VEIT	Paulina	Katja	Mn	NOTES
P69/315-1-1	60x30x30cm angular tuff block	pale green tuff, grain size 0.5-4mm consisting of lithic fragments, olivine, fdsp, small pyroxenes (<1mm). green color may stem from clay minerals.	Y	Y	Y			Y	Y				In situ origin not clear!
P69/315-1-2	30x20x15cm subangular porphyritic lava	porphyritic lava with pinkish-brown matrix. Large up to 6mm squarish fdsp phenocrysts, often with altered cores. Very fine grained brown matrix.	Y	Y	Y			Y	Y				In situ origin not clear!
P69/315-1-3	25x20x15 subangular lava block	Heavily altered aphyric basalt with dark grey, fresh core (mesocratic). Altered part is brown due to Fe-Oxyhydroxides. Grain size is < 0.5mm, homogeneous consisting mostly of fdsp and pyroxene, small green crystals could be ol. Mn crusts 1mm thick.	Y	Y	Y			Y	Y				In situ origin not clear! Veins appear to be related to tectonic deformation and are not cooling cracks. They are filled with white mineral, qz? cc?

STATION 316-1: Haxby Seamount
Western ridge on SE facing slope; steepest structure present
Dredge on bottom UTC 27/03/06 0624hrs, lat 69°06.916'S, long 123°58.203'W, depth 3336m
Dredge off bottom UTC 27/03/06 00850hrs, lat 69°06.65 'S, long 123°59.53'W, depth 2963m
20kg dropstones; no samples taken

STATION 317-1: Haxby Seamount

Southern slope of Haxby Seamount, upper section at 1900m beneath plateau edge
Dredge on bottom UTC 27/03/06 1156hrs, lat 69°10.315'S, long 123°25.456'W, depth 1983m
Dredge off bottom UTC 27/03/06 1341hrs, lat 69º10.00'S, long 123º26.16'W, depth 1584m
500kg. dropstones; carbonate crusts with basalt pebbles

SAMPLE #	SIZE & SHAPE & ROCK TYPE	DESCRIPTION	TS	CHEM	Ar	GLS / MIN	ARCH	PICT	A.VEIT	Paulina	Katja	Mn	NOTES
P69/317-1-1	20x10x10cm carbonate cemented basalt breccia	Basalt clasts are mostly angular and range from 0.3 to several cm and are totally weathered to brown color. Biggest clast has 8cm diameter with fresh, aphyric core.	Y	Y	Y			Y	Y				carbonate sampled by Gerd Kuhn
P69/317-1-2	Carbonate cemented basalt breccia similar to PS69-317-1-1.	Biggest clast is 5cm diameter with fresh, aphyric core.		Y	Y			Y			Y		
P69/317-1-3	70x40x40cm carbonate block as reference sample	Fine grained matrix with coarse fragments of corals, bioturbation infilled with foraminifera sand, 2.5Y812 pale yellow, Mn crusts on surface and in bioturbation channels (not filled).						Y		Y			carbonate sampled by Gerd Kuhn
P69/317-1-4	breccia with carbonate matrix	breccia contains highly altered hyaloclastite								Y	Y		1cm Mn crust, sample entirely to Paulina and Katja
P69/317-1-5	Mn crust up to 10cm thick	refererence sample taken								Y		Y	

STATION 318-1: Haxby Seamount
Southern plateau edge at Eastern end of plateau.
Dredge on bottom UTC 27/03/06 1530hrs, lat 69°08.64'S, long 123°13.35'W, depth 1788m
Dredge off bottom UTC 27/03/06 1652hrs, lat 69º08.28'S, long 123º12.86'W, depth 1480m
500kg. dropstones, carbonates, Mn crusts, volcanic breccias, corals

SAMPLE #	SIZE & SHAPE & ROCK TYPE	DESCRIPTION	TS	CHEM	Ar	GLS / MIN	ARCH	PICT	A.VEIT	Paulina	Katja	Mn	NOTES
P69/318-1-1	light-yellow crust	dolomite?					Y	N					
P69/318-1-2	highly altered volcanic breccia	palagonized hyaloclastite?					Y	N					
P69/318-1-3	40x40cm boulder of breccia	completely altered and covered by up to 10cm Mn crust					Y	N					

STATION 319-1: Haxby Seamount
cone on Eastern volcanic rift
Dredge on bottom UTC 27/03/06 1917hrs, lat 69°10.43S, long 122°52.60'W, depth 2009m
Dredge off bottom UTC 27/03/06 2055hrs, lat 69º09.84'S, long 122º52.70'W, depth 1475m
500kg. dropstones, fossil corals, biology, Mn crusts; no samples taken

STATION 320-1: Miller Seamount
NW corner, lower part of small volcanic rift
Dredge on bottom UTC 28/03/06 0031hrs, lat 69°21.09'S, long 121°52.12'W, depth 2500m
Dredge off bottom UTC 27/03/06 0158hrs, lat 69º20.30'S, long 121º50.40'W, depth 2432m
200kg. dropstones, one in-situ volcanic, other volcanics to be checked

SAMPLE #	SIZE & SHAPE & ROCK TYPE	DESCRIPTION	TS	CHEM	Ar	GLS / MIN	ARCH	PICT	A.VEIT	Paulina	Katja	Mn	NOTES
P69/320-1-1	30x25x13cm subangular to rounded lava boulder	Lava with brown-redish aphyric matrix, elongated unfilled vesicles up to 1cm. 2mm Mn crust.	Y	Y	Y		Y	Y	Y	Y			16x10x10cm working half, 28x15x13cm archive half.
P69/320-1-2	50x50x30cm subangular basalt boulder	dark grey, aphyric, dense , fine grained matrix, quite fresh	Y					Y	Y				20x10x8cm working half. In situ origin not clear. Compare petrography of similar samples in this dredge.
P69/320-1-3	40x25x15cm original size of subangular basalt boulder	Dark-grey, coarse grained aphyric matrix. Quite fresh. <1mm Mn coating.	Y					Y	Y				19x14x15cm working half. In situ origin not clear. Compare petrography of similar samples in this dredge.
P69/320-1-4	30x20x20cm subangular basalt boulder.	Dark-grey, coarse grained aphyric matrix; fresh. <1mm Mn coating.	Y					Y	Y				In situ origin not clear. Compare petrography of similar samples in this dredge.
P69/320-1-5	4x Mn crusts	Reference samples						Y		Y			

STATION 321-1: Miller Seamount

Southern part, SE facing slope beneath plateau edge

Dredge on bottom UTC 28/03/06 0355hrs, lat 69°21.53'S, long 121°31.94'W, depth 1670m

Dredge off bottom UTC 28/03/06 0510hrs, lat 69º21.766'S, long 121º34.906'W, depth 1431m

500kg. in-situ ol-cpx phyric basalt, aphyric basalts to be cross-checked for similarities, Mn crusts, minor dropstones

SAMPLE #	SIZE & SHAPE & ROCK TYPE	DESCRIPTION	TS	CHEM	Ar	GLS / MIN	ARCH	PICT	A.VEIT	Paulina	Katja	Mn	NOTES
P69/321-1-1	60x30x30 angular lava boulders	Dense, non-vesicular, dark-grey, very fine grained matrix. 3% altered ol, 1-3mm; << 1% fdsp, <1mm. Mn coating 3-5mm. 35x20x15cm working half	Y	Y	Y		Y	Y	Y	Y			Archive samples in 5 seperate bags. Additionally 4 boulders similar to 321-1-1 were also archived
P69/321-1-2	30x30x20 angular lava block	Dark brown, dense matrix appears quite fresh. 1-2% altered ol, <1mm; 1% cpx mostly <1mm some megacrysts up to 1cm. Different from PS69-321-1-1.	Y	Y	Y			Y	Y	Y			White secondary minerals along cracks.
P69/321-1-3	10x10x10cm angular lava pieces	Similar to PS69-321-1-2 but less ol & cpx phenocrysts, <<1%, <1mm.	Y	Y	Y			Y	Y	Y			
P69/321-1-4	40x30x30cm angular lava fragment	Dense, vesicles free matrix, dark-grey fine grained. 1-2% fresh cpx phenocrysts, 1mm, some cpx megacrysts up to 8mm. 1% ol microphenocrysts <0.5mm. < 0.5% plag, 2-3mm. Groundmass also quite fresh.	Y	Y	Y			Y	Y	Y			1-2mm Mn coating on outer surfaces.
P69/321-1-5	50x40x40cm angular lava fragments	brownish to greyish matrix, fresh inner core 3cm, <4% cpx phenocrysts up to 3mm, some megacrysts up to 2cm. Cpx appears slightly altered to red-pink.	Y	Y	Y			Y	Y	Y			
P69/321-1-6	10x10x8cm subangular to rounded dense aphyric basalt pebble.	Light grey matrix, dense, quite fresh. 1-2mm Mn coating.	Y					Y	Y				In situ origin questionable. Compare petrography of similar samples in this dredge
P69/321-1-7	11x7x5 subangular to rounded basalt clast	Grey to light grey dense aphyric matrix. Minor Mn coating	Y					Y	Y				In situ origin questionable. Compare petrography of similar samples in this dredge
P69/321-1-8	11x10x9cm subangular basalt clast	greyish to brownish dense matrix. 2% altered ol, 3mm, <1% cpx, 1-2mm. 2-3mm Mn crust	Y					Y	Y				

P69/321-1-9	16x11x8cm angular basalt clast.	Grey dense matrix, aphyric. 2-3mm Mn crust.	Y					Y	Y					In situ origin not clear.
SAMPLE #	SIZE & SHAPE & ROCK TYPE	DESCRIPTION	TS	CHEM	Ar	GLS / MIN	ARCH	PICT	A.VEIT	Paulina	Katja	Mn		NOTES
P69/321-1-10	9x7x7cm clast of basalt breccia	Clasts are mostly <1cm, angular and totally weathered to brown color. A single 5cm basalt clast has tiny fresh, aphyric core.	Y					Y						
P69/321-1-11	10x8x8cm rounded basalt pebble	Dark-grey, dense matrix. Slightly altered, <<1% altered ol phenocrysts <1mm; <0.5mm plag phenocrysts <1mm.	Y					Y						
P69/321-1-12	50x30x10cm Mn encrusted beach breccia	Recovered 6 basalt cobbles. Two best were labelled -12a and -12b.						Y						
P69/321-1-12a	10x7x5cm basalt cobble recovered from Mn encrusted beach breccia	Ol-cpx-plag basalt with fresh core. altered Ol <1%, <1mm; fresh cpx <1%, <1mm; fresh plag <1%, 1-2mm	Y					Y						
P69/321-1-12b	3cm basalt cobble recovered from Mn encrusted beach breccia.	strongly altered Ol phyric basalt. altered Ol <1%, <1mm.	Y					Y						
P69/321-1-13	Mn encrusted breccia	similar to PS69/321-1-12									Y			Katja has entire sample
P69/321-1-14	Mn crusts	partly contains highly altered breccia								Y				3 pieces taken as reference

STATION 322-1: Miller Seamount
Southern part, S facing step within slope
Dredge on bottom UTC 28/03/06 0727hrs, lat 69°28.51'S, long 121°22.30'W, depth 2249m
Dredge off bottom UTC 28/03/06 0842hrs, 69°28.22'S, long 121°22.10'W, depth 1956m
dredge empty

STATION 323-1: Miller Seamount
Southern part, S facing cliff below plateau edge
Dredge on bottom UTC 28/03/06 1011hrs, lat 69°28.064'S, long 121°23.163'W, depth 1676m
Dredge off bottom UTC 28/03/06 1117hrs, lat 69º26.748'S, long 121°17.915'W, depth 1369m
4 granitic dropstones, no samples taken

STATION 324-1: Miller Seamount

Southern part, SE facing slope in the lower section right beneath cone like structure

Dredge on bottom UTC 28/03/06 1309hrs, lat 69°30.07'S, long 121°04.00'W, depth 2622m

Dredge off bottom UTC 28/03/06 1454hrs, lat 69º29.56'S, long 121º02.80'W, depth 2205m

400kg. dropstones, Mn-crusts, lava fragments of possible in-situ origin, volcaniclastic breccias

SAMPLE #	SIZE & SHAPE & ROCK TYPE	DESCRIPTION	TS	CHEM	Ar	GLS / MIN	ARCH	PICT	A.VEIT	Paulina	Katja	Mn	NOTES
P69/324-1-1	21x14x15cm angular basalt	Medium to fine grained dense, greyish matrix. Somewhat platy appearance. 5% cpx, 1-2mm, 3% fdsp <1mm a few up to 2mm. Almost too fresh for old submarine lava	Y	Y	Y			Y	Y				
P69/324-1-2	16x12x12cm subangular basalt piece	Fine grained, light grey matrix. Less fdsp and cpx phenocrysts than sample PS69-324-1-1.	Y	Y	Y			Y	Y				
P69/324-1-3	14x10x10cm angular basalt	Ol-cpx phyric. 3% fresh Ol, 0.5-1mm; 1% fresh cpx, 1-2mm, <0.5mm.	Y	Y	Y			Y					Mn coating on all sides.
P69/324-1-4	14x7x6cm angular basalt	Px and fdsp make up the entire fine grained, holocrystalline matrix.	N	Y	Y			Y					Check thin section for similarities with sample PS69-324-1-1.
P69/324-1-5	13x5x4cm angular basalt	similar to PS69-324-1-4	N	Y	Y			Y		Y			Very little Mn coating
P69/324-1-6	9x5x10 subangular basalt clast	Sample consists for the most part of aphyric, dense, dark grey, slightly altered basalt. One fourth of the sample is however vesicular, 20% vesicles, 0.2-1mm, partially filled or lined with secondary minerals. The vesicular zone has irregular contact to the dense aphyric part; flow contact?	N	Y	Y			Y					
P69/324-1-7A	30x30x10 volcanicalstic breccia	Some of the clasts are basaltic and up to 10cm. Mn encrusted. Breccia appears carbonate cemented.	Y					Y	Y	Y			
P69/324-1-7B	20x15x15 volcanicalstic breccia	similar to PS69-324-1-7A	Y					Y					
P69/324-1-7C	17x16x16 volcanicalstic breccia	similar to PS69-324-1-7A						Y					
P69/324-1-7D		similar to PS69-324-1-7A						N		Y	Y		entire sample to Paulina & Katja
P69/324-1-7E	20x15x6 volcanicalstic breccia	similar to PS69-324-1-7A						Y					
P69/324-1-7F	numereous pieces of volcanicalstic breccia	similar to PS69-324-1-7A						Y					

STATION 324-1 (continued)

SAMPLE #	SIZE & SHAPE & ROCK TYPE	DESCRIPTION	TS	CHEM	Ar	GLS / MIN	ARCH	PICT	A.VEIT	Paulina	Katja	Mn	NOTES
P69/324-1-8	20x15x10cm subangular sediment	yellowish lithified sediment (dolomitic?)	Y					Y	Y				
P69/324-1-9	3 pieces of Mn crusts up to 12 cm							N		Y	Y		

STATION 325-1: Miller Seamount

Southern flank, upper section, cone like structure

Dredge on bottom UTC 28/03/06 1617hrs, lat 69°27.23'S, long 120°55.38'W, depth 1560m

Dredge off bottom UTC 28/03/06 1723hrs, lat 69º26.90'S, long 120º54.94'W, depth 1527m

500kg. Dredge got stuck very early. dropstones, fdsp phyric vesicular lava (in-situ); single basalt with possible in-situ origin, fine grained greyish rocks that could be either basalts or sediments

SAMPLE #	SIZE & SHAPE & ROCK TYPE	DESCRIPTION	TS	CHEM	Ar	GLS / MIN	ARCH	PICT	A.VEIT	Paulina	Katja	Mn	NOTES
P69/325-1-1	30x30x20 angular basalt	Medium grey basalt with 1-3mm phenocrysts. 5% plag, 1% ol, <1% px, Fine grained <0.5mm matrix. Very fresh, no alteration visible. Slight Mn coating.	Y	Y	Y			Y	Y				3 seperate sample bags: 22x12x7; 16x18x8; two small pieces
P69/325-1-2A	30x10x15cm angular lava	Fairly fine grained, brown matrix with 10% vesicles up to 5mm, some filled with zeoliths? or cc? Open vesicles are lined with Fe-Oxyhydroxides. 2% plag phenocrysts up to 5mm length (laths). Some orange brown patches.	Y	Y	Y			Y	Y	Y			
P69/325-1-2B	20x10x10cm angular lava	similar to PS69-325-1-2A, but slightly more grey- brown and less altered	Y	Y	Y			Y					
P69/325-1-2C	8x5x5cm angular lava	similar to PS69-325-1-2A	Y	Y	Y			Y					
P69/325-1-2D	5x3x3cm, angular lava	similar to PS69-325-1-2A	Y	Y	Y			Y					
P69/325-1-3	50x30x30 angular block	Medium grey, very fine grained (<<0.5mm) material. Matrix has sugary texture and no visible crytals. This could be a sediment.	Y					Y	Y				working half 20x10x8cm piece of original block. Check thin section prior to further analyses. Two archive sample bags

STATION 325-1 (continued)

SAMPLE #	SIZE & SHAPE & ROCK TYPE	DESCRIPTION	TS	CHEM	Ar	GLS / MIN	ARCH	PICT	A.VEIT	Paulina	Katja	Mn	NOTES
P69/325-1-4	12x11x7 subangular clast	Very fine grained, greenish-grey. No recognizable phenocrysts. Appears to be a fine grained sediment. Quarzite?	Y					Y	Y				Check thin section prior to further analyses.
P69/325-1-5	8x4x4cm angular basalt clast	Dark brown, fine to medium grained. 2% fdsp, 1mm; 1% cpx, <1mm. 1mm Mn coating.	N					Y					
P69/325-1-6	5x4x4 angular clast	Very fine grained, brownish grey matrix, aphyric rock with sugary texture. This is probably a sediment.	N					Y					Check thin section prior to further analyses.
P69/325-1-7	6x5x5cm angular basalt	Greenish to dark grey matrix. Minor small 1mm, green crystals. Identification not possible.	N					Y					
P69/325-1-8	8x8x4cm subangular rock	Greenish-brown fine grained matrix. Quite similar to PS69-325-1-7. Not sure whether this is volcanic	N					Y					
P69/325-1-9	18x10x6cm angular basalt	Dark brown fine grained matrix with 5-10% cpx and plag (up to 7mm) phenocrysts. Cpx has sometimes altered brown rims.	Y					Y	Y				
P69/325-1-10	10x10x5 angular clast	similar to PS69-324-1-4. Small <0.5mm pale spots could be fdsp. Not sure whether this is volcanic.	Y					Y	Y				
P69/325-1-11	60x30x30cm angular basalt	Medium grained 0.5-1mm, medium grey basalt with prominent altered outer rim (2cm thick). Greyish crystals fdsp? and pyroxenes visible. 2mm thin Mn crust.	Y					Y	Y				two archive samples: 40x20x20cm; 30x20x20cm
P69/325-1-12	8x10x3cm angular rock	dark brown aphyric rock with sugary texture. A few small, pale spots on cut surface. Coiuld be a sediment	Y					Y					

STATION 327-1: Seamount C
cone at Western slope of the structure
Dredge on bottom UTC 29/03/06 0940hrs, lat 69°11.054'S, long 117°38.659'W, depth 2957m
Dredge off bottom UTC 29/03/06 1127hrs, lat 69º11.660'S, long 117º38.589'W, depth 2515m
500kg. vesicular, ol phyric pillow lava; dense lava of possible in-situ origin; Mn-crusts; dropstones

SAMPLE #	SIZE & SHAPE & ROCK TYPE	DESCRIPTION	TS	CHEM	Ar	GLS / MIN	ARCH	PICT	A.VEIT	Paulina	Katja	Mn	NOTES
P69/327-1-1	25x25cm pillow fragments	Relatively dense, 5% fdsp <1mm, 5% altered ol <2mm. Matrix appears to be relatively fresh in places. For the most part the sample is quite altered.	Y	Y	Y		Y	Y	Y				1 archive sample
P69/327-1-2	30x40cm pillow fragment	similar to PS69-3271-1 with more vesicles. Vesicles are often partly filled. Ol <5mm is completely altered.	Y	Y	Y		Y	Y	Y		Y		2 archive samples; 15x12x10 working half
P69/327-1-3	20x20 pillow fragment	similar to PS69-327-1-2.	N				Y	Y					1 archive sample; 17x12x8 working half
P69/327-1-4	25x25 pillow fragment	similar to PS69-327-1-2, more altered	N				Y	Y					1 archive sample
P69/327-1-5	20x20 pillow fragment	similar to PS69-327-1-2.	N					Y					
P69/327-1-6	20x15x15cm angular lava fragment	dense fresh, plag phyric lava. Fdsp <1mm. Very little Mn coating.	Y					Y					Check thin section whether sample -6 through -9 are same lithology.
P69/327-1-7	15x15x10cm angular lava fragment	similar to PS69/327-1-6	N					Y					Check thin section whether sample -6 through -9 are same lithology.
P69/327-1-8	15x10x12cm subangular lava fragment	similar to PS69/327-1-6	Y					Y	Y				Check thin section whether sample -6 through -9 are same lithology.
P69/327-1-9	25x25cm angular pieces of pillow fragments	similar to PS69/327-1-6	Y					Y					Check thin section whether sample -6 through -9 are same lithology.
P69/327-1-10 -A through -K	variable sized pillow fragments	similar to PS69-327-1-1/2	Y					Y					
P69/327-1-11	Mn crust up to 7cm	reference sample								Y			

STATION 328-1: Ridge E of Seamount C

ridge like structure 5nm E of Seamount C, western flank. Dredge on gentle slope due to incorrect map

Dredge on bottom UTC 29/03/06 1410hrs, lat 69°09.95'S, long 117°08.80'W, depth 3136m

Dredge off bottom UTC 29/03/06 1512hrs, lat 69º10.26'S, long 117º08.32'W, depth 3015m

500kg. white semiconsolidated sediment, small lava fragments of unknown origin, small dropstones

SAMPLE #	SIZE & SHAPE & ROCK TYPE	DESCRIPTION	TS	CHEM	Ar	GLS / MIN	ARCH	PICT	A.VEIT	Paulina	Katja	Mn	NOTES
P69/328-1-1A	9x8x4cm angular basalt clast	Grey fine crystalline matrix with 40% fdsp up to 3mm and subordinate altered ol. Very little Mn coating.	Y					Y	Y				probably not in-situ.
P69/328-1-1B	18x12x7cm subangular basalt clast	still sediment attached on all sides. 20-30% fsdp phenocrysts, similar to PS69-328-1-1.						Y					
P69/328-1-2	9x8x4cm angular gabbro? fragment	holocrystalline rock consisting of fdsp up to 2mm and cpx <0.5mm. This could be a fine grained gabbro.	N					Y					probably not in-situ.
P69/328-1-3	7x4x3cm subangular fragment	plag phyric basalt. 5-10% vesicles, lined with Mn. 20% fdsp, 1mm, <2% cpx, 1-2mm	N					Y					probably not in-situ.
P69/328-1-4	30cm diameter sediment piece	semi-consolidated sediment; soft clay stone; 5Y8/2; 2.5Y8/4, pale yellow with darke bioturbated parts 2.5Y5/2; grayish brown no carbonate, siliceous microfossils, possible Eocene											entire sample to Gerd Kuhn

STATION 329-1: Ridge E of Seamount C

repeat of 328-1 due to incorrect map

Dredge on bottom UTC 29/03/06 1732hrs, lat 69°09.76'S, long 117°07.80'W, depth 3267m

Dredge off bottom UTC 29/03/06 1823hrs, lat 69º10.03'S, long 117º07.05'W, depth 2984m

dredge empty

STATION PI: Peter 1st Island
sampling by helicopter of eruption center at GPS station
UTC 31/03/06 1800hrs, lat 68°51.81'S, long 90°25.56'W, depth 40m absl
20 kg, mostly Mn encrusted breccia, some amygdaloidal olivine basalts

SAMPLE #	SIZE & SHAPE & ROCK TYPE	DESCRIPTION	TS	CHEM	Ar	GLS / MIN	ARCH	PICT	A.VEIT	Paulina	Katja	Mn	NOTES
PI-1	30x30x15cm angular lava	dark grey matrix, aphyric, fresh. 15% vesicles, 0.3-1cm, open but lined with greenish and red material.	Y	Y									Eastern plateau edge, 45m absl, surficially eroded lava flow.
PI-2	Total of 3 angular pieces collected: 25x15x10cm; 15x10x8cm; 20x10x8cm	Lava, dark grey matrix, aphyric, fresh but more dense than PI-1. 5% vesicles, 0.3-1cm, open not lined with any material.	Y	Y									Northern plateau edge, 40m absl, Possibly the base of flow PI-1.
PI-3	10x10x8cm, angular	4 pieces of agglutinate, black outer rim 0.5cm (glass?), red oxidized inner core, 15% vesicles, 0.5-2mm.	Y	Y									Northern plateau edge, 40m absl, Same location as PI-2
PI-4	20x10x10cm, rounded	3 pieces of volcanic bomb. redish brown matrix, 10-20% vesicles, some parts dark grey.	Y	Y									Western plateau edge, 50m absl. Uppermost layer mainly consisting of fallout.

A.3 Station List

Station	Date	Time	Position Lat	Position Lon	Depth [m]	Gear Abbreviat.	Action
PS69/239-1	15.02.06	22:00	66° 21,38' S	71° 17,06' W	1017,0	CTD/RO	surface
PS69/239-1	15.02.06	22:13	66° 21,26' S	71° 17,31' W	1054,0	CTD/RO	at depth
PS69/239-1	15.02.06	22:36	66° 21,24' S	71° 17,08' W	1034,0	CTD/RO	on deck
PS69/239-2	15.02.06	22:46	66° 21,23' S	71° 17,00' W	1033,0	BONGO	surface
PS69/239-2	15.02.06	22:58	66° 21,21' S	71° 17,01' W	1039,0	BONGO	at depth
PS69/239-2	15.02.06	23:14	66° 21,15' S	71° 16,95' W	1058,0	BONGO	on deck
PS69/240-1	16.02.06	12:58	68° 12,10' S	69° 48,34' W	498,7	CTD/RO	surface
PS69/240-1	16.02.06	13:13	68° 12,13' S	69° 48,20' W	497,6	CTD/RO	at depth
PS69/240-1	16.02.06	13:30	68° 12,19' S	69° 48,09' W	495,1	CTD/RO	on deck
PS69/241-1	17.02.06	09:17	68° 16,08' S	75° 33,32' W	1091,2	CTD/RO	surface
PS69/241-1	17.02.06	09:30	68° 16,13' S	75° 33,47' W	1045,3	CTD/RO	at depth
PS69/241-1	17.02.06	09:46	68° 16,12' S	75° 33,41' W	1044,3	CTD/RO	on deck
PS69/242-1	18.02.06	13:08	68° 40,80' S	87° 6,13' W	3447,3	CTD/RO	surface
PS69/242-1	18.02.06	13:22	68° 40,79' S	87° 6,09' W	3447,9	CTD/RO	at depth
PS69/242-1	18.02.06	13:38	68° 40,77' S	87° 6,15' W	3445,8	CTD/RO	on deck
PS69/243-1	18.02.06	20:36	68° 43,94' S	90° 5,04' W	2964,0	CTD/RO	surface
PS69/243-1	18.02.06	21:00	68° 44,02' S	90° 5,18' W	2953,0	CTD/RO	at depth
PS69/243-1	18.02.06	21:15	68° 44,02' S	90° 5,26' W	2946,0	CTD/RO	on deck
PS69/243-2	18.02.06	21:25	68° 44,07' S	90° 5,20' W	2940,0	CTD/RO	surface
PS69/243-2	18.02.06	22:20	68° 44,17' S	90° 5,05' W	2902,0	CTD/RO	at depth
PS69/243-2	18.02.06	23:10	68° 44,24' S	90° 5,05' W	2843,0	CTD/RO	on deck
PS69/244-1	19.02.06	00:45	68° 43,75' S	90° 21,83' W	2198,0	DRG	surface
PS69/244-1	19.02.06	01:23	68° 44,16' S	90° 21,26' W	1880,0	DRG	start dredging
PS69/244-1	19.02.06	01:49	68° 44,49' S	90° 20,85' W	1679,0	DRG	stop dredging
PS69/244-1	19.02.06	02:44	68° 44,48' S	90° 20,90' W	1656,0	DRG	Information
PS69/244-1	19.02.06	03:13	68° 44,50' S	90° 20,87' W	1688,0	DRG	on deck
PS69/245-1	19.02.06	05:50	68° 53,64' S	90° 18,02' W	1649,0	DRG	surface
PS69/245-1	19.02.06	06:20	68° 54,14' S	90° 18,64' W	1591,0	DRG	Information

Station	Date	Time	Position Lat	Position Lon	Depth [m]	Gear Abbreviat.	Action
PS69/245-1	19.02.06	06:49	68° 54,58' S	90° 18,88' W	1465,0	DRG	start dredging
PS69/245-1	19.02.06	07:18	68° 54,67' S	90° 18,87' W	1528,0	DRG	Information
PS69/245-1	19.02.06	07:40	68° 54,38' S	90° 18,60' W	1391,0	DRG	Information
PS69/245-1	19.02.06	08:15	68° 54,21' S	90° 18,09' W	1680,0	DRG	on deck
PS69/246-1	20.02.06	23:00	65° 12,12' S	92° 40,85' W	3446,0	PC	surface
PS69/246-1	21.02.06	00:03	65° 12,11' S	92° 40,86' W	3442,0	PC	at sea bottom
PS69/246-1	21.02.06	01:03	65° 12,13' S	92° 40,89' W	3440,0	PC	on Deck
PS69/247-1	21.02.06	06:06	64° 48,56' S	93° 34,82' W	4230,0	PC	surface
PS69/247-1	21.02.06	07:27	64° 48,58' S	93° 34,80' W	4239,0	PC	at sea bottom
PS69/247-1	21.02.06	08:46	64° 48,44' S	93° 34,32' W	4214,0	PC	on Deck
PS69/248-1	21.02.06	12:33	65° 2,22' S	92° 57,87' W	921,4	BONGO	surface
PS69/248-1	21.02.06	12:46	65° 2,23' S	92° 57,87' W	912,7	BONGO	at depth
PS69/248-1	21.02.06	13:00	65° 2,23' S	92° 57,87' W	912,4	BONGO	on deck
PS69/249-1	22.02.06	13:03	68° 19,09' S	97° 34,74' W	4575,0	CTD/RO	surface
PS69/249-1	22.02.06	13:18	68° 19,13' S	97° 34,88' W	4573,0	CTD/RO	at depth
PS69/249-1	22.02.06	13:36	68° 19,20' S	97° 34,88' W	4573,0	CTD/RO	on deck
PS69/250-1	22.02.06	19:47	69° 5,85' S	98° 51,38' W	4455,0	PC	surface
PS69/250-1	22.02.06	21:25	69° 5,87' S	98° 51,51' W	4456,0	PC	at sea bottom
PS69/250-1	22.02.06	22:39	69° 5,23' S	98° 49,70' W	4464,0	PC	on Deck
PS69/251-1	25.02.06	03:23	72° 6,90' S	104° 48,28' W	570,8	GBG	surface
PS69/251-1	25.02.06	03:33	72° 6,86' S	104° 48,31' W	573,2	GBG	at sea bottom
PS69/251-1	25.02.06	03:44	72° 6,75' S	104° 48,28' W	572,4	GBG	on deck
PS69/251-2	25.02.06	04:11	72° 6,74' S	104° 48,57' W	572,3	GC	surface
PS69/251-2	25.02.06	04:19	72° 6,75' S	104° 48,64' W	572,3	GC	at sea bottom
PS69/251-2	25.02.06	04:32	72° 6,73' S	104° 48,76' W	572,0	GC	on deck
PS69/252-1	25.02.06	11:04	71° 51,46' S	106° 19,12' W	569,0	CTD/RO	surface
PS69/252-1	25.02.06	11:21	71° 51,39' S	106° 18,98' W	569,7	CTD/RO	at depth
PS69/252-1	25.02.06	11:42	71° 51,35' S	106° 19,04' W	567,6	CTD/RO	on deck
PS69/252-2	25.02.06	11:50	71° 51,33' S	106° 19,07' W	566,5	BONGO	surface

Station	Date	Time	Position Lat	Position Lon	Depth [m]	Gear Abbreviat.	Action
PS69/252-2	25.02.06	12:03	71° 51,29' S	106° 18,99' W	568,2	BONGO	at depth
PS69/252-2	25.02.06	12:17	71° 51,22' S	106° 18,86' W	569,3	BONGO	on deck
PS69/253-1	25.02.06	12:36	71° 52,24' S	106° 13,09' W	568,2	WHW	begin
PS69/253-1	25.02.06	13:06	71° 54,89' S	105° 58,48' W	556,6	WHW	end
PS69/254-1	25.02.06	13:49	71° 58,52' S	105° 39,77' W	500,2	SEISREFL	Streamer into water
PS69/254-1	25.02.06	14:05	71° 57,64' S	105° 38,48' W	504,3	SEISREFL	Remark
PS69/254-1	25.02.06	14:36	71° 55,61' S	105° 36,56' W	518,8	SEISREFL	airguns in the water
PS69/254-1	25.02.06	14:43	71° 55,08' S	105° 35,60' W	514,0	SEISREFL	profile start
PS69/254-1	25.02.06	22:07	71° 20,24' S	104° 48,79' W	572,0	SEISREFL	alter course
PS69/254-1	25.02.06	23:22	71° 20,01' S	104° 29,70' W	563,6	SEISREFL	Remark
PS69/254-1	25.02.06	23:36	71° 19,92' S	104° 27,20' W	563,1	SEISREFL	Remark
PS69/254-1	25.02.06	23:48	71° 19,81' S	104° 25,03' W	574,1	SEISREFL	streamer on deck
PS69/255-1	26.02.06	12:59	71° 48,08' S	104° 21,30' W	654,5	GC	surface
PS69/255-1	26.02.06	13:10	71° 48,08' S	104° 21,09' W	656,5	GC	at sea bottom
PS69/255-1	26.02.06	13:10	71° 48,08' S	104° 21,09' W	656,5	GC	off ground hoisting
PS69/255-1	26.02.06	13:23	71° 48,22' S	104° 21,44' W	657,2	GC	on deck
PS69/255-2	26.02.06	13:37	71° 48,05' S	104° 21,02' W	658,7	GBG	surface
PS69/255-2	26.02.06	13:47	71° 48,01' S	104° 21,17' W	654,9	GBG	at sea bottom
PS69/255-2	26.02.06	14:00	71° 47,96' S	104° 21,29' W	653,3	GBG	on deck
PS69/255-3	26.02.06	14:08	71° 47,86' S	104° 21,61' W	655,7	GBG	surface
PS69/255-3	26.02.06	14:19	71° 47,83' S	104° 21,69' W	654,2	GBG	at sea bottom
PS69/255-3	26.02.06	14:31	71° 47,83' S	104° 21,59' W	655,9	GBG	on deck
PS69/256-1	26.02.06	16:00	71° 55,33' S	104° 20,08' W	669,8	GC	surface
PS69/256-1	26.02.06	16:12	71° 55,36' S	104° 20,27' W	667,5	GC	at sea bottom
PS69/256-1	26.02.06	16:27	71° 55,35' S	104° 20,30' W	667,4	GC	on deck
PS69/257-1	28.02.06	12:31	73° 6,12' S	114° 48,55' W	727,1	CTD/RO	surface
PS69/257-1	28.02.06	12:51	73° 5,89' S	114° 48,29' W	727,1	CTD/RO	at depth
PS69/257-1	28.02.06	13:11	73° 5,77' S	114° 48,09' W	727,0	CTD/RO	on deck
PS69/257-2	28.02.06	13:16	73° 5,75' S	114° 47,99' W	727,4	BONGO	surface

Station	Date	Time	Position Lat	Position Lon	Depth [m]	Gear Abbreviat.	Action
PS69/257-2	28.02.06	13:38	73° 5,64' S	114° 47,93' W	724,4	BONGO	at depth
PS69/257-2	28.02.06	13:57	73° 5,56' S	114° 47,89' W	722,8	BONGO	on deck
PS69/258-1	01.03.06	16:47	74° 19,73' S	110° 16,15' W	276,1	CTD/RO	surface
PS69/258-1	01.03.06	16:58	74° 19,72' S	110° 16,22' W	271,4	CTD/RO	at depth
PS69/258-1	01.03.06	17:14	74° 19,72' S	110° 16,51' W	256,0	CTD/RO	on deck
PS69/259-1	01.03.06	17:55	74° 18,09' S	110° 15,99' W	257,8	GC	surface
PS69/259-1	01.03.06	18:01	74° 18,10' S	110° 15,92' W	257,7	GC	at sea bottom
PS69/259-1	01.03.06	18:10	74° 18,04' S	110° 15,86' W	251,3	GC	on deck
PS69/260-1	01.03.06	20:16	74° 19,76' S	110° 16,21' W	268,8	MN	surface
PS69/260-1	01.03.06	20:25	74° 19,71' S	110° 16,50' W	256,4	MN	at depth
PS69/260-1	01.03.06	20:42	74° 19,67' S	110° 16,21' W	268,4	MN	on deck
PS69/261-1	02.03.06	01:53	73° 55,12' S	111° 40,65' W	556,9	OBS	surface
PS69/261-2	02.03.06	03:12	73° 50,12' S	112° 10,92' W	709,1	OBS	surface
PS69/261-3	02.03.06	04:31	73° 44,54' S	112° 40,89' W	712,1	OBS	surface
PS69/261-4	02.03.06	05:47	73° 39,11' S	113° 10,80' W	684,0	OBS	surface
PS69/261-5	02.03.06	06:57	73° 33,85' S	113° 40,69' W	736,4	OBS	surface
PS69/261-6	02.03.06	08:11	73° 28,46' S	114° 10,34' W	796,6	OBS	surface
PS69/261-7	02.03.06	09:26	73° 23,09' S	114° 39,99' W	888,5	OBS	surface
PS69/261-8	02.03.06	10:40	73° 17,77' S	115° 9,32' W	915,8	OBS	surface
PS69/261-9	02.03.06	12:01	73° 12,37' S	115° 38,23' W	804,0	OBS	surface
PS69/262-1	02.03.06	12:36	73° 9,39' S	115° 51,38' W	731,0	WHW	begin
PS69/262-1	02.03.06	13:02	73° 6,75' S	116° 1,31' W	703,5	WHW	end
PS69/263-1	02.03.06	13:39	73° 4,15' S	116° 2,56' W	685,0	SEISREFL	Streamer into water
PS69/263-1	02.03.06	14:00	73° 5,23' S	116° 2,31' W	695,8	SEISREFL	airguns in the water
PS69/263-1	02.03.06	14:24	73° 6,93' S	115° 59,55' W	708,7	SEISREFL	profile start
PS69/263-1	03.03.06	00:00	73° 33,69' S	113° 41,44' W	735,0	SEISREFL	alter course
PS69/263-1	03.03.06	05:15	73° 50,30' S	112° 39,94' W	805,2	SEISREFL	alter course
PS69/263-1	03.03.06	12:20	73° 55,95' S	111° 37,93' W	612,2	SEISREFL	end of profile
PS69/263-1	03.03.06	12:26	73° 56,38' S	111° 37,37' W	615,3	SEISREFL	array on deck

Station	Date	Time	Position Lat	Position Lon	Depth [m]	Gear Abbreviat.	Action
PS69/263-1	03.03.06	12:40	73° 56,97' S	111° 37,01' W	589,9	SEISREFL	streamer on deck
PS69/264-1	03.03.06	13:41	73° 55,12' S	111° 40,86' W	557,7	OBS	on deck
PS69/264-2	03.03.06	15:32	73° 50,27' S	112° 10,74' W	708,5	OBS	on deck
PS69/264-3	03.03.06	16:55	73° 44,54' S	112° 40,94' W	712,8	OBS	released
PS69/264-3	03.03.06	17:02	73° 44,48' S	112° 40,97' W	712,8	OBS	at surface
PS69/264-3	03.03.06	17:14	73° 44,55' S	112° 40,77' W	712,9	OBS	on deck
PS69/265-1	03.03.06	18:38	73° 40,09' S	113° 2,08' W	693,9	CTD/RO	surface
PS69/265-1	03.03.06	18:57	73° 40,12' S	113° 2,10' W	692,7	CTD/RO	at depth
PS69/265-1	03.03.06	19:16	73° 40,11' S	113° 2,14' W	695,6	CTD/RO	on deck
PS69/265-2	03.03.06	19:21	73° 40,11' S	113° 2,21' W	696,1	BONGO	surface
PS69/265-2	03.03.06	19:32	73° 40,10' S	113° 2,15' W	694,8	BONGO	at depth
PS69/265-2	03.03.06	19:45	73° 40,13' S	113° 2,12' W	693,3	BONGO	on deck
PS69/265-3	03.03.06	19:59	73° 40,13' S	113° 2,25' W	693,7	GC	surface
PS69/265-3	03.03.06	20:06	73° 40,14' S	113° 2,31' W	691,8	GC	at sea bottom
PS69/265-3	03.03.06	20:21	73° 40,16' S	113° 2,39' W	691,7	GC	on deck
PS69/264-4	03.03.06	20:56	73° 39,02' S	113° 10,76' W	682,1	OBS	released
PS69/264-4	03.03.06	21:03	73° 38,90' S	113° 10,78' W	681,6	OBS	at surface
PS69/264-4	03.03.06	21:27	73° 38,85' S	113° 10,84' W	679,6	OBS	on deck
PS69/264-5	03.03.06	22:54	73° 33,81' S	113° 40,67' W	736,6	OBS	released
PS69/264-5	03.03.06	22:57	73° 33,78' S	113° 40,78' W	735,7	OBS	at surface
PS69/264-5	03.03.06	23:17	73° 33,76' S	113° 40,96' W	738,0	OBS	on deck
PS69/266-1	03.03.06	23:37	73° 32,52' S	113° 44,47' W	745,5	GC	surface
PS69/266-1	03.03.06	23:49	73° 32,53' S	113° 44,48' W	745,2	GC	at sea bottom
PS69/266-1	04.03.06	00:00	73° 32,51' S	113° 44,51' W	744,9	GC	on deck
PS69/264-6	04.03.06	01:27	73° 28,45' S	114° 10,28' W	794,7	OBS	released
PS69/264-6	04.03.06	02:08	73° 28,51' S	114° 10,59' W	803,1	OBS	at surface
PS69/264-6	04.03.06	02:21	73° 28,36' S	114° 10,52' W	797,7	OBS	on deck
PS69/267-1	04.03.06	03:32	73° 23,69' S	114° 33,39' W	863,4	GC	surface
PS69/267-1	04.03.06	03:44	73° 23,72' S	114° 33,55' W	863,1	GC	at sea bottom

Station	Date	Time	Position Lat	Position Lon	Depth [m]	Gear Abbreviat.	Action
PS69/267-1	04.03.06	03:57	73° 23,72' S	114° 33,91' W	864,8	GC	on deck
PS69/267-2	04.03.06	04:09	73° 23,73' S	114° 34,08' W	863,7	GKG	surface
PS69/267-2	04.03.06	04:22	73° 23,71' S	114° 33,91' W	864,2	GKG	at sea bottom
PS69/267-2	04.03.06	04:35	73° 23,72' S	114° 34,03' W	863,1	GKG	on deck
PS69/264-7	04.03.06	05:15	73° 23,06' S	114° 40,47' W	892,5	OBS	released
PS69/264-7	04.03.06	05:30	73° 23,01' S	114° 40,04' W	887,1	OBS	released
PS69/264-7	04.03.06	05:42	73° 22,93' S	114° 40,32' W	889,4	OBS	at surface
PS69/264-7	04.03.06	05:58	73° 23,06' S	114° 40,69' W	893,0	OBS	on deck
PS69/268-1	04.03.06	06:58	73° 19,01' S	115° 0,15' W	907,5	CTD/RO	surface
PS69/268-1	04.03.06	07:21	73° 18,88' S	115° 0,11' W	910,7	CTD/RO	at depth
PS69/268-1	04.03.06	07:42	73° 18,78' S	115° 0,32' W	909,7	CTD/RO	on deck
PS69/264-8	04.03.06	08:35	73° 17,75' S	115° 9,14' W	915,7	OBS	released
PS69/264-8	04.03.06	08:45	73° 17,72' S	115° 9,48' W	917,0	OBS	at surface
PS69/264-8	04.03.06	08:49	73° 17,75' S	115° 9,43' W	916,5	OBS	on deck
PS69/269-1	04.03.06	10:00	73° 13,12' S	115° 34,71' W	848,5	GKG	surface
PS69/269-1	04.03.06	10:13	73° 13,16' S	115° 34,62' W	849,5	GKG	at sea bottom
PS69/269-1	04.03.06	10:27	73° 13,12' S	115° 34,72' W	848,0	GKG	on deck
PS69/269-2	04.03.06	10:42	73° 13,13' S	115° 34,70' W	848,4	GC	surface
PS69/269-2	04.03.06	10:54	73° 13,11' S	115° 34,79' W	847,0	GC	at sea bottom
PS69/269-2	04.03.06	11:09	73° 13,12' S	115° 34,81' W	847,2	GC	on deck
PS69/264-9	04.03.06	11:48	73° 12,46' S	115° 38,57' W	800,8	OBS	released
PS69/264-9	04.03.06	11:54	73° 12,48' S	115° 38,46' W	801,4	OBS	at surface
PS69/264-9	04.03.06	12:10	73° 12,44' S	115° 38,16' W	804,8	OBS	on deck
PS69/269-3	04.03.06	12:26	73° 12,41' S	115° 38,05' W	805,5	CTD	surface
PS69/269-3	04.03.06	12:46	73° 12,49' S	115° 38,05' W	805,5	CTD	at depth
PS69/269-3	04.03.06	13:07	73° 12,51' S	115° 38,08' W	805,4	CTD	on deck
PS69/269-4	04.03.06	13:08	73° 12,52' S	115° 38,08' W	805,4	BONGO	surface
PS69/269-4	04.03.06	13:33	73° 12,66' S	115° 38,04' W	806,0	BONGO	at depth
PS69/269-4	04.03.06	13:43	73° 12,62' S	115° 38,05' W	805,2	BONGO	on deck

Station	Date	Time	Position Lat	Position Lon	Depth [m]	Gear Abbreviat.	Action
PS69/270-1	04.03.06	14:57	73° 9,95' S	115° 40,81' W	802,0	WHW	begin
PS69/270-1	04.03.06	15:21	73° 6,44' S	115° 41,23' W	774,0	WHW	end
PS69/271-1	04.03.06	15:35	73° 6,26' S	115° 40,59' W	772,3	SEISREFL	Streamer into water
PS69/271-1	04.03.06	15:50	73° 6,84' S	115° 41,65' W	773,7	SEISREFL	airguns in the water
PS69/271-1	04.03.06	15:53	73° 7,00' S	115° 42,20' W	773,3	SEISREFL	profile start
PS69/271-1	04.03.06	19:34	73° 24,99' S	115° 30,05' W	902,5	SEISREFL	alter course
PS69/271-1	04.03.06	20:34	73° 30,10' S	115° 30,58' W	916,5	SEISREFL	alter course
PS69/271-1	05.03.06	09:38	73° 57,08' S	118° 33,72' W	1428,0	SEISREFL	alter course
PS69/271-1	05.03.06	12:28	73° 43,95' S	118° 48,02' W	393,9	SEISREFL	alter course
PS69/271-1	05.03.06	13:04	73° 41,75' S	118° 42,15' W	546,5	SEISREFL	alter course
PS69/271-1	05.03.06	15:17	73° 48,91' S	118° 12,43' W	807,0	SEISREFL	end of profile
PS69/271-1	05.03.06	15:21	73° 49,24' S	118° 12,35' W	863,7	SEISREFL	array on deck
PS69/271-1	05.03.06	15:30	73° 49,63' S	118° 12,77' W	1108,0	SEISREFL	streamer on deck
PS69/272-1	06.03.06	14:15	73° 53,84' S	118° 30,01' W	1589,0	CTD/RO	surface
PS69/272-1	06.03.06	14:31	73° 53,78' S	118° 30,14' W	1595,0	CTD/RO	Information
PS69/272-1	06.03.06	14:41	73° 53,70' S	118° 30,23' W	1578,0	CTD/RO	on deck
PS69/272-1	06.03.06	14:45	73° 53,63' S	118° 30,35' W	1573,0	CTD/RO	surface
PS69/272-1	06.03.06	15:18	73° 53,35' S	118° 30,68' W	1556,0	CTD/RO	at depth
PS69/272-1	06.03.06	15:50	73° 53,05' S	118° 30,95' W	1494,0	CTD/RO	on deck
PS69/272-2	06.03.06	16:10	73° 53,66' S	118° 28,90' W	1579,0	GC	surface
PS69/272-2	06.03.06	16:27	73° 53,57' S	118° 29,17' W	1578,0	GC	at sea bottom
PS69/272-2	06.03.06	16:48	73° 53,43' S	118° 29,52' W	1571,0	GC	on deck
PS69/272-3	06.03.06	17:04	73° 53,62' S	118° 28,36' W	1568,0	GKG	surface
PS69/272-3	06.03.06	17:24	73° 53,53' S	118° 28,70' W	1576,0	GKG	at sea bottom
PS69/272-3	06.03.06	17:43	73° 53,39' S	118° 29,01' W	1569,0	GKG	on deck
PS69/273-1	06.03.06	22:36	73° 57,85' S	117° 50,14' W	1339,0	CTD/RO	surface
PS69/273-1	06.03.06	23:06	73° 57,89' S	117° 50,43' W	1319,6	CTD/RO	at depth
PS69/273-1	06.03.06	23:37	73° 57,97' S	117° 50,60' W	1346,0	CTD/RO	on deck
PS69/273-2	07.03.06	00:32	73° 57,65' S	117° 50,49' W	1349,0	GC	surface

Station	Date	Time	Position Lat	Position Lon	Depth [m]	Gear Abbreviat.	Action
PS69/273-2	07.03.06	00:48	73° 57,70' S	117° 50,60' W	1352,0	GC	at sea bottom
PS69/273-2	07.03.06	01:09	73° 57,78' S	117° 50,79' W	1350,0	GC	on deck
PS69/274-1	07.03.06	02:31	73° 51,32' S	117° 46,57' W	1449,0	GC	surface
PS69/274-1	07.03.06	02:48	73° 51,36' S	117° 46,54' W	1452,0	GC	at sea bottom
PS69/274-1	07.03.06	03:10	73° 51,37' S	117° 46,43' W	1446,0	GC	on deck
PS69/275-1	07.03.06	03:50	73° 53,31' S	117° 32,95' W	1521,0	GC	surface
PS69/275-1	07.03.06	04:06	73° 53,33' S	117° 32,90' W	1518,0	GC	at sea bottom
PS69/275-1	07.03.06	04:18	73° 53,32' S	117° 32,84' W	1520,0	GC	on deck
PS69/275-2	07.03.06	04:39	73° 53,31' S	117° 32,88' W	1518,0	GKG	surface
PS69/275-2	07.03.06	05:00	73° 53,32' S	117° 32,91' W	1517,0	GKG	at sea bottom
PS69/275-2	07.03.06	05:19	73° 53,38' S	117° 32,77' W	1499,0	GKG	on deck
PS69/276-1	07.03.06	07:02	73° 49,12' S	116° 59,92' W	833,1	MOR	surface
PS69/276-1	07.03.06	07:03	73° 49,08' S	116° 59,91' W	823,5	MOR	surface
PS69/276-1	07.03.06	07:04	73° 49,05' S	116° 59,90' W	813,1	MOR	surface
PS69/276-1	07.03.06	07:05	73° 49,03' S	116° 59,90' W	803,5	MOR	surface
PS69/276-1	07.03.06	07:06	73° 49,01' S	116° 59,91' W	804,1	MOR	slipped
PS69/276-2	07.03.06	07:17	73° 48,57' S	117° 0,34' W	958,5	CTD/RO	surface
PS69/276-1	07.03.06	07:41	73° 48,60' S	117° 0,59' W	946,7	MOR	at depth
PS69/276-2	07.03.06	07:41	73° 48,60' S	117° 0,59' W	946,7	CTD/RO	at depth
PS69/276-2	07.03.06	08:04	73° 48,55' S	117° 0,38' W	943,1	CTD/RO	on deck
PS69/277-1	07.03.06	14:23	73° 57,17' S	116° 52,23' W	147,7	SEP	on deck
PS69/278-1	07.03.06	20:03	73° 50,31' S	115° 33,01' W	893,1	MOR	surface
PS69/278-1	07.03.06	20:04	73° 50,33' S	115° 32,91' W	892,5	MOR	slipped
PS69/278-2	07.03.06	20:18	73° 50,84' S	115° 34,41' W	951,2	CTD/RO	surface
PS69/278-2	07.03.06	20:42	73° 50,79' S	115° 34,28' W	945,7	CTD/RO	at depth
PS69/278-2	07.03.06	21:01	73° 50,77' S	115° 34,19' W	942,8	CTD/RO	on deck
PS69/278-3	07.03.06	21:06	73° 50,76' S	115° 34,36' W	944,9	BONGO	surface
PS69/278-3	07.03.06	21:20	73° 50,76' S	115° 34,38' W	947,2	BONGO	at depth
PS69/278-3	07.03.06	21:32	73° 50,76' S	115° 34,10' W	937,5	BONGO	on deck

Station	Date	Time	Position Lat	Position Lon	Depth [m]	Gear Abbreviat.	Action
PS69/279-1	08.03.06	03:42	74° 3,48' S	112° 25,15' W	877,0	MOR	surface
PS69/279-1	08.03.06	03:43	74° 3,49' S	112° 25,07' W	881,7	MOR	slipped
PS69/279-2	08.03.06	03:50	74° 3,57' S	112° 24,85' W	889,2	CTD/RO	surface
PS69/279-2	08.03.06	04:15	74° 3,66' S	112° 24,82' W	894,8	CTD/RO	at depth
PS69/279-2	08.03.06	04:31	74° 3,68' S	112° 24,84' W	892,0	CTD/RO	on deck
PS69/280-1	08.03.06	06:20	73° 56,19' S	111° 37,54' W	623,2	GC	surface
PS69/280-1	08.03.06	06:31	73° 56,15' S	111° 37,41' W	624,9	GC	at sea bottom
PS69/280-1	08.03.06	06:43	73° 56,14' S	111° 37,40' W	625,1	GC	on deck
PS69/280-2	08.03.06	06:58	73° 56,19' S	111° 37,30' W	625,5	GKG	surface
PS69/280-2	08.03.06	07:08	73° 56,17' S	111° 37,32' W	626,9	GKG	at sea bottom
PS69/280-2	08.03.06	07:10	73° 56,16' S	111° 37,33' W	626,3	GKG	
PS69/280-2	08.03.06	07:12	73° 56,16' S	111° 37,34' W	630,1	GKG	at sea bottom
PS69/280-2	08.03.06	07:24	73° 56,13' S	111° 37,43' W	624,7	GKG	on deck
PS69/281-1	08.03.06	12:58	74° 19,78' S	110° 12,39' W	217,1	BONGO	surface
PS69/281-1	08.03.06	13:10	74° 19,78' S	110° 12,37' W	216,1	BONGO	at depth
PS69/281-1	08.03.06	13:23	74° 19,76' S	110° 12,35' W	215,3	BONGO	on deck
PS69/281-2	08.03.06	13:32	74° 19,75' S	110° 12,41' W	214,3	GKG	surface
PS69/281-2	08.03.06	13:37	74° 19,75' S	110° 12,44' W	213,2	GKG	at sea bottom
PS69/281-2	08.03.06	13:41	74° 19,76' S	110° 12,45' W	213,7	GKG	
PS69/281-2	08.03.06	13:43	74° 19,76' S	110° 12,45' W	213,6	GKG	surface
PS69/281-2	08.03.06	13:46	74° 19,77' S	110° 12,46' W	213,1	GKG	at sea bottom
PS69/281-2	08.03.06	13:53	74° 19,77' S	110° 12,50' W	213,3	GKG	on deck
PS69/282-1	08.03.06	18:44	74° 13,26' S	110° 14,15' W	152,6	SEISREFL	Streamer into water
PS69/282-1	08.03.06	18:57	74° 13,91' S	110° 14,82' W	152,0	SEISREFL	airguns in the water
PS69/282-1	08.03.06	19:08	74° 13,88' S	110° 17,73' W	103,8	SEISREFL	profile start
PS69/282-1	10.03.06	15:06	72° 45,82' S	115° 21,65' W	610,7	SEISREFL	end of profile
PS69/282-1	10.03.06	15:13	72° 46,09' S	115° 21,07' W	610,4	SEISREFL	array on deck
PS69/282-1	10.03.06	15:29	72° 46,32' S	115° 19,43' W	616,5	SEISREFL	streamer on deck
PS69/283-1	10.03.06	15:49	72° 46,36' S	115° 19,25' W	614,4	CTD/RO	surface

Station	Date	Time	Position Lat	Position Lon	Depth [m]	Gear Abbreviat.	Action
PS69/283-1	10.03.06	16:05	72° 46,30' S	115° 19,22' W	617,5	CTD/RO	at depth
PS69/283-1	10.03.06	16:22	72° 46,34' S	115° 19,15' W	615,7	CTD/RO	on deck
PS69/283-2	10.03.06	16:31	72° 46,38' S	115° 19,14' W	615,5	MN	surface
PS69/283-2	10.03.06	16:34	72° 46,39' S	115° 19,15' W	615,4	MN	Error - Restart
PS69/283-2	10.03.06	16:39	72° 46,37' S	115° 19,09' W	614,5	MN	
PS69/283-2	10.03.06	16:58	72° 46,39' S	115° 19,14' W	616,0	MN	at depth
PS69/283-2	10.03.06	17:20	72° 46,41' S	115° 19,05' W	616,3	MN	on deck
PS69/283-3	10.03.06	17:24	72° 46,41' S	115° 19,05' W	616,7	BONGO	surface
PS69/283-3	10.03.06	17:36	72° 46,41' S	115° 19,00' W	615,9	BONGO	at depth
PS69/283-3	10.03.06	17:51	72° 46,40' S	115° 19,00' W	616,4	BONGO	on deck
PS69/283-4	10.03.06	18:16	72° 46,40' S	115° 19,12' W	617,0	MN	surface
PS69/283-4	10.03.06	18:34	72° 46,41' S	115° 19,13' W	616,4	MN	at depth
PS69/283-4	10.03.06	18:58	72° 46,50' S	115° 19,33' W	615,0	MN	on deck
PS69/283-5	10.03.06	18:58	72° 46,50' S	115° 19,33' W	615,0	GKG	surface
PS69/283-5	10.03.06	19:33	72° 45,86' S	115° 22,62' W	611,9	GKG	at sea bottom
PS69/283-5	10.03.06	19:43	72° 45,88' S	115° 22,57' W	611,2	GKG	on deck
PS69/283-6	10.03.06	20:01	72° 45,86' S	115° 22,65' W	612,2	GC	surface
PS69/283-6	10.03.06	20:11	72° 45,86' S	115° 22,66' W	612,7	GC	at sea bottom
PS69/283-6	10.03.06	20:23	72° 45,81' S	115° 22,73' W	611,6	GC	on deck
PS69/284-1	10.03.06	22:05	73° 1,38' S	115° 24,04' W	763,7	GC	surface
PS69/284-1	10.03.06	22:16	73° 1,40' S	115° 24,20' W	763,6	GC	at sea bottom
PS69/284-1	10.03.06	22:16	73° 1,40' S	115° 24,20' W	763,6	GC	off ground hoisting
PS69/284-1	10.03.06	22:25	73° 1,42' S	115° 23,99' W	763,5	GC	on deck
PS69/284-2	10.03.06	22:40	73° 1,32' S	115° 23,97' W	764,2	GKG	surface
PS69/284-2	10.03.06	22:51	73° 1,21' S	115° 24,08' W	762,7	GKG	at sea bottom
PS69/284-2	10.03.06	23:03	73° 1,05' S	115° 24,42' W	761,6	GKG	on deck
PS69/285-1	11.03.06	17:40	74° 30,15' S	109° 41,97' W	847,5	CTD/RO	surface
PS69/285-1	11.03.06	17:59	74° 30,18' S	109° 41,74' W	798,7	CTD/RO	at depth
PS69/285-1	11.03.06	18:14	74° 30,20' S	109° 41,59' W	763,1	CTD/RO	on deck

Station	Date	Time	Position Lat	Position Lon	Depth [m]	Gear Abbreviat.	Action
PS69/286-1	12.03.06	21:13	74° 42,91' S	106° 3,72' W	689,4	CTD/RO	surface
PS69/286-1	12.03.06	21:31	74° 42,94' S	106° 3,83' W	703,8	CTD/RO	on deck
PS69/287-1	13.03.06	02:48	74° 50,44' S	104° 57,07' W	1015,0	SEISREFL	Streamer into water
PS69/287-1	13.03.06	03:03	74° 50,93' S	104° 54,21' W	961,5	SEISREFL	airguns in the water
PS69/287-1	13.03.06	03:07	74° 51,08' S	104° 53,11' W	1026,0	SEISREFL	profile start
PS69/287-1	13.03.06	09:31	74° 30,08' S	103° 20,27' W	924,8	SEISREFL	alter course
PS69/287-1	13.03.06	11:44	74° 20,02' S	103° 0,03' W	258,7	SEISREFL	alter course
PS69/287-1	13.03.06	13:29	74° 14,46' S	102° 37,70' W	328,9	SEISREFL	end of profile
PS69/287-1	13.03.06	13:34	74° 14,23' S	102° 36,51' W	418,1	SEISREFL	array on deck
PS69/287-1	13.03.06	13:47	74° 13,97' S	102° 34,50' W	468,4	SEISREFL	streamer on deck
PS69/288-1	13.03.06	17:17	74° 24,92' S	102° 59,69' W	772,6	GC	surface
PS69/288-1	13.03.06	17:25	74° 24,92' S	102° 59,61' W	773,1	GC	at sea bottom
PS69/288-1	13.03.06	17:48	74° 24,93' S	102° 59,60' W	772,6	GC	on deck
PS69/288-2	13.03.06	18:07	74° 24,91' S	102° 59,60' W	772,9	GKG	surface
PS69/288-2	13.03.06	18:19	74° 24,92' S	102° 59,53' W	773,0	GKG	at sea bottom
PS69/288-2	13.03.06	18:33	74° 24,93' S	102° 59,57' W	773,2	GKG	on deck
PS69/288-3	13.03.06	19:42	74° 24,93' S	102° 59,53' W	772,2	GC	surface
PS69/288-3	13.03.06	19:51	74° 24,95' S	102° 59,48' W	772,1	GC	at sea bottom
PS69/288-3	13.03.06	20:10	74° 24,99' S	102° 59,26' W	770,6	GC	on deck
PS69/289-1	13.03.06	21:22	74° 30,48' S	103° 21,63' W	930,4	CTD/RO	surface
PS69/289-1	13.03.06	21:42	74° 30,50' S	103° 21,44' W	922,5	CTD/RO	at depth
PS69/289-1	13.03.06	22:04	74° 30,43' S	103° 20,97' W	932,5	CTD/RO	on deck
PS69/289-2	13.03.06	22:10	74° 30,43' S	103° 21,00' W	933,2	BONGO	surface
PS69/289-2	13.03.06	22:24	74° 30,45' S	103° 21,15' W	926,8	BONGO	at depth
PS69/289-2	13.03.06	22:38	74° 30,44' S	103° 21,21' W	931,9	BONGO	on deck
PS69/289-3	13.03.06	23:11	74° 30,42' S	103° 21,62' W	940,9	GC	surface
PS69/289-3	13.03.06	23:24	74° 30,42' S	103° 21,55' W	942,8	GC	at sea bottom
PS69/289-3	13.03.06	23:38	74° 30,37' S	103° 21,70' W	945,1	GC	on deck
PS69/290-1	14.03.06	00:58	74° 36,56' S	103° 52,22' W	849,8	MOR	surface

Station	Date	Time	Position Lat	Position Lon	Depth [m]	Gear Abbreviat.	Action
PS69/290-1	14.03.06	00:59	74° 36,53' S	103° 52,26' W	848,1	MOR	surface
PS69/290-1	14.03.06	01:00	74° 36,51' S	103° 52,31' W	847,8	MOR	surface
PS69/290-1	14.03.06	01:00	74° 36,51' S	103° 52,31' W	847,8	MOR	surface
PS69/290-1	14.03.06	01:01	74° 36,49' S	103° 52,36' W	849,7	MOR	slipped
PS69/290-2	14.03.06	01:08	74° 36,43' S	103° 52,47' W	839,8	CTD/RO	surface
PS69/290-2	14.03.06	01:28	74° 36,34' S	103° 53,04' W	854,1	CTD/RO	at depth
PS69/290-2	14.03.06	01:43	74° 36,30' S	103° 52,98' W	856,7	CTD/RO	on deck
PS69/291-1	14.03.06	02:44	74° 41,16' S	104° 9,36' W	1024,0	GC	surface
PS69/291-1	14.03.06	02:56	74° 41,16' S	104° 9,51' W	1023,0	GC	at sea bottom
PS69/291-1	14.03.06	03:16	74° 41,27' S	104° 9,60' W	1021,0	GC	on deck
PS69/292-1	14.03.06	05:15	74° 40,91' S	105° 11,56' W	1405,0	CTD/RO	surface
PS69/292-1	14.03.06	05:44	74° 40,89' S	105° 11,50' W	1401,0	CTD/RO	at depth
PS69/292-1	14.03.06	06:10	74° 40,92' S	105° 11,56' W	1405,0	CTD/RO	on deck
PS69/292-2	14.03.06	06:20	74° 40,92' S	105° 11,62' W	1407,0	GC	surface
PS69/292-2	14.03.06	06:35	74° 40,92' S	105° 11,61' W	1407,0	GC	at sea bottom
PS69/292-2	14.03.06	06:55	74° 40,90' S	105° 11,37' W	1390,0	GC	on deck
PS69/292-3	14.03.06	07:11	74° 40,98' S	105° 11,35' W	1391,0	GKG	surface
PS69/292-3	14.03.06	07:29	74° 40,95' S	105° 11,60' W	1406,0	GKG	at sea bottom
PS69/292-3	14.03.06	07:48	74° 40,98' S	105° 11,64' W	1404,0	GKG	on deck
PS69/293-1	14.03.06	11:08	74° 34,89' S	103° 33,26' W	876,8	SEISREFL	Streamer into water
PS69/293-1	14.03.06	11:21	74° 34,72' S	103° 30,41' W	685,1	SEISREFL	airguns in the water
PS69/293-1	14.03.06	11:24	74° 34,82' S	103° 29,59' W	621,6	SEISREFL	profile start
PS69/293-1	14.03.06	17:57	74° 17,48' S	104° 59,57' W	918,8	SEISREFL	alter course
PS69/293-1	15.03.06	05:51	73° 25,21' S	103° 30,21' W	625,8	SEISREFL	alter course
PS69/293-1	15.03.06	10:58	73° 0,99' S	103° 57,01' W	566,7	SEISREFL	end of profile
PS69/293-1	15.03.06	11:14	73° 0,98' S	103° 53,11' W	547,5	SEISREFL	streamer on deck
PS69/293-1	15.03.06	11:18	73° 1,00' S	103° 52,13' W	544,5	SEISREFL	array on deck
PS69/294-1	15.03.06	11:50	72° 59,96' S	103° 59,65' W	546,4	CTD/RO	surface
PS69/294-1	15.03.06	12:04	72° 59,96' S	103° 59,66' W	543,6	CTD/RO	at depth

Station	Date	Time	Position Lat	Position Lon	Depth [m]	Gear Abbreviat.	Action
PS69/294-1	15.03.06	12:20	73° 0,06' S	103° 59,76' W	544,0	CTD/RO	on deck
PS69/294-2	15.03.06	12:27	73° 0,13' S	104° 0,00' W	542,8	BONGO	surface
PS69/294-2	15.03.06	12:41	73° 0,20' S	103° 59,93' W	542,7	BONGO	at depth
PS69/294-2	15.03.06	12:53	73° 0,25' S	103° 59,80' W	544,4	BONGO	on deck
PS69/295-1	16.03.06	00:40	74° 28,72' S	104° 5,93' W	1151,0	GC	surface
PS69/295-1	16.03.06	00:53	74° 28,74' S	104° 6,09' W	1151,0	GC	at sea bottom
PS69/295-1	16.03.06	01:10	74° 28,72' S	104° 6,55' W	1149,0	GC	on deck
PS69/296-1	16.03.06	03:00	74° 21,42' S	104° 44,94' W	1434,0	GC	surface
PS69/296-1	16.03.06	03:16	74° 21,41' S	104° 45,08' W	1433,0	GC	at sea bottom
PS69/296-1	16.03.06	03:42	74° 21,41' S	104° 45,16' W	1432,0	GC	on deck
PS69/297-1	16.03.06	06:46	74° 4,77' S	103° 40,06' W	479,9	GKG	surface
PS69/297-1	16.03.06	06:54	74° 4,79' S	103° 40,06' W	481,0	GKG	at sea bottom
PS69/297-1	16.03.06	07:03	74° 4,77' S	103° 40,13' W	477,5	GKG	on deck
PS69/298-1	16.03.06	09:44	73° 42,32' S	103° 49,95' W	919,5	GC	surface
PS69/298-1	16.03.06	09:55	73° 42,31' S	103° 49,95' W	922,0	GC	at sea bottom
PS69/298-1	16.03.06	10:09	73° 42,31' S	103° 49,96' W	919,2	GC	on deck
PS69/299-1	16.03.06	12:12	73° 26,66' S	103° 38,97' W	706,4	GKG	surface
PS69/299-1	16.03.06	12:22	73° 26,62' S	103° 38,89' W	717,8	GKG	at sea bottom
PS69/299-1	16.03.06	12:33	73° 26,59' S	103° 38,78' W	728,0	GKG	on deck
PS69/300-1	16.03.06	13:46	73° 16,22' S	103° 40,71' W	767,0	GC	surface
PS69/300-1	16.03.06	13:55	73° 16,23' S	103° 40,76' W	766,1	GC	at sea bottom
PS69/300-1	16.03.06	14:06	73° 16,31' S	103° 40,79' W	770,3	GC	on deck
PS69/301-1	16.03.06	16:24	73° 1,93' S	103° 56,41' W	581,5	SEISREFL	Streamer into water
PS69/301-1	16.03.06	16:38	73° 2,29' S	103° 53,60' W	569,3	SEISREFL	airguns in the water
PS69/301-1	16.03.06	16:43	73° 2,24' S	103° 52,36' W	558,0	SEISREFL	profile start
PS69/301-1	17.03.06	00:44	72° 25,87' S	104° 0,39' W	661,0	SEISREFL	end of profile
PS69/301-1	17.03.06	00:48	72° 25,72' S	103° 59,66' W	664,3	SEISREFL	array on deck
PS69/301-1	17.03.06	00:58	72° 25,80' S	103° 58,39' W	678,6	SEISREFL	streamer on deck
PS69/302-1	18.03.06	14:54	71° 8,29' S	105° 40,01' W	565,8	MOR	surface

Station	Date	Time	Position Lat	Position Lon	Depth [m]	Gear Abbreviat.	Action
PS69/302-1	18.03.06	14:55	71° 8,24' S	105° 39,99' W	565,8	MOR	surface
PS69/302-1	18.03.06	14:56	71° 8,21' S	105° 39,97' W	566,3	MOR	slipped
PS69/302-2	18.03.06	15:06	71° 7,97' S	105° 39,97' E	566,3	CTD/RO	surface
PS69/302-2	18.03.06	15:22	71° 8,09' S	105° 39,88' E	566,2	CTD/RO	at depth
PS69/302-2	18.03.06	15:33	71° 8,15' S	105° 39,88' W	565,8	CTD/RO	on deck
PS69/302-3	18.03.06	16:27	71° 7,90' S	105° 38,20' W	565,0	GKG	surface
PS69/302-3	18.03.06	16:45	71° 7,90' S	105° 38,30' W	565,0	GKG	at sea bottom
PS69/302-3	18.03.06	16:58	71° 7,90' S	105° 38,40' W	565,0	GKG	on deck
PS69/302-4	18.03.06	17:10	71° 7,90' S	105° 38,50' W	564,0	GC	surface
PS69/302-4	18.03.06	17:25	71° 7,90' S	105° 38,40' W	564,0	GC	at sea bottom
PS69/302-4	18.03.06	17:37	71° 7,90' S	105° 38,40' W	564,0	GC	on deck
PS69/303-1	18.03.06	18:57	71° 0,00' S	105° 39,50' W	1515,0	CTD/RO	surface
PS69/303-1	18.03.06	19:17	71° 0,05' S	105° 39,67' W	1528,0	CTD/RO	at depth
PS69/303-1	18.03.06	19:36	71° 0,07' S	105° 40,21' W	1531,0	CTD/RO	on deck
PS69/303-2	18.03.06	19:44	71° 0,06' S	105° 40,43' W	1527,0	MN	surface
PS69/303-2	18.03.06	20:26	71° 0,06' S	105° 41,25' W	1505,0	MN	at depth
PS69/303-2	18.03.06	21:01	71° 0,06' S	105° 41,84' W	1501,0	MN	on deck
PS69/303-3	18.03.06	21:11	71° 0,06' S	105° 42,06' W	1503,0	BONGO	surface
PS69/303-3	18.03.06	21:24	71° 0,02' S	105° 42,41' W	1507,0	BONGO	at depth
PS69/303-3	18.03.06	21:37	71° 0,02' S	105° 42,83' W	1507,0	BONGO	on deck
PS69/303-4	18.03.06	21:45	70° 59,97' S	105° 43,01' W	1517,0	MN	surface
PS69/303-4	18.03.06	22:23	70° 59,94' S	105° 44,06' W	1509,0	MN	at depth
PS69/303-4	18.03.06	23:06	71° 0,02' S	105° 45,33' W	1497,0	MN	on deck
PS69/304-1	19.03.06	01:12	71° 9,38' S	105° 32,98' W	569,7	SEISREFL	airguns in the water
PS69/304-1	19.03.06	01:15	71° 9,15' S	105° 32,68' W	569,5	SEISREFL	profile start
PS69/304-1	19.03.06	13:16	70° 10,16' S	105° 29,77' W	3567,0	SEISREFL	alter course
PS69/304-1	19.03.06	14:29	70° 10,76' S	105° 12,11' W	3470,0	SEISREFL	end of profile
PS69/304-1	19.03.06	14:33	70° 10,87' S	105° 11,24' W	3469,0	SEISREFL	array on deck
PS69/304-1	19.03.06	14:58	70° 11,02' S	105° 5,44' W	3584,0	SEISREFL	airguns in the water

Station	Date	Time	Position Lat	Position Lon	Depth [m]	Gear Abbreviat.	Action
PS69/304-1	19.03.06	15:01	70° 11,08' S	105° 4,76' W	3606,0	SEISREFL	profile start
PS69/304-1	19.03.06	20:52	70° 15,29' S	103° 30,20' W	3793,0	SEISREFL	alter course
PS69/304-1	20.03.06	01:41	70° 17,32' S	104° 54,06' W	3735,0	SEISREFL	alter course
PS69/304-1	20.03.06	17:05	70° 2,85' S	109° 10,03' W	3801,0	SEISREFL	Remark
PS69/304-1	20.03.06	17:08	70° 2,71' S	109° 10,72' W	3792,0	SEISREFL	Remark
PS69/304-1	20.03.06	18:07	70° 2,15' S	109° 24,63' W	3735,0	SEISREFL	airguns in the water
PS69/304-1	20.03.06	18:19	70° 1,83' S	109° 27,41' W	3736,0	SEISREFL	profile start
PS69/304-1	20.03.06	20:20	70° 0,01' S	109° 59,67' W	3590,0	SEISREFL	alter course
PS69/304-1	20.03.06	21:42	70° 1,56' S	110° 21,68' W	3531,0	SEISREFL	Remark
PS69/304-1	20.03.06	21:55	70° 1,97' S	110° 25,21' W	3552,0	SEISREFL	airguns in the water
PS69/304-1	22.03.06	03:25	70° 39,99' S	118° 44,93' W	2857,0	SEISREFL	end of profile
PS69/304-1	22.03.06	03:29	70° 39,95' S	118° 45,94' W	2854,0	SEISREFL	array on deck
PS69/304-1	22.03.06	03:40	70° 39,57' S	118° 47,09' W	2849,0	SEISREFL	streamer on deck
PS69/305-1	22.03.06	13:09	70° 15,03' S	119° 41,22' W	2950,0	CTD/RO	surface
PS69/305-1	22.03.06	13:24	70° 15,04' S	119° 41,14' W	2948,0	CTD/RO	at depth
PS69/305-1	22.03.06	13:43	70° 15,06' S	119° 41,22' W	2948,0	CTD/RO	on deck
PS69/305-2	22.03.06	13:49	70° 15,07' S	119° 41,22' W	2948,0	BONGO	surface
PS69/305-2	22.03.06	14:02	70° 15,09' S	119° 41,21' W	2949,0	BONGO	at depth
PS69/305-2	22.03.06	14:15	70° 15,07' S	119° 41,26' W	2945,0	BONGO	on deck
PS69/306-1	22.03.06	14:21	70° 15,07' S	119° 41,27' W	2947,0	OBS	surface
PS69/306-2	22.03.06	15:41	70° 24,43' S	119° 30,88' W	2923,0	OBS	surface
PS69/306-3	22.03.06	17:02	70° 33,80' S	119° 19,82' W	2863,0	OBS	surface
PS69/306-4	22.03.06	18:23	70° 43,13' S	119° 9,62' W	2820,0	OBS	surface
PS69/306-5	22.03.06	19:45	70° 52,49' S	118° 58,77' W	2771,0	OBS	surface
PS69/306-6	22.03.06	21:06	71° 1,81' S	118° 48,20' W	2698,0	OBS	surface
PS69/306-7	22.03.06	22:25	71° 11,18' S	118° 37,08' W	2540,0	OBS	surface
PS69/307-1	23.03.06	02:03	71° 33,31' S	118° 11,43' W	1748,0	SEISREFL	Streamer into water
PS69/307-1	23.03.06	02:16	71° 32,57' S	118° 11,41' W	1783,0	SEISREFL	airguns in the water
PS69/307-1	23.03.06	02:23	71° 32,38' S	118° 11,14' W	1787,0	SEISREFL	array on deck

Station	Date	Time	Position Lat	Position Lon	Depth [m]	Gear Abbreviat.	Action
PS69/307-1	23.03.06	02:53	71° 31,84' S	118° 12,03' W	1820,0	SEISREFL	airguns in the water
PS69/307-1	23.03.06	02:58	71° 31,46' S	118° 12,40' W	1833,0	SEISREFL	profile start
PS69/307-1	23.03.06	16:13	70° 30,38' S	119° 24,12' W	2902,0	SEISREFL	Remark
PS69/307-1	23.03.06	21:30	70° 5,67' S	119° 51,87' W	2979,0	SEISREFL	end of profile
PS69/307-1	23.03.06	21:57	70° 4,09' S	119° 51,39' W	2984,0	SEISREFL	streamer on deck
PS69/307-1	23.03.06	22:06	70° 3,62' S	119° 51,08' W	2975,0	SEISREFL	array on deck
PS69/308-1	23.03.06	23:41	70° 15,05' S	119° 41,44' W	2952,0	OBS	released
PS69/308-1	24.03.06	00:55	70° 15,07' S	119° 41,27' W	2948,0	OBS	released
PS69/308-1	24.03.06	01:34	70° 15,20' S	119° 40,36' W	2951,0	OBS	released
PS69/308-1	24.03.06	02:32	70° 15,24' S	119° 41,02' W	2952,0	OBS	
PS69/308-2	24.03.06	03:57	70° 24,50' S	119° 30,65' W	2912,1	OBS	released
PS69/308-2	24.03.06	04:16	70° 24,42' S	119° 30,97' W	2912,7	OBS	released
PS69/308-2	24.03.06	05:25	70° 24,48' S	119° 30,66' W	2911,3	OBS	
PS69/308-3	24.03.06	06:46	70° 33,84' S	119° 20,33' W	2856,8	OBS	released
PS69/308-3	24.03.06	06:51	70° 33,84' S	119° 20,27' W	2856,7	OBS	
PS69/308-3	24.03.06	07:01	70° 33,84' S	119° 20,12' W	2855,6	OBS	released
PS69/308-3	24.03.06	07:20	70° 33,75' S	119° 20,56' W	2858,3	OBS	released
PS69/308-3	24.03.06	07:31	70° 33,87' S	119° 20,48' W	2858,1	OBS	at surface
PS69/308-3	24.03.06	07:45	70° 33,93' S	119° 19,90' W	2851,3	OBS	on deck
PS69/309-1	24.03.06	08:20	70° 33,71' S	119° 20,26' W	2870,0	PC	surface
PS69/309-1	24.03.06	09:15	70° 33,67' S	119° 20,23' W	2869,0	PC	at sea bottom
PS69/309-1	24.03.06	10:25	70° 33,72' S	119° 20,39' W	2869,0	PC	on Deck
PS69/308-4	24.03.06	11:56	70° 43,13' S	119° 9,61' W	2805,1	OBS	released
PS69/308-4	24.03.06	12:29	70° 43,08' S	119° 9,38' W	2818,0	OBS	at surface
PS69/308-4	24.03.06	12:42	70° 43,03' S	119° 8,85' W	2820,0	OBS	on deck
PS69/308-5	24.03.06	14:12	70° 52,44' S	118° 58,66' W	2772,0	OBS	released
PS69/308-5	24.03.06	14:37	70° 52,41' S	118° 58,42' W	2758,3	OBS	at surface
PS69/308-5	24.03.06	14:50	70° 52,43' S	118° 58,16' W	2758,1	OBS	on deck
PS69/308-6	24.03.06	16:19	71° 1,80' S	118° 48,07' W	2685,8	OBS	released

Station	Date	Time	Position Lat	Position Lon	Depth [m]	Gear Abbreviat.	Action
PS69/308-6	24.03.06	16:53	71° 1,79' S	118° 48,32' W	2683,9	OBS	at surface
PS69/308-6	24.03.06	16:57	71° 1,84' S	118° 48,38' W	2684,2	OBS	on deck
PS69/308-7	24.03.06	18:20	71° 11,21' S	118° 37,45' W	2527,9	OBS	released
PS69/308-7	24.03.06	18:53	71° 11,17' S	118° 37,53' W	2528,9	OBS	at surface
PS69/308-7	24.03.06	19:04	71° 11,29' S	118° 37,56' W	2526,6	OBS	on deck
PS69/310-1	24.03.06	22:03	71° 8,97' S	119° 57,39' W	2123,0	PC	surface
PS69/310-1	24.03.06	22:42	71° 8,94' S	119° 57,56' W	2126,0	PC	at sea bottom
PS69/310-1	24.03.06	23:23	71° 8,96' S	119° 57,21' W	2123,0	PC	on Deck
PS69/308-8	25.03.06	03:40	70° 24,44' S	119° 30,78' W	2911,3	OBS	released
PS69/308-8	25.03.06	04:20	70° 24,49' S	119° 31,85' W	2911,9	OBS	at surface
PS69/308-8	25.03.06	04:37	70° 24,45' S	119° 30,69' W	2923,0	OBS	on deck
PS69/308-9	25.03.06	05:56	70° 15,13' S	119° 41,33' W	2937,5	OBS	released
PS69/308-9	25.03.06	06:06	70° 15,15' S	119° 41,24' W	2936,9	OBS	released
PS69/308-9	25.03.06	07:36	70° 15,07' S	119° 41,55' W	2950,0	OBS	
PS69/311-1	26.03.06	09:32	69° 52,13' S	126° 7,98' W	2442,0	DRG	surface
PS69/311-1	26.03.06	09:55	69° 51,44' S	126° 6,23' W	2280,0	DRG	start dredging
PS69/311-1	26.03.06	10:37	69° 50,99' S	126° 4,89' W	1802,0	DRG	stop dredging
PS69/311-1	26.03.06	11:41	69° 50,70' S	126° 4,43' W	1718,0	DRG	on deck
PS69/312-1	26.03.06	12:34	69° 47,31' S	125° 53,36' W	2514,0	DRG	surface
PS69/312-1	26.03.06	13:15	69° 47,47' S	125° 57,10' W	1990,0	DRG	start dredging
PS69/312-1	26.03.06	13:28	69° 47,49' S	125° 57,63' W	1773,0	DRG	stop dredging
PS69/312-1	26.03.06	14:11	69° 47,43' S	125° 57,92' W	1723,0	DRG	start dredging
PS69/312-1	26.03.06	14:26	69° 47,50' S	125° 58,66' W	1505,0	DRG	stop dredging
PS69/312-1	26.03.06	15:22	69° 47,38' S	125° 58,55' W	1584,0	DRG	on deck
PS69/313-1	26.03.06	15:46	69° 47,37' S	125° 58,50' W	1592,0	CTD/RO	surface
PS69/313-1	26.03.06	16:02	69° 47,36' S	125° 58,53' W	1591,0	CTD/RO	at depth
PS69/313-1	26.03.06	16:21	69° 47,40' S	125° 58,46' W	1587,0	CTD/RO	on deck
PS69/313-2	26.03.06	16:29	69° 47,43' S	125° 58,42' W	1582,0	BONGO	surface
PS69/313-2	26.03.06	16:43	69° 47,45' S	125° 58,43' W	1570,0	BONGO	at depth

Station	Date	Time	Position Lat	Position Lon	Depth [m]	Gear Abbreviat.	Action
PS69/313-2	26.03.06	16:55	69° 47,48' S	125° 58,35' W	1592,0	BONGO	on deck
PS69/314-1	26.03.06	17:56	69° 42,14' S	126° 12,30' W	2532,0	DRG	surface
PS69/314-1	26.03.06	18:30	69° 43,05' S	126° 11,57' W	2099,0	DRG	Information
PS69/314-1	26.03.06	19:02	69° 43,52' S	126° 10,80' W	1942,0	DRG	start dredging
PS69/314-1	26.03.06	19:36	69° 43,52' S	126° 10,74' W	1947,0	DRG	stop dredging
PS69/314-1	26.03.06	20:17	69° 43,62' S	126° 10,37' W	1932,0	DRG	on deck
PS69/315-1	26.03.06	22:14	69° 36,14' S	125° 21,90' W	3155,0	DRG	surface
PS69/315-1	26.03.06	22:48	69° 35,50' S	125° 19,72' W	2543,0	DRG	start dredging
PS69/315-1	26.03.06	23:16	69° 35,19' S	125° 18,65' W	2261,0	DRG	Information
PS69/315-1	26.03.06	23:45	69° 35,15' S	125° 18,58' W	2276,0	DRG	stop dredging
PS69/315-1	27.03.06	00:21	69° 35,11' S	125° 18,45' W	2301,0	DRG	on deck
PS69/316-1	27.03.06	06:24	69° 7,67' S	123° 54,77' W	3216,0	DRG	surface
PS69/316-1	27.03.06	07:18	69° 6,91' S	123° 58,20' W	3392,0	DRG	Information
PS69/316-1	27.03.06	07:47	69° 6,67' S	123° 59,37' W	3058,0	DRG	start dredging
PS69/316-1	27.03.06	08:50	69° 6,65' S	123° 59,53' W	3044,0	DRG	stop dredging
PS69/316-1	27.03.06	09:29	69° 6,60' S	123° 59,78' W	3021,0	DRG	on deck
PS69/317-1	27.03.06	11:22	69° 11,03' S	123° 23,45' W	2520,0	DRG	surface
PS69/317-1	27.03.06	11:56	69° 10,31' S	123° 25,45' W	2033,0	DRG	Information
PS69/317-1	27.03.06	12:23	69° 9,97' S	123° 26,33' W	1590,0	DRG	start dredging
PS69/317-1	27.03.06	13:39	69° 9,99' S	123° 26,15' W	1607,0	DRG	stop dredging
PS69/317-1	27.03.06	14:16	69° 9,98' S	123° 25,81' W	1662,0	DRG	on deck
PS69/318-1	27.03.06	15:00	69° 9,46' S	123° 13,02' W	2349,0	DRG	surface
PS69/318-1	27.03.06	15:30	69° 8,63' S	123° 13,32' W	1834,0	DRG	start dredging
PS69/318-1	27.03.06	16:52	69° 8,23' S	123° 12,86' W	1508,0	DRG	stop dredging
PS69/318-1	27.03.06	17:20	69° 8,18' S	123° 12,63' W	1519,0	DRG	on deck
PS69/319-1	27.03.06	18:43	69° 11,59' S	122° 52,60' W	2857,0	DRG	surface
PS69/319-1	27.03.06	19:17	69° 10,44' S	122° 52,57' W	2076,0	DRG	Information
PS69/319-1	27.03.06	19:45	69° 10,00' S	122° 52,62' W	1543,0	DRG	start dredging
PS69/319-1	27.03.06	20:55	69° 9,86' S	122° 52,67' W	1498,0	DRG	stop dredging

Station	Date	Time	Position Lat	Position Lon	Depth [m]	Gear Abbreviat.	Action
PS69/319-1	27.03.06	21:18	69° 9,77' S	122° 52,77' W	1517,0	DRG	on deck
PS69/320-1	27.03.06	23:56	69° 22,07' S	121° 53,70' W	3113,0	DRG	surface
PS69/320-1	28.03.06	00:31	69° 21,09' S	121° 52,12' W	2577,0	DRG	Information
PS69/320-1	28.03.06	00:50	69° 20,89' S	121° 51,77' W	2344,0	DRG	start dredging
PS69/320-1	28.03.06	01:56	69° 20,43' S	121° 52,27' W	2521,0	DRG	stop dredging
PS69/320-1	28.03.06	02:27	69° 20,19' S	121° 53,20' W	2688,0	DRG	on deck
PS69/321-1	28.03.06	03:15	69° 21,80' S	121° 35,16' W	2154,0	DRG	surface
PS69/321-1	28.03.06	04:13	69° 21,48' S	121° 31,23' W	1462,0	DRG	start dredging
PS69/321-1	28.03.06	04:44	69° 21,46' S	121° 29,81' W	1345,0	DRG	stop dredging
PS69/321-1	28.03.06	05:40	69° 21,52' S	121° 31,54' W	1539,0	DRG	on deck
PS69/322-1	28.03.06	06:49	69° 29,65' S	121° 22,09' W	2883,0	DRG	surface
PS69/322-1	28.03.06	07:25	69° 28,59' S	121° 22,31' W	2381,0	DRG	Information
PS69/322-1	28.03.06	07:44	69° 28,35' S	121° 22,24' W	2097,0	DRG	start dredging
PS69/322-1	28.03.06	08:45	69° 28,22' S	121° 22,10' W	1985,0	DRG	stop dredging
PS69/322-1	28.03.06	09:12	69° 28,15' S	121° 22,05' W	1974,0	DRG	on deck
PS69/323-1	28.03.06	09:40	69° 28,07' S	121° 17,97' W	2359,0	DRG	surface
PS69/323-1	28.03.06	10:11	69° 27,07' S	121° 17,98' W	1726,0	DRG	Information
PS69/323-1	28.03.06	10:29	69° 26,80' S	121° 17,98' W	1424,0	DRG	start dredging
PS69/323-1	28.03.06	11:17	69° 26,75' S	121° 17,91' W	1401,0	DRG	stop dredging
PS69/323-1	28.03.06	11:37	69° 26,69' S	121° 17,95' W	1366,0	DRG	on deck
PS69/324-1	28.03.06	12:28	69° 31,01' S	121° 6,18' W	3413,0	DRG	surface
PS69/324-1	28.03.06	13:25	69° 29,86' S	121° 3,41' W	2359,0	DRG	Information
PS69/324-1	28.03.06	13:30	69° 29,84' S	121° 3,27' W	2299,0	DRG	start dredging
PS69/324-1	28.03.06	14:45	69° 29,57' S	121° 2,78' W	2250,0	DRG	stop dredging
PS69/324-1	28.03.06	15:17	69° 29,61' S	121° 2,28' W	2328,0	DRG	on deck
PS69/325-1	28.03.06	15:45	69° 28,31' S	120° 54,88' W	2011,0	DRG	surface
PS69/325-1	28.03.06	16:17	69° 27,23' S	120° 55,37' W	1605,0	DRG	Information
PS69/325-1	28.03.06	16:41	69° 26,82' S	120° 55,58' W	1392,0	DRG	start dredging
PS69/325-1	28.03.06	17:23	69° 26,91' S	120° 54,93' W	1555,0	DRG	stop dredging

Station	Date	Time	Position Lat	Position Lon	Depth [m]	Gear Abbreviat.	Action
PS69/325-1	28.03.06	17:48	69° 26,77' S	120° 54,48' W	1588,0	DRG	on deck
PS69/326-1	29.03.06	00:13	70° 15,10' S	119° 41,22' W	2936,9	CTD/RO	surface
PS69/326-1	29.03.06	00:27	70° 15,09' S	119° 41,24' W	2942,0	CTD/RO	at depth
PS69/326-2	29.03.06	00:38	70° 15,09' S	119° 41,29' W	2943,0	OBS	at surface
PS69/326-1	29.03.06	00:41	70° 15,08' S	119° 41,31' W	2944,0	CTD/RO	on deck
PS69/326-2	29.03.06	00:55	70° 15,17' S	119° 41,33' W	2943,0	OBS	on deck
PS69/327-1	29.03.06	08:58	69° 9,77' S	117° 38,67' W	3318,0	DRG	surface
PS69/327-1	29.03.06	09:41	69° 11,05' S	117° 38,67' W	3023,0	DRG	Information
PS69/327-1	29.03.06	10:19	69° 11,66' S	117° 38,65' W	2591,0	DRG	start dredging
PS69/327-1	29.03.06	11:22	69° 11,66' S	117° 38,58' W	2592,0	DRG	stop dredging
PS69/327-1	29.03.06	11:57	69° 11,71' S	117° 38,68' W	2626,0	DRG	on deck
PS69/328-1	29.03.06	13:19	69° 8,88' S	117° 8,76' W	3403,0	DRG	surface
PS69/328-1	29.03.06	14:11	69° 9,86' S	117° 8,81' W	3222,0	DRG	Information
PS69/328-1	29.03.06	14:40	69° 10,23' S	117° 8,23' W	3071,0	DRG	start dredging
PS69/328-1	29.03.06	15:12	69° 10,26' S	117° 8,33' W	3079,0	DRG	stop dredging
PS69/328-1	29.03.06	15:54	69° 10,18' S	117° 8,22' W	3070,0	DRG	on deck
PS69/329-1	29.03.06	16:48	69° 8,89' S	117° 9,38' W	3450,0	DRG	surface
PS69/329-1	29.03.06	17:32	69° 9,77' S	117° 7,79' W	3319,0	DRG	surface
PS69/329-1	29.03.06	17:48	69° 9,98' S	117° 7,64' W	3059,0	DRG	start dredging
PS69/329-1	29.03.06	18:23	69° 10,03' S	117° 7,52' W	3044,0	DRG	stop dredging
PS69/329-1	29.03.06	19:07	69° 10,17' S	117° 7,23' W	3056,0	DRG	on deck
PS69/330-1	30.03.06	05:14	70° 8,10' S	111° 44,83' W	3419,0	PC	surface
PS69/330-1	30.03.06	06:29	70° 8,12' S	111° 45,04' W	3417,0	PC	at sea bottom
PS69/330-1	30.03.06	08:15	70° 7,98' S	111° 44,60' W	3421,0	PC	on Deck
PS69/331-1	31.03.06	18:16	68° 58,15' S	90° 41,81' W	1286,0	CTD/RO	surface
PS69/331-1	31.03.06	18:30	68° 58,14' S	90° 41,95' W	1304,0	CTD/RO	at depth
PS69/331-1	31.03.06	18:48	68° 58,17' S	90° 41,95' W	1314,0	CTD/RO	on deck
PS69/331-2	31.03.06	19:32	68° 58,10' S	90° 42,05' W	1312,0	MN	surface
PS69/331-2	31.03.06	20:06	68° 58,08' S	90° 41,91' W	1289,0	MN	at depth

Station	Date	Time	Position Lat	Position Lon	Depth [m]	Gear Abbreviat.	Action
PS69/331-2	31.03.06	20:48	68° 58,08' S	90° 42,01' W	1306,0	MN	on deck
PS69/332-1	01.04.06	11:15	68° 31,37' S	82° 43,93' W	2581,0	PC	surface
PS69/332-1	01.04.06	12:17	68° 31,40' S	82° 44,16' W	3507,0	PC	at sea bottom
PS69/332-1	01.04.06	13:14	68° 31,35' S	82° 44,04' W	3509,0	PC	on Deck
PS69/333-1	02.04.06	19:21	67° 40,67' S	73° 20,41' W	495,4	MOR	surface
PS69/333-1	02.04.06	19:22	67° 40,67' S	73° 20,27' W	494,6	MOR	surface
PS69/333-1	02.04.06	19:23	67° 40,66' S	73° 20,16' W	496,3	MOR	slipped
PS69/333-1	02.04.06	19:23	67° 40,66' S	73° 20,16' W	496,3	MOR	surface
PS69/334-1	05.04.06	21:43	62° 14,79' S	58° 42,40' W	131,7	CTD/RO	surface
PS69/334-1	05.04.06	21:50	62° 14,78' S	58° 42,40' W	133,5	CTD/RO	at depth
PS69/334-1	05.04.06	21:54	62° 14,77' S	58° 42,40' W	132,4	CTD/RO	on deck
PS69/334-2	05.04.06	22:05	62° 14,76' S	58° 42,38' W	130,3	GKG	surface
PS69/334-2	05.04.06	22:10	62° 14,77' S	58° 42,43' W	135,5	GKG	at sea bottom
PS69/334-2	05.04.06	22:17	62° 14,80' S	58° 42,40' W	128,3	GKG	on deck
PS69/335-1	06.04.06	10:10	62° 15,52' S	58° 46,55' W	469,3	GKG	surface
PS69/335-1	06.04.06	10:19	62° 15,51' S	58° 46,39' W	461,8	GKG	at sea bottom
PS69/335-1	06.04.06	10:29	62° 15,47' S	58° 46,42' W	461,3	GKG	on deck
PS69/335-2	06.04.06	10:54	62° 15,49' S	58° 46,37' W	461,1	GC	surface
PS69/335-2	06.04.06	11:00	62° 15,50' S	58° 46,35' W	460,5	GC	at sea bottom
PS69/335-2	06.04.06	11:13	62° 15,51' S	58° 46,31' W	459,5	GC	on deck
PS69/336-1	06.04.06	11:46	62° 17,35' S	58° 41,65' W	445,9	GC	surface
PS69/336-1	06.04.06	11:52	62° 17,33' S	58° 41,68' W	444,6	GC	at sea bottom
PS69/336-1	06.04.06	12:03	62° 17,32' S	58° 41,65' W	444,0	GC	on deck
PS69/336-2	06.04.06	12:17	62° 17,33' S	58° 41,62' W	443,7	GKG	surface
PS69/336-2	06.04.06	12:24	62° 17,35' S	58° 41,51' W	443,7	GKG	at sea bottom
PS69/336-2	06.04.06	12:33	62° 17,35' S	58° 41,44' W	444,1	GKG	on deck
PS69/337-1	06.04.06	13:36	62° 14,79' S	58° 42,20' W	114,7	GC	surface
PS69/337-1	06.04.06	13:40	62° 14,77' S	58° 42,14' W	115,2	GC	at sea bottom
PS69/337-1	06.04.06	13:48	62° 14,77' S	58° 42,13' W	115,2	GC	on deck

Station	Date	Time	Position Lat	Position Lon	Depth [m]	Gear Abbreviat.	Action
PS69/337-2	06.04.06	14:09	62° 14,80' S	58° 42,15' W	112,7	GC	surface
PS69/337-2	06.04.06	14:12	62° 14,79' S	58° 42,12' W	109,1	GC	at sea bottom
PS69/337-2	06.04.06	14:19	62° 14,79' S	58° 42,13' W	109,6	GC	on deck
PS69/338-1	06.04.06	18:00	62° 14,30' S	58° 48,81' W	454,8	GC	surface
PS69/338-1	06.04.06	18:07	62° 14,30' S	58° 48,81' W	454,6	GC	at sea bottom
PS69/338-1	06.04.06	18:15	62° 14,31' S	58° 48,79' W	453,9	GC	on deck
PS69/339-1	06.04.06	21:34	62° 12,10' S	58° 51,53' W	268,8	GC	surface
PS69/339-1	06.04.06	21:38	62° 12,08' S	58° 51,49' W	268,2	GC	at sea bottom
PS69/339-1	06.04.06	21:47	62° 12,08' S	58° 51,53' W	268,8	GC	on deck